Frequency-based decay electron spectroscopy to measure neutrino mass and exotic interactions

Prof. Dr. Martin Fertl

Searching for New Physics at the Quantum Technology Frontier

CSF, Ascona

July 6th, 2023

JOHANNES GUTENBERG UNIVERSITÄT MAINZ

Outline

Short introduction to neutrino masses

The current state of the art: KATRIN and its latest results

Project 8: Narrow-range CRES for a neutrino mass measurement

He-6: Broad-band CRES to search for chirality flipping interactions

Summary

Non-zero neutrino masses are firmly established …

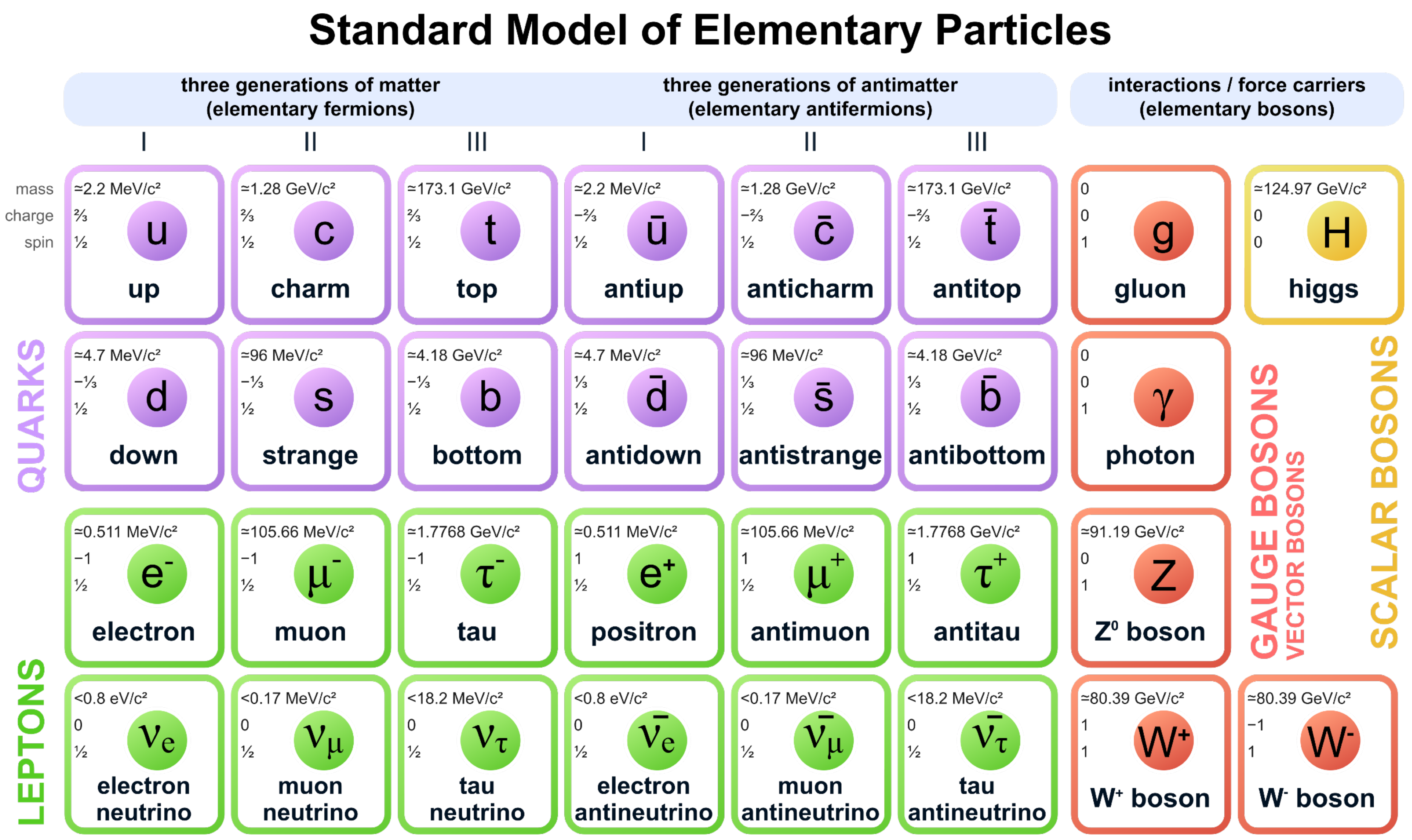

Figure adapted and updated from https://commons.wikimedia.org/wiki/File:Standard_Model_of_Elementary_Particles_Anti.svg

… through neutrino flavor oscillation experiments, …

… but neutrinos remain only SM particle without measured mass …

… and the mass generation mechanism remains unclear.

Neutrino mass from tritium β decay spectrum

With neutrino mixing and nuclear recoil for T_{nuc}:

$$\frac{dN}{dE_e} = \frac{G_F^2 m_e^5 \cos^2\theta_C}{2\pi^3\hbar^7} \left|M_{nuc}\right|^2 F(Z, E_e)\, p_e\,(E_e + m_e) \sum_i \left|U_{ei}\right|^2 (E_{max} - E_e) \times \sqrt{(E_{max} - E_e)^2 - m_{\nu i}^2} \cdot \Theta\,(E_{max} - E_e - m_{\nu i})$$

Neutrino mass from tritium β decay spectrum

With <u>neutrino mixing</u> and nuclear recoil for T_{nuc}:

physical constants

$$\frac{dN}{dE_e} = \frac{G_F^2 m_e^5 \cos^2\theta_C}{2\pi^3\hbar^7} |M_{nuc}|^2 F(Z, E_e) p_e (E_e + m_e) \sum_i |U_{ei}|^2 (E_{max} - E_e)$$

$$\times \sqrt{(E_{max} - E_e)^2 - m_{\nu i}^2} \cdot \Theta(E_{max} - E_e - m_{\nu i})$$

Neutrino mass from tritium β decay spectrum

With neutrino mixing and nuclear recoil for T_{nuc}:

physical constants — energy indep. matrix element

$$\frac{dN}{dE_e} = \frac{G_F^2 m_e^5 \cos^2\theta_C}{2\pi^3\hbar^7} \left|M_{nuc}\right|^2 F\left(Z, E_e\right) p_e \left(E_e + m_e\right) \sum_i \left|U_{ei}\right|^2 \left(E_{max} - E_e\right) \times \sqrt{\left(E_{max} - E_e\right)^2 - m_{\nu i}^2} \cdot \Theta\left(E_{max} - E_e - m_{\nu i}\right)$$

Neutrino mass from tritium β decay spectrum

With <u>neutrino mixing</u> and nuclear recoil for T_{nuc}:

physical constants

energy indep. matrix element

$$\frac{dN}{dE_e} = \frac{G_F^2 m_e^5 \cos^2\theta_C}{2\pi^3\hbar^7} |M_{nuc}|^2 F(Z, E_e) p_e (E_e + m_e) \sum_i |U_{ei}|^2 (E_{max} - E_e)$$

$$\times \sqrt{(E_{max} - E_e)^2 - m_{\nu i}^2} \cdot \Theta(E_{max} - E_e - m_{\nu i})$$

purely kinematic parameters

Neutrino mass from tritium β decay spectrum

With neutrino mixing and nuclear recoil for T_{nuc}:

physical constants — energy indep. matrix element

$$\frac{dN}{dE_e} = \frac{G_F^2 m_e^5 \cos^2\theta_C}{2\pi^3\hbar^7} |M_{nuc}|^2 F(Z,E_e)\, p_e\,(E_e + m_e) \sum_i |U_{ei}|^2 (E_{max} - E_e) \times \sqrt{(E_{max} - E_e)^2 - m_{\nu i}^2} \cdot \Theta(E_{max} - E_e - m_{\nu i})$$

purely kinematic parameters

For unresolved neutrino mass splitting:

$$m(\nu_e) = \sqrt{\sum_i |U_{e,i}|^2 m_i^2}$$

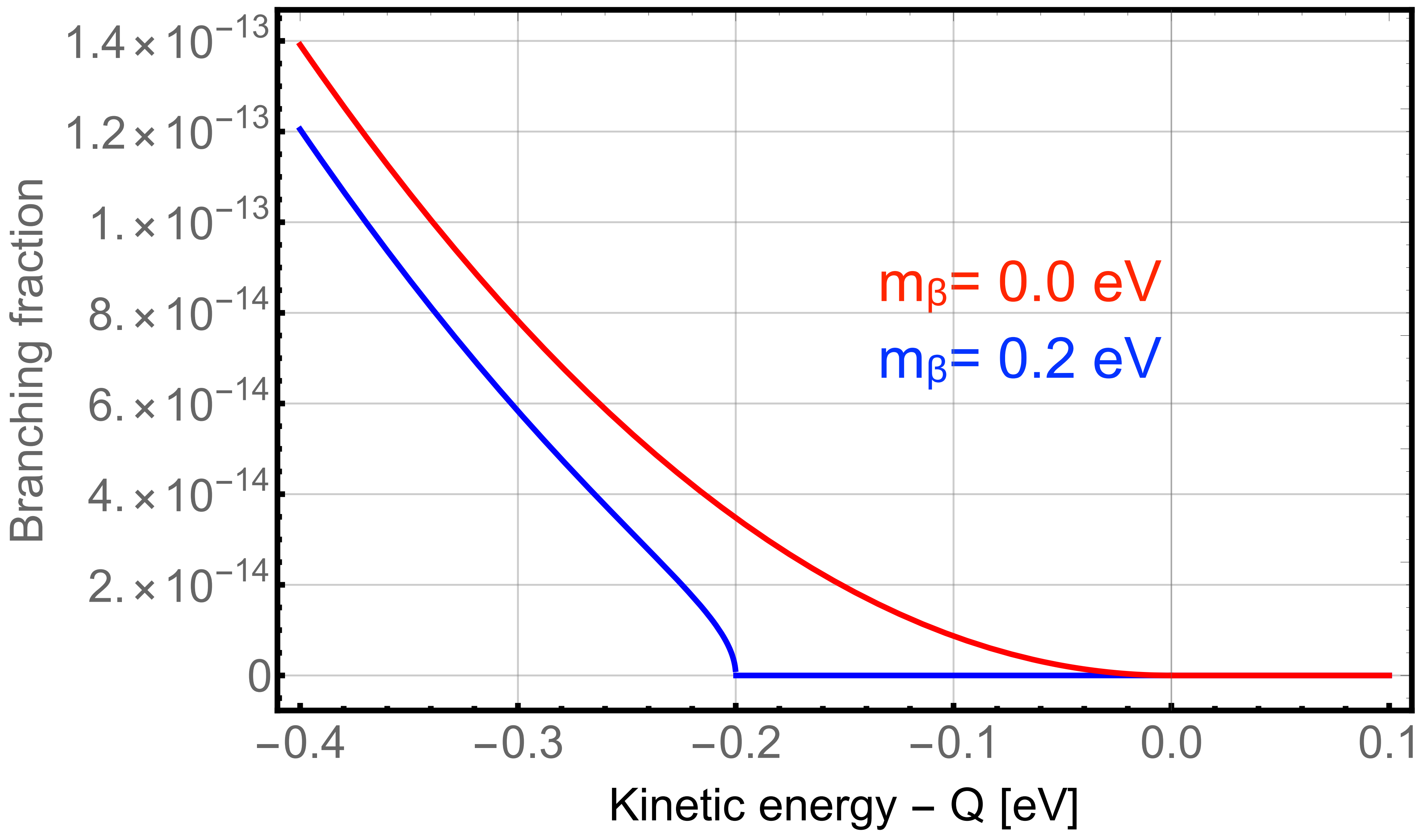

Neutrino mass from tritium β decay spectrum

With neutrino mixing and nuclear recoil for T_{nuc}:

physical constants — energy indep. matrix element

$$\frac{dN}{dE_e} = \frac{G_F^2 m_e^5 \cos^2\theta_C}{2\pi^3\hbar^7} |M_{nuc}|^2 F(Z, E_e)\, p_e (E_e + m_e) \sum_i |U_{ei}|^2 (E_{max} - E_e)$$
$$\times \sqrt{(E_{max} - E_e)^2 - m_{\nu i}^2} \cdot \Theta(E_{max} - E_e - m_{\nu i})$$

purely kinematic parameters

For unresolved neutrino mass splitting: $m(\nu_e) = \sqrt{\sum_i |U_{e,i}|^2 m_i^2}$

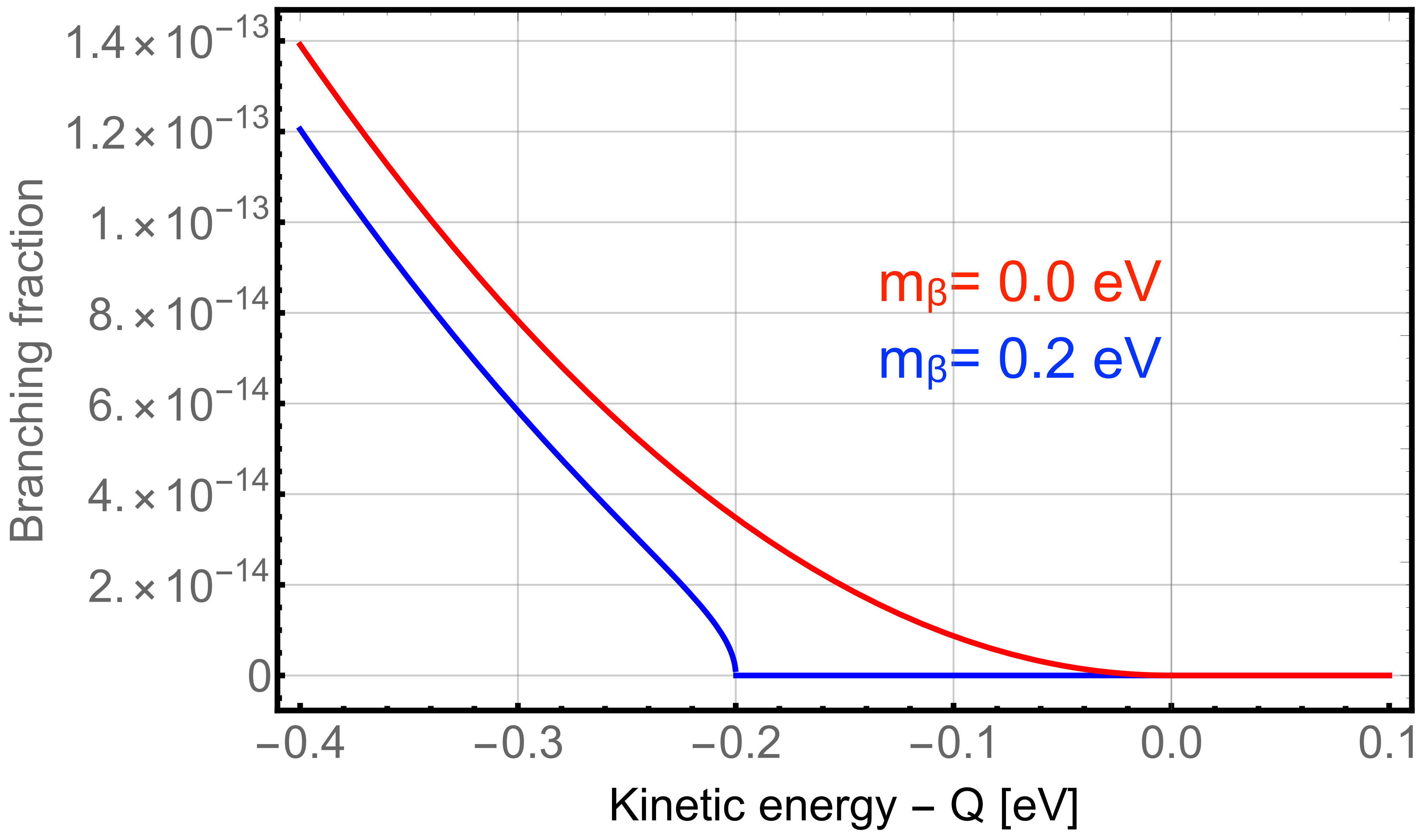

Branching fraction into endpoint region:

$$BR \approx \left(\frac{\delta E}{E_0}\right)^3$$

Neutrino mass from tritium β decay spectrum

With neutrino mixing and nuclear recoil for T_{nuc}:

physical constants — energy indep. matrix element

$$\frac{dN}{dE_e} = \frac{G_F^2 m_e^5 \cos^2\theta_C}{2\pi^3\hbar^7} |M_{nuc}|^2 F(Z, E_e)\, p_e (E_e + m_e) \sum_i |U_{ei}|^2 (E_{max} - E_e) \times \sqrt{(E_{max} - E_e)^2 - m_{\nu i}^2} \cdot \Theta(E_{max} - E_e - m_{\nu i})$$

purely kinematic parameters

For unresolved neutrino mass splitting:

$$m(\nu_e) = \sqrt{\sum_i |U_{e,i}|^2 m_i^2}$$

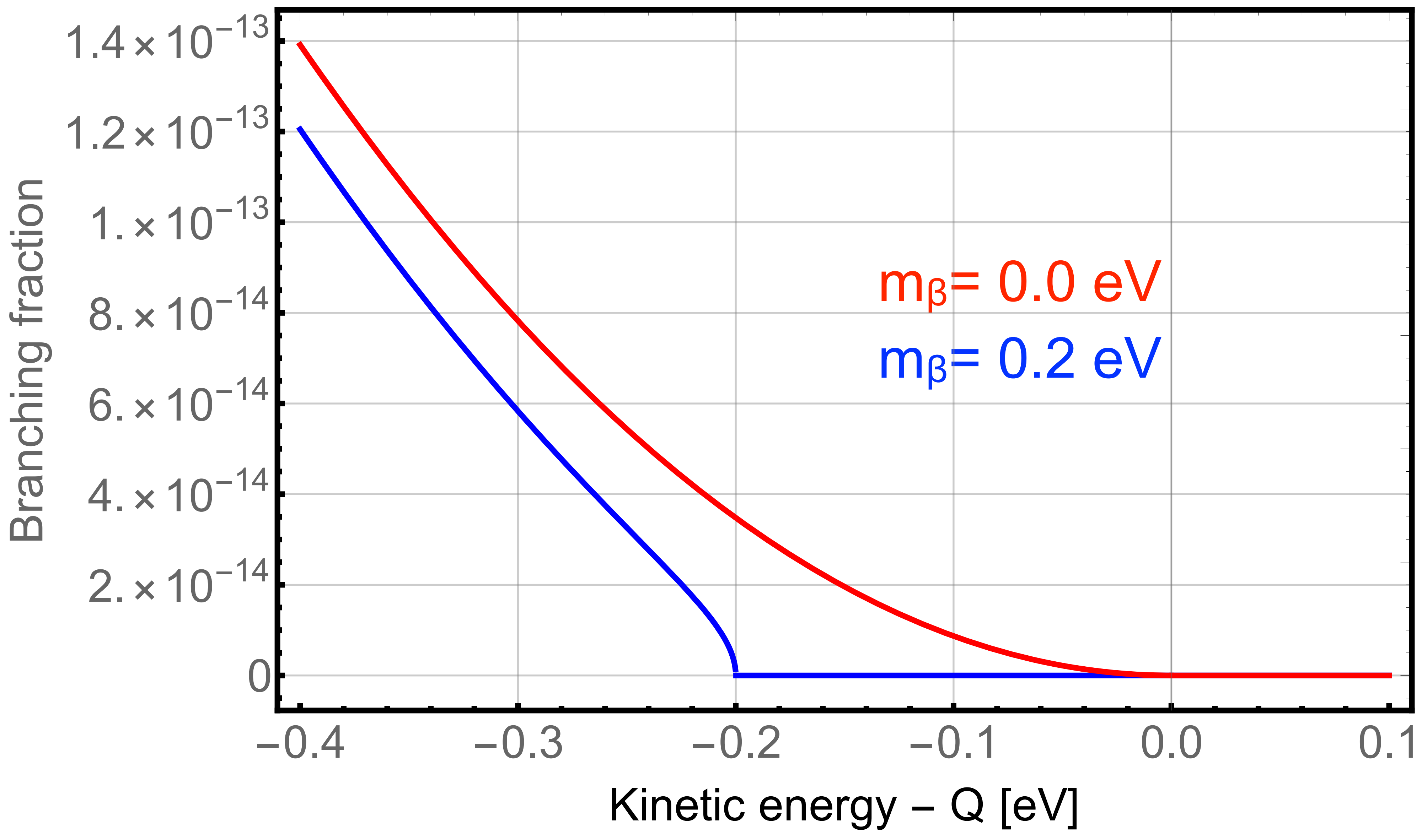

Branching fraction into endpoint region:

$$BR \approx \left(\frac{\delta E}{E_0}\right)^3$$

Tritium
E_0 (T_A) = 18.59201(7) keV
Super allowed transition
$T_{1/2}$ = 12.32 y
BR (1eV) = 2 x 10^{-13}

Myers et al, PRL 114, 013033, 2015

Neutrino mass from tritium β decay spectrum

With <u>neutrino mixing</u> and nuclear recoil for T_{nuc}:

physical constants — energy indep. matrix element

$$\frac{dN}{dE_e} = \frac{G_F^2 m_e^5 \cos^2\theta_C}{2\pi^3\hbar^7} |M_{nuc}|^2 F(Z,E_e)\, p_e (E_e + m_e) \sum_i |U_{ei}|^2 (E_{max} - E_e)$$

$$\times \sqrt{(E_{max} - E_e)^2 - m_{\nu i}^2} \cdot \Theta(E_{max} - E_e - m_{\nu i})$$

purely kinematic parameters

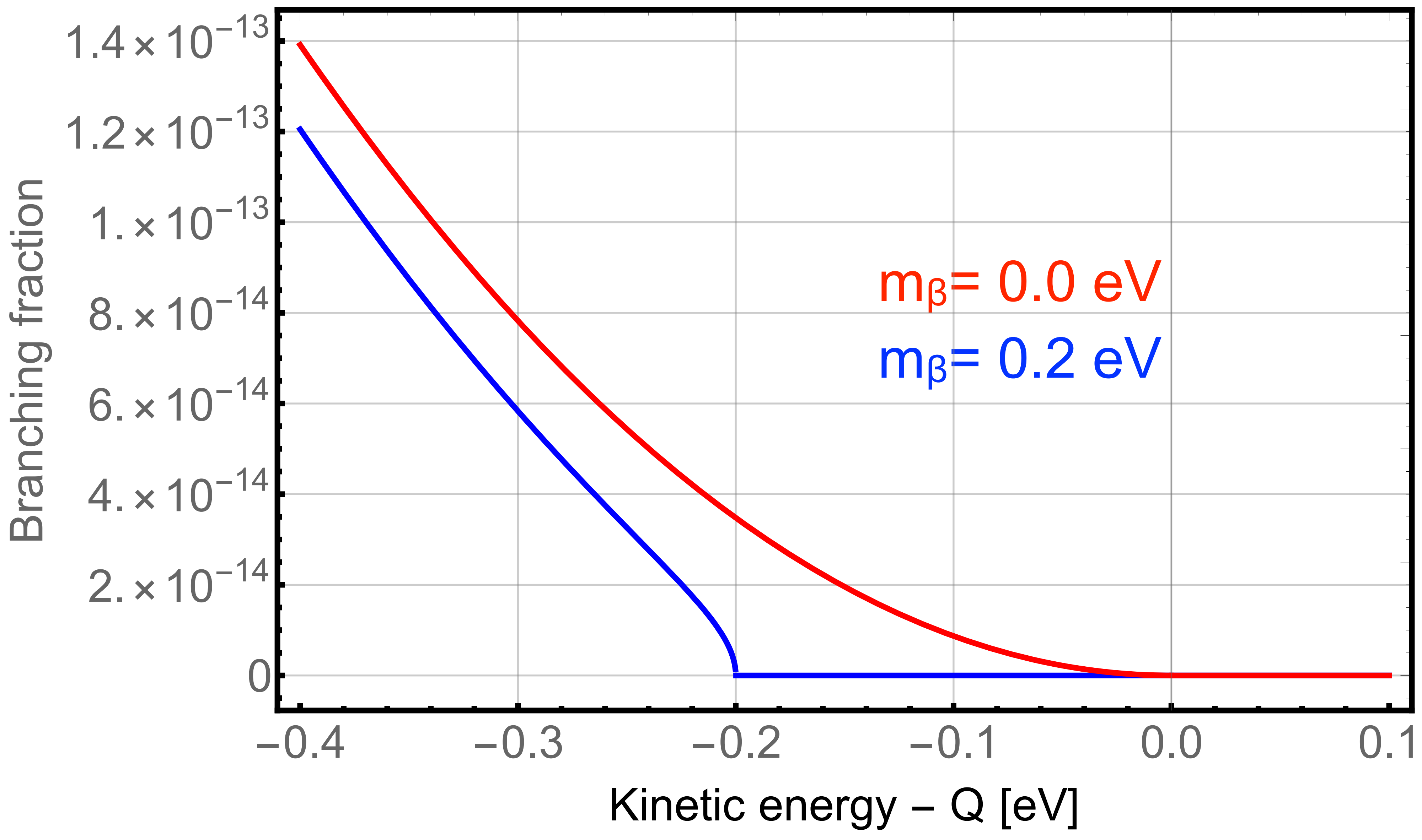

For unresolved neutrino mass splitting: $m(\nu_e) = \sqrt{\sum_i |U_{e,i}|^2 m_i^2}$

Branching fraction into endpoint region:

$$BR \approx \left(\frac{\delta E}{E_0}\right)^3$$

Tritium
E_0 (T_A) = 18.59201(7) keV
Super allowed transition
$T_{1/2}$ = 12.32 y
BR (1eV) = 2 x 10^{-13}

Myers et al, PRL 114, 013033, 2015

What we have so far:

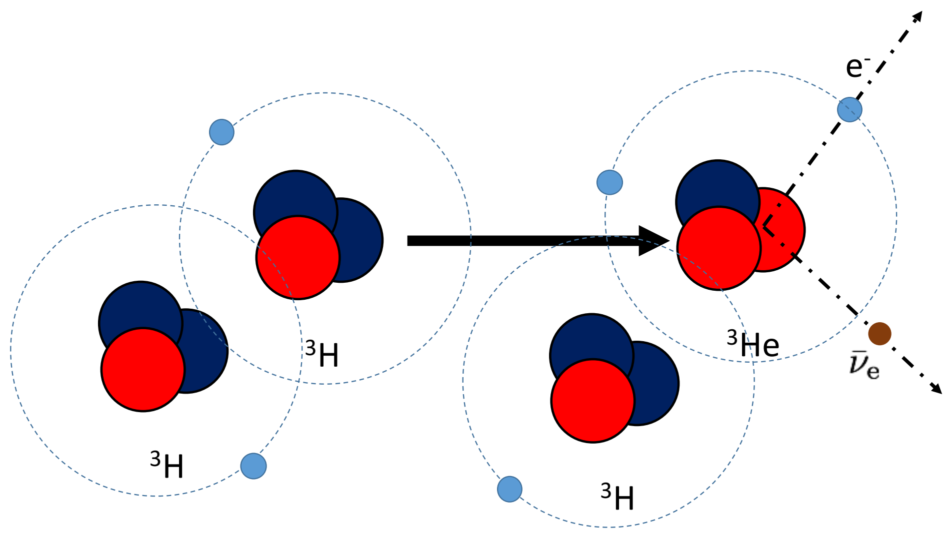

What we want:

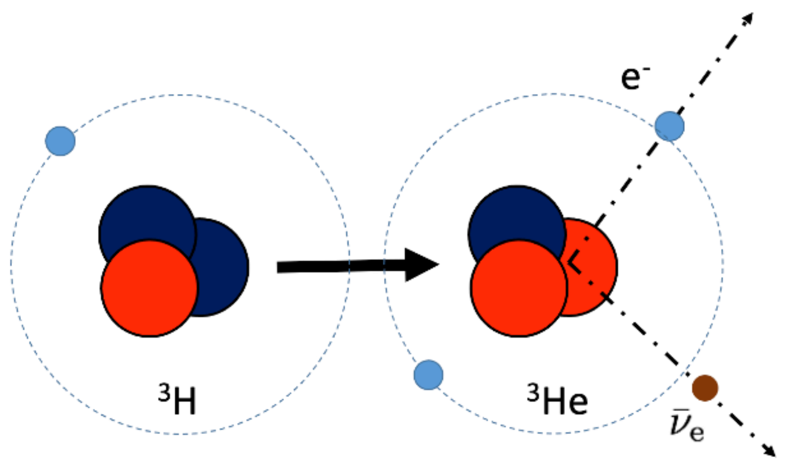

KATRIN: pushing a MAC-E filter at all boundaries to the extremes!

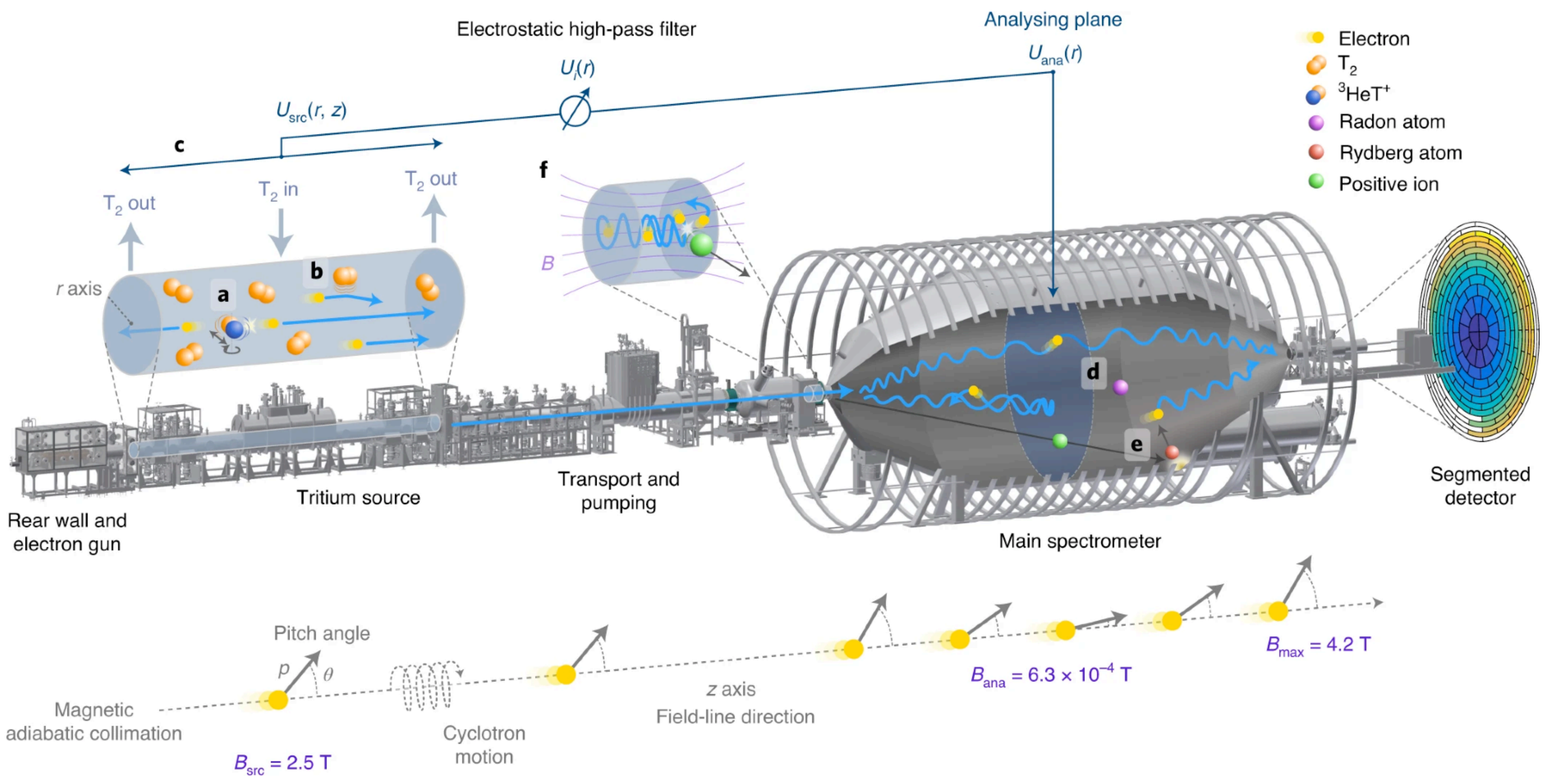

Source: Direct neutrino-mass measurement with sub-electronvolt sensitivity,
The KATRIN Collaboration, Nature Physics, volume 18, pages 160–166 (2022)

KATRIN: pushing a MAC-E filter at all boundaries to the extremes!

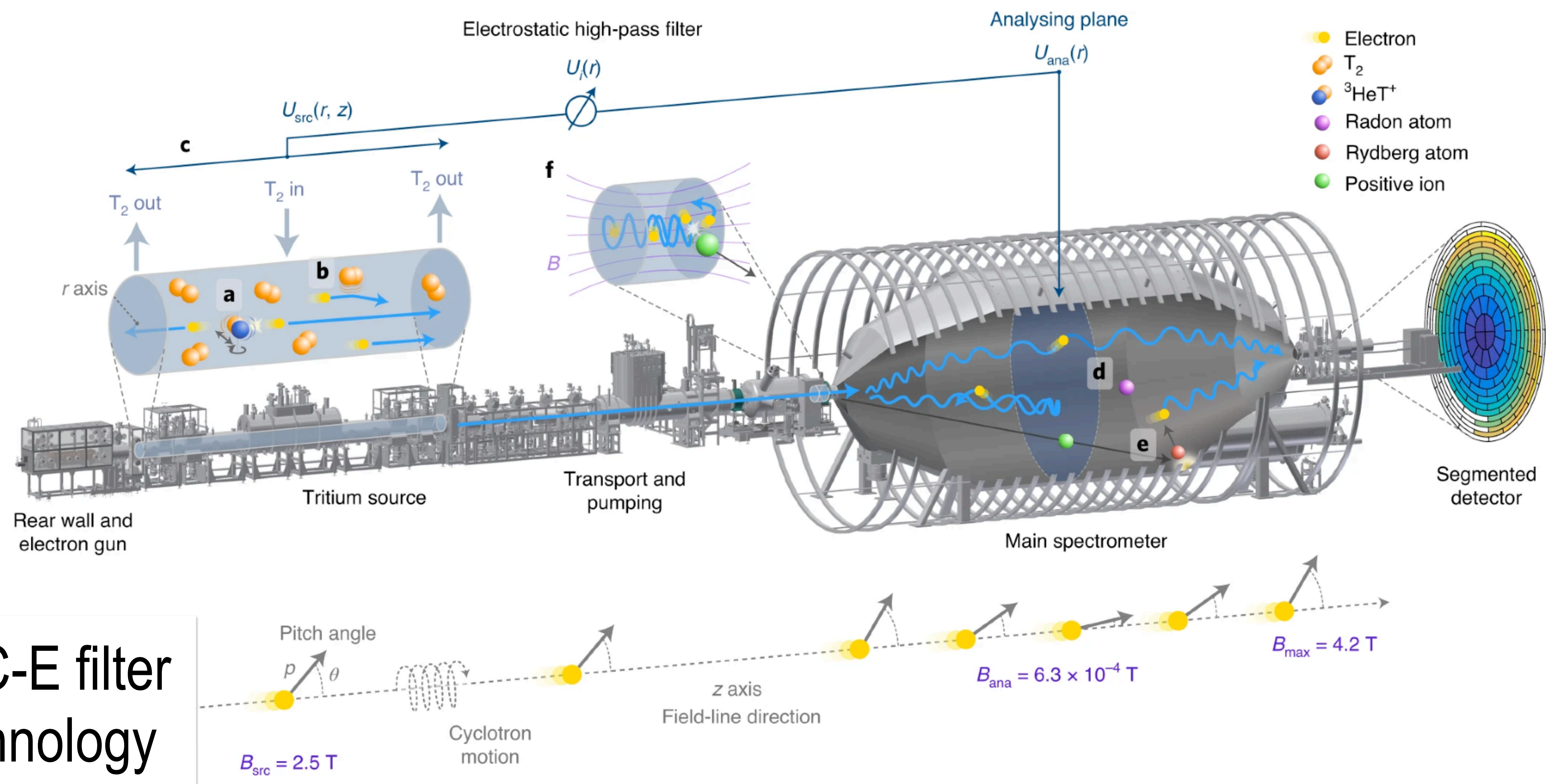

MAC-E filter technology

Source: Direct neutrino-mass measurement with sub-electronvolt sensitivity, The KATRIN Collaboration, Nature Physics, volume 18, pages 160–166 (2022)

KATRIN: pushing a MAC-E filter at all boundaries to the extremes!

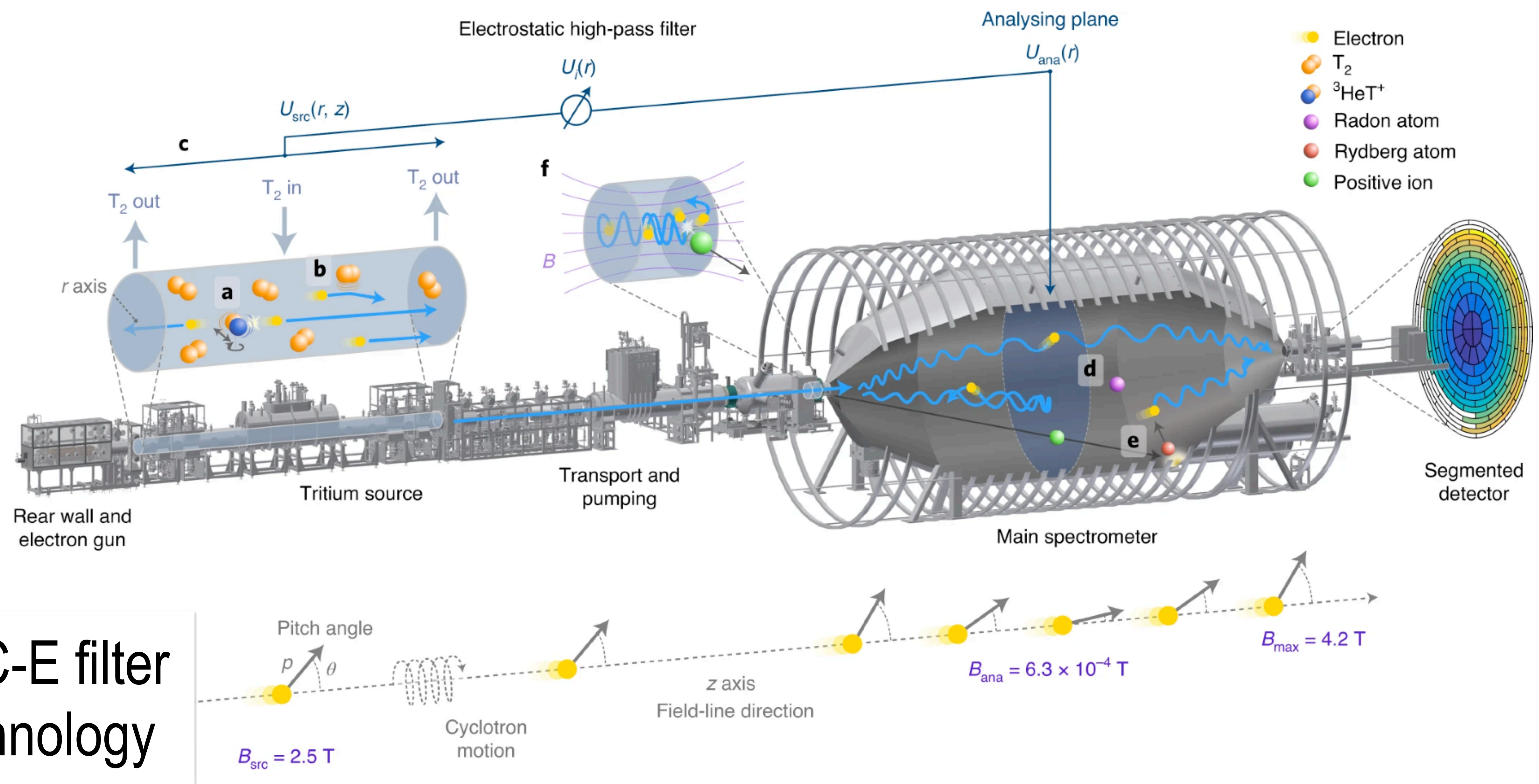

MAC-E filter technology

- Source decay rate > 10^{11} Bq
- Tritium suppression > 10^{12}
- MAC-E filter width: 0.93 eV @ 18.6 keV
- Main spectrometer at < 10^{-10} mbar
- Exquisite MC model of experiment

Source: Direct neutrino-mass measurement with sub-electronvolt sensitivity, The KATRIN Collaboration, Nature Physics, volume 18, pages 160–166 (2022)

KATRIN: pushing a MAC-E filter at all boundaries to the extremes!

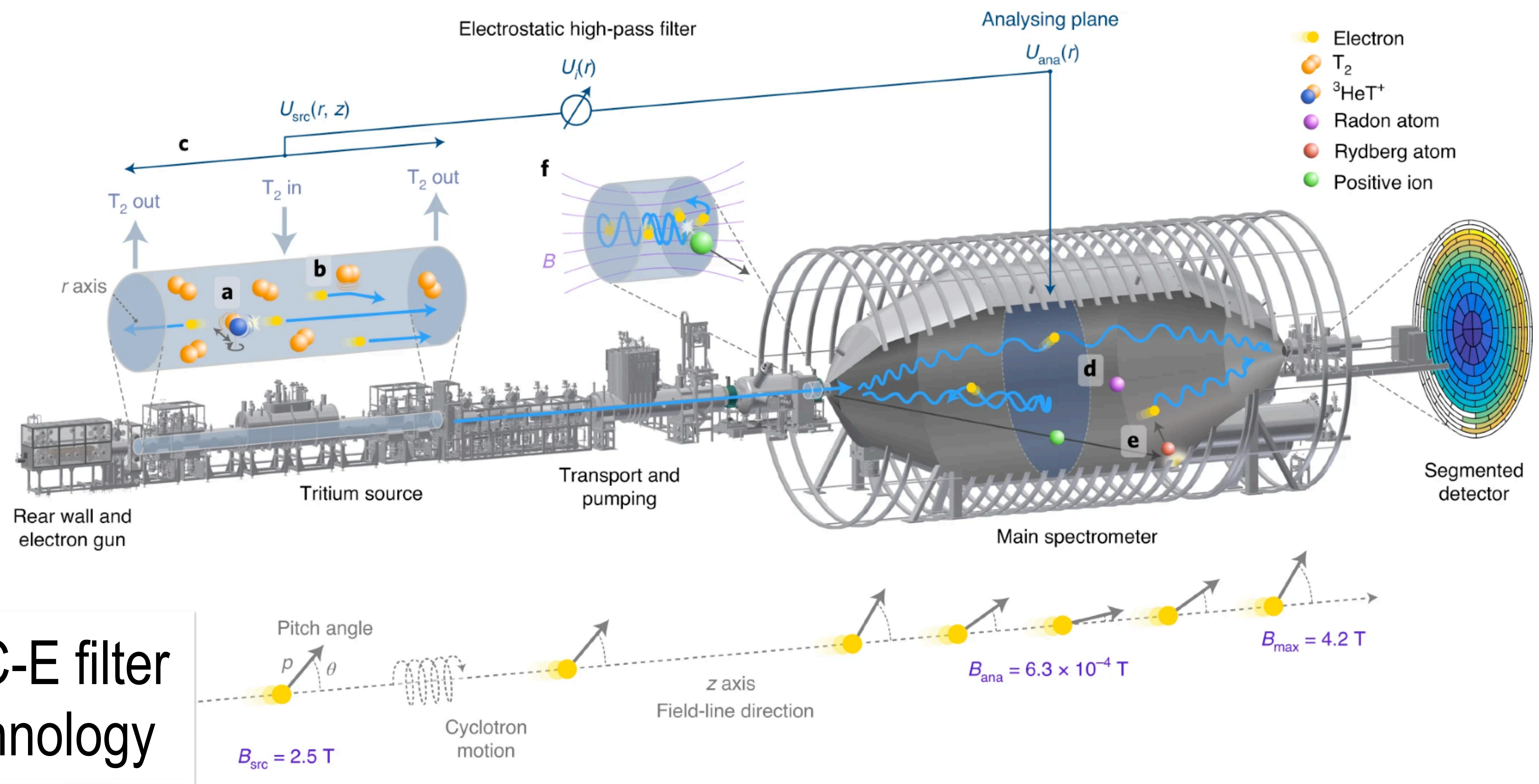

MAC-E filter technology

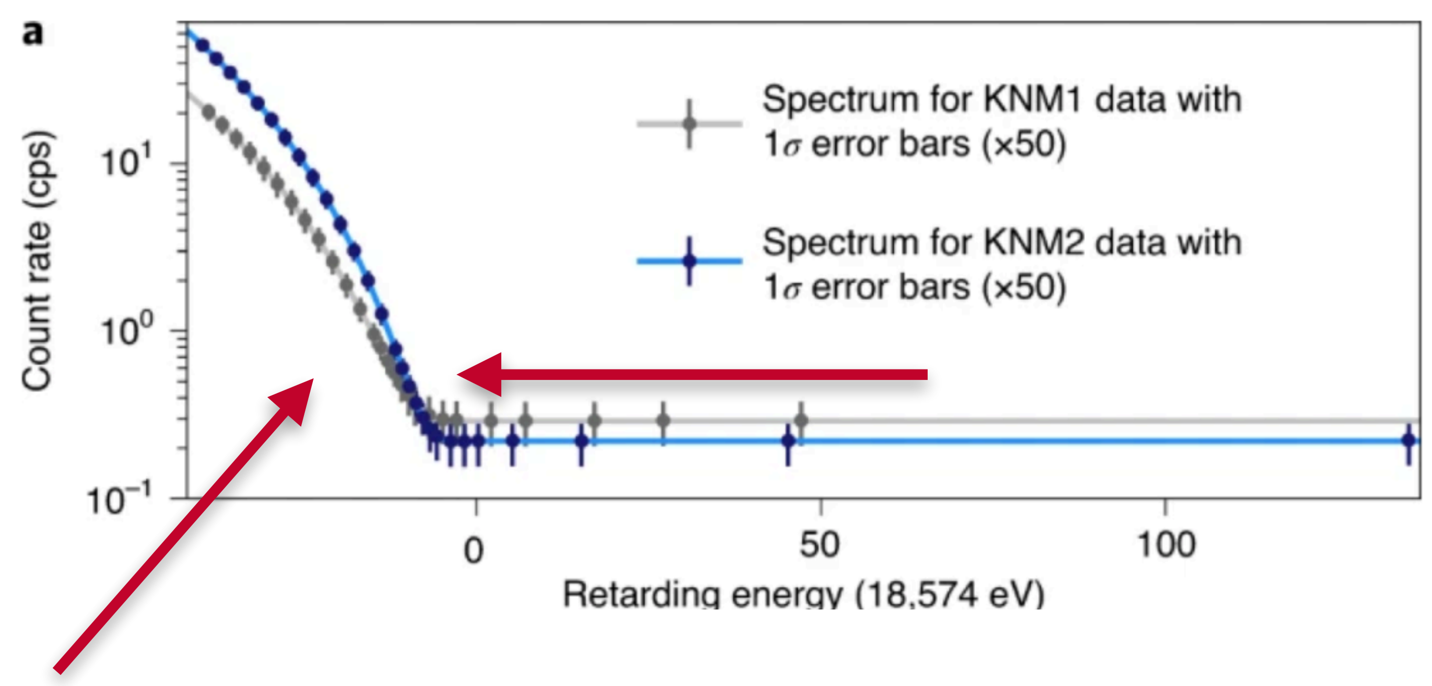

Neutrino mass signature:
change of shape and shift of endpoint

- Source decay rate > 10^{11} Bq
- Tritium suppression > 10^{12}
- MAC-E filter width: 0.93 eV @ 18.6 keV
- Main spectrometer at < 10^{-10} mbar
- Exquisite MC model of experiment

Source: Direct neutrino-mass measurement with sub-electronvolt sensitivity, The KATRIN Collaboration, Nature Physics, volume 18, pages 160–166 (2022)

KATRIN: pushing a MAC-E filter at all boundaries to the extremes!

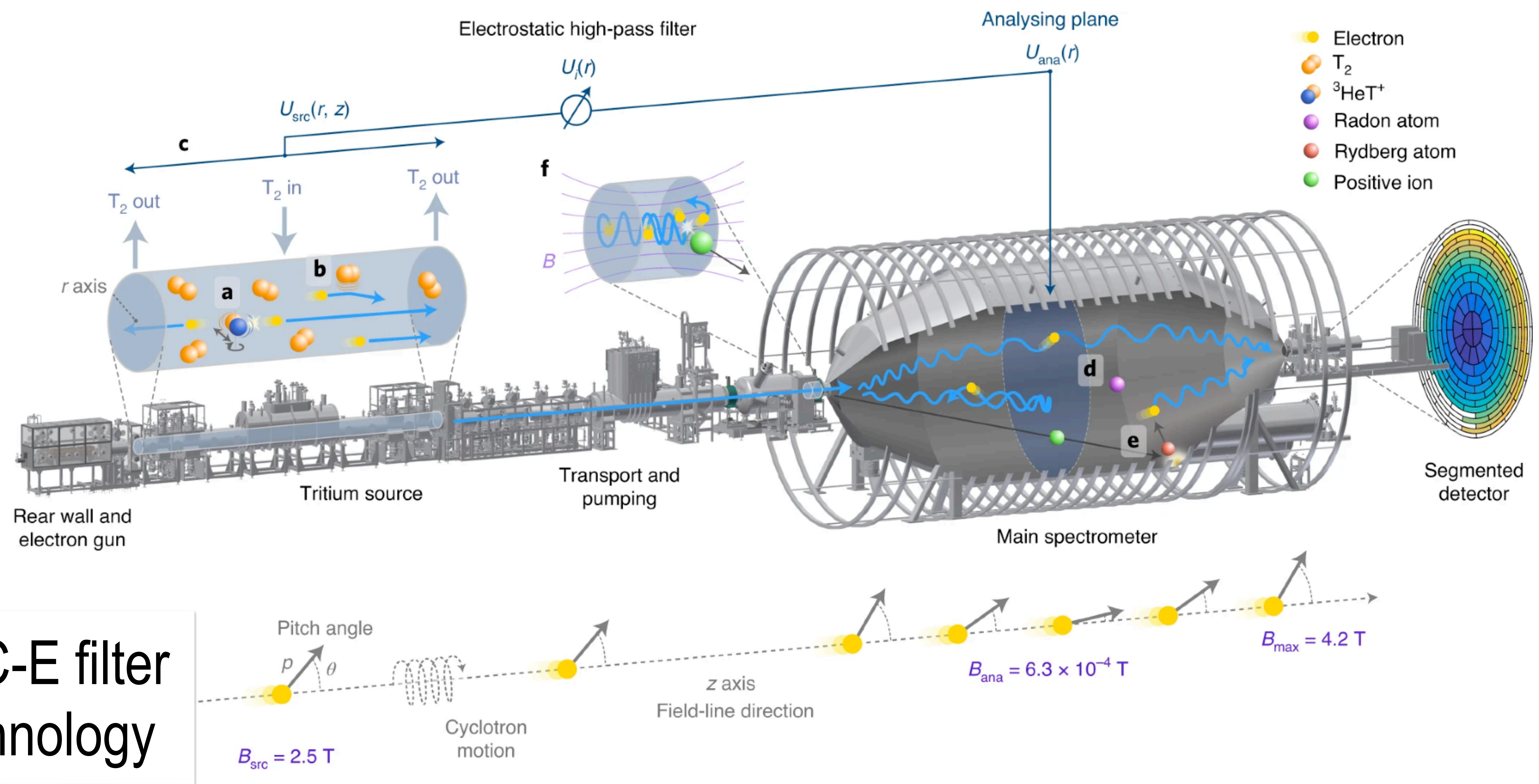

MAC-E filter technology

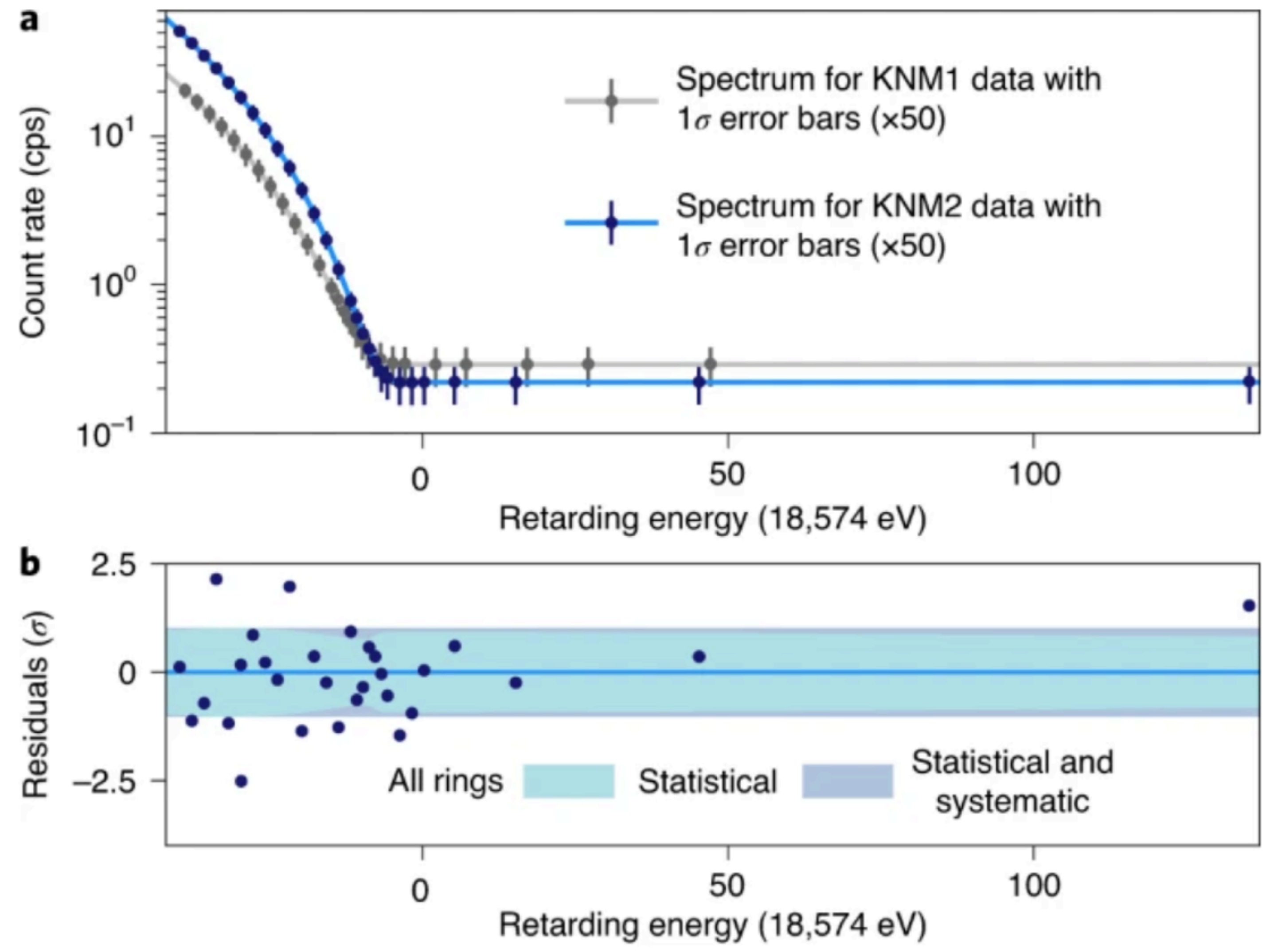

- Source decay rate > 10^{11} Bq
- Tritium suppression > 10^{12}
- MAC-E filter width: 0.93 eV @ 18.6 keV
- Main spectrometer at < 10^{-10} mbar
- Exquisite MC model of experiment

Source: Direct neutrino-mass measurement with sub-electronvolt sensitivity, The KATRIN Collaboration, Nature Physics, volume 18, pages 160–166 (2022)

KATRIN: pushing a MAC-E filter at all boundaries to the extremes!

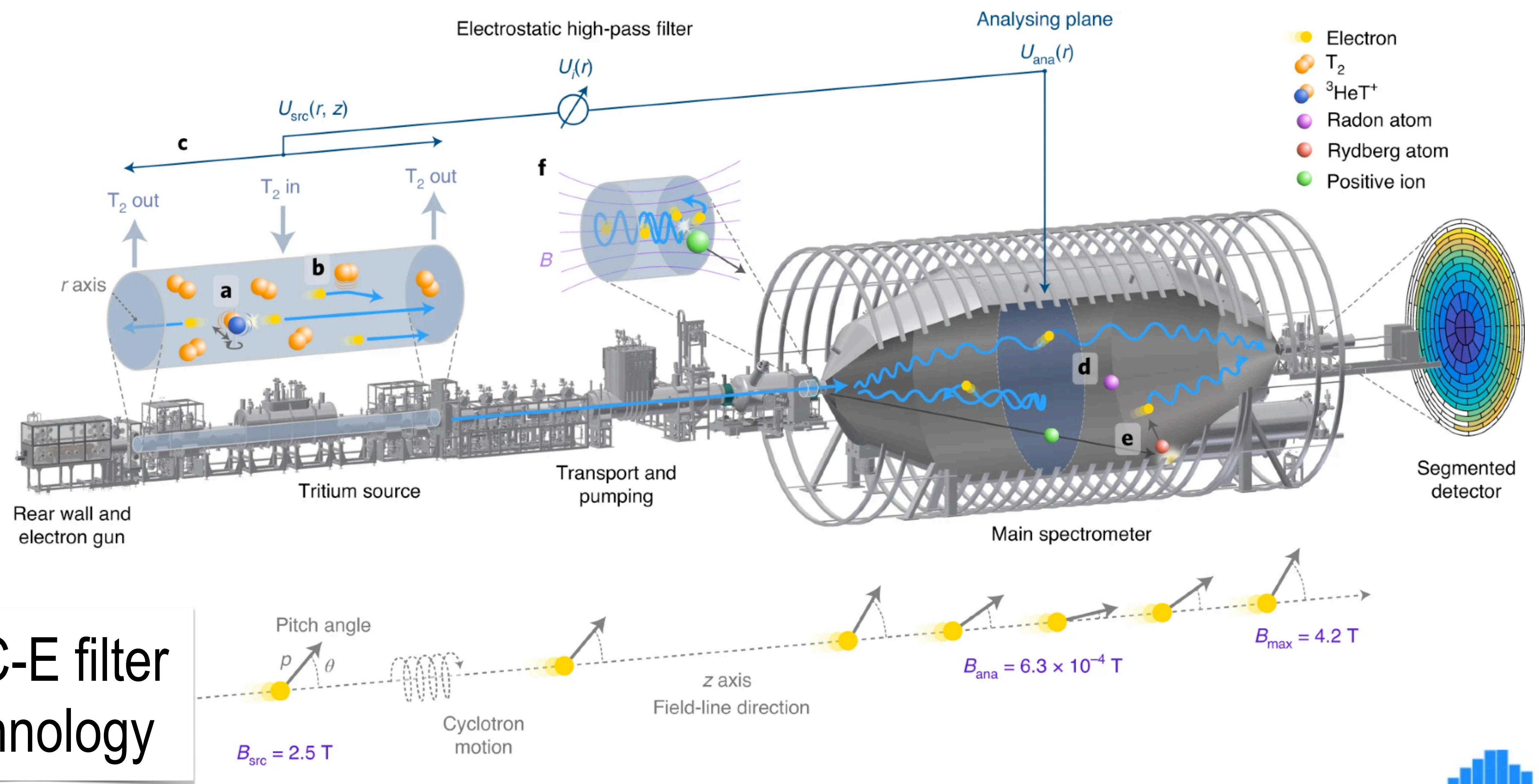

MAC-E filter technology

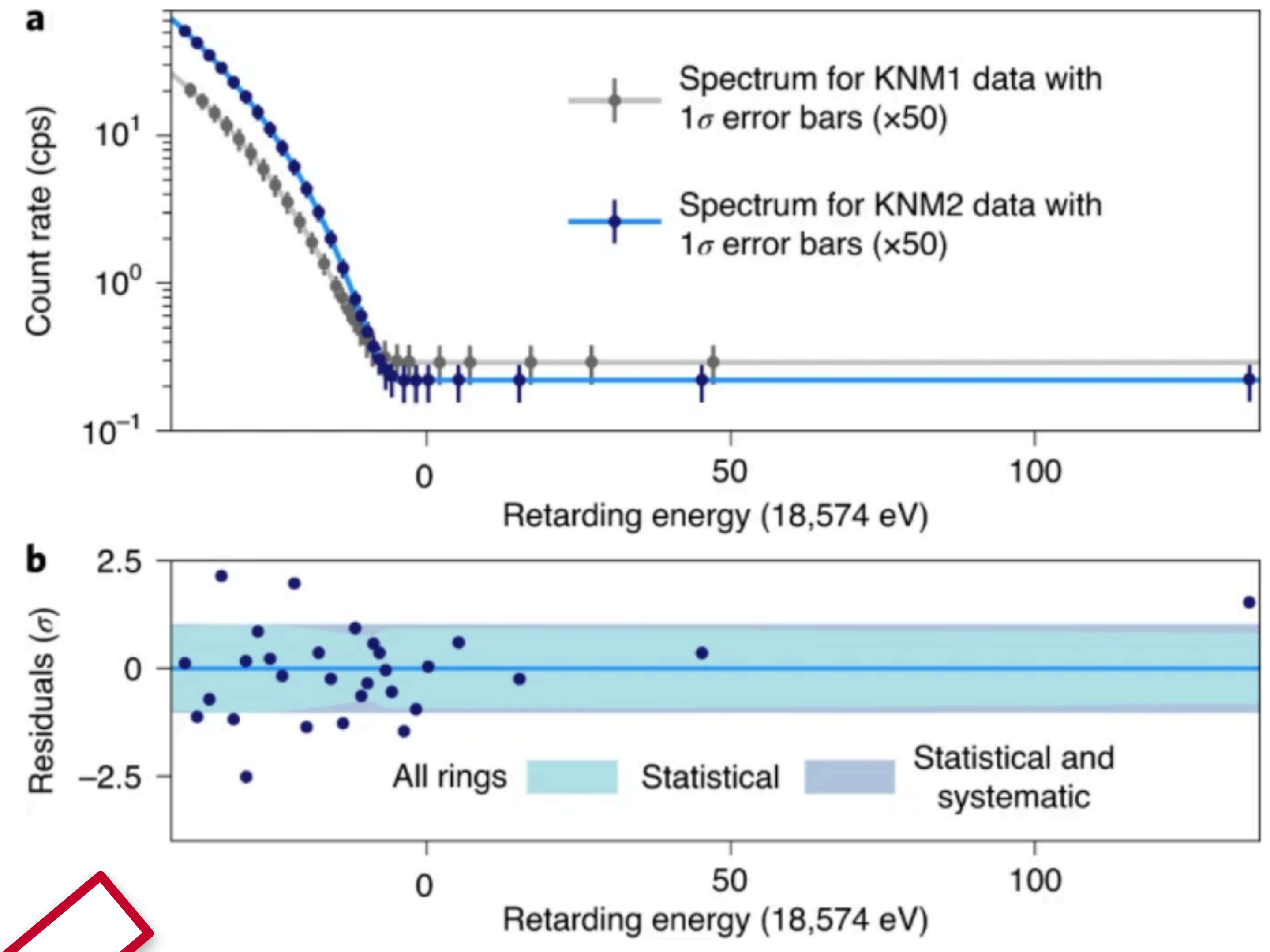

- Source decay rate > 10^{11} Bq
- Tritium suppression > 10^{12}
- MAC-E filter width: 0.93 eV @ 18.6 keV
- Main spectrometer at < 10^{-10} mbar
- Exquisite MC model of experiment

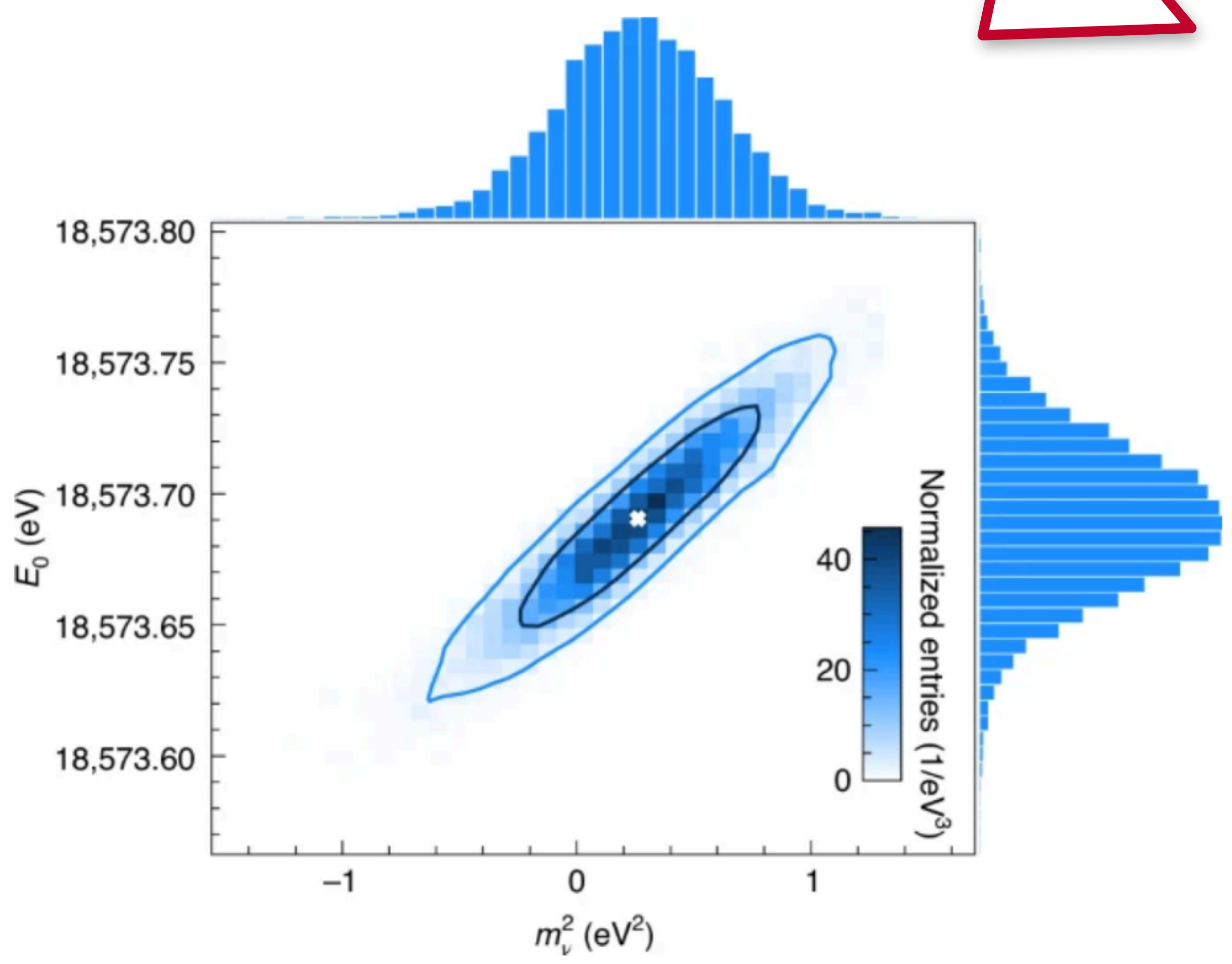

Source: Direct neutrino-mass measurement with sub-electronvolt sensitivity, The KATRIN Collaboration, Nature Physics, volume 18, pages 160–166 (2022)

KATRIN: pushing a MAC-E filter at all boundaries to the extremes!

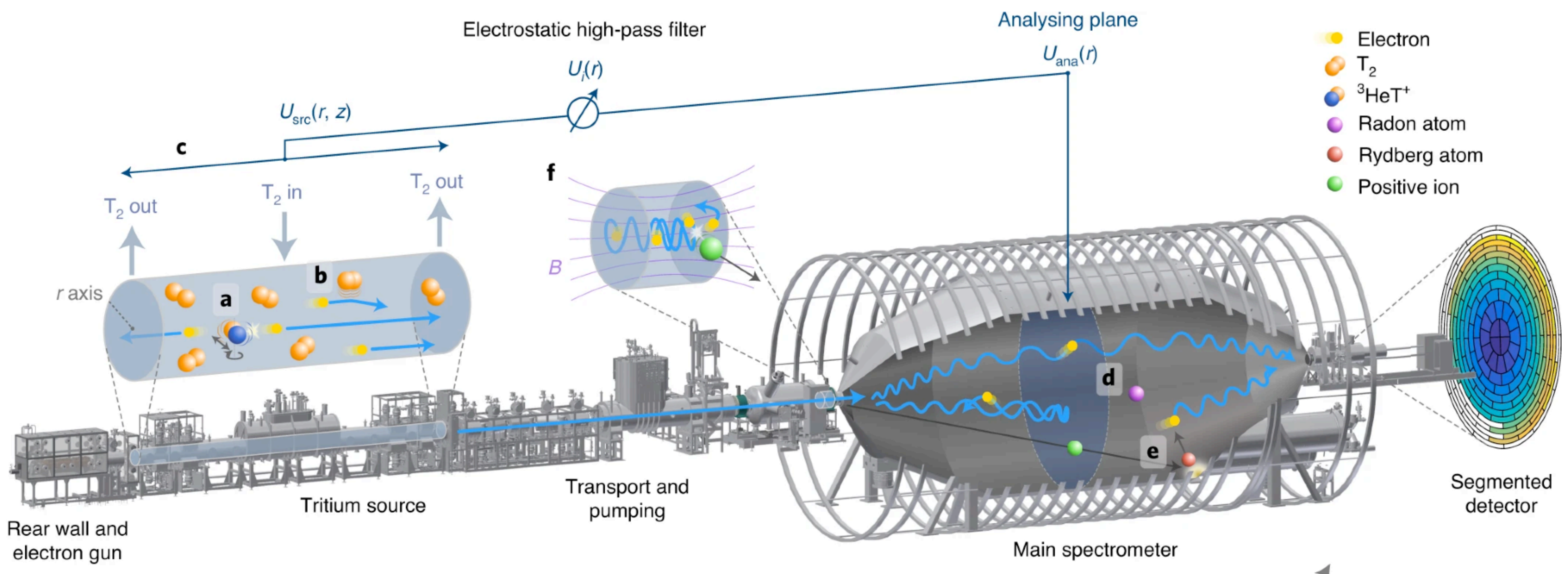

MAC-E filter technology

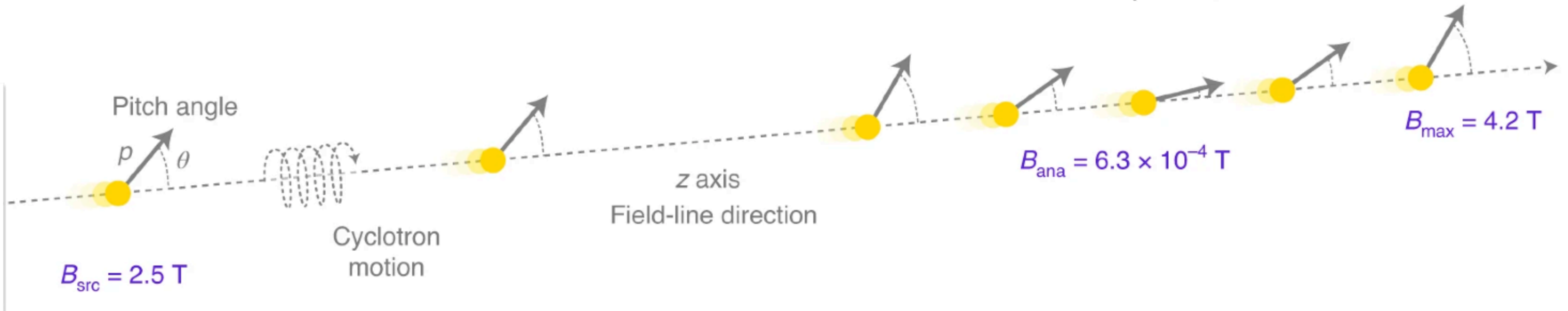

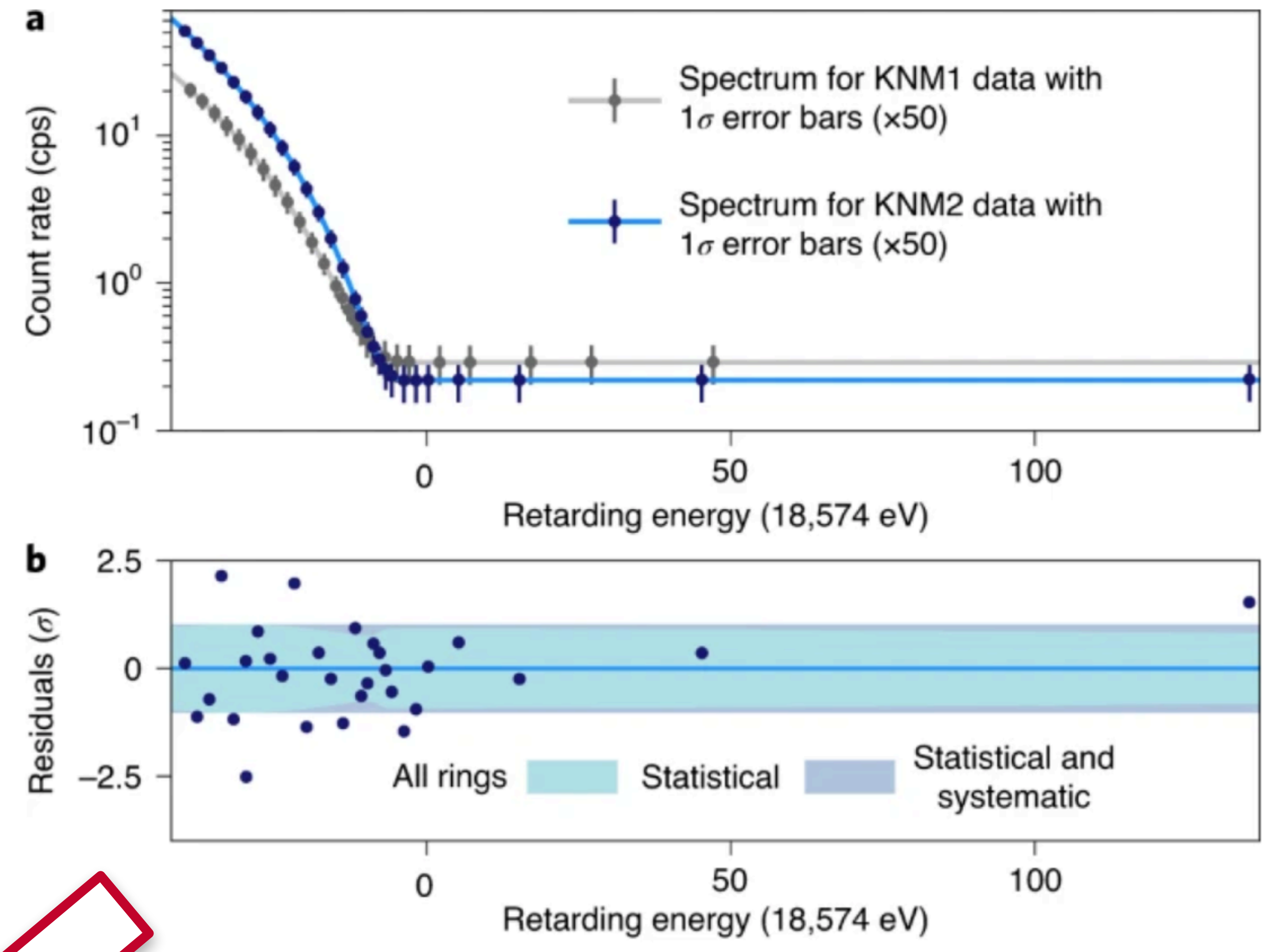

- Source decay rate > 10^{11} Bq
- Tritium suppression > 10^{12}
- MAC-E filter width: 0.93 eV @ 18.6 keV
- Main spectrometer at < 10^{-10} mbar
- Exquisite MC model of experiment

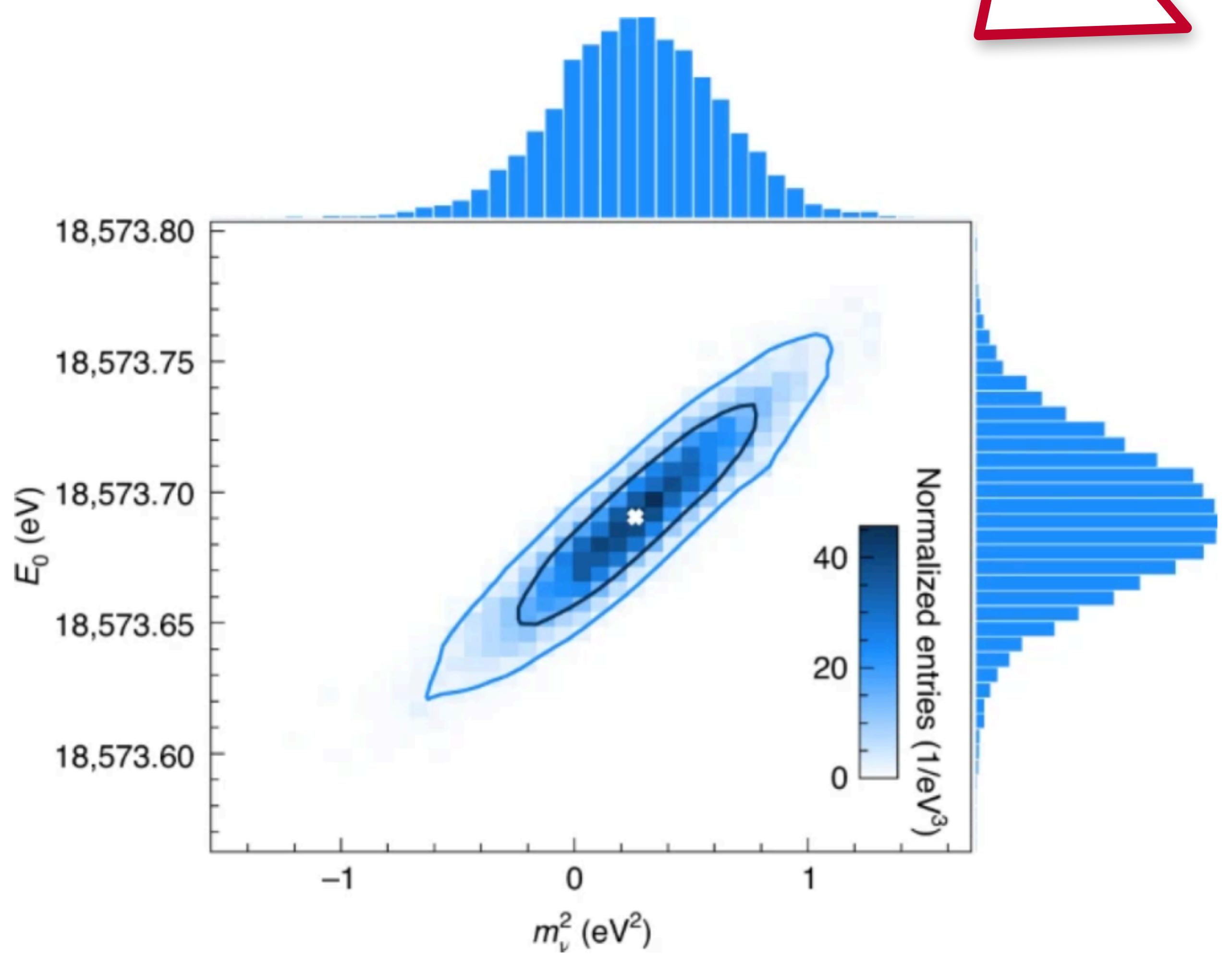

Best upper limit on neutrino mass
$$m_\nu < 0.8\,\mathrm{eV/c^2}\text{ at }90\,\%\,\mathrm{CL}$$

Anticipated sensitivity:
$$m_\nu < 0.2\,\mathrm{eV/c^2}\text{ at }90\,\%\,\mathrm{CL}$$

Source: Direct neutrino-mass measurement with sub-electronvolt sensitivity, The KATRIN Collaboration, Nature Physics, volume 18, pages 160–166 (2022)

The challenges to higher mass sensitivity: systematics and statistics

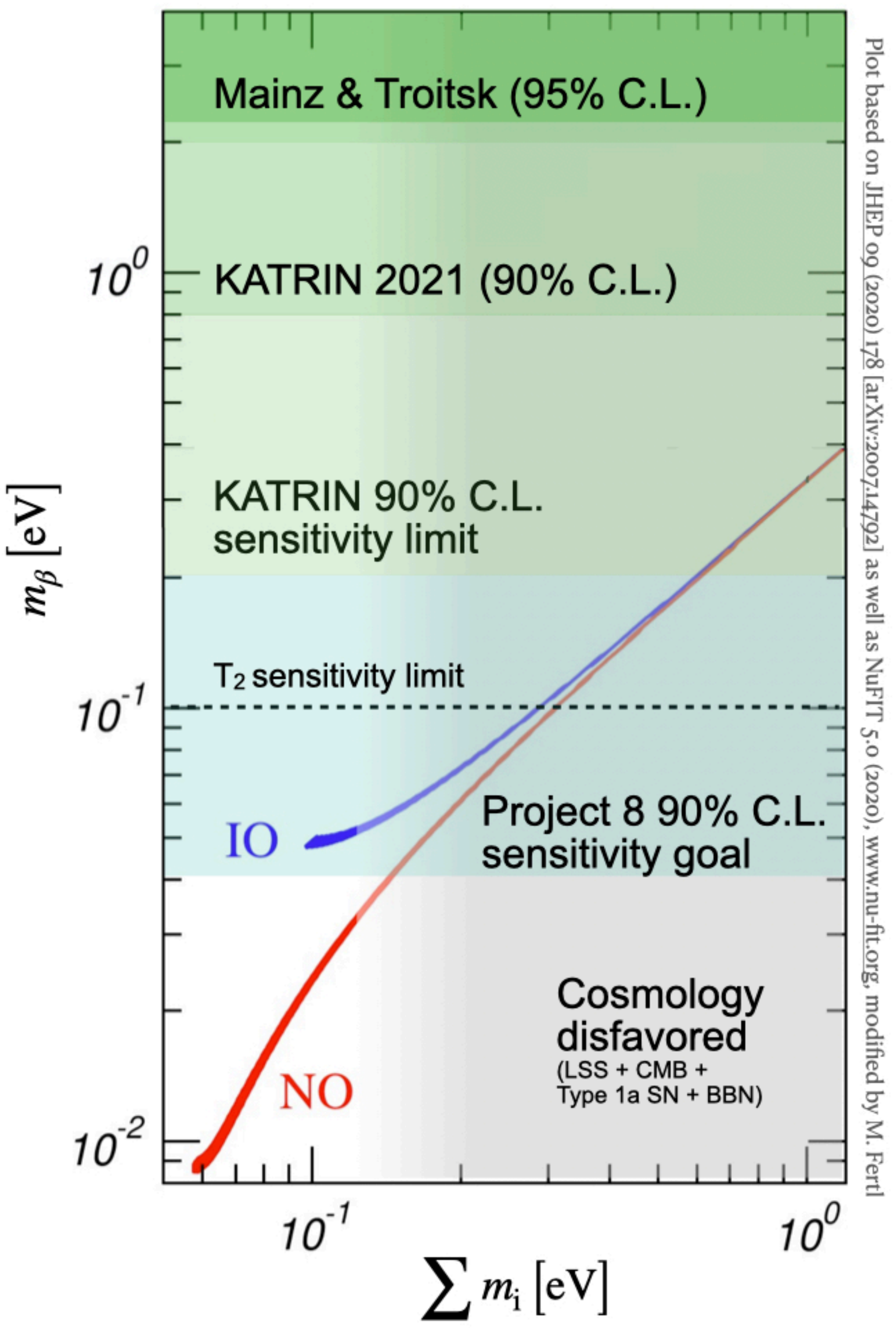

The challenges to higher mass sensitivity: systematics and statistics

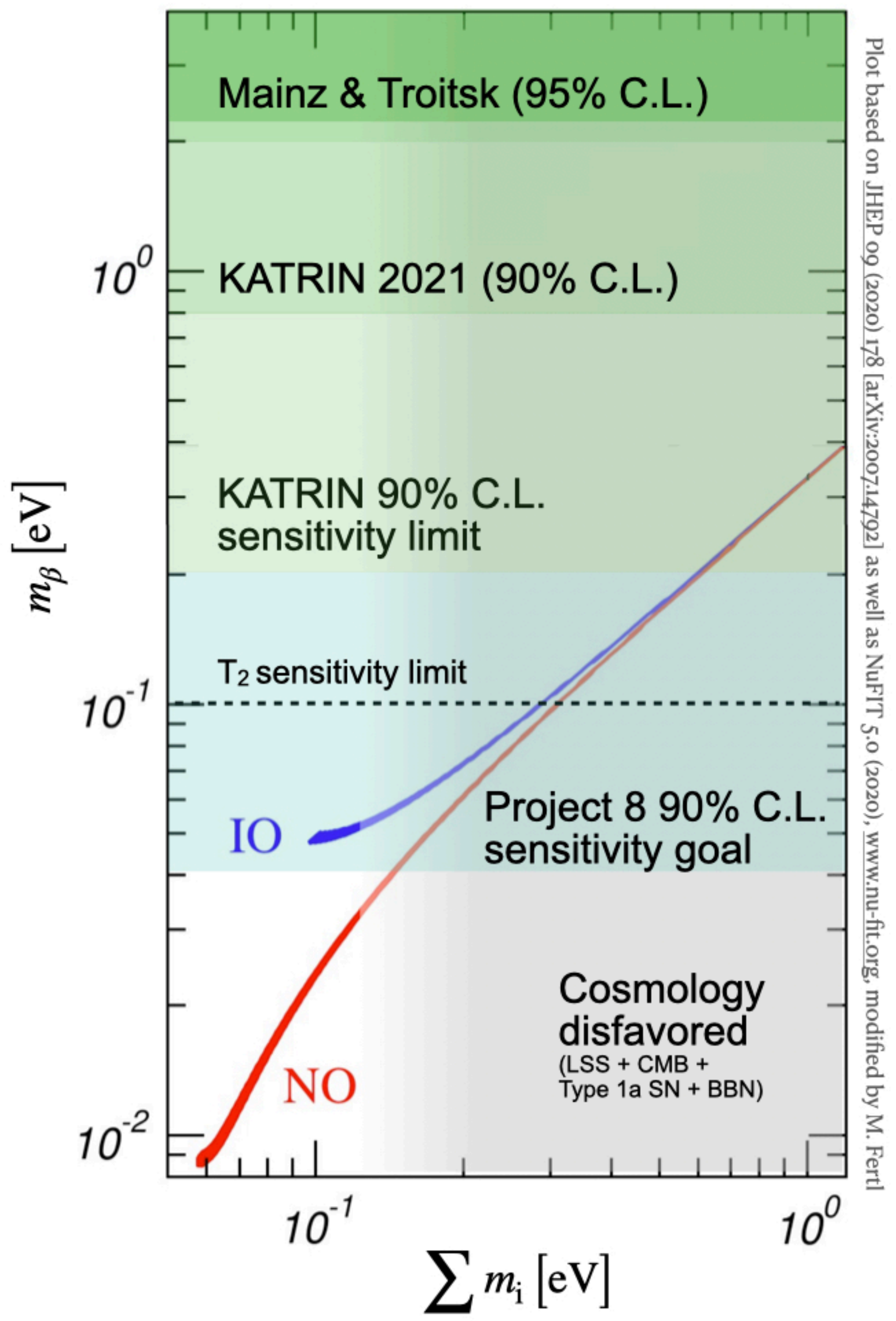

- MAC-E filter resolution scales with inverse area of analysis plane ($\vec{\nabla} \cdot \vec{B} = 0$!) Can't build a larger vacuum tank!

The challenges to higher mass sensitivity: systematics <u>and</u> statistics

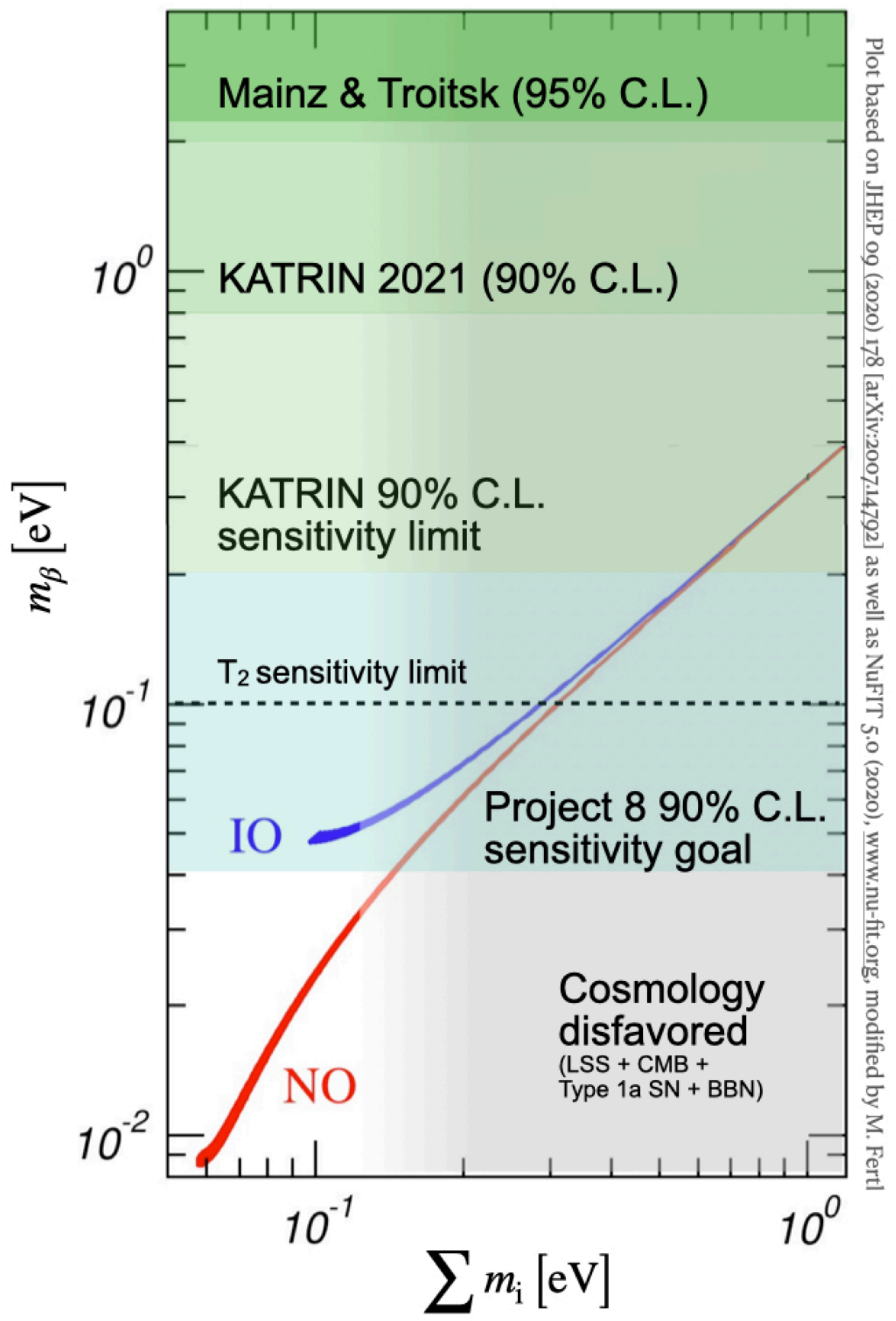

- MAC-E filter resolution scales with inverse area of analysis plane ($\vec{\nabla} \cdot \vec{B} = 0!$) Can't build a larger vacuum tank!
- Already at max. T_2 column density and length: inelastic scattering!

The challenges to higher mass sensitivity: systematics and statistics

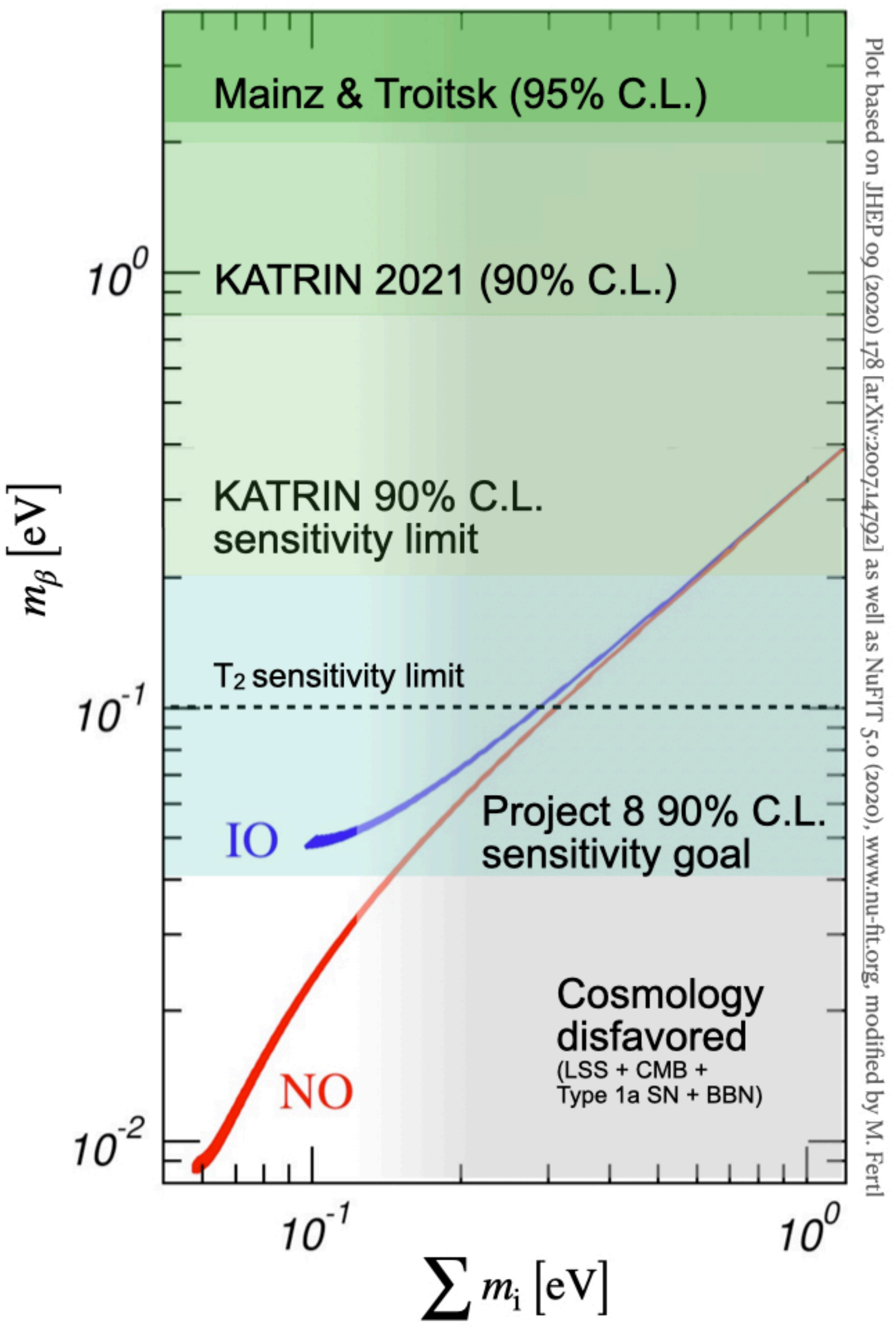

- MAC-E filter resolution scales with inverse area of analysis plane ($\vec{\nabla} \cdot \vec{B} = 0$!)
  Can't build a larger vacuum tank!
- Already at max. T_2 column density and length: inelastic scattering!
- Integrating MAC-E filter spectrometer → Stepping of retardation voltage, slow, stability!
- Intrinsic final state distribution of $^3HeT^+$ molecular ion causes smearing of decay endpoint

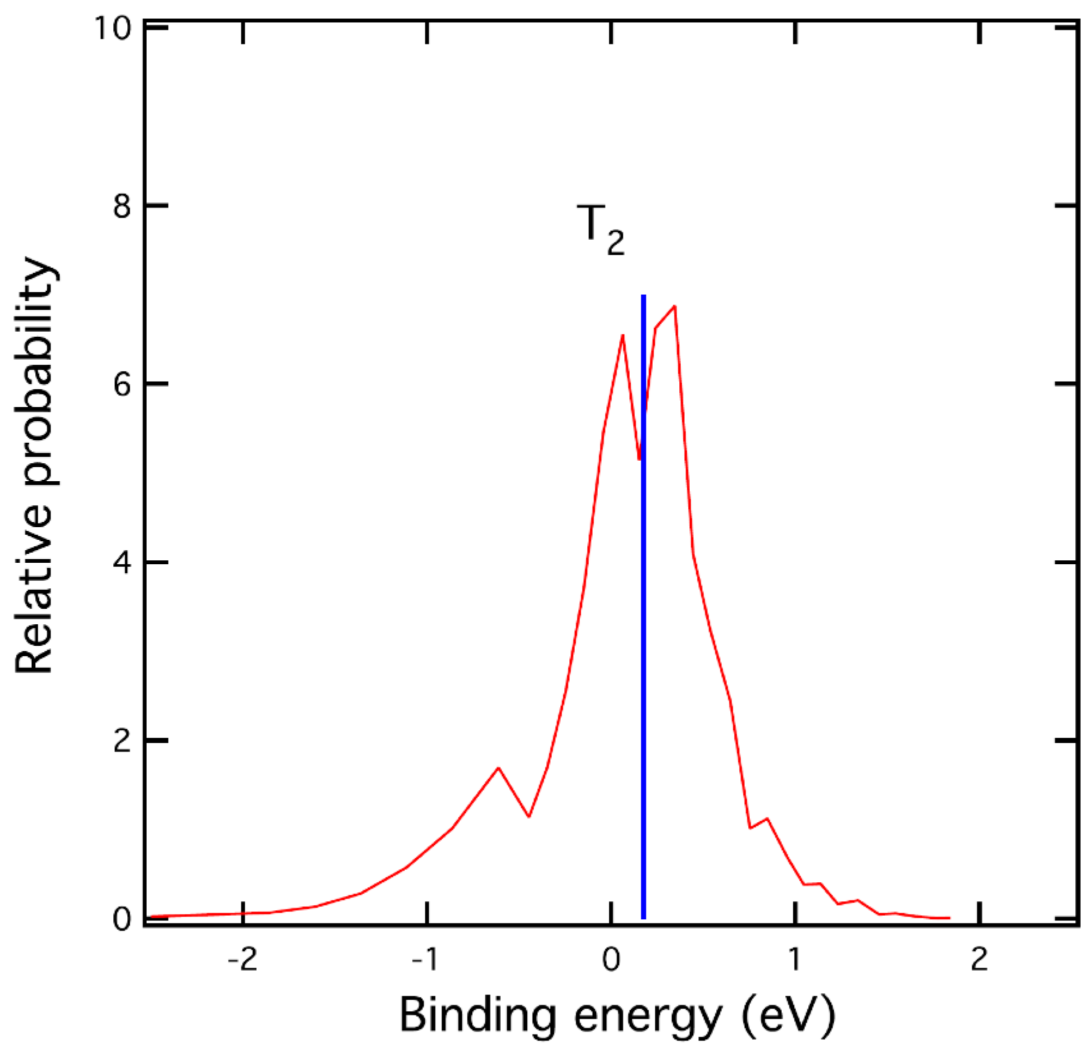

L. Bodine, et al, Phys. Rev. C 91, 035505 , 2015

The challenges to higher mass sensitivity: systematics and statistics

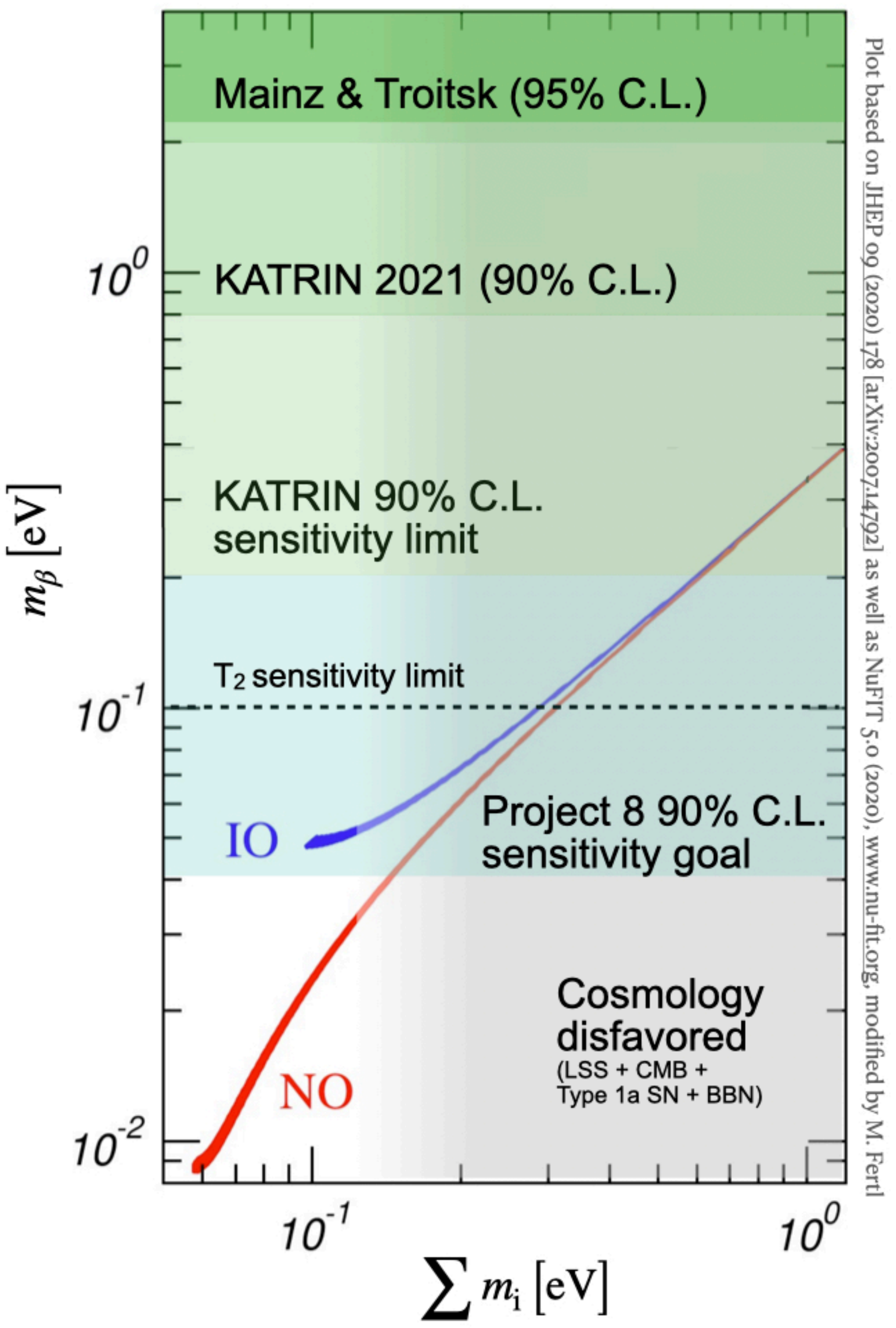

- MAC-E filter resolution scales with inverse area of analysis plane ($\vec{\nabla} \cdot \vec{B} = 0$!)
  Can't build a larger vacuum tank!
- Already at max. T_2 column density and length: inelastic scattering!
- Integrating MAC-E filter spectrometer → Stepping of retardation voltage, slow, stability!
- Intrinsic final state distribution of $^3HeT^+$ molecular ion causes smearing of decay endpoint

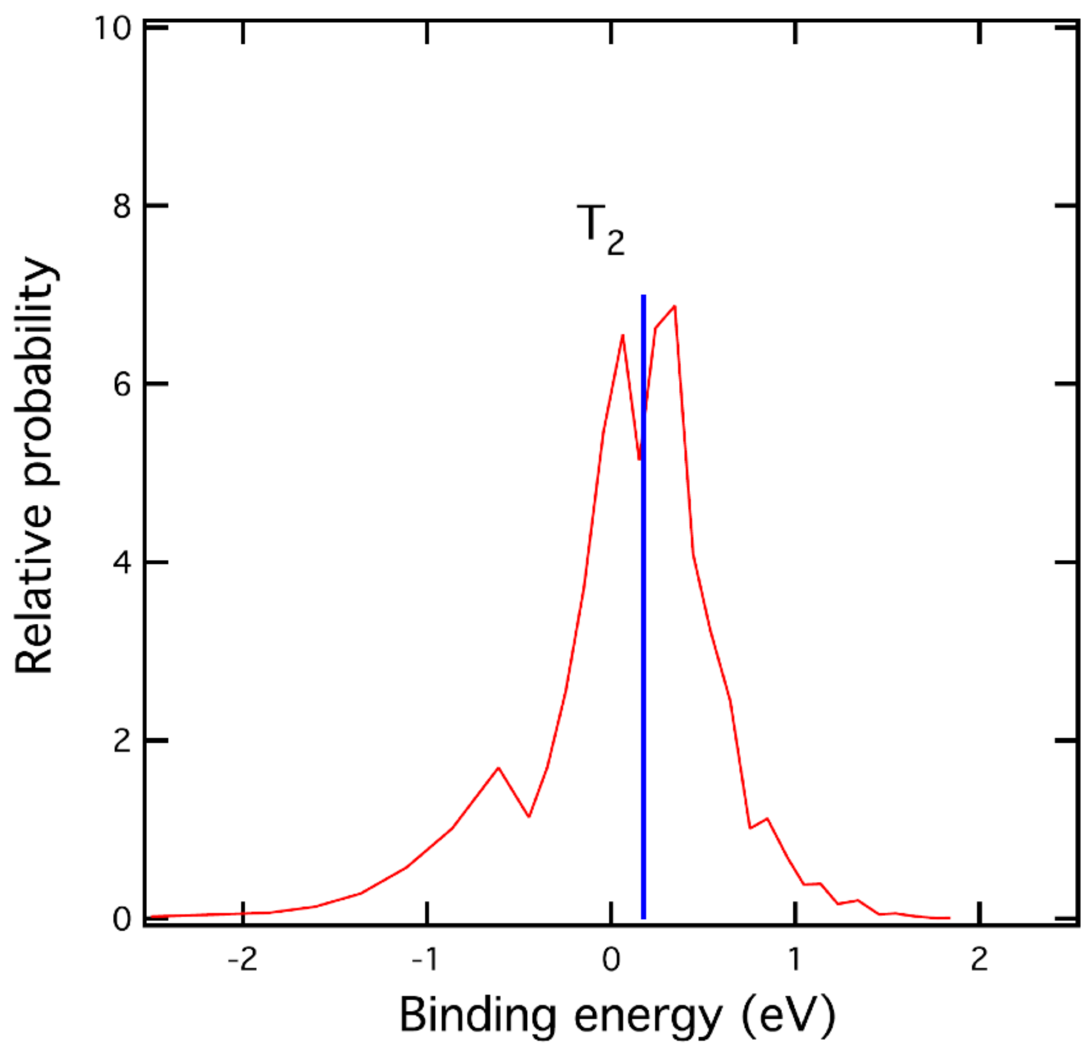

L. Bodine, et al, Phys. Rev. C 91, 035505 , 2015

Project 8

A frequency-based approach towards the measurement of the neutrino mass using ultra cold atomic tritium with 40 meV/c² sensitivity

Project 8: Cyclotron radiation emission spectroscopy of $T_{(2)}$

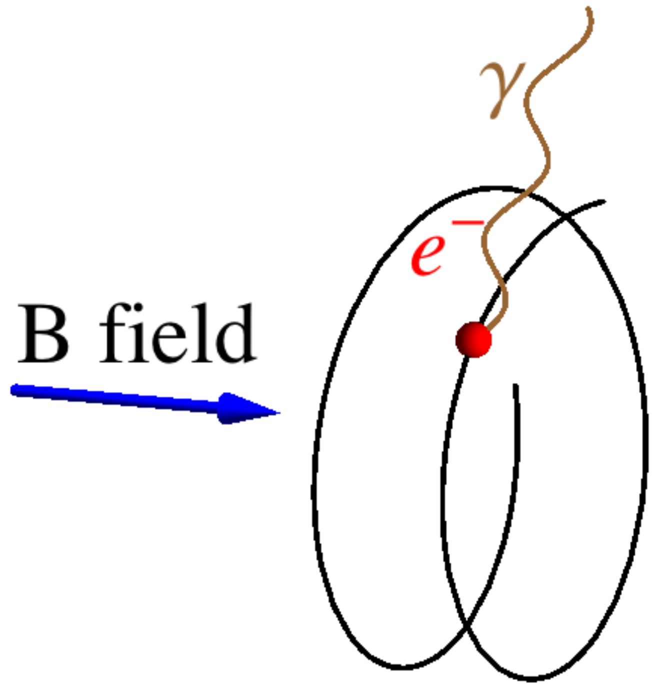

Project 8: Cyclotron radiation emission spectroscopy of $T_{(2)}$

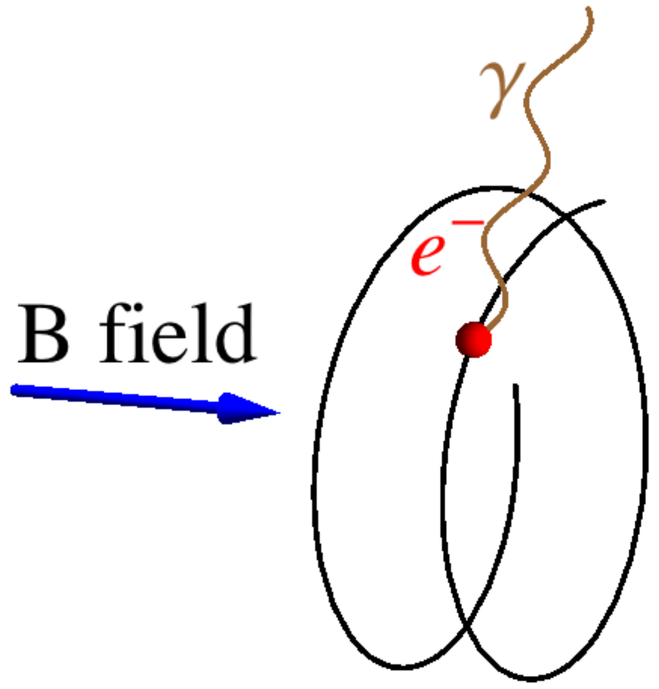

Novel approach: J. Formaggio and B. Monreal, Phys. Rev D 80:051301 (2009)

- Cyclotron radiation from single electrons
- Source transparent to microwave radiation
- No e⁻ transport from source to detector
- Highly precise frequency measurement

$$f_c = \frac{f_{c,0}}{\gamma} = \frac{1}{2\pi} \frac{eB}{m_e + E_{kin}/c^2}$$

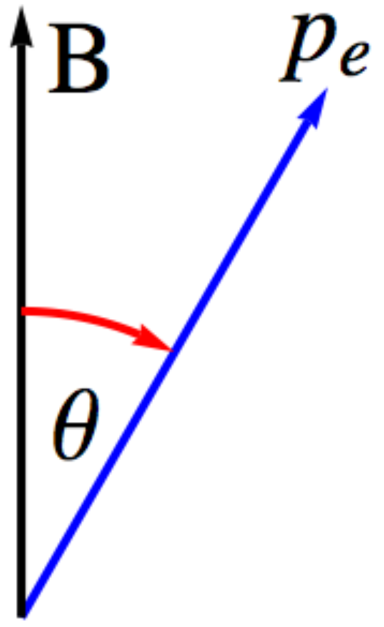

Project 8: Cyclotron radiation emission spectroscopy of T(2)

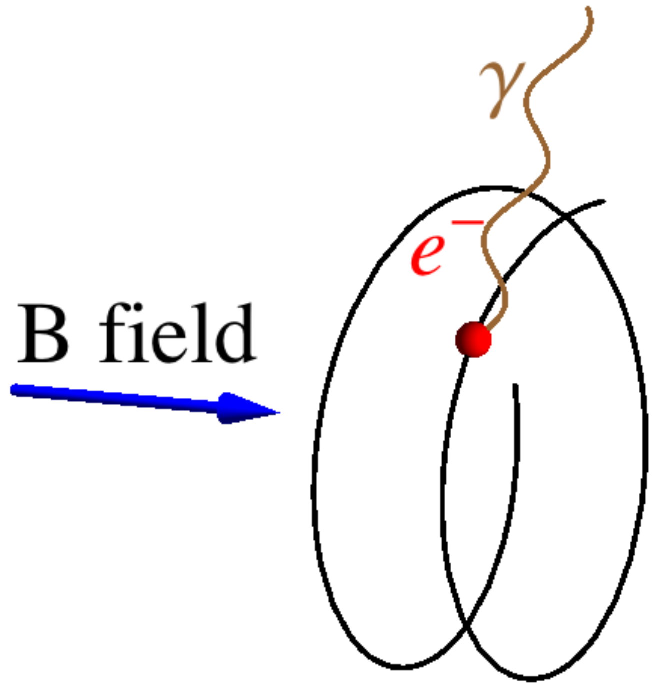

Novel approach: J. Formaggio and B. Monreal, Phys. Rev D 80:051301 (2009)

- Cyclotron radiation from single electrons
- Source transparent to microwave radiation
- No e- transport from source to detector
- Highly precise frequency measurement

$$f_c = \frac{f_{c,0}}{\gamma} = \frac{1}{2\pi} \frac{eB}{m_e + E_{kin}/c^2}$$

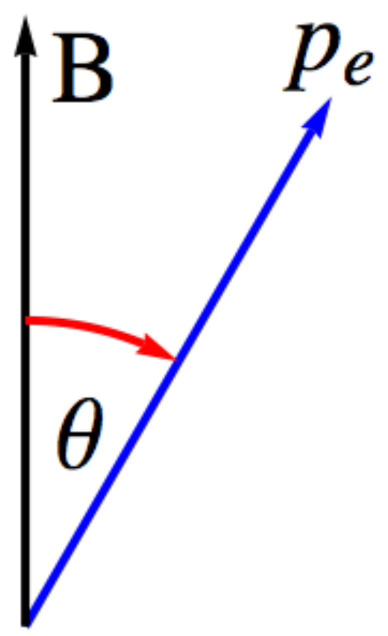

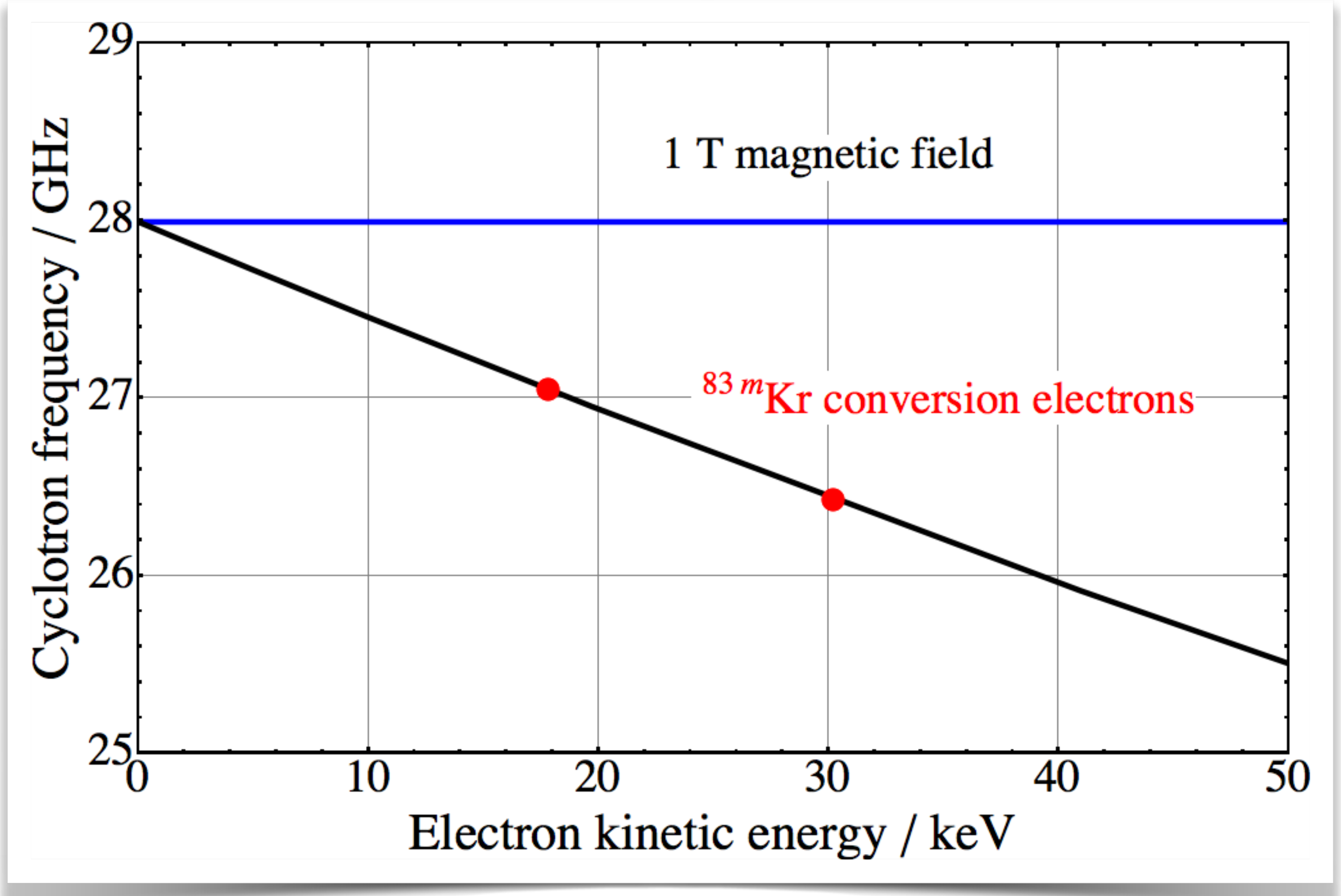

Project 8: Cyclotron radiation emission spectroscopy of $T_{(2)}$

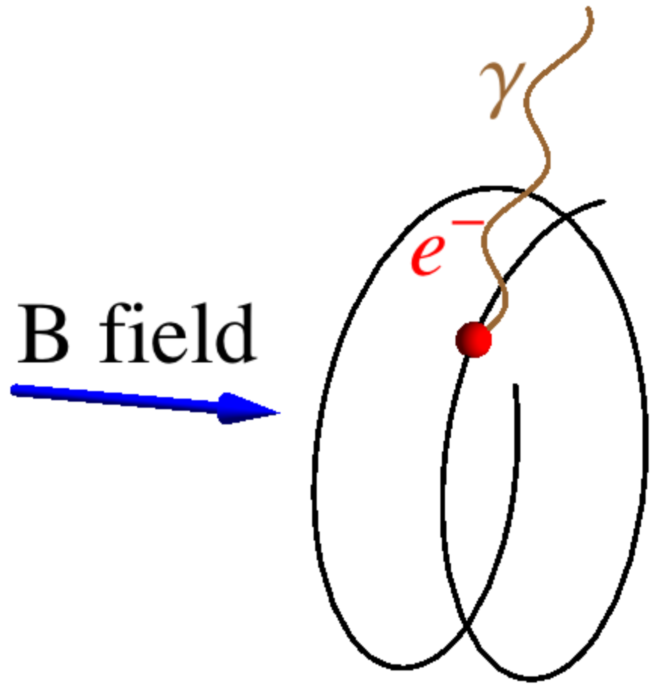

Novel approach: J. Formaggio and B. Monreal, Phys. Rev D 80:051301 (2009)

- Cyclotron radiation from single electrons
- Source transparent to microwave radiation
- No e^- transport from source to detector
- Highly precise frequency measurement

$$f_c = \frac{f_{c,0}}{\gamma} = \frac{1}{2\pi} \frac{eB}{m_e + E_{kin}/c^2}$$

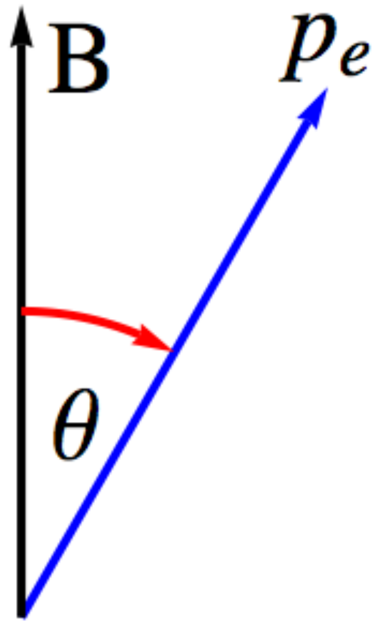

$$P\left(E_{kin}, m, \theta\right) = \frac{1}{4\pi\epsilon_0} \frac{2}{3} \frac{e^4}{m^4 c^5} B^2 \left(E_{kin}^2 + 2\, E_{kin}\, m\, c^2\right) \sin^2\theta$$

$$P\left(17.8\,\mathrm{keV}, 90^\circ, 1\,\mathrm{T}\right) = 1\,\mathrm{fW}$$

$$P\left(30.2\,\mathrm{keV}, 90^\circ, 1\,\mathrm{T}\right) = 1.7\,\mathrm{fW}$$

Small but readily detectable with state-of-the-art detectors

Project 8: Cyclotron radiation emission spectroscopy of $T_{(2)}$

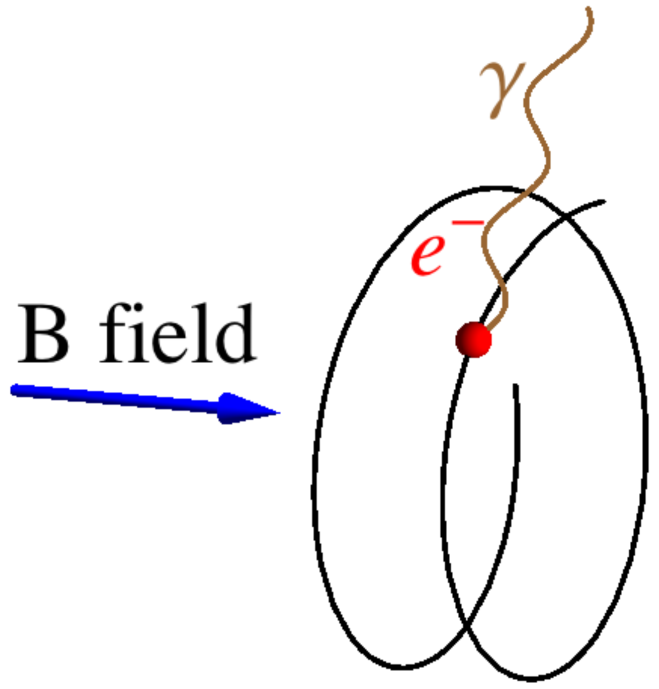

Novel approach: J. Formaggio and B. Monreal, Phys. Rev D 80:051301 (2009)

- Cyclotron radiation from single electrons
- Source transparent to microwave radiation
- No e^- transport from source to detector
- Highly precise frequency measurement

$$f_c = \frac{f_{c,0}}{\gamma} = \frac{1}{2\pi}\frac{eB}{m_e + E_{kin}/c^2}$$

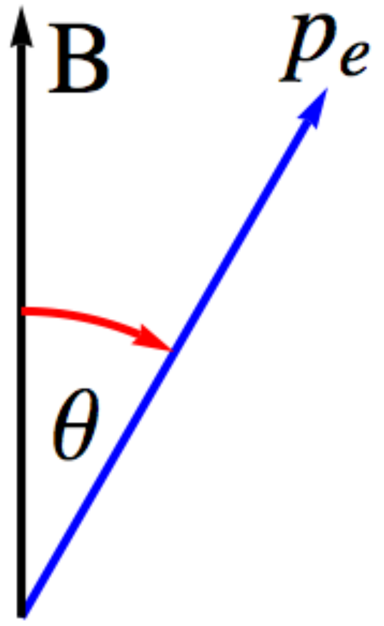

$$P(E_{kin}, m, \theta) = \frac{1}{4\pi\epsilon_0}\frac{2}{3}\frac{e^4}{m^4 c^5} B^2 \left(E_{kin}^2 + 2\,E_{kin}\,m\,c^2\right)\sin^2\theta$$

$$P(17.8\,\mathrm{keV}, 90°, 1\,\mathrm{T}) = 1\,\mathrm{fW}$$

$$P(30.2\,\mathrm{keV}, 90°, 1\,\mathrm{T}) = 1.7\,\mathrm{fW}$$

Small but readily detectable with state-of-the-art detectors

$$P\left(17.8\,\mathrm{keV}, 90°, 0.04\,\mathrm{T}\right) = 1\,\mathrm{aW} \,@\, 1\,\mathrm{GHz}$$

Atomic physics drives us to lower fields
→ need for quantum amplifiers!

Project 8 phase I: First demonstration of CRES

Demonstrate the path to an electron neutrino mass experiment step by step!

2015	2016	2017	2018	2019	2020	2021	2022	2023	2024	2025	2026

Phase I Proof of principle to show the feasibility of CRES: Use mono-energetic conversion electrons from ^{83m}Kr gas in waveguide

Project 8 phase I: First demonstration of CRES

Demonstrate the path to an electron neutrino mass experiment step by step!

2015 2016 2017 2018 2019 2020 2021 2022 2023 2024 2025 2026

Phase I Proof of principle to show the feasibility of CRES: Use mono-energetic conversion electrons from ^{83m}Kr gas in waveguide

Amplification, digitization, mixing, and Fourier transformation

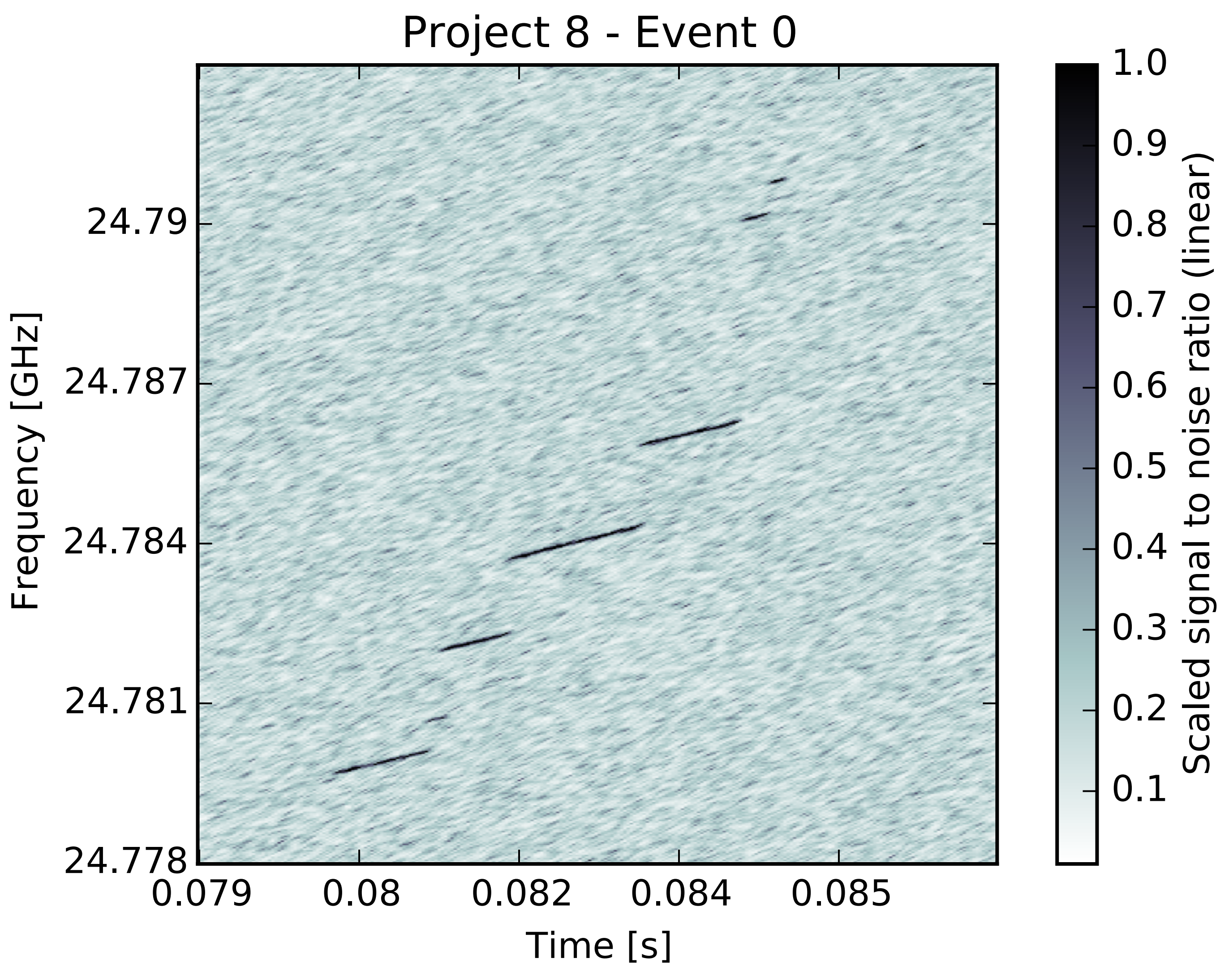

Project 8 phase I: First demonstration of CRES

Demonstrate the path to an electron neutrino mass experiment step by step!

2015 2016 2017 2018 2019 2020 2021 2022 2023 2024 2025 2026

Phase I Proof of principle to show the feasibility of CRES: Use mono-energetic conversion electrons from ^{83m}Kr gas in waveguide

Amplification, digitization, mixing, and Fourier transformation

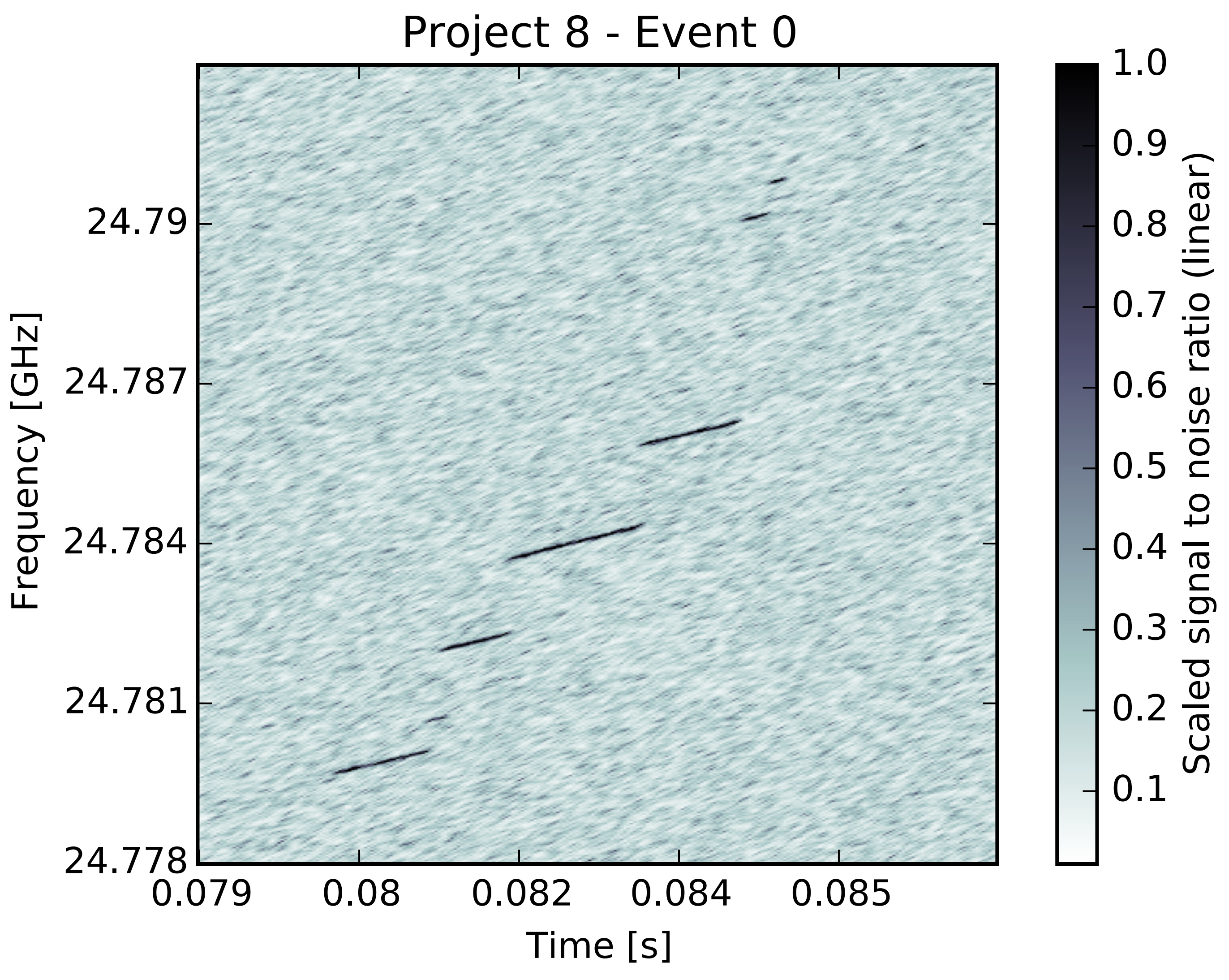

Very first CRES spectrum of ^{83m}Kr

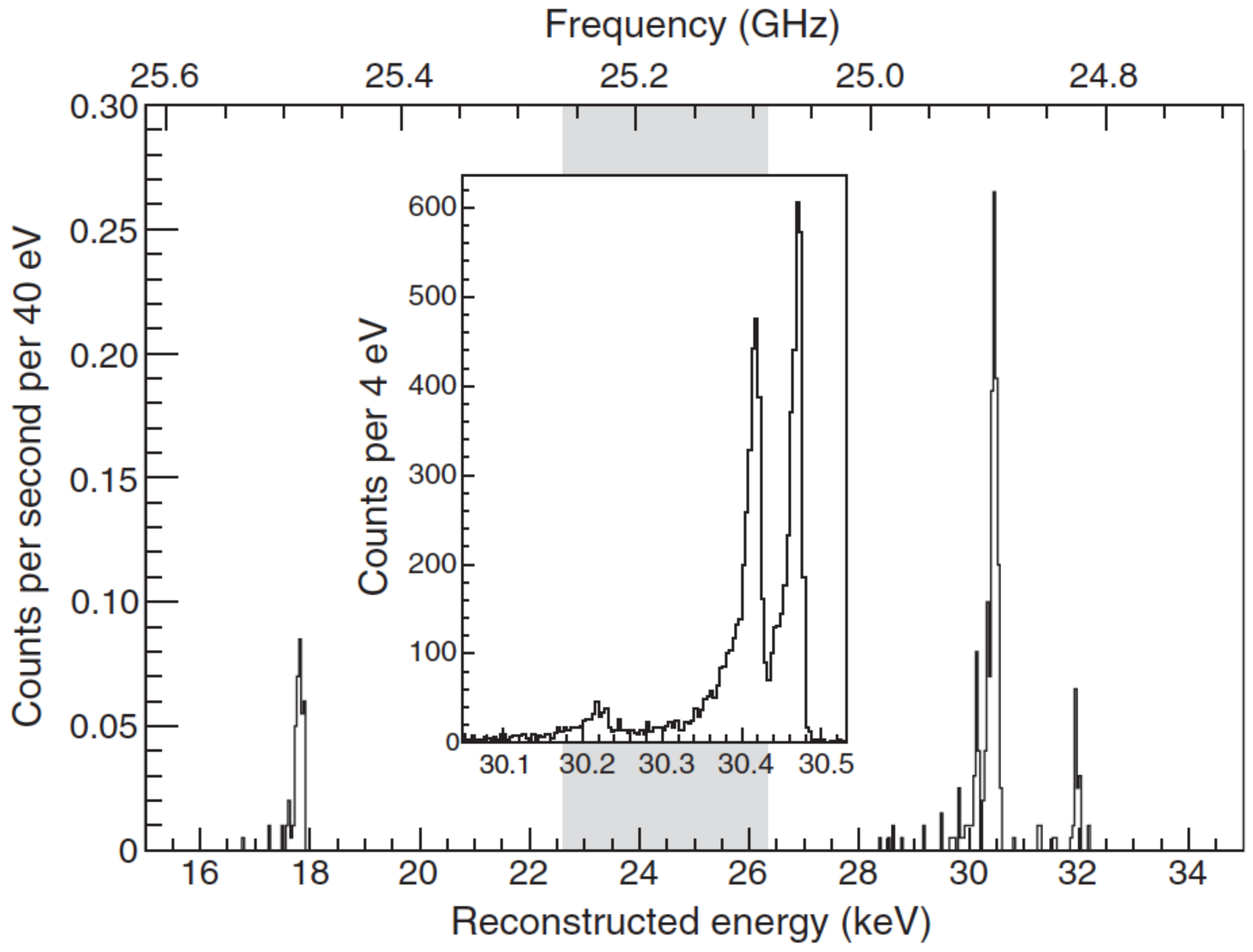

Asner et al., Physical Review Letters, 114, 162501 (2015)

Project 8 phase I: First demonstration of CRES

Demonstrate the path to an electron neutrino mass experiment step by step!

2015 2016 2017 2018 2019 2020 2021 2022 2023 2024 2025 2026

Phase I Proof of principle to show the feasibility of CRES: Use mono-energetic conversion electrons from ^{83m}Kr gas in waveguide

Amplification, digitization, mixing, and Fourier transformation

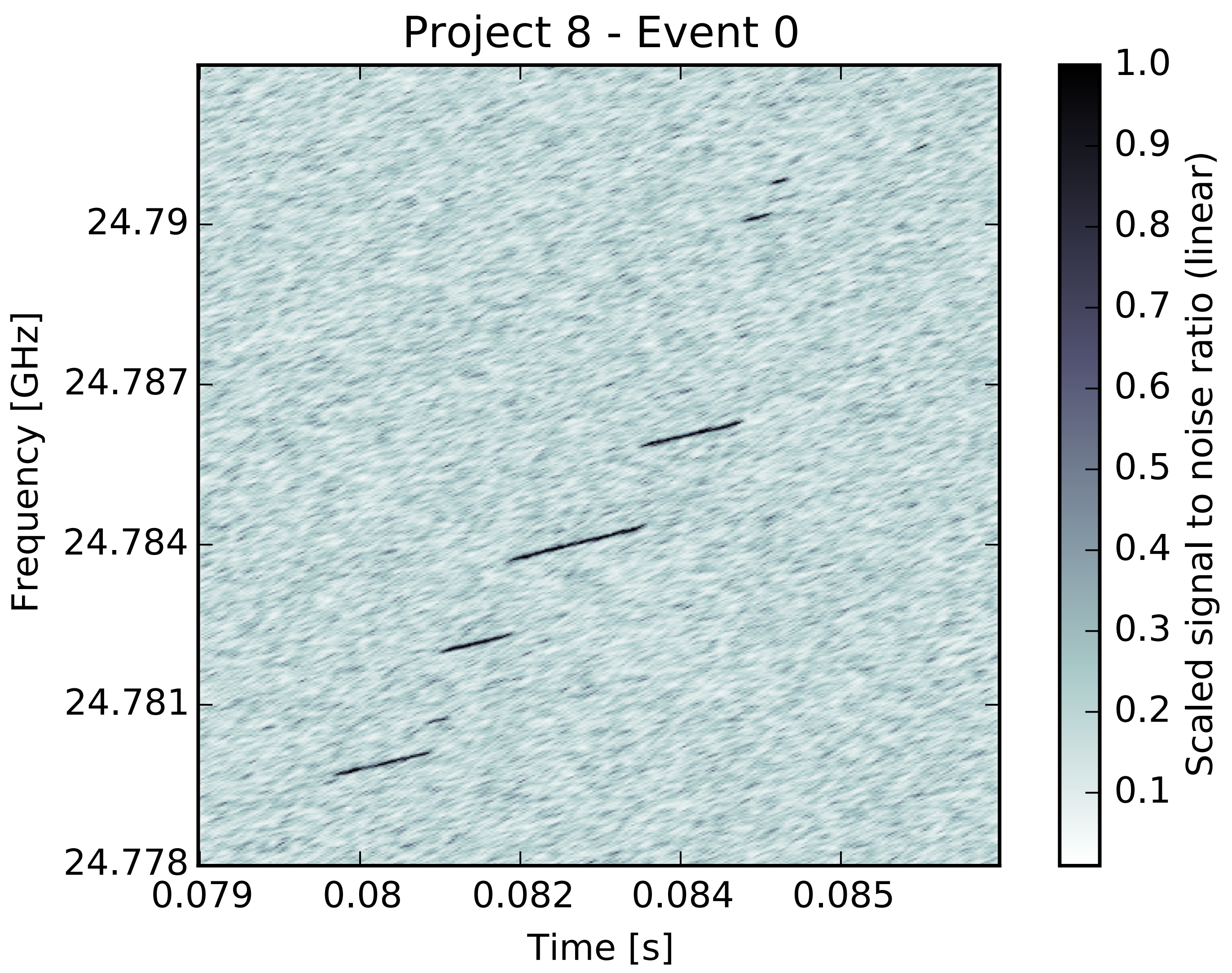

Very first CRES spectrum of ^{83m}Kr

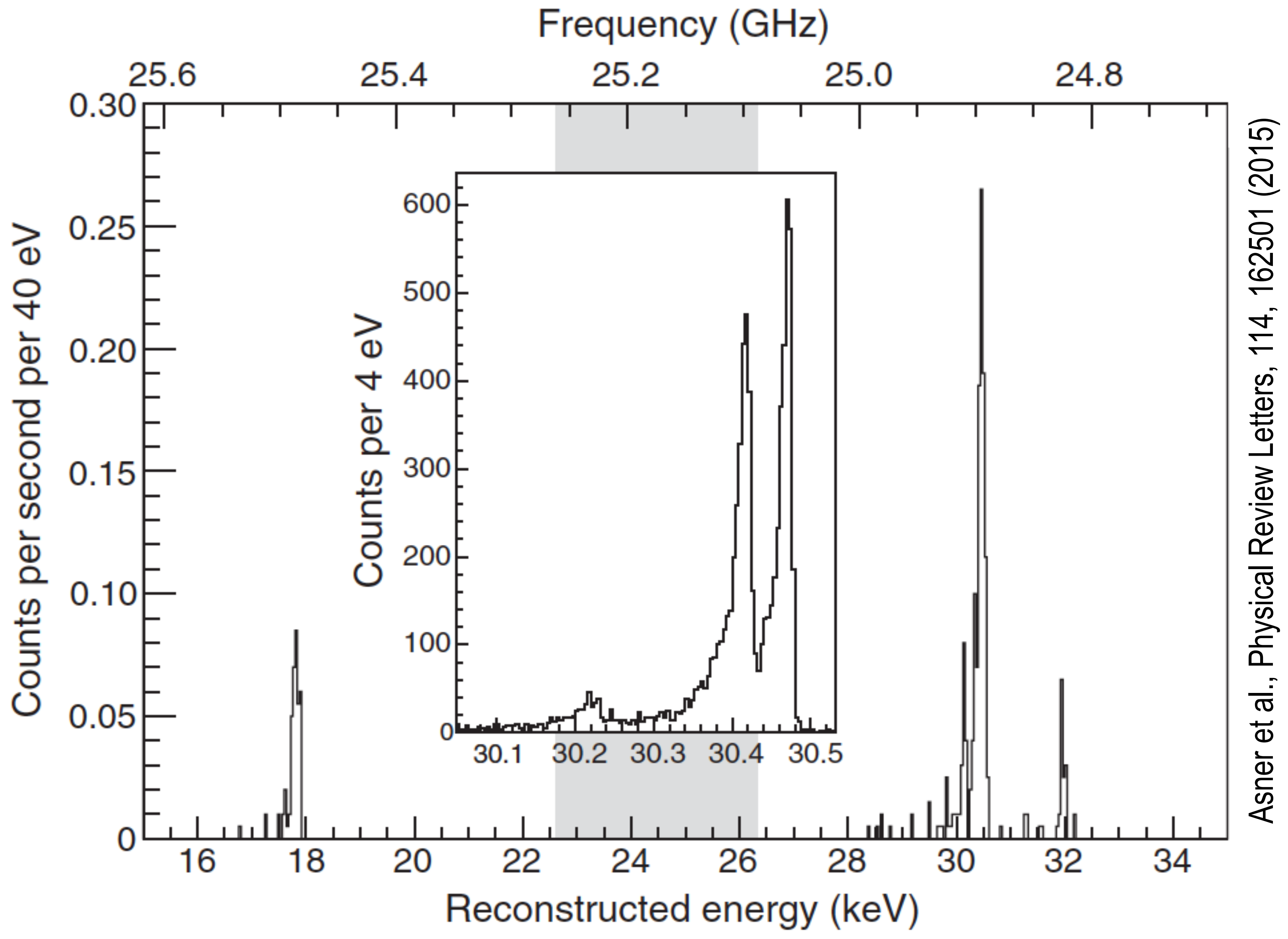

High res. CRES spectrum of ^{83m}Kr

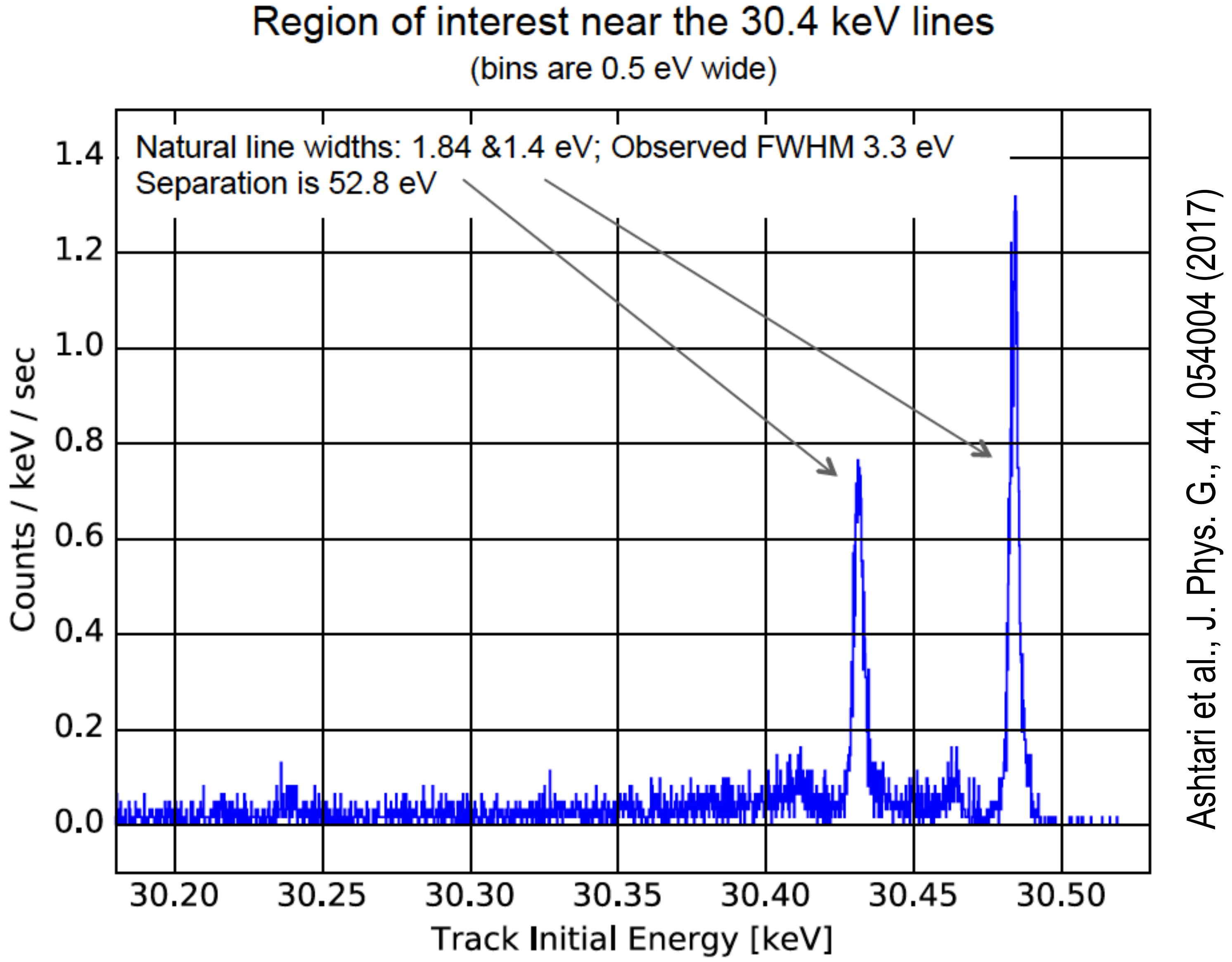

CRES compared to classical spectroscopy

^{83m}Kr commissioning run: Observation of single 17.8 keV CE electrons on real time spectrum analyzer

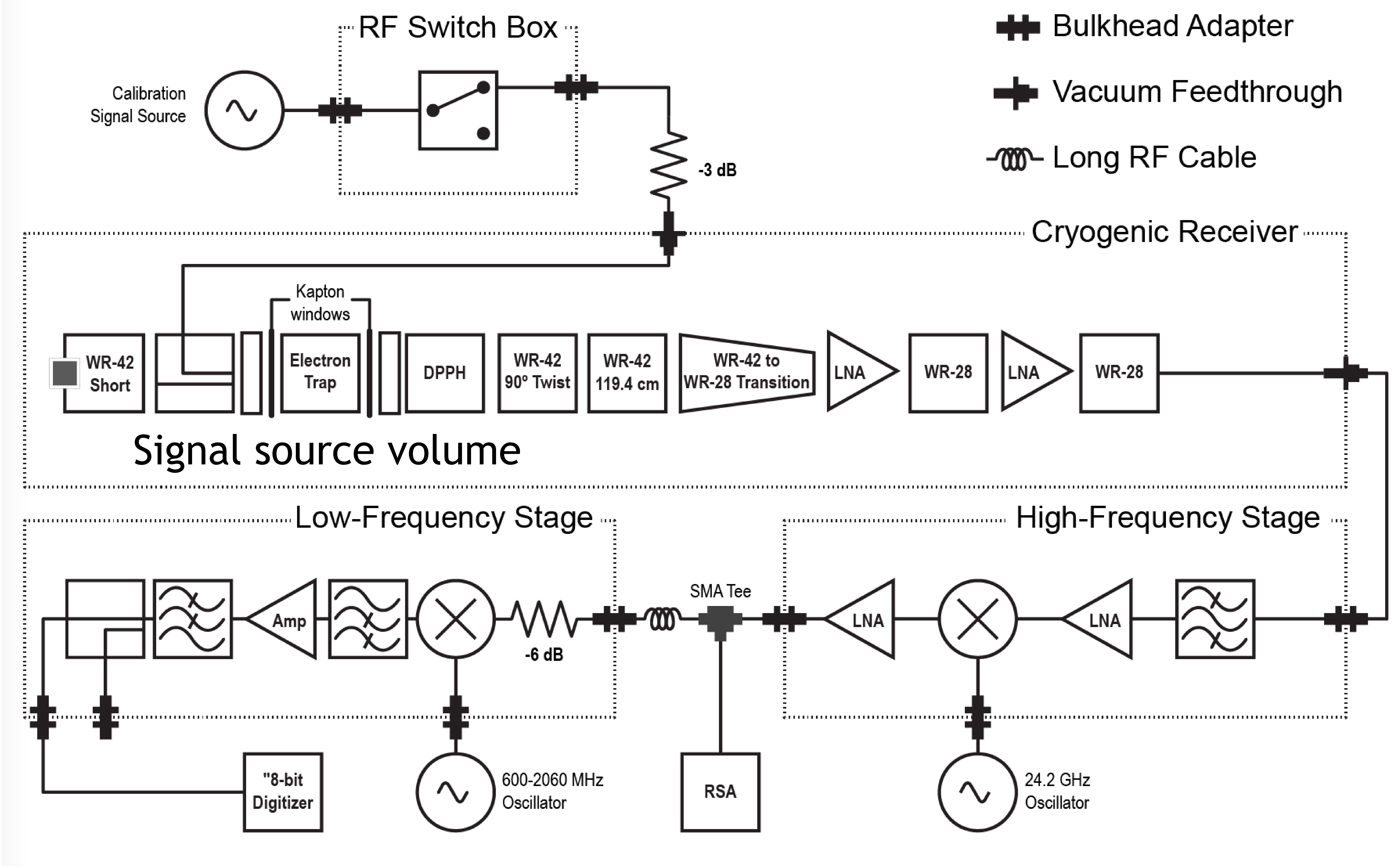

CRES compared to classical spectroscopy

^{83m}Kr commissioning run: Observation of single 17.8 keV CE electrons on real time spectrum analyzer

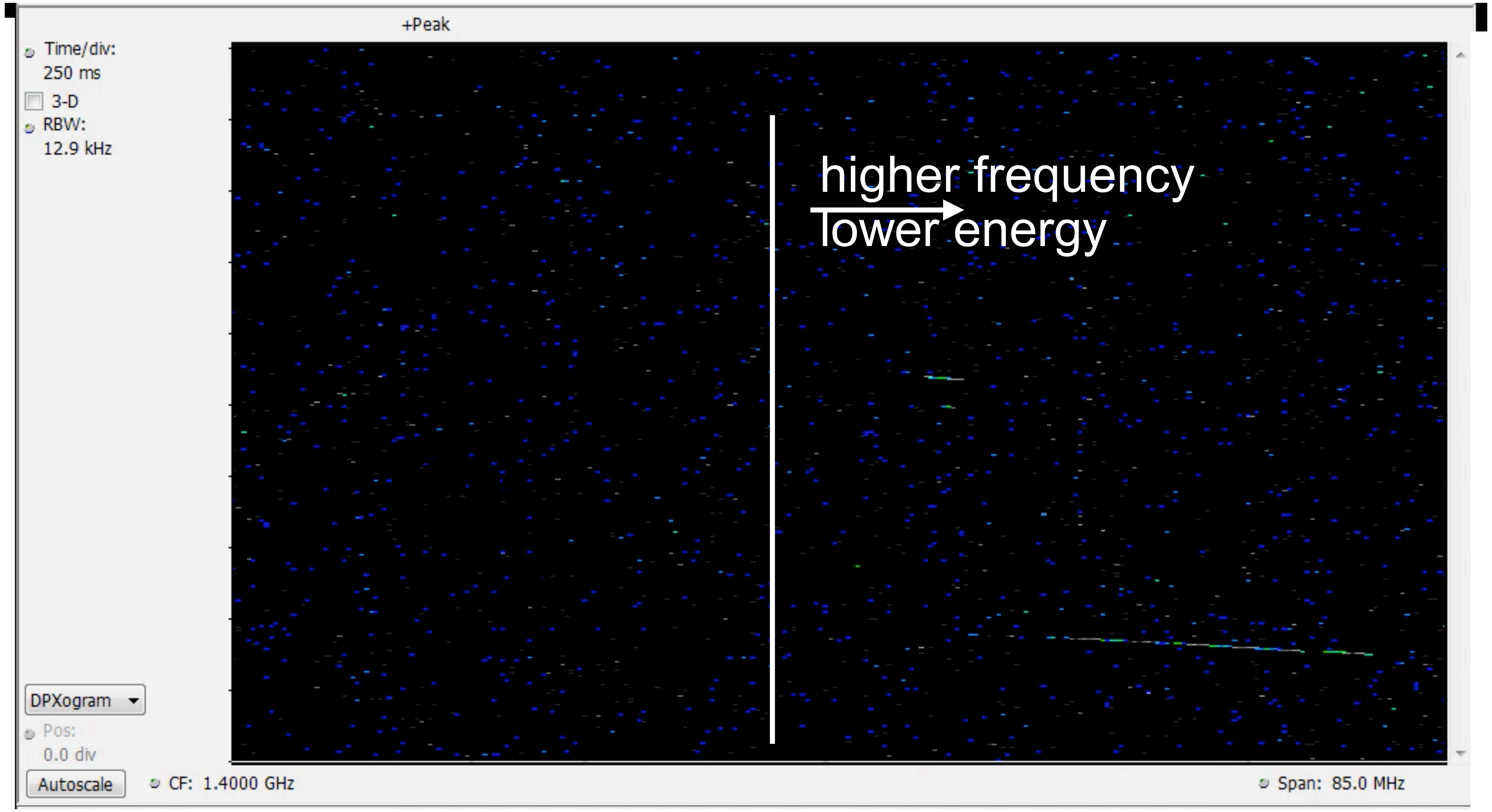

85 MHz window around 1.4 GHz central frequency

CRES compared to classical spectroscopy

^{83m}Kr commissioning run: Observation of single 17.8 keV CE electrons on real time spectrum analyzer

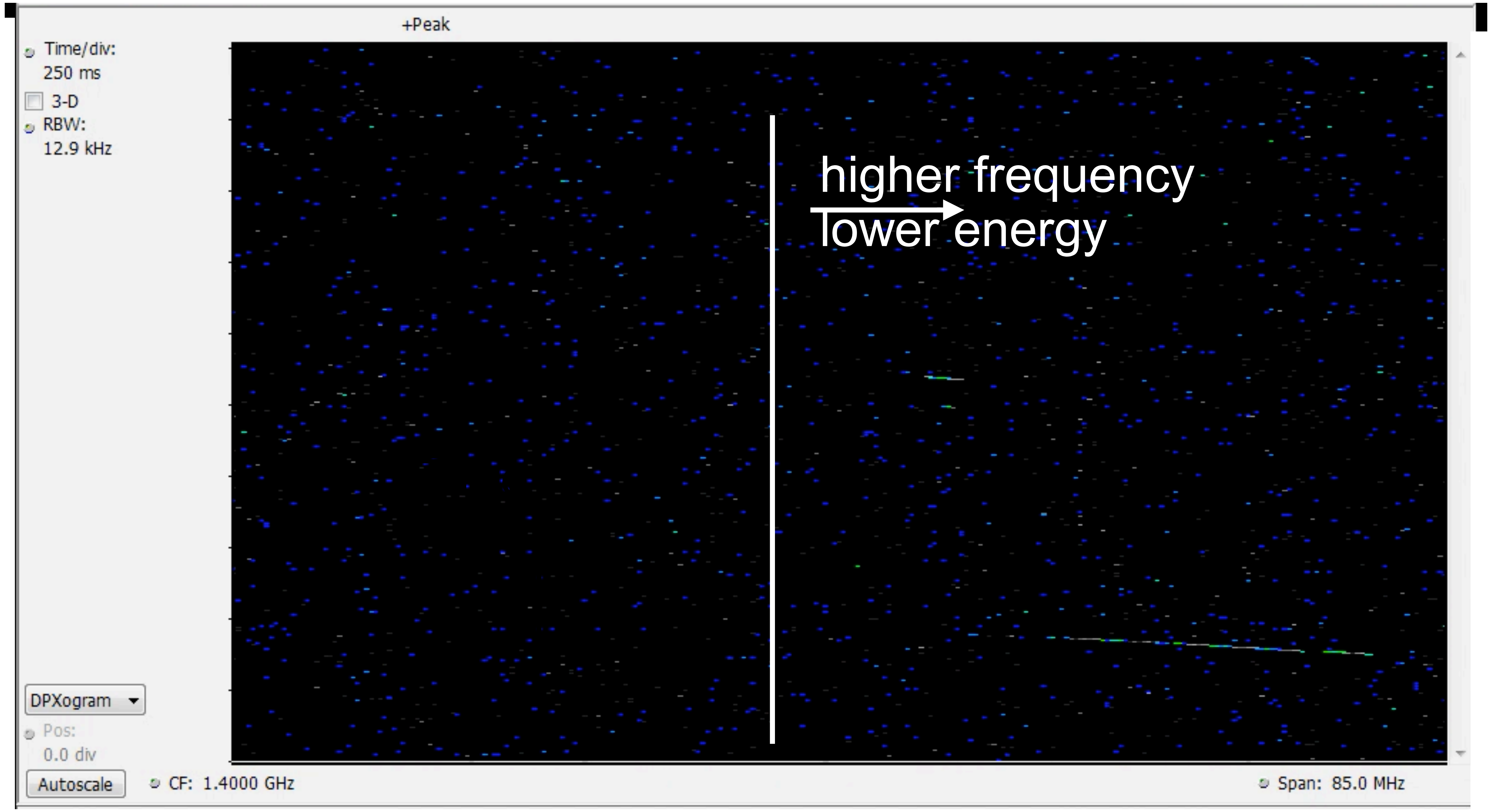

85 MHz window around 1.4 GHz central frequency

CRES compared to classical spectroscopy

^{83m}Kr commissioning run: Observation of single 17.8 keV CE electrons on real time spectrum analyzer

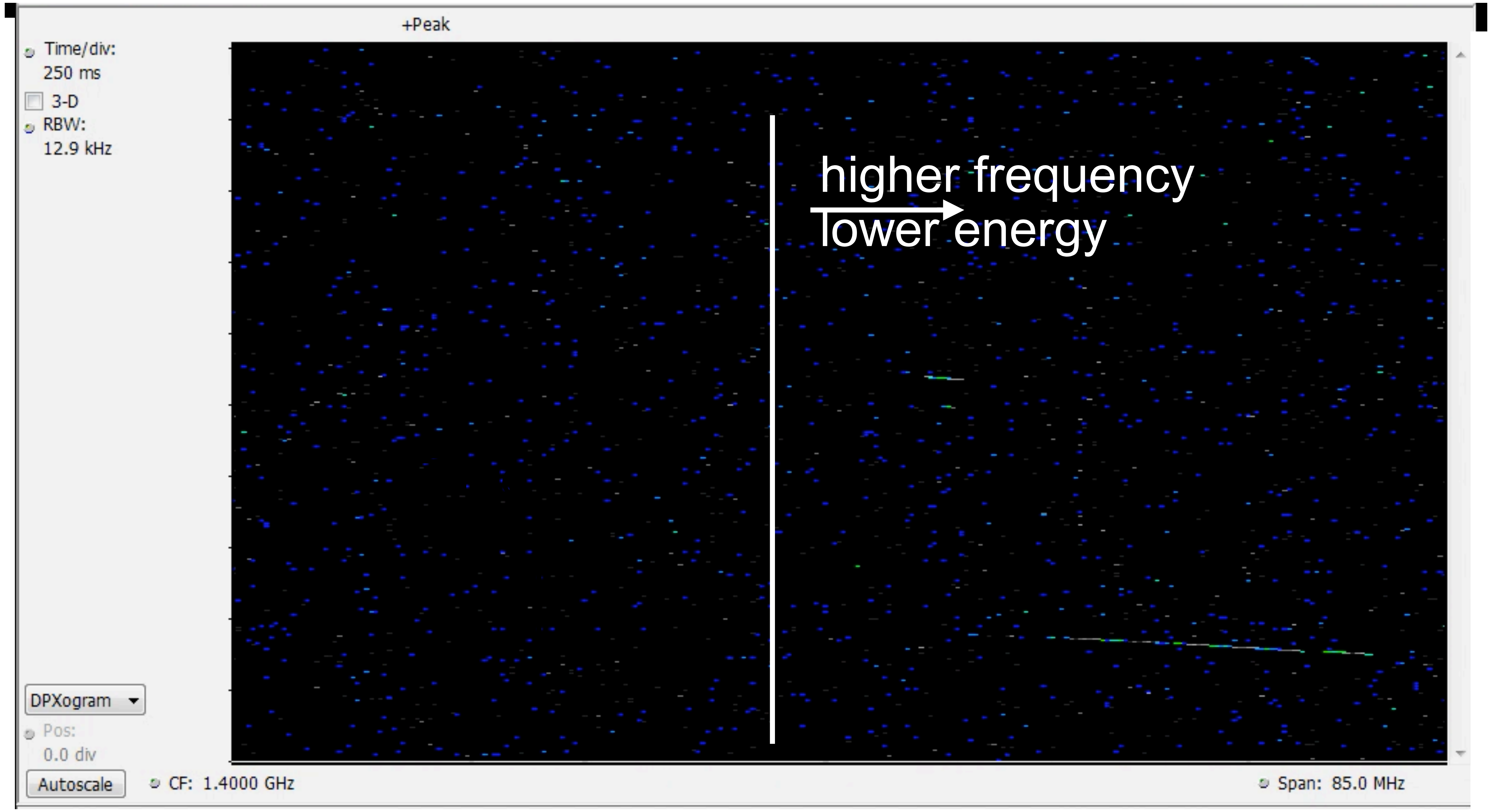

85 MHz window around 1.4 GHz central frequency

Unique features of CRES:

- Pile-up(?)

CRES compared to classical spectroscopy

^{83m}Kr commissioning run: Observation of single 17.8 keV CE electrons on real time spectrum analyzer

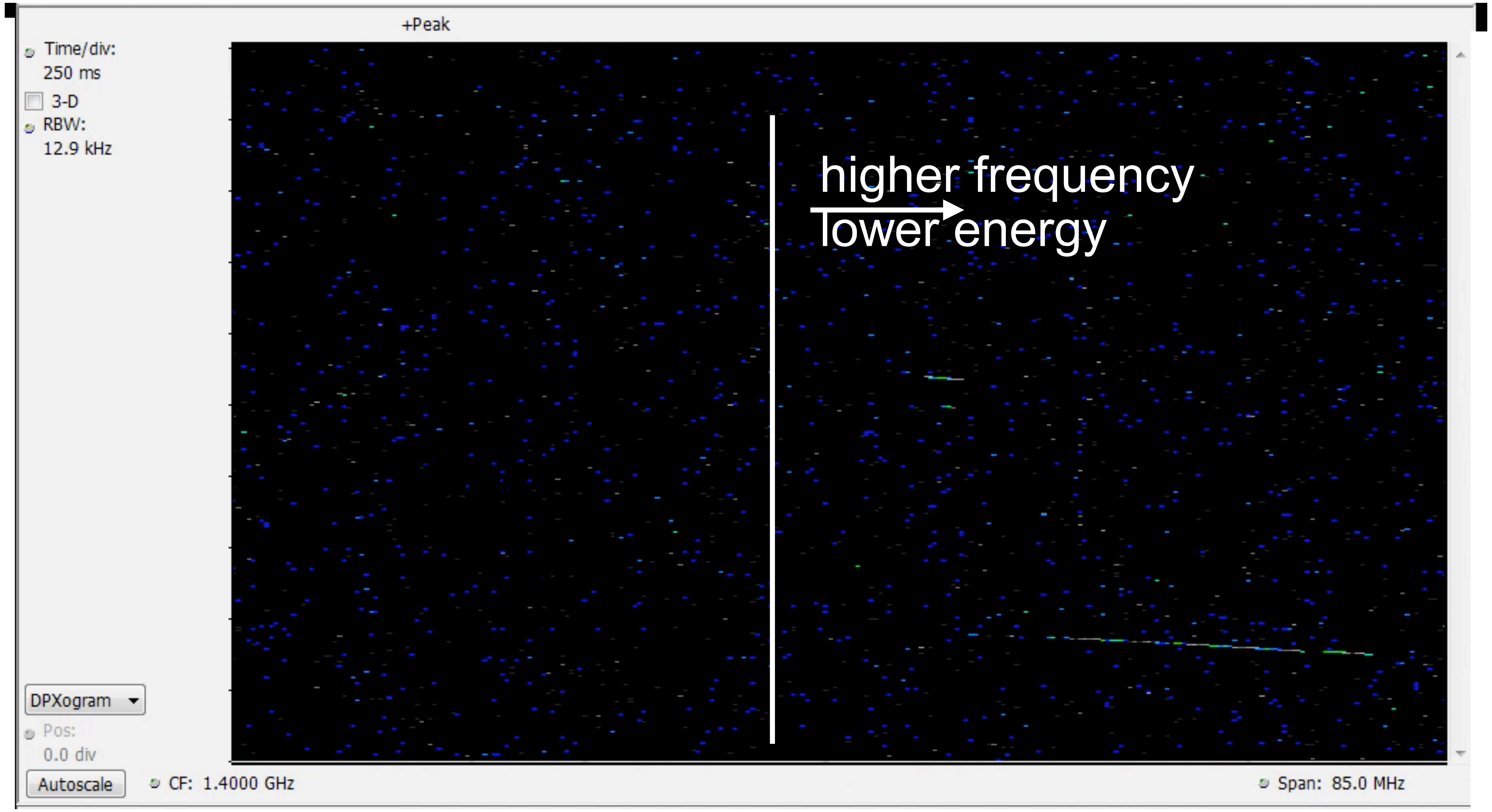

85 MHz window around 1.4 GHz central frequency

Unique features of CRES:

- Pile-up(?)
  - Distinct signal start frequencies
  - Distinct signal start times
  - Distinct scattering pattern
  - Detected power level

CRES compared to classical spectroscopy

^{83m}Kr commissioning run: Observation of single 17.8 keV CE electrons on real time spectrum analyzer

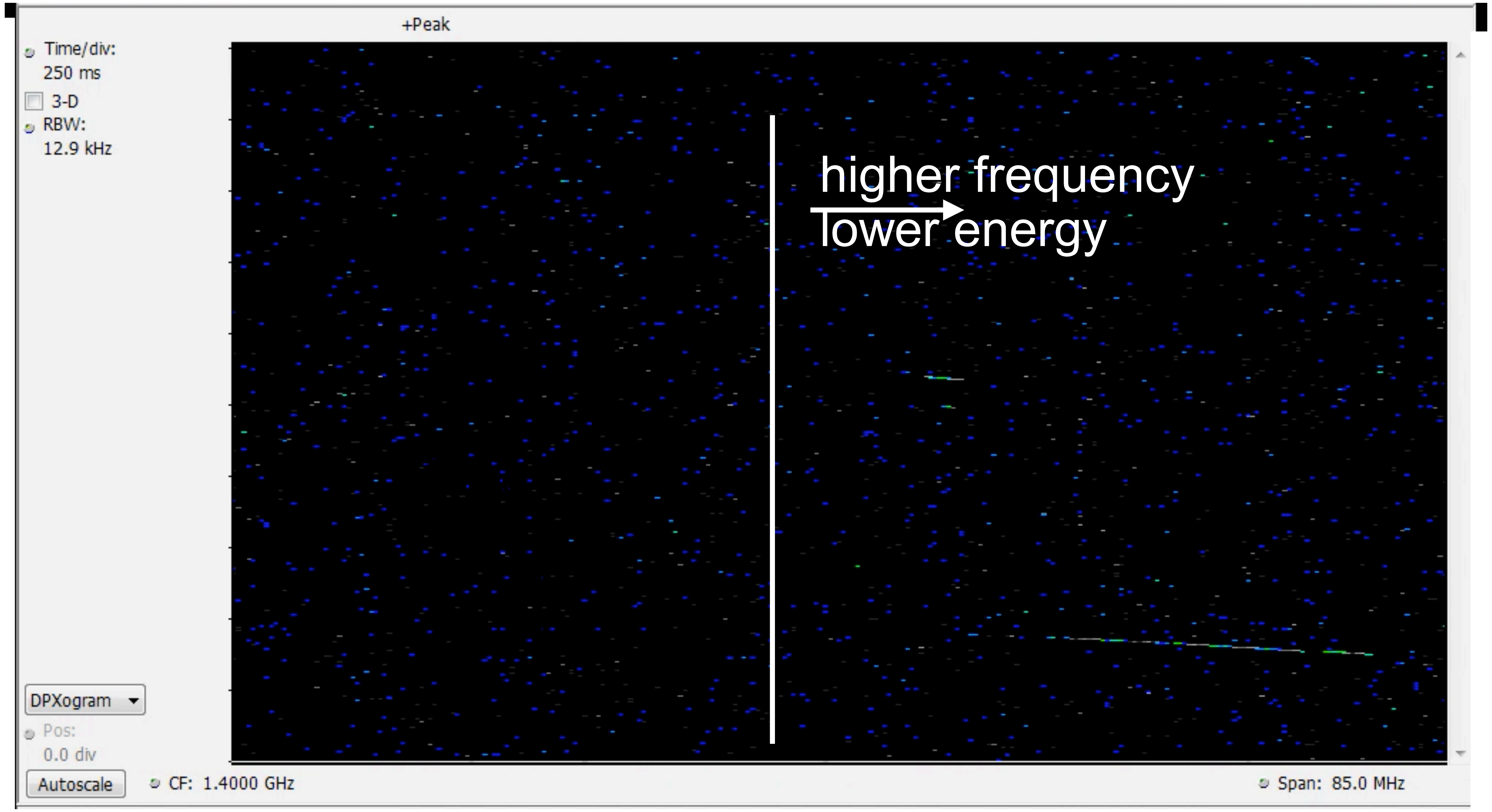

85 MHz window around 1.4 GHz central frequency

Unique features of CRES:

- Pile-up(?)
  - Distinct signal start frequencies
  - Distinct signal start times
  - Distinct scattering pattern
  - Detected power level
- Fully differential measurement scheme (compared to the MAC-E scheme)

CRES compared to classical spectroscopy

^{83m}Kr commissioning run: Observation of single 17.8 keV CE electrons on real time spectrum analyzer

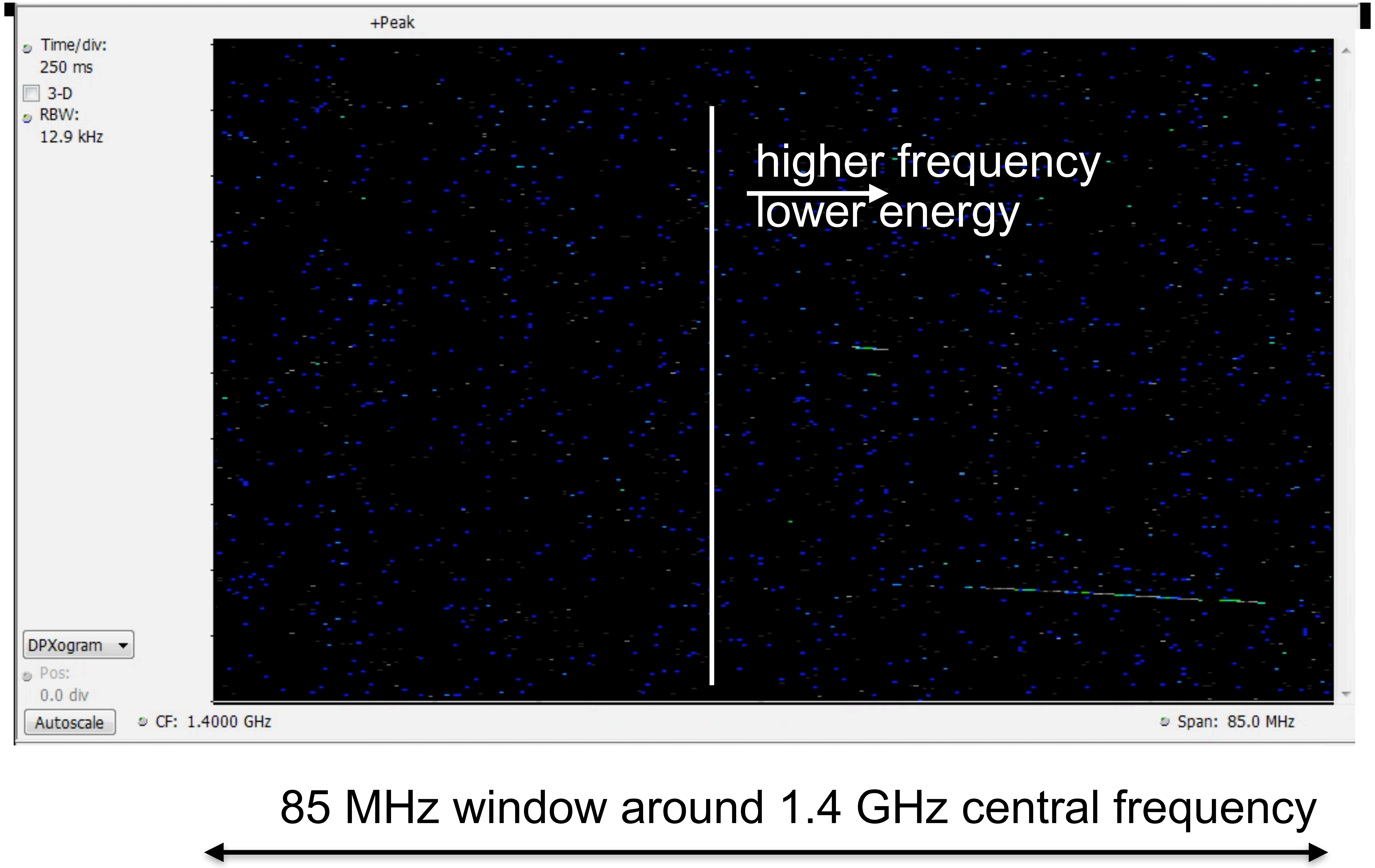

Unique features of CRES:

- Pile-up(?)
  - Distinct signal start frequencies
  - Distinct signal start times
  - Distinct scattering pattern
  - Detected power level
- Fully differential measurement scheme (compared to the MAC-E scheme)

Very different set of cut parameters compared to classical e⁻ spectroscopy!

Project 8 phase II: CRES application to a continuous spectrum

Demonstrate the path to an electron neutrino mass experiment step by step!

2015	2016	2017	2018	2019	2020	2021	2022	2023	2024	2025	2026

Project 8 phase II: CRES application to a continuous spectrum

Demonstrate the path to an electron neutrino mass experiment step by step!

	2015	2016	2017	2018	2019	2020	2021	2022	2023	2024	2025	2026
Phase II	Construction			Data taking			Analysis					

Goals:

- 1st application of CRES to continuous β spectrum
- 1st frequency-based neutrino mass limit
- Demonstration of:
  - high energy resolution
  - zero background
  - control of systematic effects

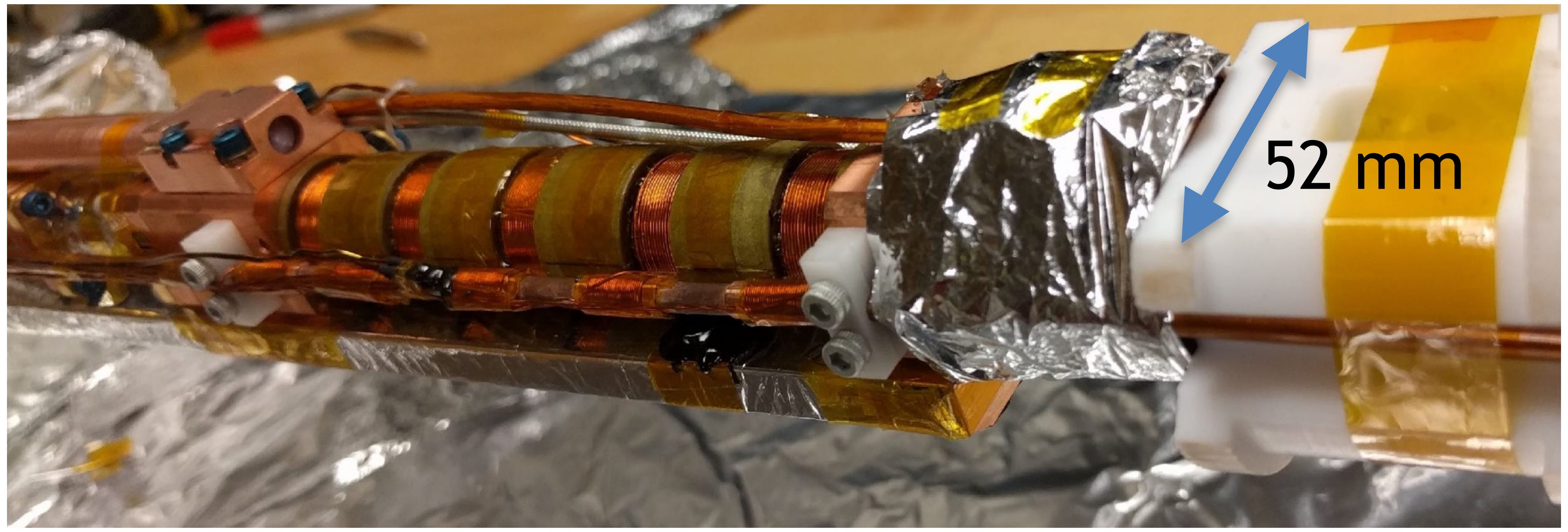

Project 8 phase II: Calibration measurement using ^{83m}Kr

Trap depth determines the energy resolution and the line shape!
→ Calibration with mono-energetic ^{83m}Kr conversion electrons

Project 8 phase II: Calibration measurement using ^{83m}Kr

Trap depth determines the energy resolution and the line shape!
→ Calibration with mono-energetic ^{83m}Kr conversion electrons

"Shallow trap" configuration with:
- small pitch angle acceptance
- small magnetic field variation
- but high energy resolution

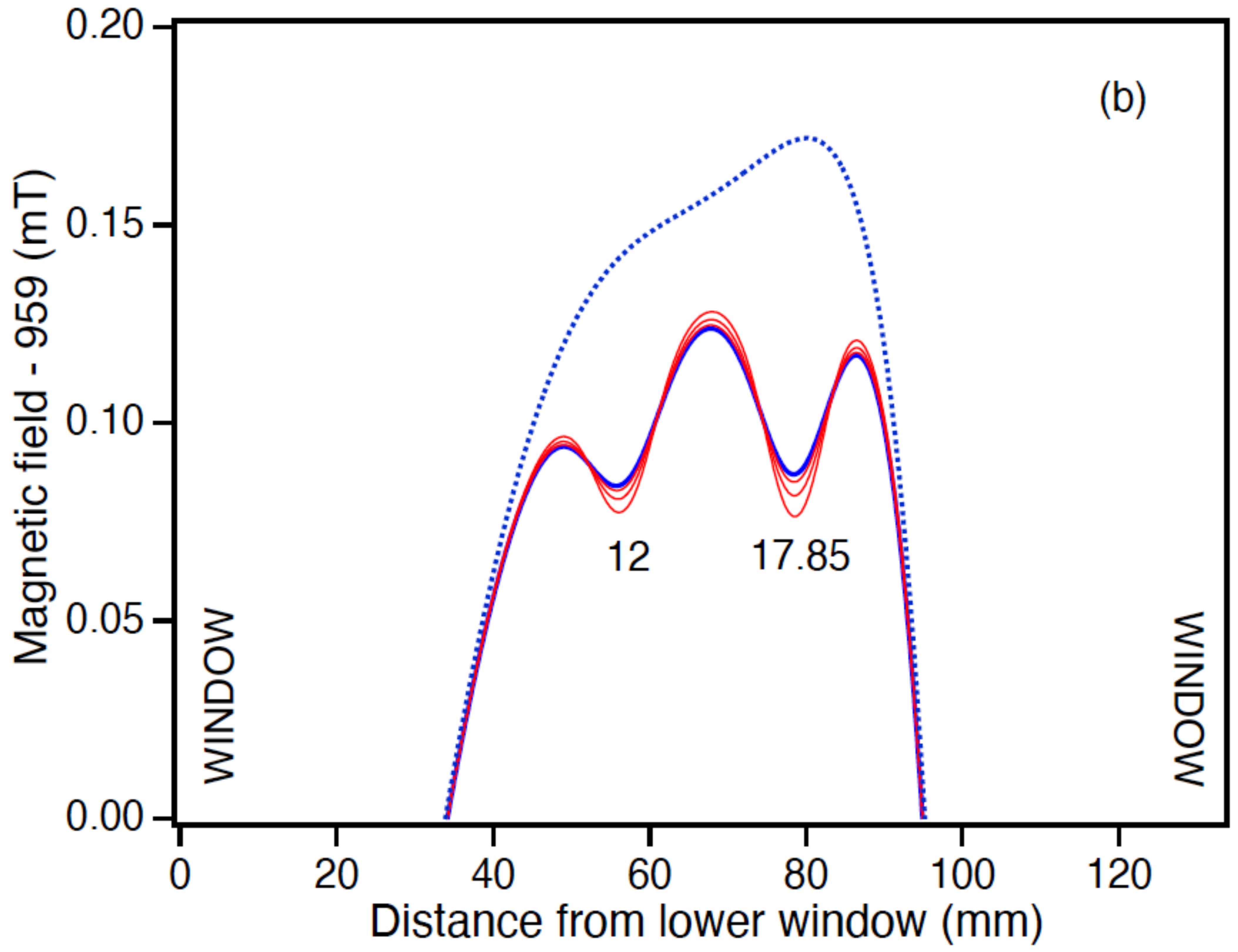

Project 8 phase II: Calibration measurement using ^{83m}Kr

Trap depth determines the energy resolution and the line shape!
→ Calibration with mono-energetic ^{83m}Kr conversion electrons

"Shallow trap" configuration with:
- small pitch angle acceptance
- small magnetic field variation
- but high energy resolution

Development of line shape model:
- Kr decay physics: shake-up and shake-off
  - ^{83m}Kr used in many other experiment too
    New paper: H. Robertson and *V. Venkatapathy*, Phys. Rev. C 102, 035502, 2020
- e$^-$ - scattering in (high-density) gas column, background gases, missed first track

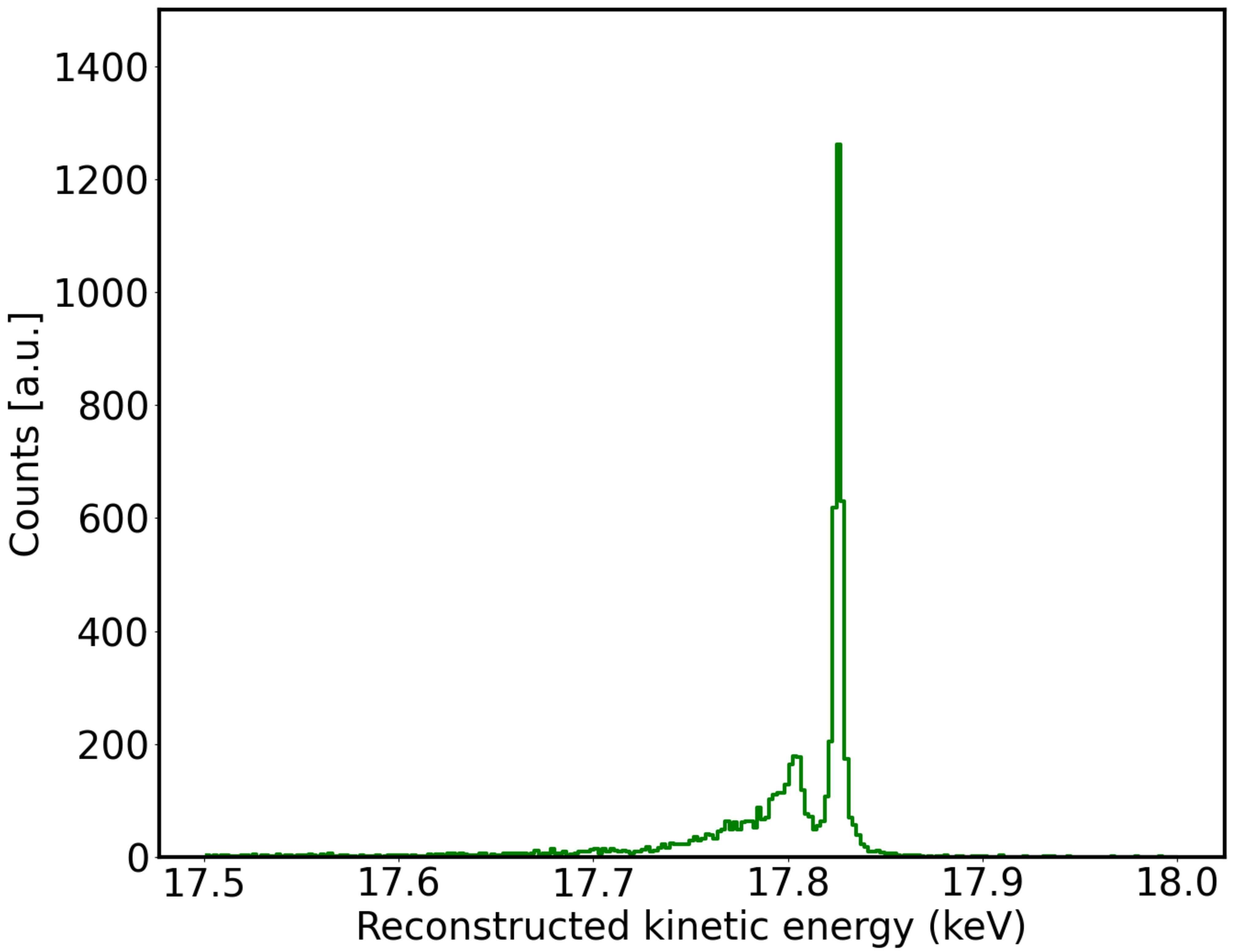

Project 8 phase II: Calibration measurement using ^{83m}Kr

Trap depth determines the energy resolution and the line shape!
→ Calibration with mono-energetic ^{83m}Kr conversion electrons

"Shallow trap" configuration with:
- small pitch angle acceptance
- small magnetic field variation
- but high energy resolution

Development of line shape model:
- Kr decay physics: shake-up and shake-off
  - ^{83m}Kr used in many other experiment too
    New paper: H. Robertson and *V. Venkatapathy*, Phys. Rev. C 102, 035502, 2020
- e^- - scattering in (high-density) gas column, background gases, missed first track

Measured line width: (2.8 ± 0.1) eV
Instrumental width: (1.7 ± 0.2) eV

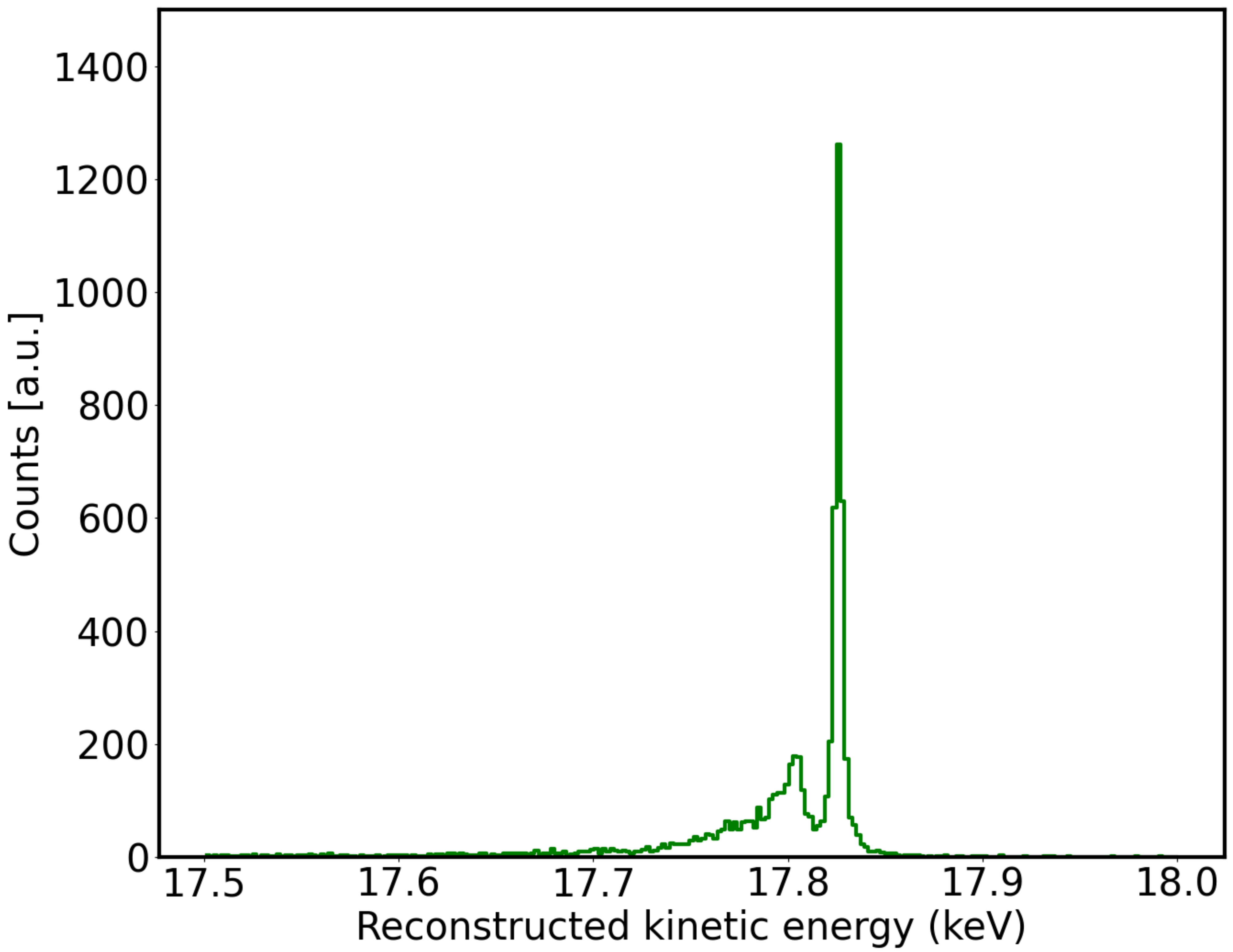

Project 8 phase II: Calibration measurement using ^{83m}Kr

Trap depth determines the energy resolution and the line shape!
→ Calibration with mono-energetic ^{83m}Kr conversion electrons

Esfahani, et al, arXiv:2303.12055

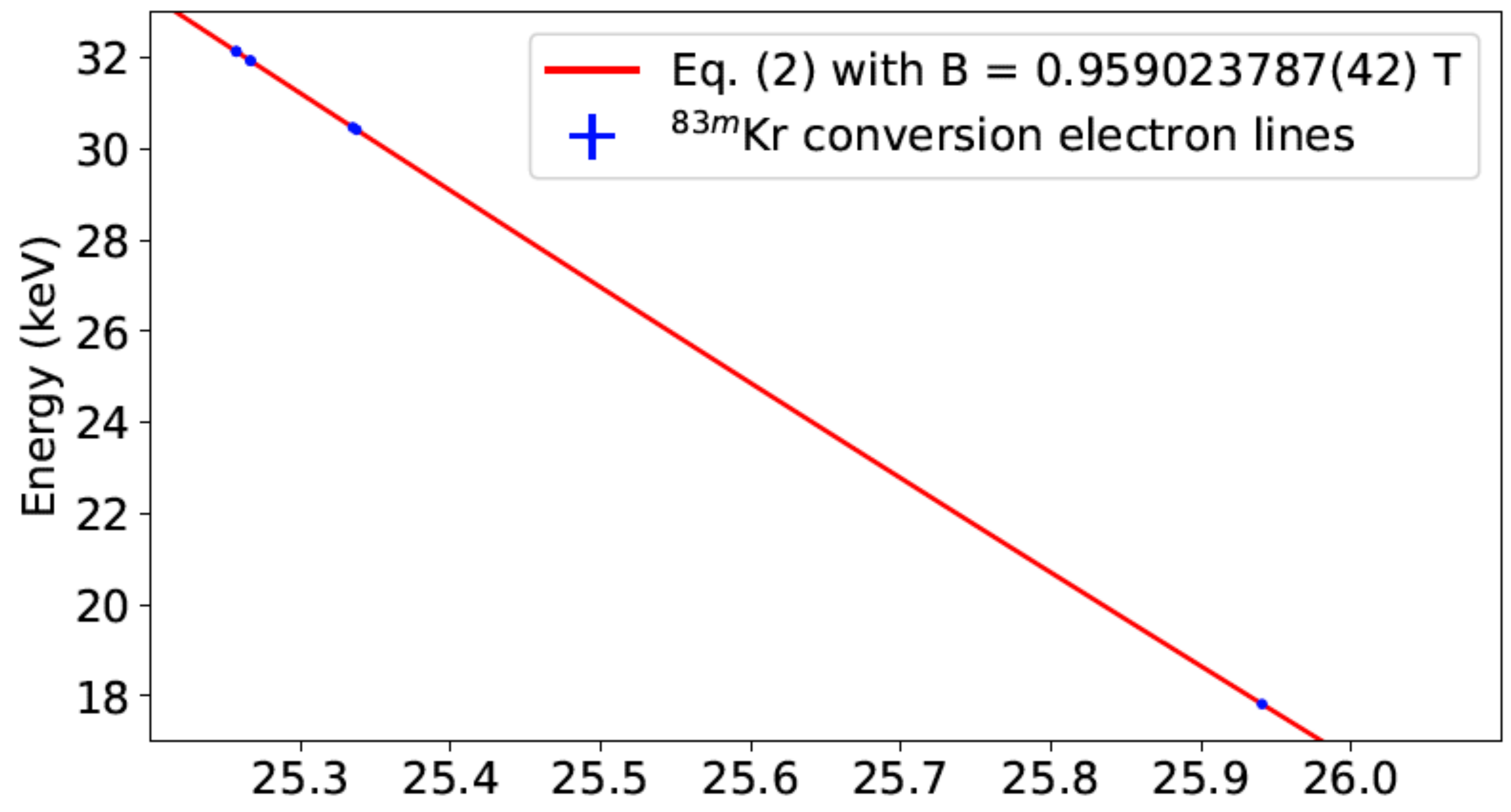

Project 8 phase II: Calibration measurement using ^{83m}Kr

Trap depth determines the energy resolution and the line shape!
→ Calibration with mono-energetic ^{83m}Kr conversion electrons

Esfahani, et al, arXiv:2303.12055

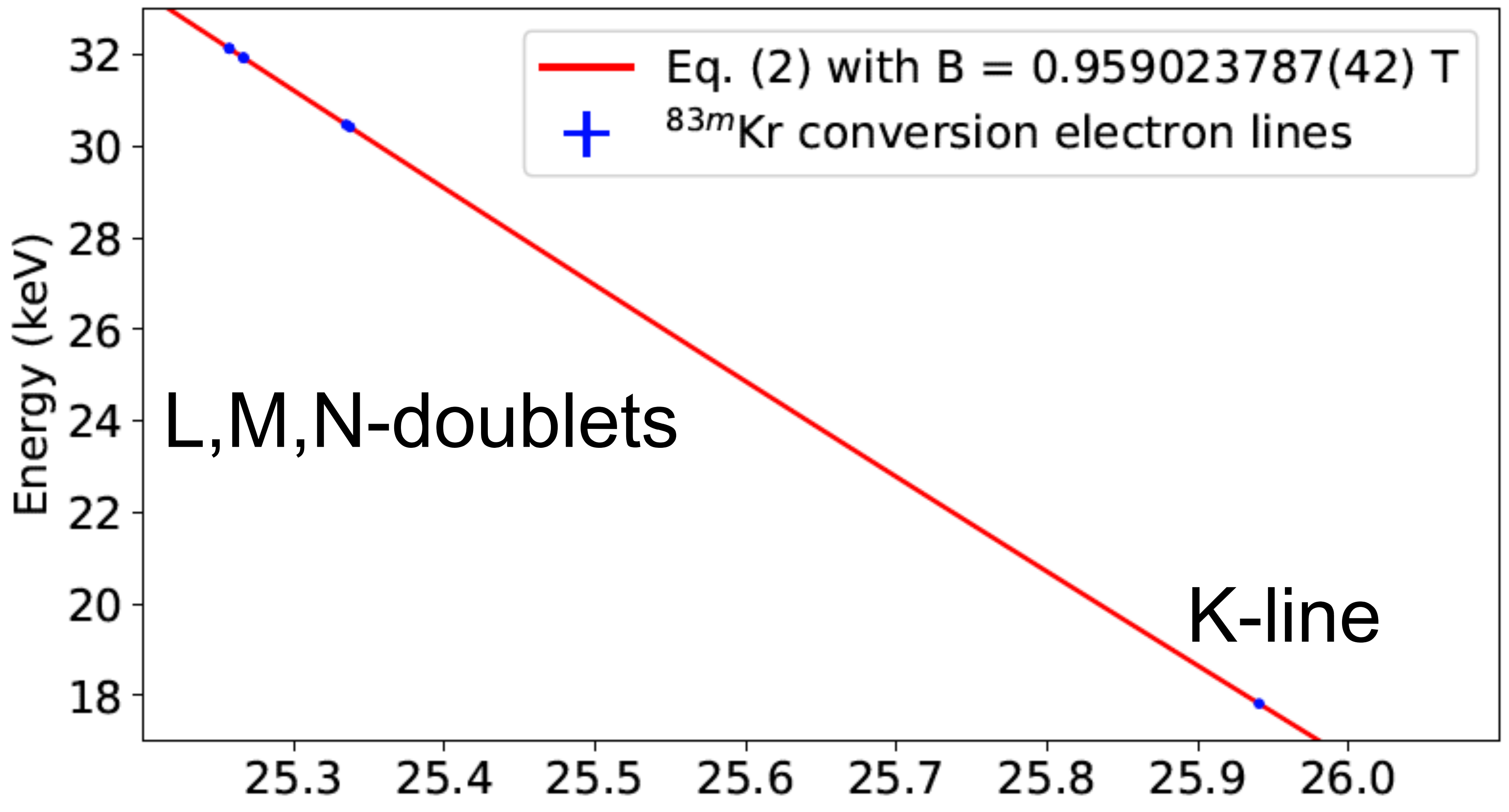

"Shallow trap" configuration:

- Extreme energy precision of CRES demonstrated

Project 8 phase II: Calibration measurement using ^{83m}Kr

Trap depth determines the energy resolution and the line shape!
→ Calibration with mono-energetic ^{83m}Kr conversion electrons

"Shallow trap" configuration:

- Extreme energy precision of CRES demonstrated
- Kin. energy vs. frequency fit: χ^2/ndf = 0.3
  Residuals mostly < 50 meV (across 14 keV, $< 3 \cdot 10^{-6}$)

Esfahani, et al, arXiv:2303.12055

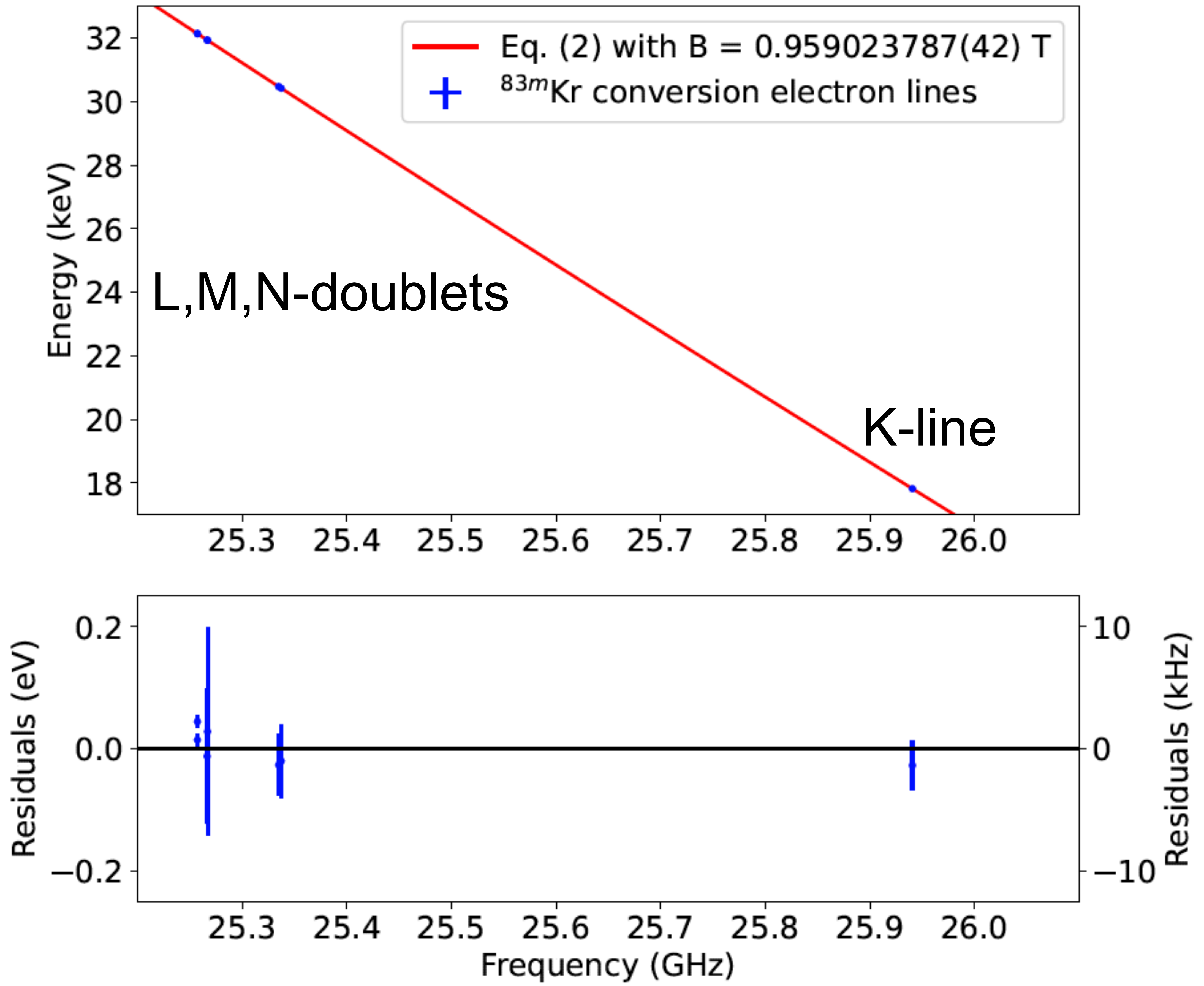

Project 8 phase II: Calibration measurement using ^{83m}Kr

Trap depth determines the energy resolution and the line shape!
→ Calibration with mono-energetic ^{83m}Kr conversion electrons

"Shallow trap" configuration:

- Extreme energy precision of CRES demonstrated
- Kin. energy vs. frequency fit: χ^2/ndf = 0.3
  Residuals mostly < 50 meV (across 14 keV, $< 3 \cdot 10^{-6}$)
- Determine energy of 32-keV γ-line: (32153.6 ± 2.4) eV
  Excellent agreement with literature value: (32151.7± 0.5) eV
  Venos et al., NIM A 560, 2, 352-359, 2006

Esfahani, et al, arXiv:2303.12055

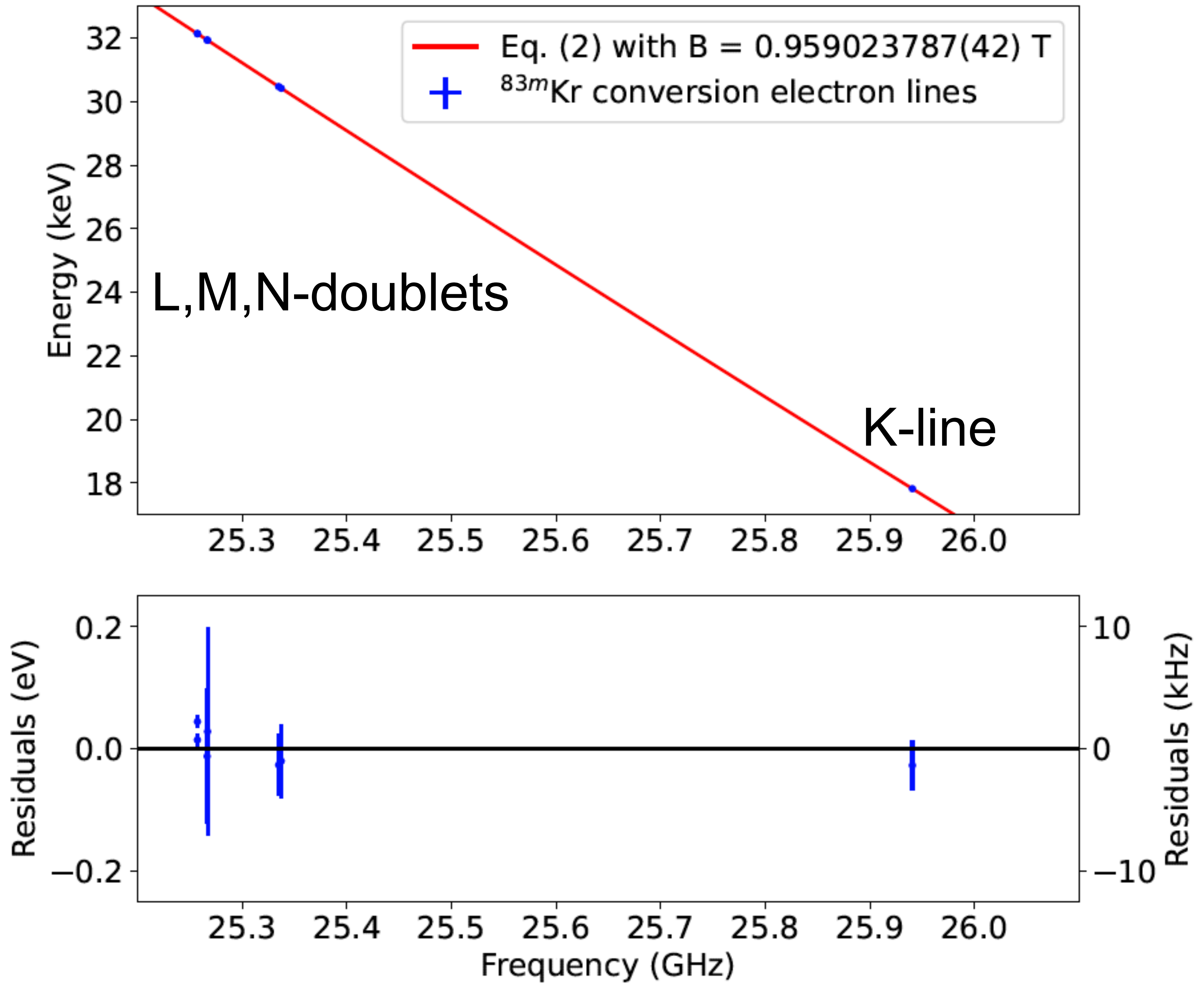

Project 8 phase II: Calibration measurement using ^{83m}Kr

Trap depth determines the energy resolution and the line shape!
→ Calibration with mono-energetic ^{83m}Kr conversion electrons

“Shallow trap” configuration:

- Extreme energy precision of CRES demonstrated
- Kin. energy vs. frequency fit: χ^2/ndf = 0.3
  Residuals mostly < 50 meV (across 14 keV, $< 3 \cdot 10^{-6}$)
- Determine energy of 32-keV γ-line: (32153.6 ± 2.4) eV
  Excellent agreement with literature value: (32151.7± 0.5) eV
  Venos et al., NIM A 560, 2, 352-359, 2006

Plot: A. Esfahani

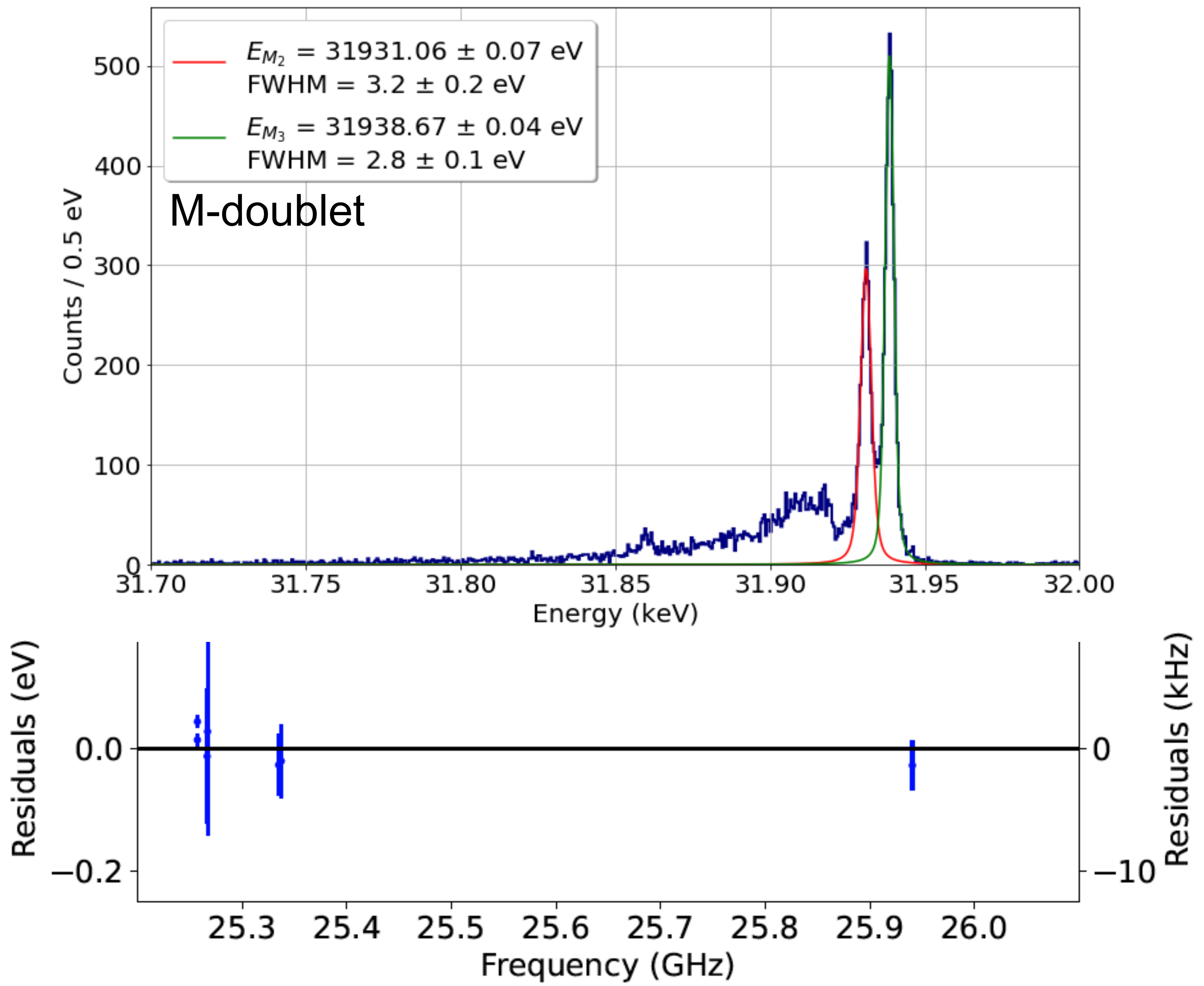

Project 8 phase II: Calibration measurement using ^{83m}Kr

Project 8 phase II: Calibration measurement using ^{83m}Kr

Challenge with shallow trap:
Low T_2 decay rate at the CRES
compatible gas density!

Project 8 phase II: Calibration measurement using ^{83m}Kr

Esfahani, et al, arXiv:2303.12055

Challenge with shallow trap:
Low T_2 decay rate at the CRES compatible gas density!

“Deep trap” configuration with:
- large pitch angle acceptance
- larger magnetic field variation
- but lower energy resolution

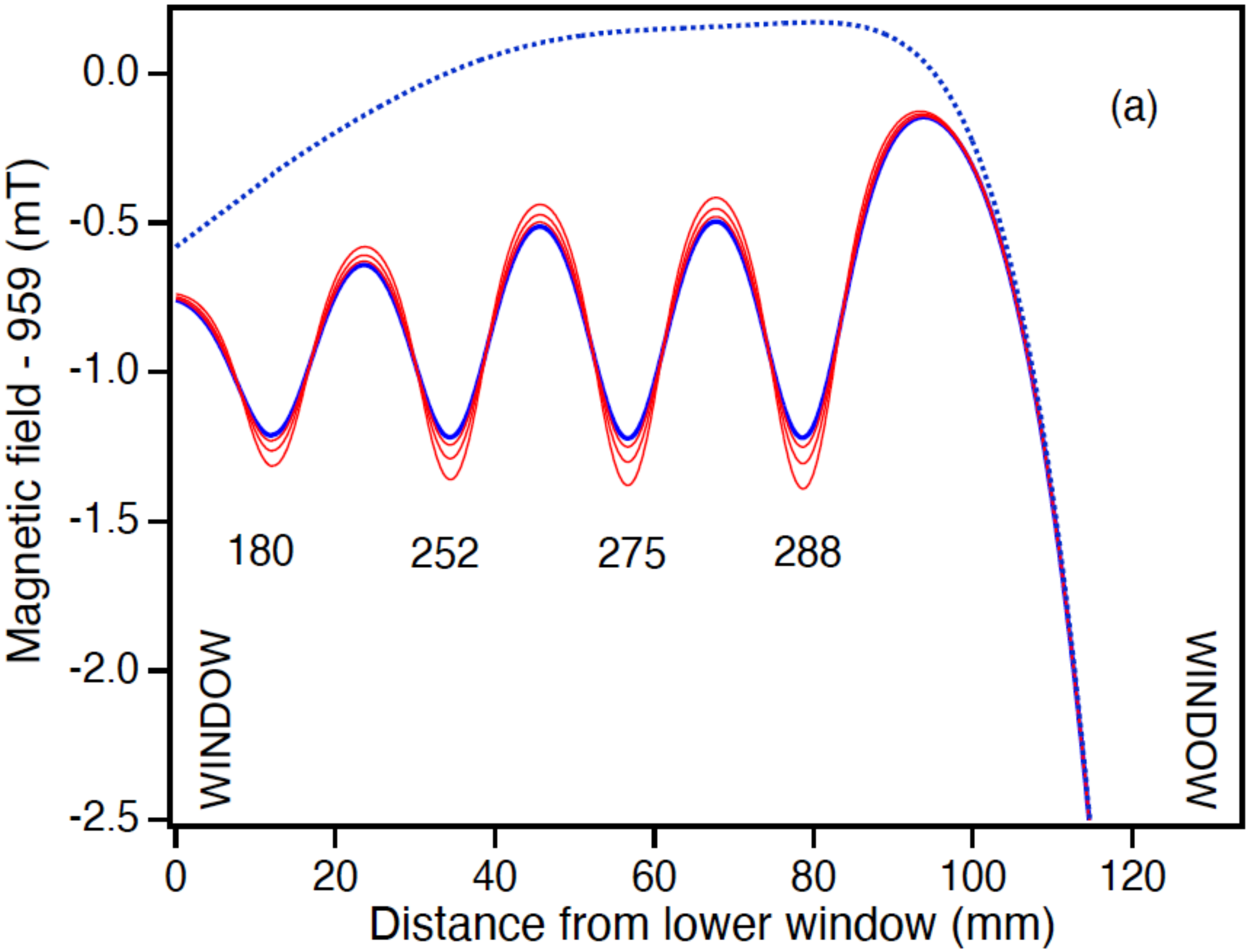

Project 8 phase II: Calibration measurement using ^{83m}Kr

Esfahani, et al, arXiv:2303.12055

Challenge with shallow trap:
Low T_2 decay rate at the CRES compatible gas density!

"Deep trap" configuration with:
- large pitch angle acceptance
- larger magnetic field variation
- but lower energy resolution

Detector response model verified for deep trap configuration!

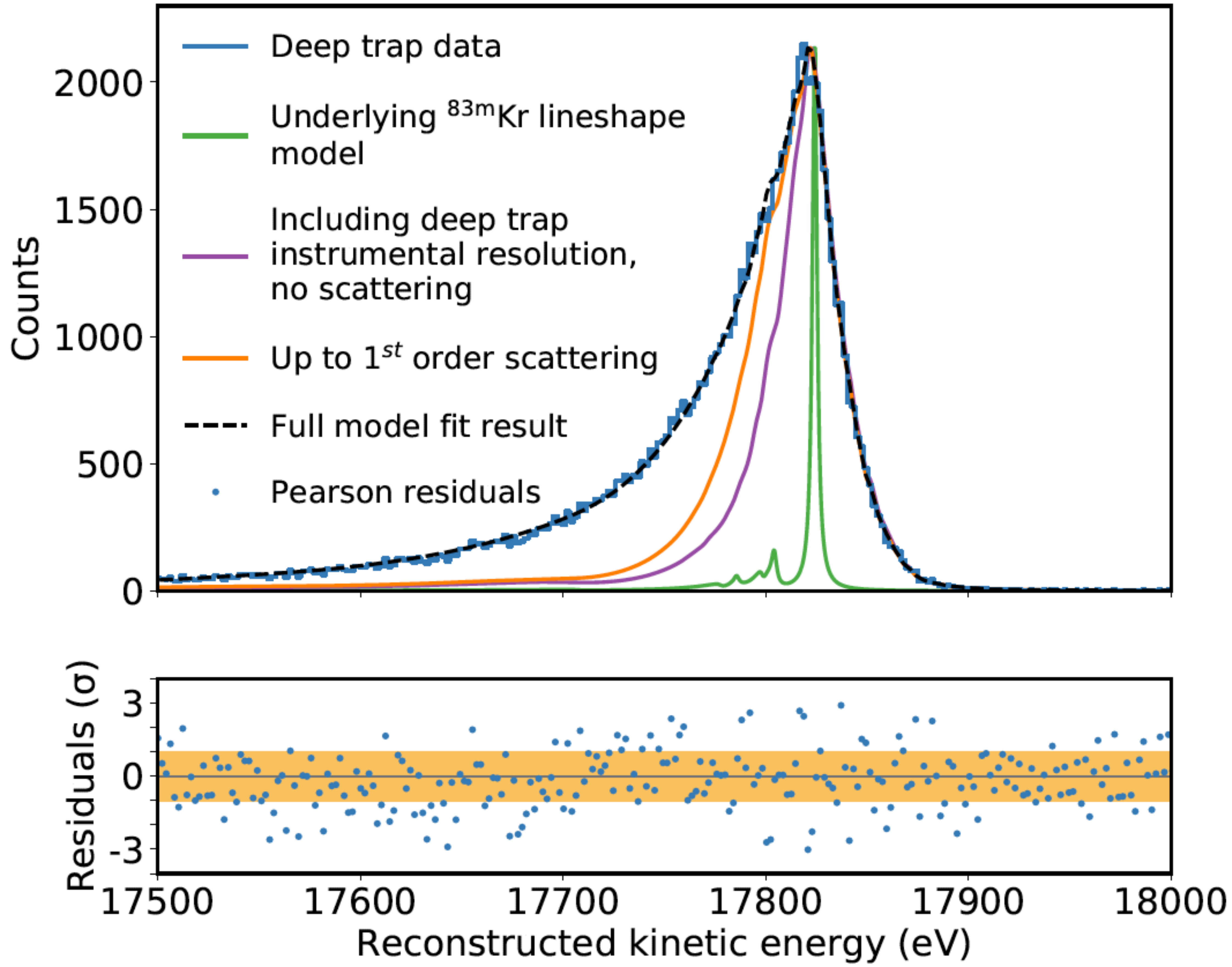

Project 8 phase II: Calibration measurement using ^{83m}Kr

Project 8 phase II: Calibration measurement using ^{83m}Kr

Detector response is frequency dependent!

Sweep position of 17.8 keV ^{83m}Kr across frequency ROI by changing the background field!

$$f_c = \frac{1}{2\pi} \frac{eB}{m_e + E_{kin}/c^2}$$

Project 8 phase II: Calibration measurement using ^{83m}Kr

Detector response is frequency dependent!

Sweep position of 17.8 keV ^{83m}Kr across frequency ROI by changing the background field!

$$f_c = \frac{1}{2\pi} \frac{eB}{m_e + E_{kin}/c^2}$$

Direct characterization of frequency response variation of waveguide setup

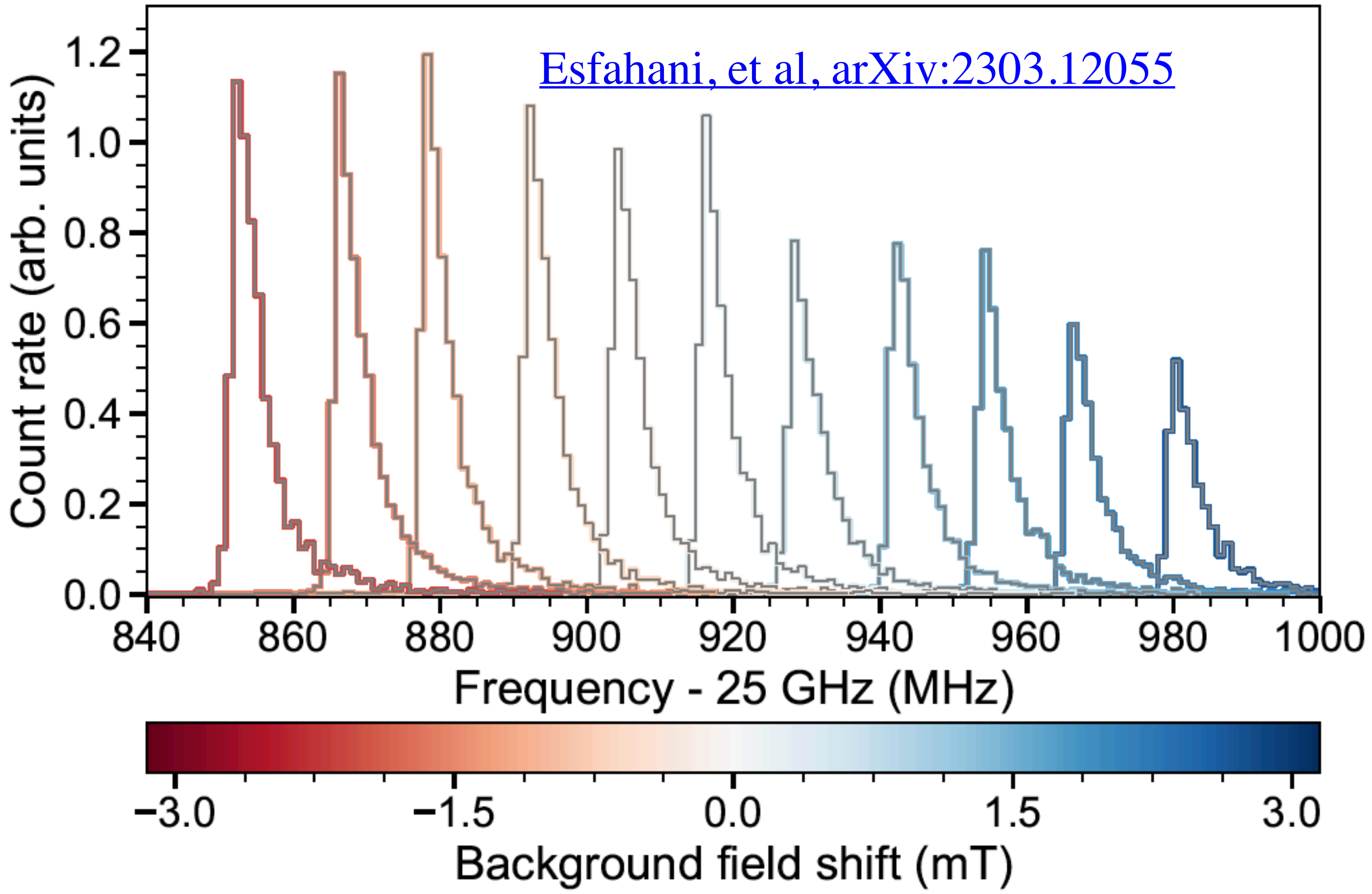

JG|U

Project 8 phase II: Calibration measurement using ^{83m}Kr

Detector response is frequency dependent!

Sweep position of 17.8 keV ^{83m}Kr across frequency ROI by changing the background field!

$$f_c = \frac{1}{2\pi} \frac{eB}{m_e + E_{kin}/c^2}$$

Direct characterization of frequency response variation of waveguide setup

Notch in detection efficiency:

- TM01 mode interaction in the waveguide "cavity" due to imperfections
- Characterized, quantitatively understood and accounted in the spectral analysis

Esfahani, et al, arXiv:2212.05048

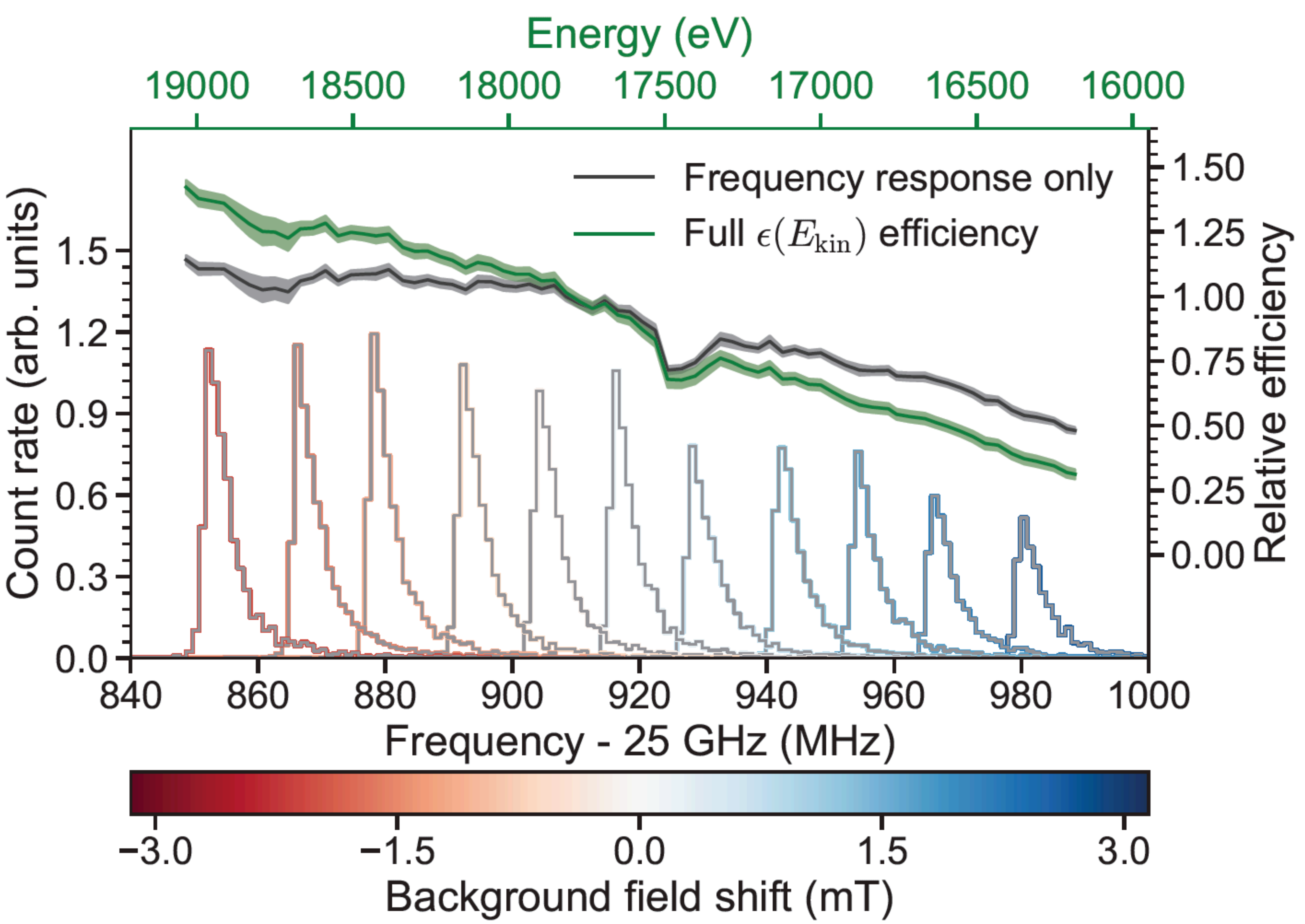

The complete analysis flow

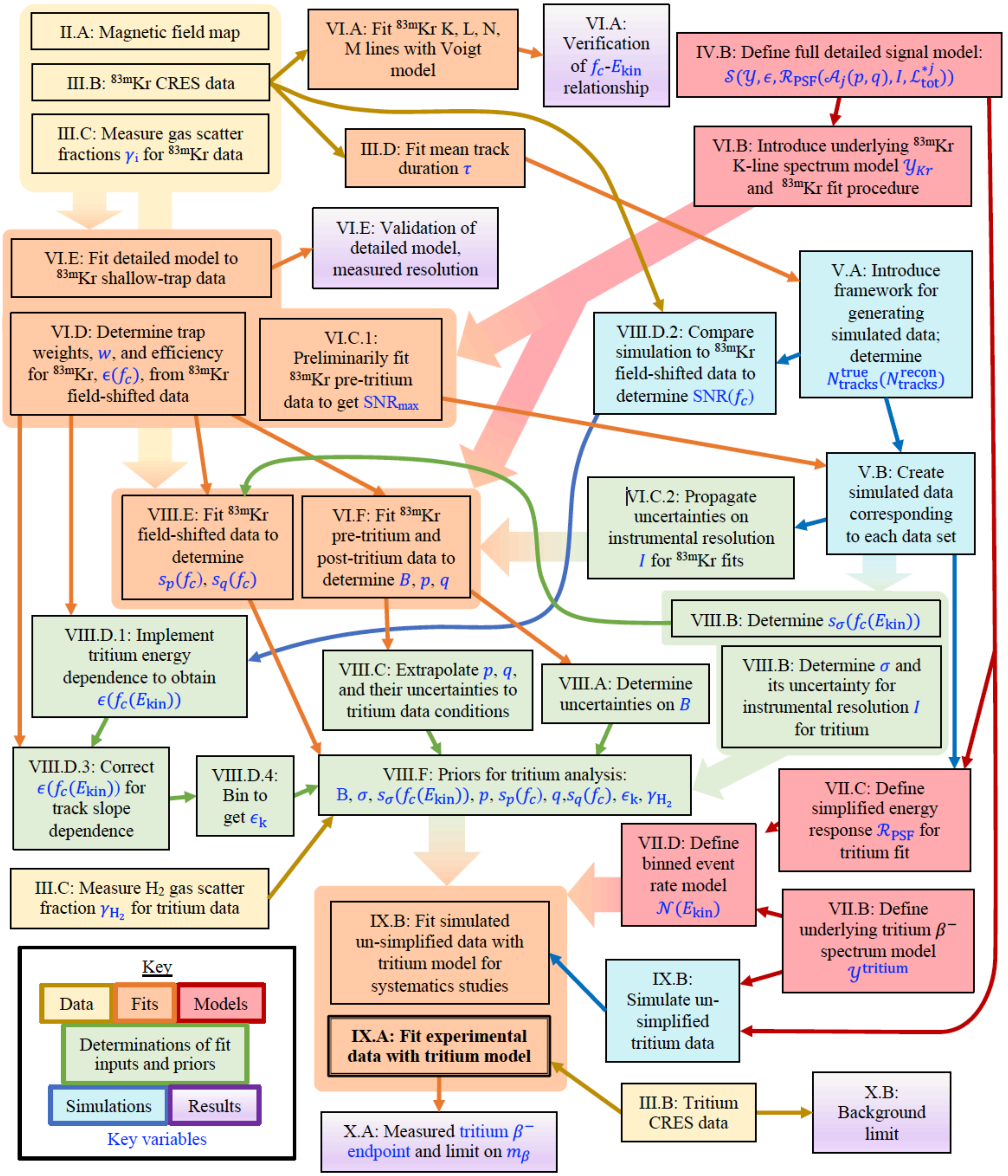

arXiv:2303.12055

The waveguide prototype setup revealed a lot of signal features that were unknown at the time of the waveguide cell construction

→ Development of a complex signal model to reflect

- Instrumental RF properties
- Instrumental thermodynamic properties
- Change of gas composition (^{3}He build-up)

→ Completely new analysis approach for new type of data!

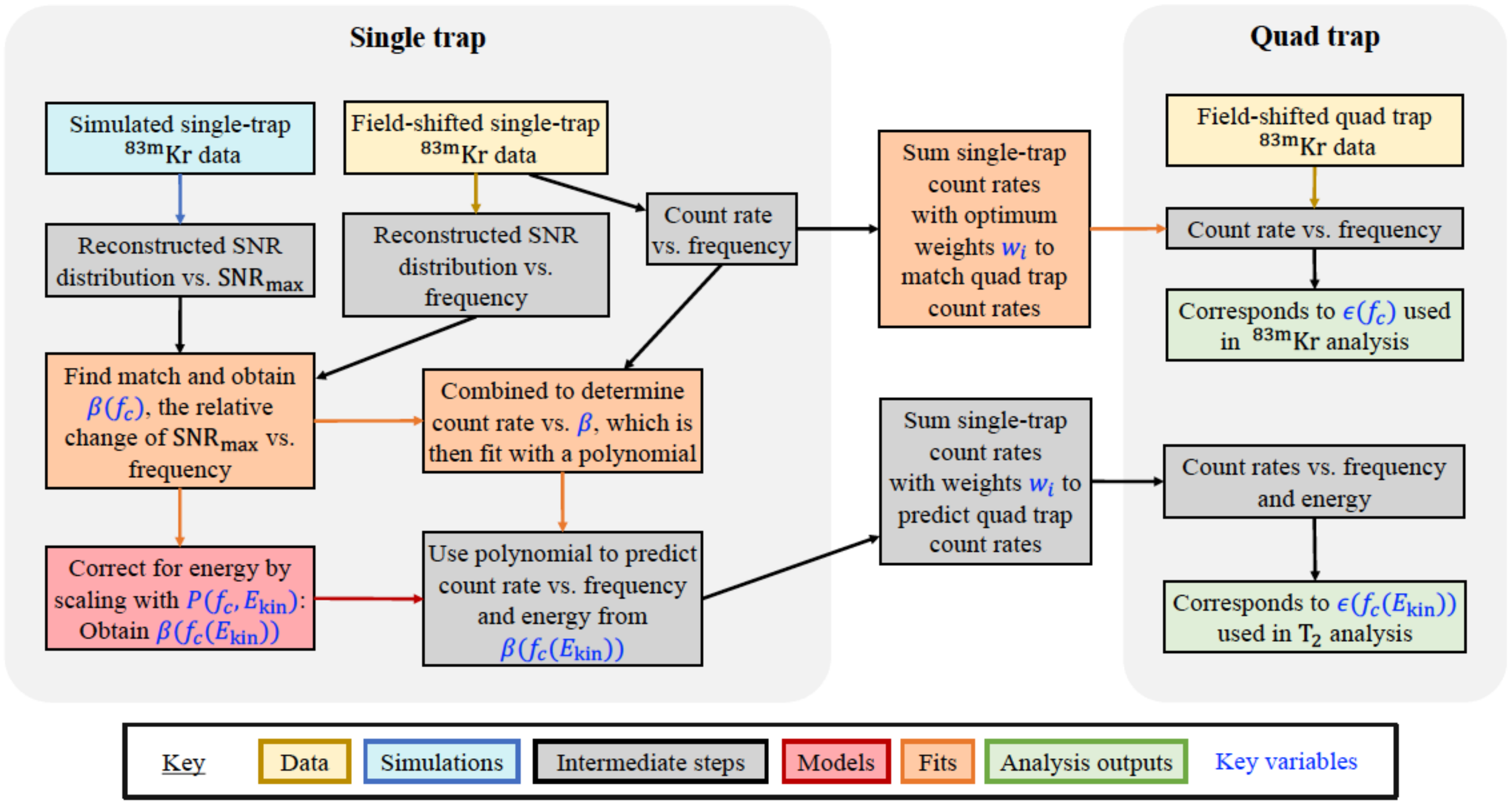

Project 8 phase II: results from molecular tritium

T_2 endpoint consistent with literature value

Esfahani, et al, arXiv:2303.12055

First frequency-based neutrino mass measurement

Extremely low background rate, no events beyond the endpoint region

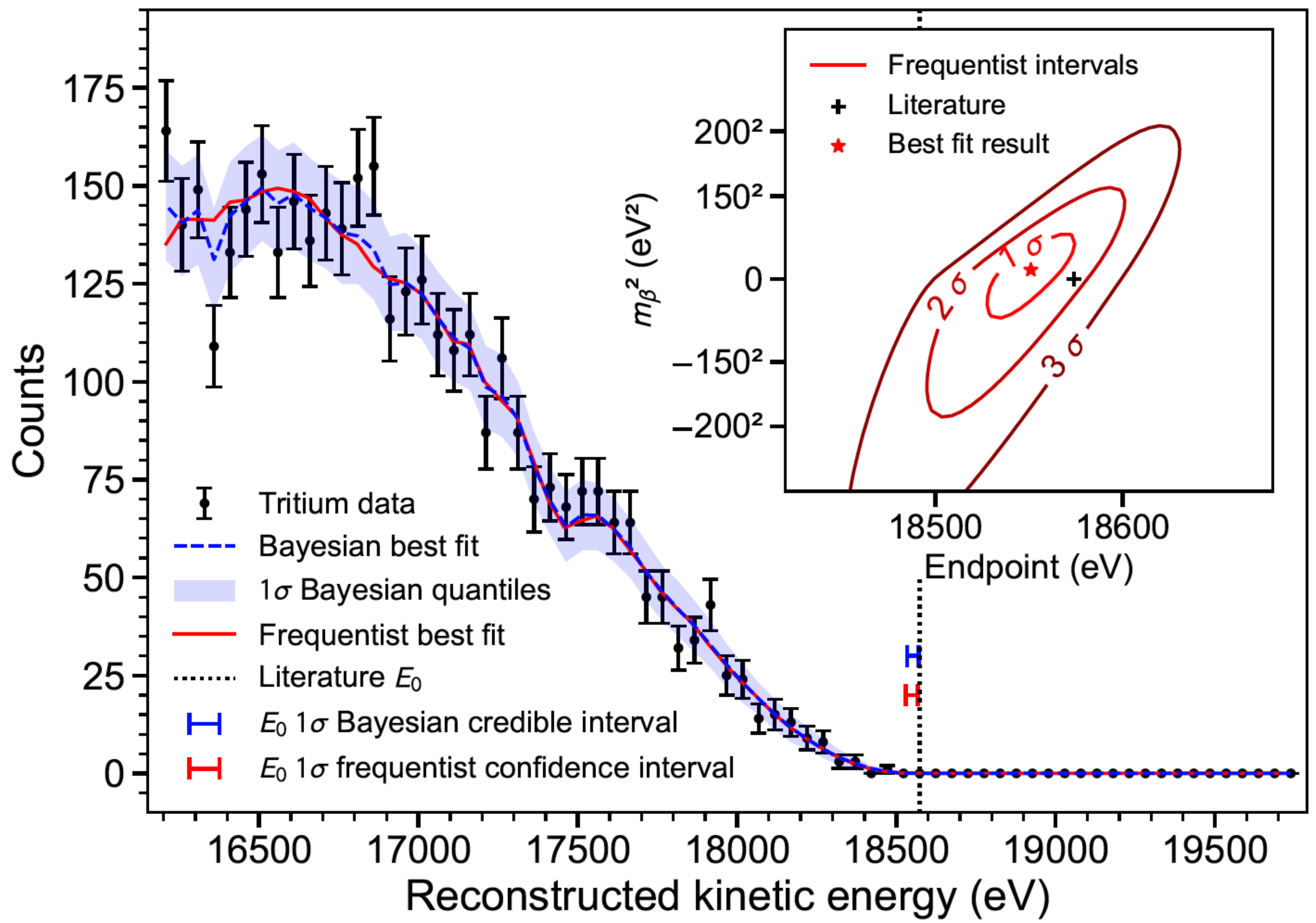

Frequentist and Bayesian analyses:

T2 endpoint: $E_0^{\text{Freq.}} = \left(18548^{+19}_{-19}\right)\ \text{eV}\ (1\sigma)$
$E_0^{\text{Bay.}} = \left(18553^{+18}_{-19}\right)\ \text{eV}\ (1\sigma)$

Neutrino mass: $m_\beta^{\text{Freq.}} \leq 152\,\text{eV/c}^2\ (90\,\%\,\text{C.L.})$
$m_\beta^{\text{Bay.}} \leq 155\,\text{eV/c}^2\ (90\,\%\,\text{C.I.})$

Background rate: $\leq 3 \times 10^{-10}\,\text{eV}^{-1}\text{s}^{-1}\ (90\,\%\,\text{C.I.})$

Project 8: The road to higher neutrino mass sensitivity …

Project 8: The road to higher neutrino mass sensitivity …

Improved control of systematic effects:

- Magnetic field optimization
- Magnetic field characterization
- Control of gas scattering
- Control of gas column composition and stability

Project 8: The road to higher neutrino mass sensitivity …

Improved control of systematic effects:

- Magnetic field optimization
- Magnetic field characterization
- Control of gas scattering
- Control of gas column composition and stability

Higher density ⇒ higher statistics, but much shorter tracks?

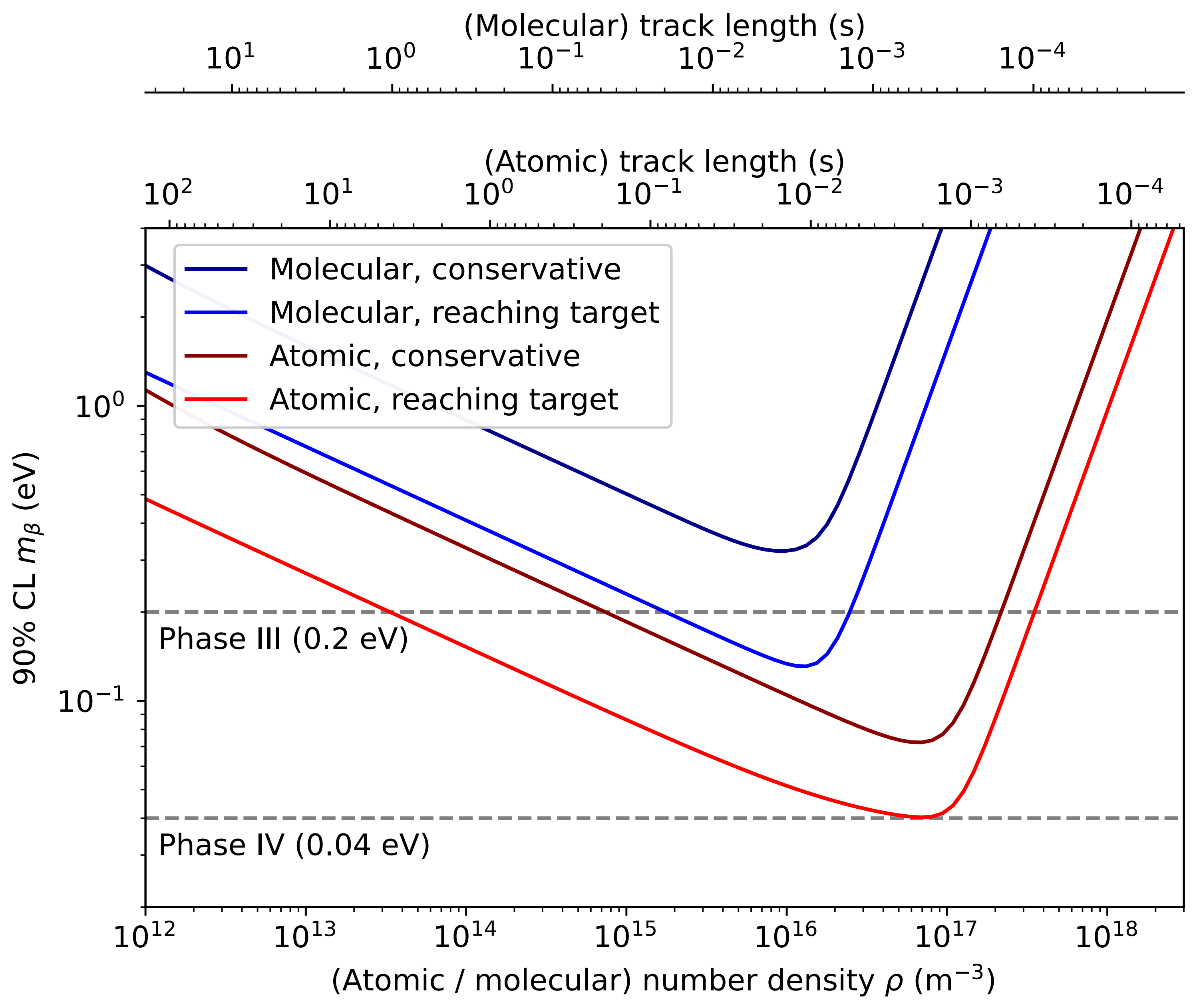

Project 8: The road to higher neutrino mass sensitivity …

Improved control of systematic effects:

- Magnetic field optimization
- Magnetic field characterization
- Control of gas scattering
- Control of gas column composition and stability

Higher density ⇒ higher statistics, but much shorter tracks?

Larger volume ⇒ higher statistics, but signal dilution

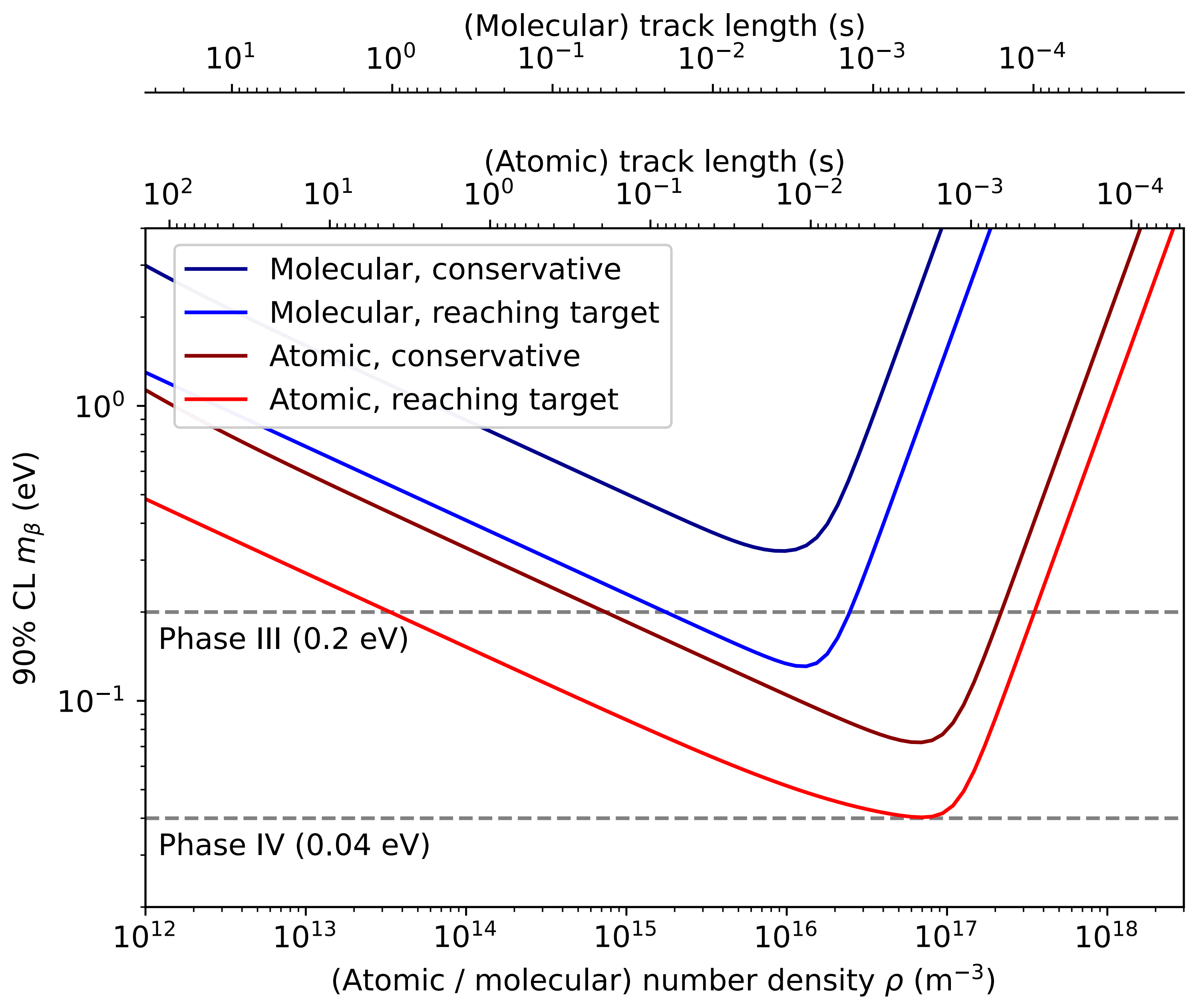

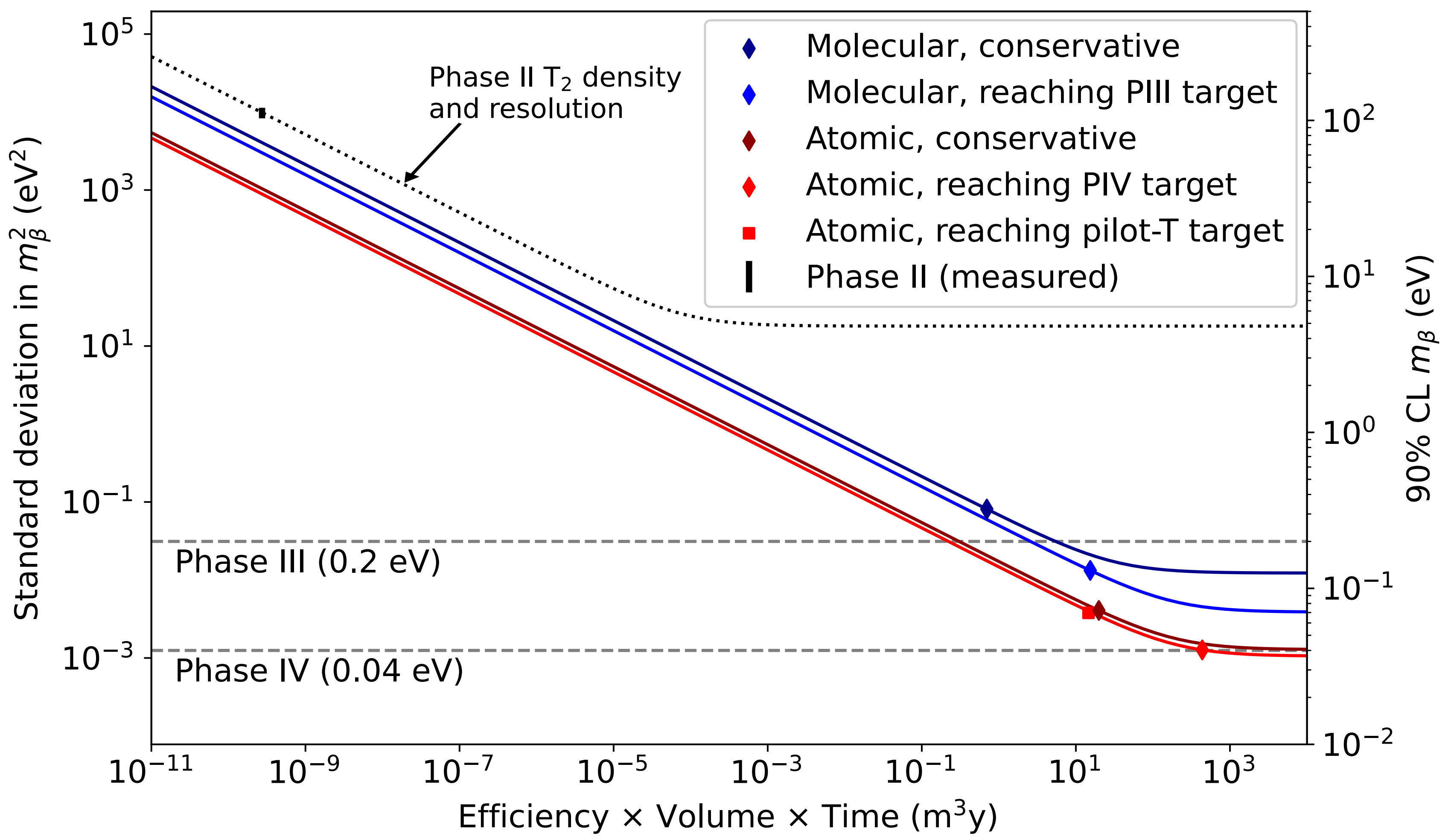

Project 8: The road to higher neutrino mass sensitivity …

Improved control of systematic effects:

- Magnetic field optimization
- Magnetic field characterization
- Control of gas scattering
- Control of gas column composition and stability

Higher density ⇒ higher statistics, but much shorter tracks?

Larger volume ⇒ higher statistics, but signal dilution

Development of cold atomic hydrogen/tritium sources

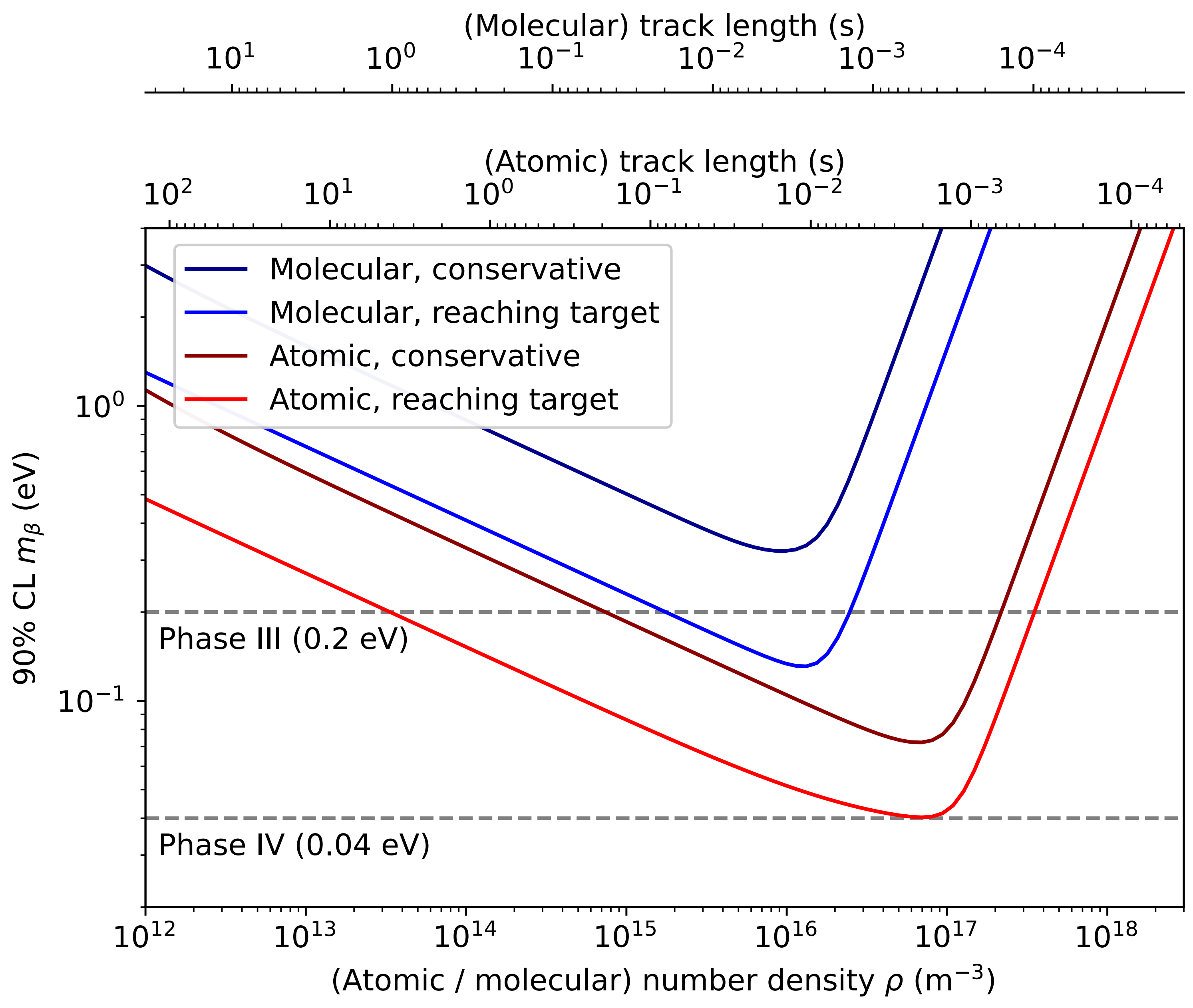

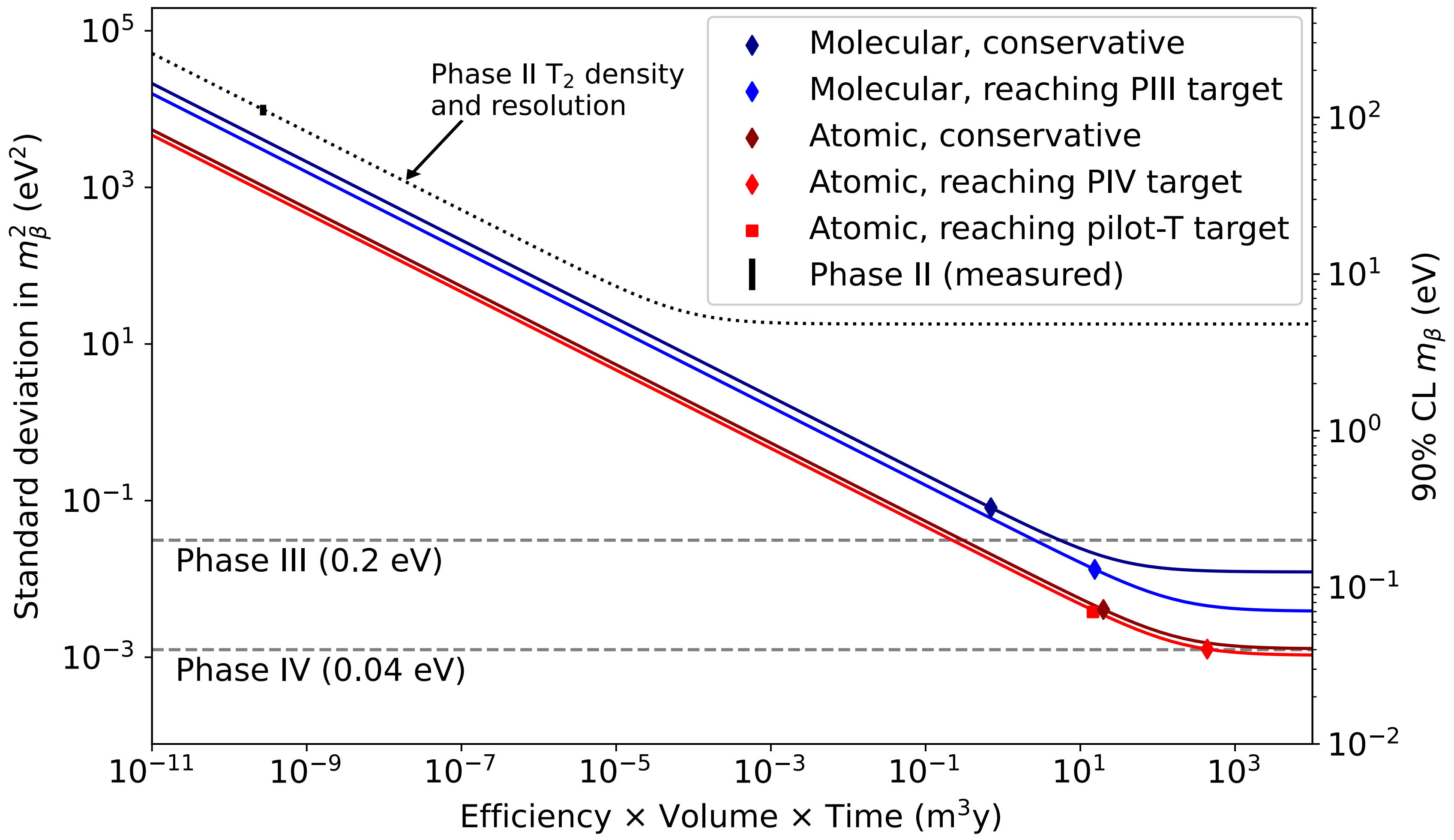

Future phases of Project 8: Larger volumes, atomic tritium, lower magnetic fields, …

Future phases of Project 8: Larger volumes, atomic tritium, lower magnetic fields, …

Phase I+ II have established CRES as a high-precision frequency-based single electron spectroscopy technology

JG|U

Future phases of Project 8: Larger volumes, atomic tritium, lower magnetic fields, …

Phase I+ II have established CRES as a high-precision frequency-based single electron spectroscopy technology

Phase III aims to establish the scaling relations to design an experiment with 40 meV mass sensitivity:

- Signal detection in a small RF cavity instead of a waveguide
  ⇒ Cavity CRES Apparatus (CCA)
- Scaling of the gas volume from mm^3 to m^3 and in low field
  ⇒ Low field Apparatus (LUCKEY/LFA)
- Production of trapped cold atomic hydrogen/tritium
  ⇒ Atomic Tritium Demonstrator (ATD)
- Scientific milestone measurements along the way!

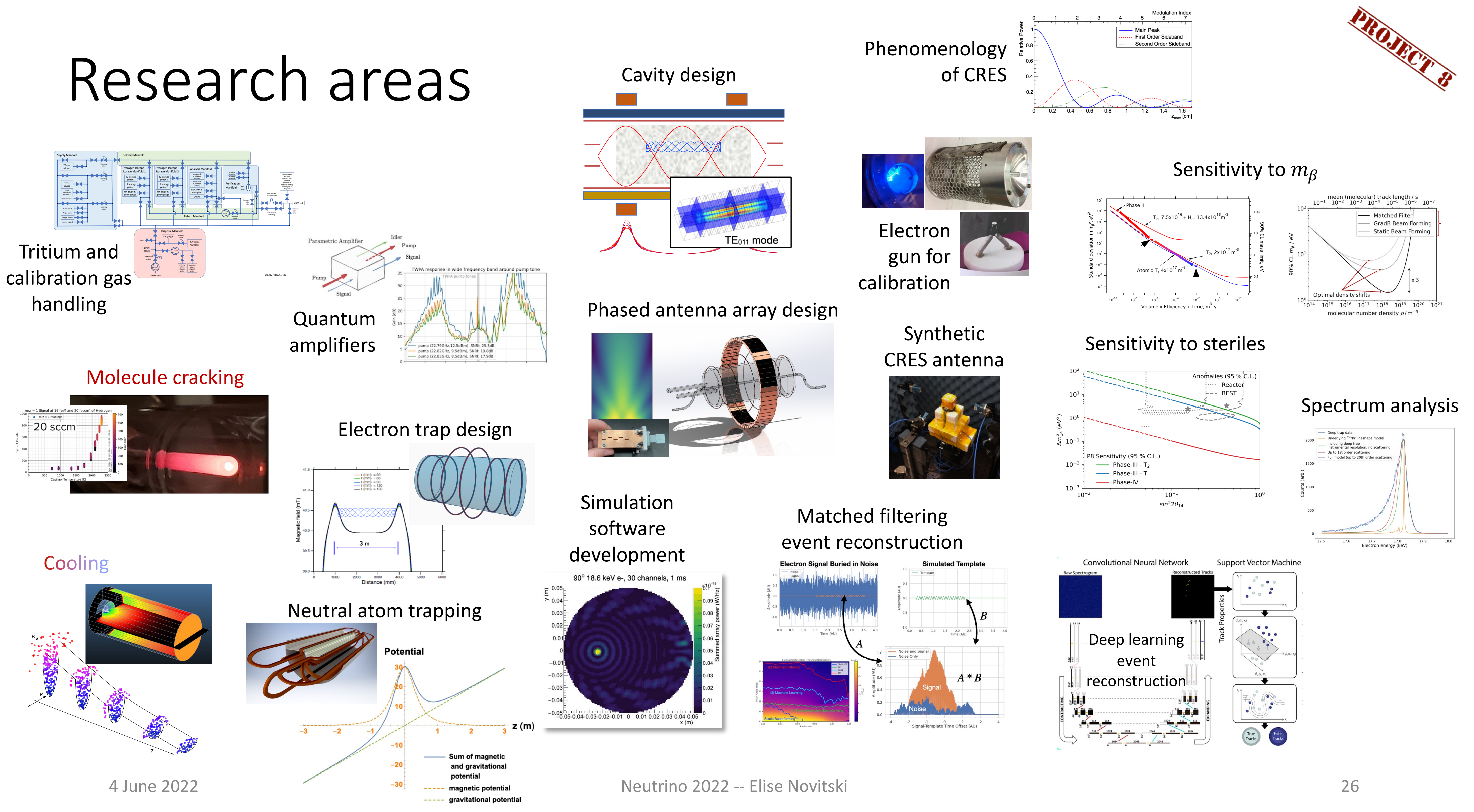

Future phases of Project 8: Larger volumes, atomic tritium, lower magnetic fields, …

Phase I+ II have established CRES as a high-precision frequency-based single electron spectroscopy technology

Phase III aims to establish the scaling relations to design an experiment with 40 meV mass sensitivity:

- Signal detection in a small RF cavity instead of a waveguide
  $\Rightarrow$ Cavity CRES Apparatus (CCA)
- Scaling of the gas volume from mm^3 to m^3 and in low field
  $\Rightarrow$ Low field Apparatus (LUCKEY/LFA)
- Production of trapped cold atomic hydrogen/tritium
  $\Rightarrow$ Atomic Tritium Demonstrator (ATD)
- Scientific milestone measurements along the way!

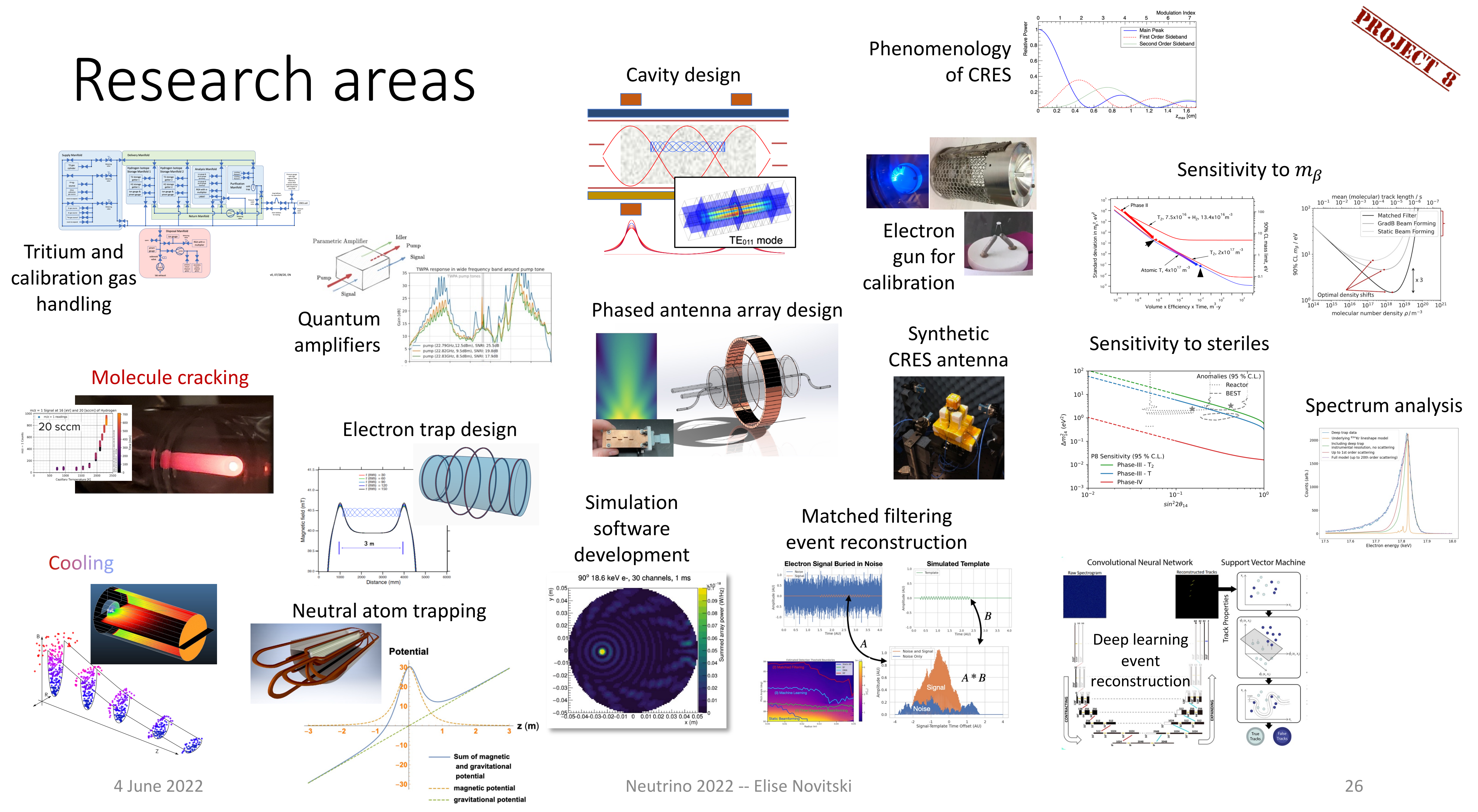

Phase IV: Ultimate sensitivity phase with (then) established technology

Phase III: development of all required technologies

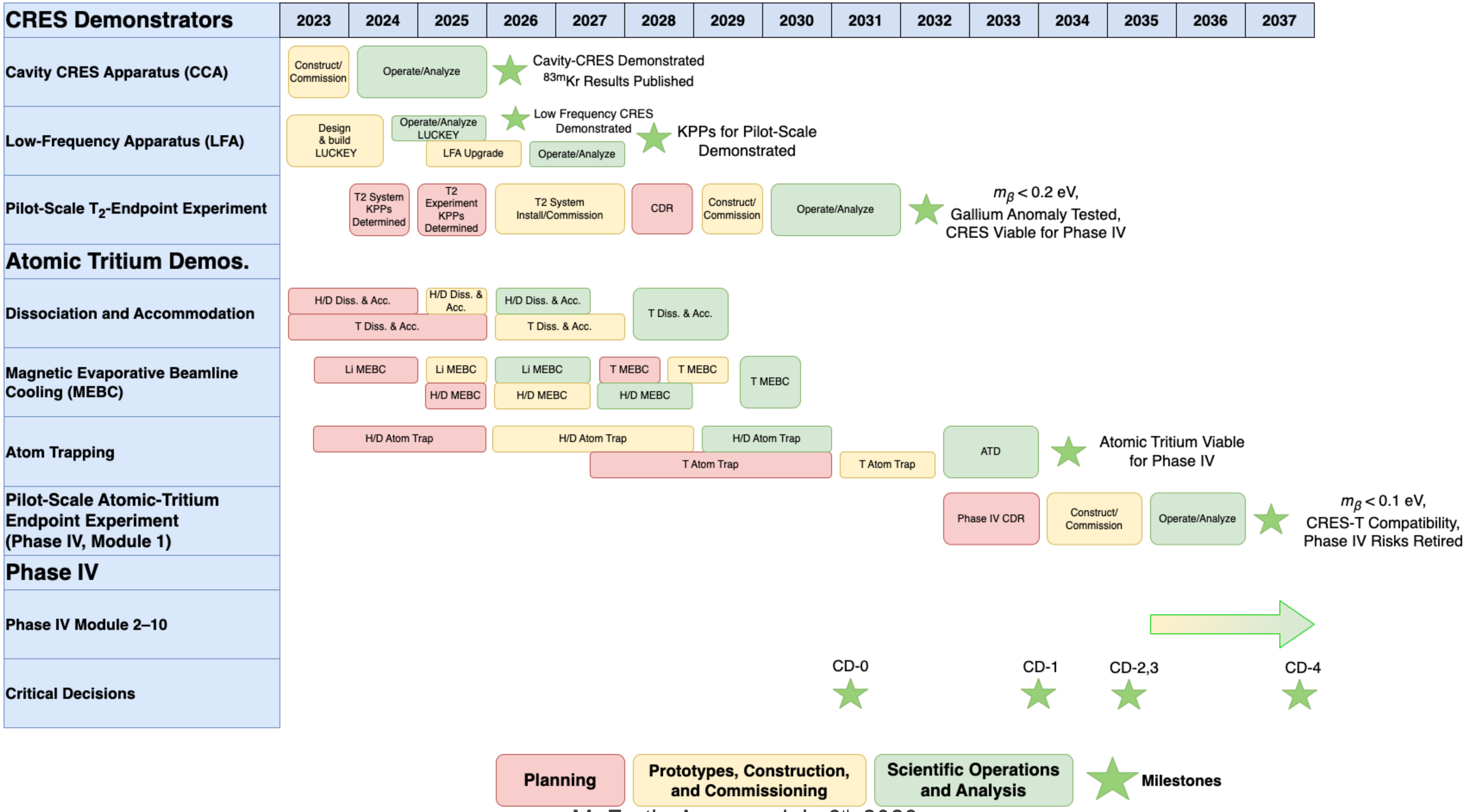

Phase III: development of all required technologies

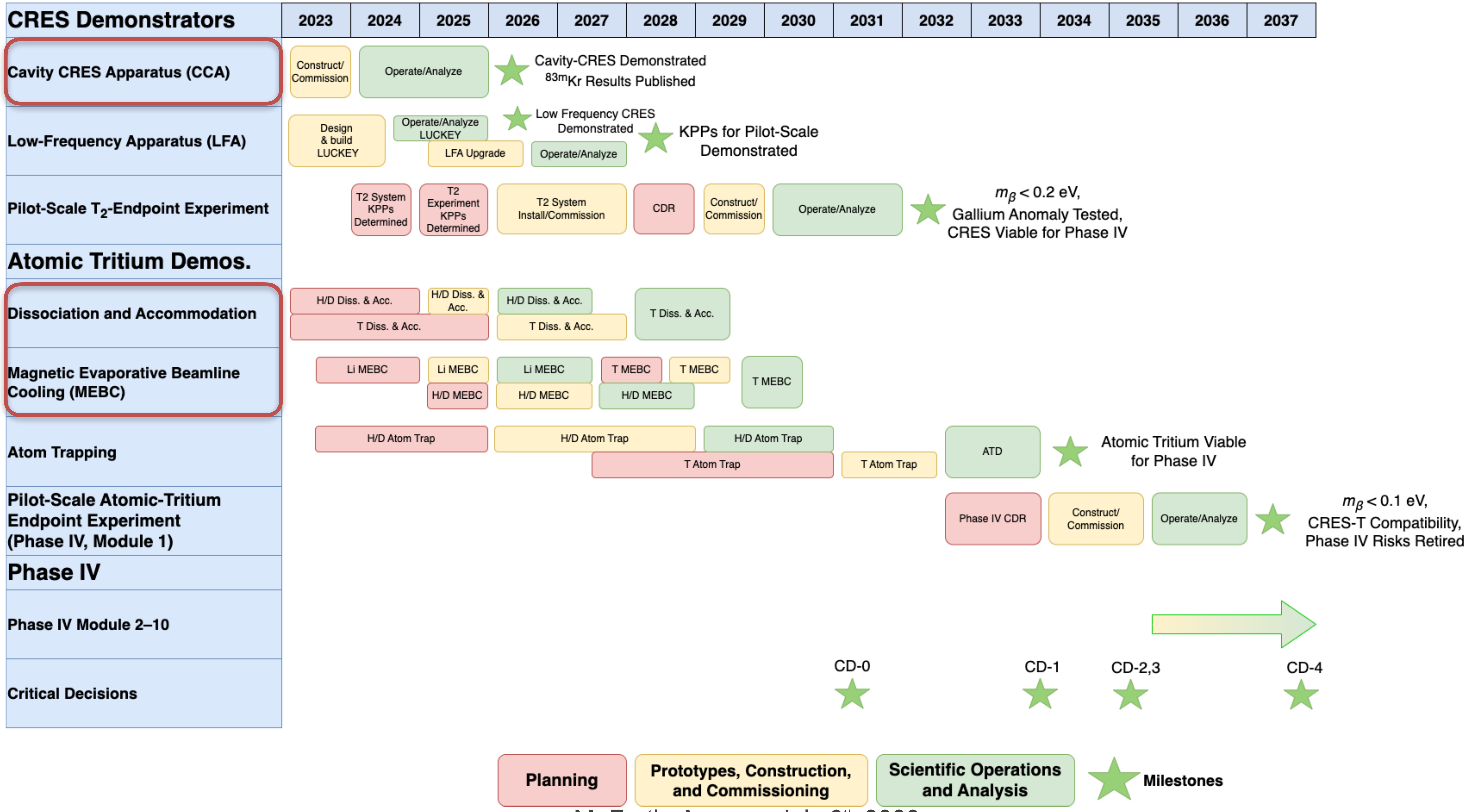

JG|U

Phase III Cavity CRES apparatus (CCA)

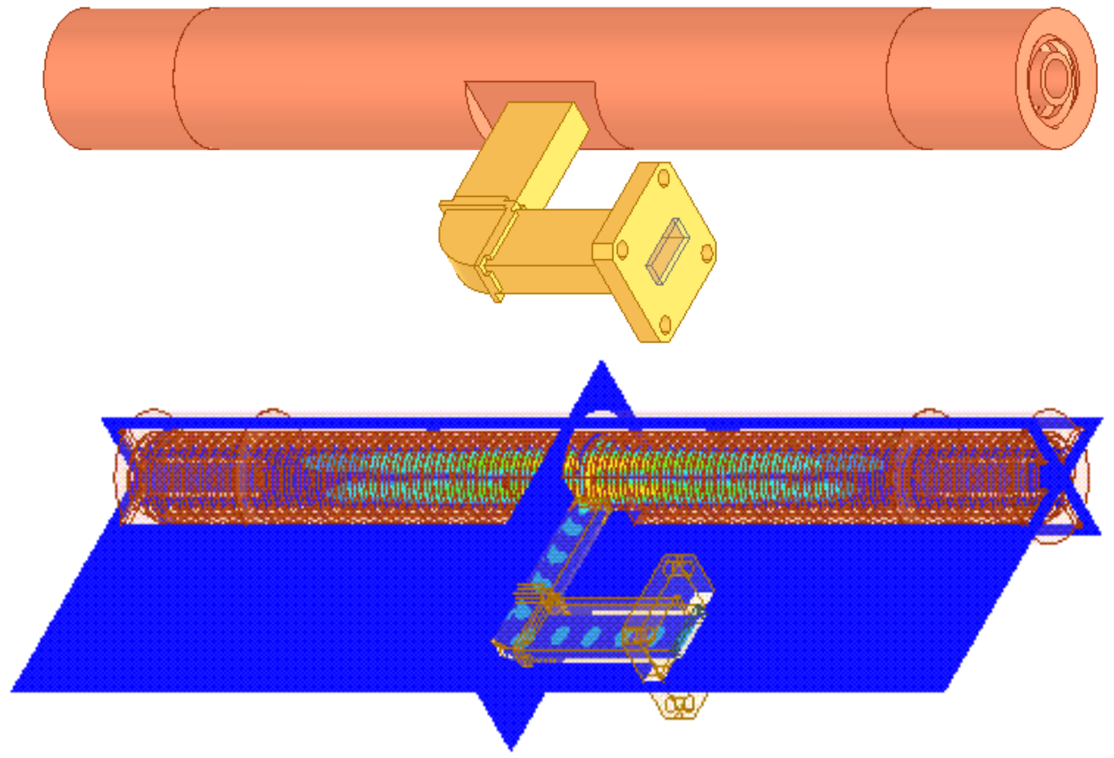

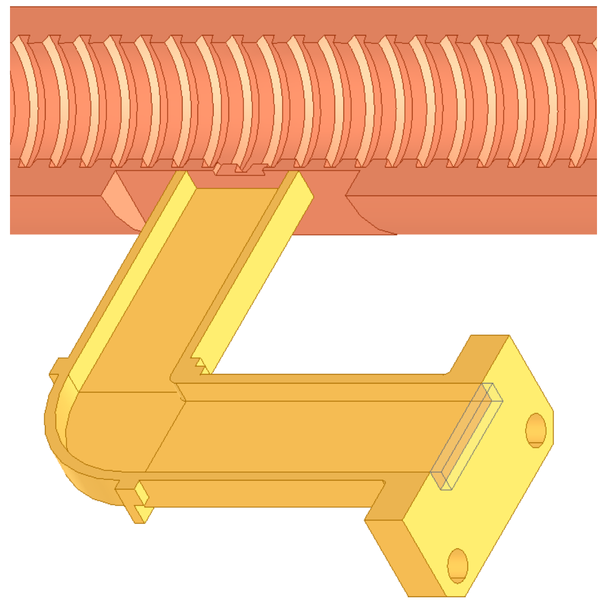

Phase III Cavity CRES apparatus (CCA)

Physically open ended cavity with coupling to waveguide

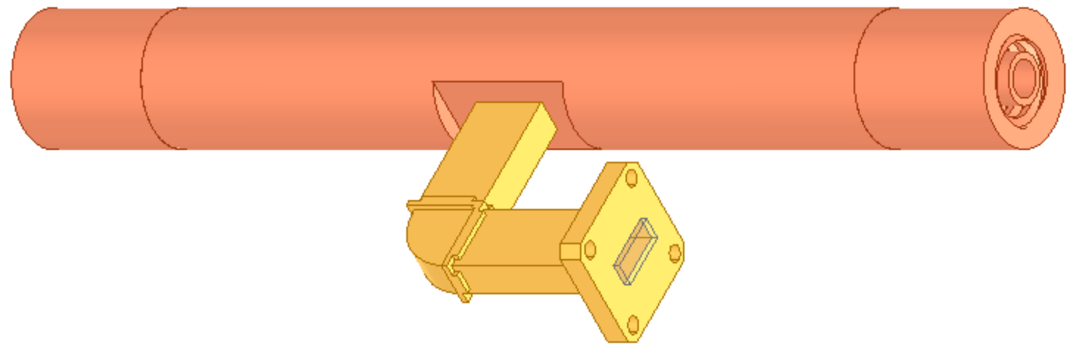

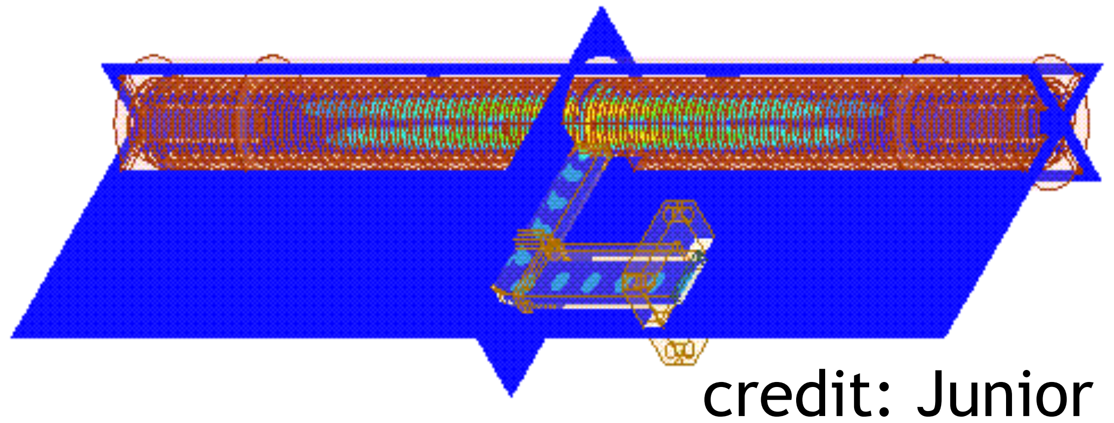

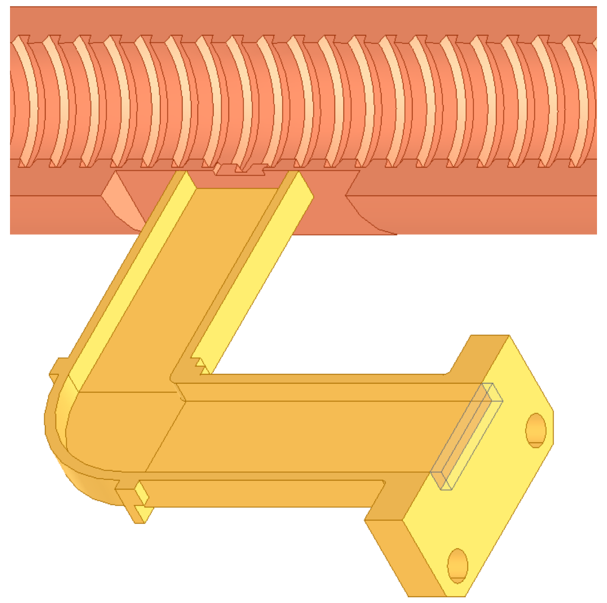

credit: Junior Peña and Juliana Stachurska

Phase III Cavity CRES apparatus (CCA)

Physically open ended cavity with coupling to waveguide

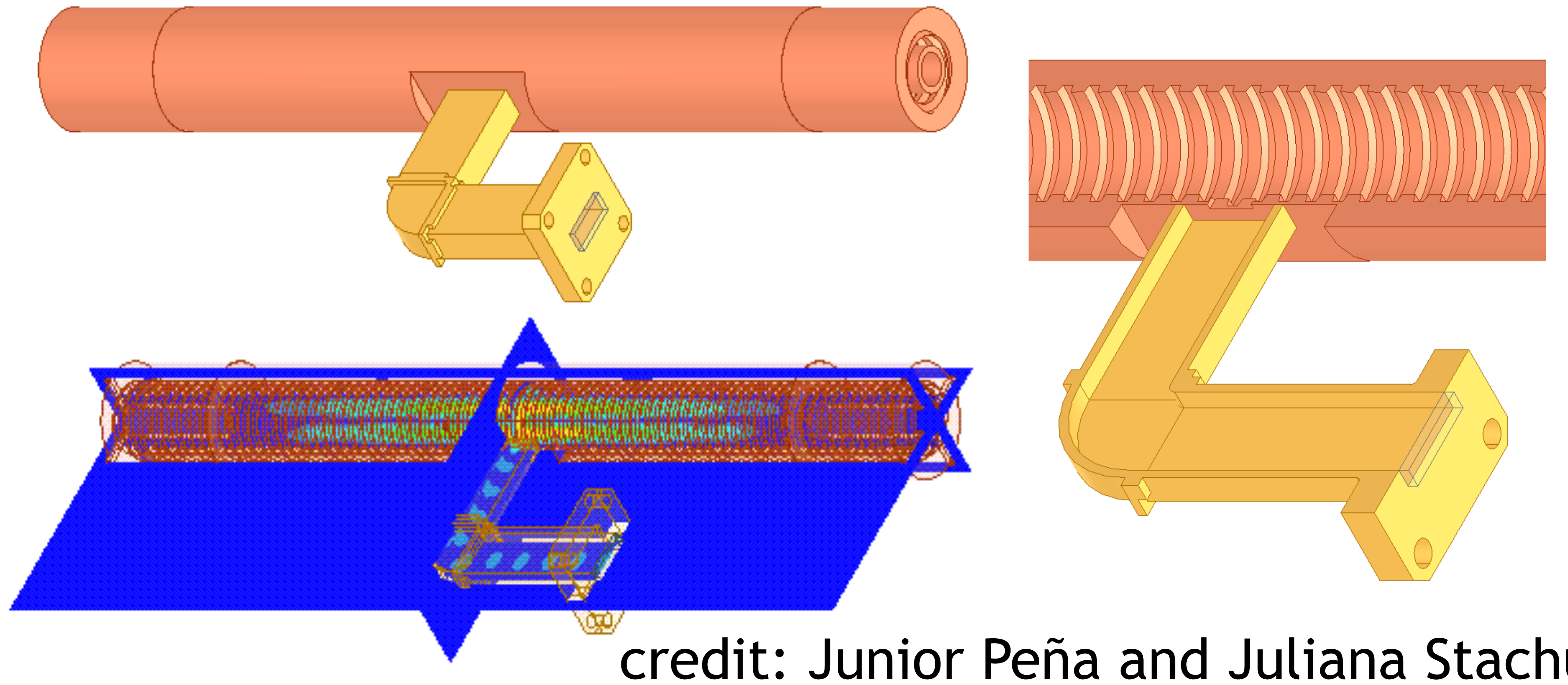

credit: Junior Peña and Juliana Stachurska

- Need to establish the signal model for e in cavity
- Need to demonstrate sufficient power collection
- Need to demonstrate the analysis capabilities

JG|U

Phase III Cavity CRES apparatus (CCA)

Physically open ended cavity with coupling to waveguide

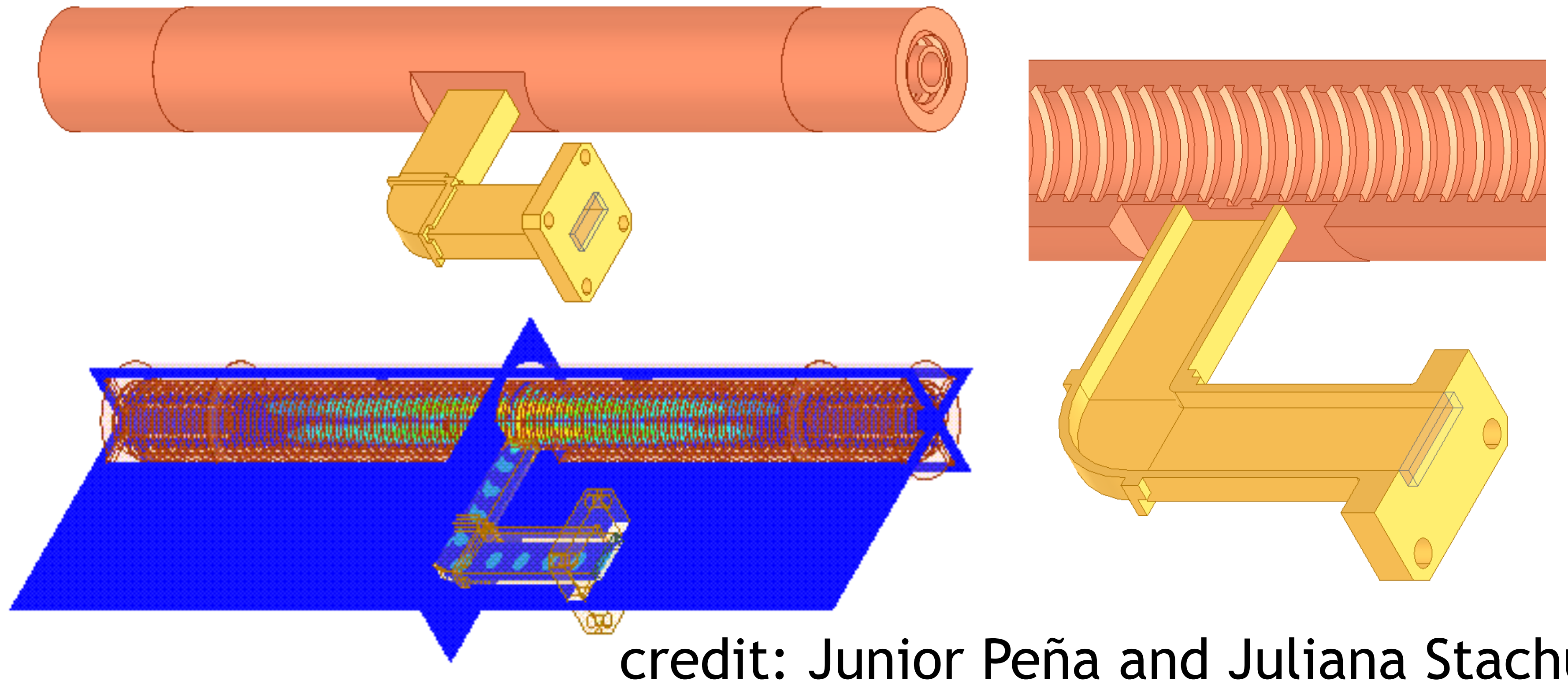

credit: Junior Peña and Juliana Stachurska

- Need to establish the signal model for e in cavity
- Need to demonstrate sufficient power collection
- Need to demonstrate the analysis capabilities
- Will use a ~1T MRI magnet for re-use of RF instrumentation

Phase III Cavity CRES apparatus (CCA)

Physically open ended cavity with coupling to waveguide

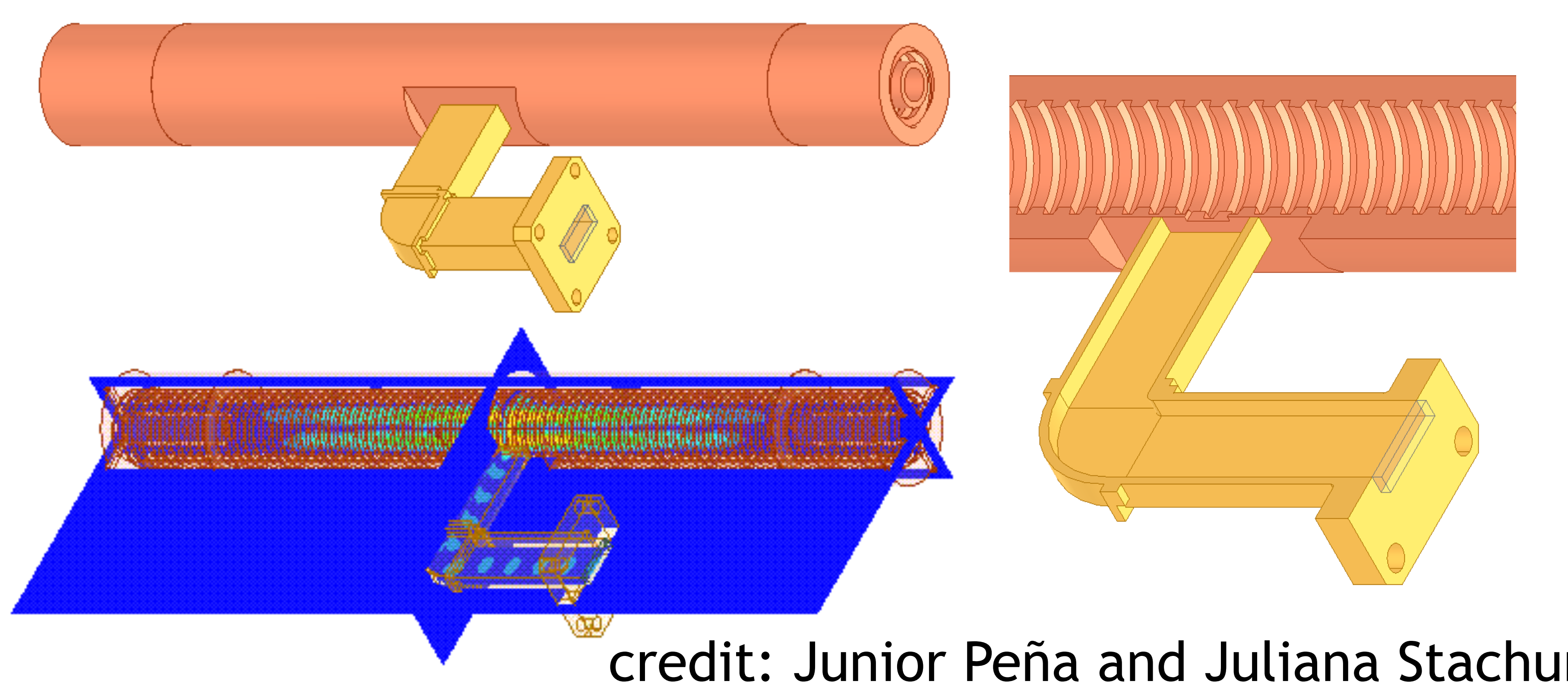

credit: Junior Peña and Juliana Stachurska

- Need to establish the signal model for e in cavity
- Need to demonstrate sufficient power collection
- Need to demonstrate the analysis capabilities
- Will use a ~1T MRI magnet for re-use of RF instrumentation

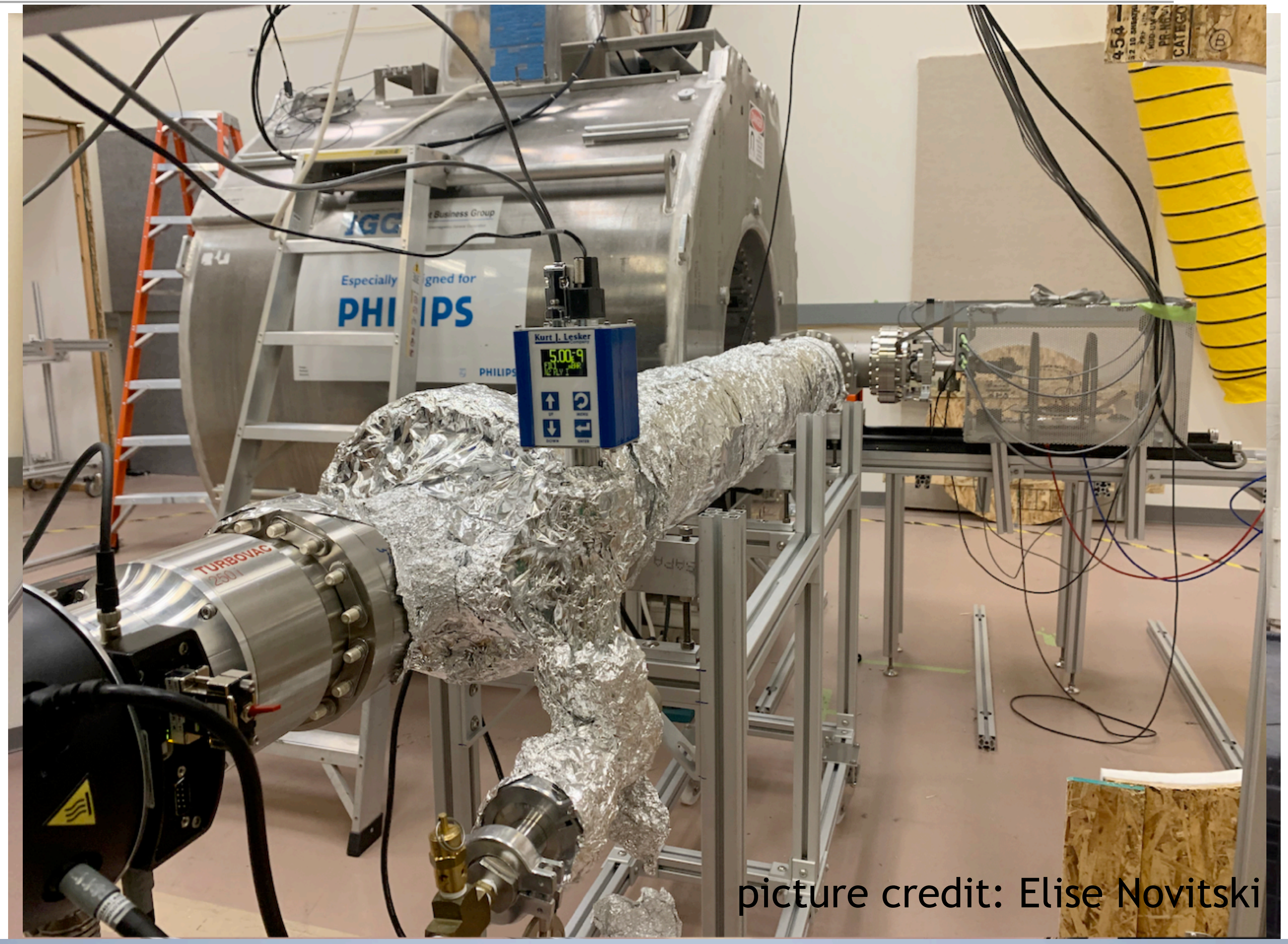

picture credit: Elise Novitski

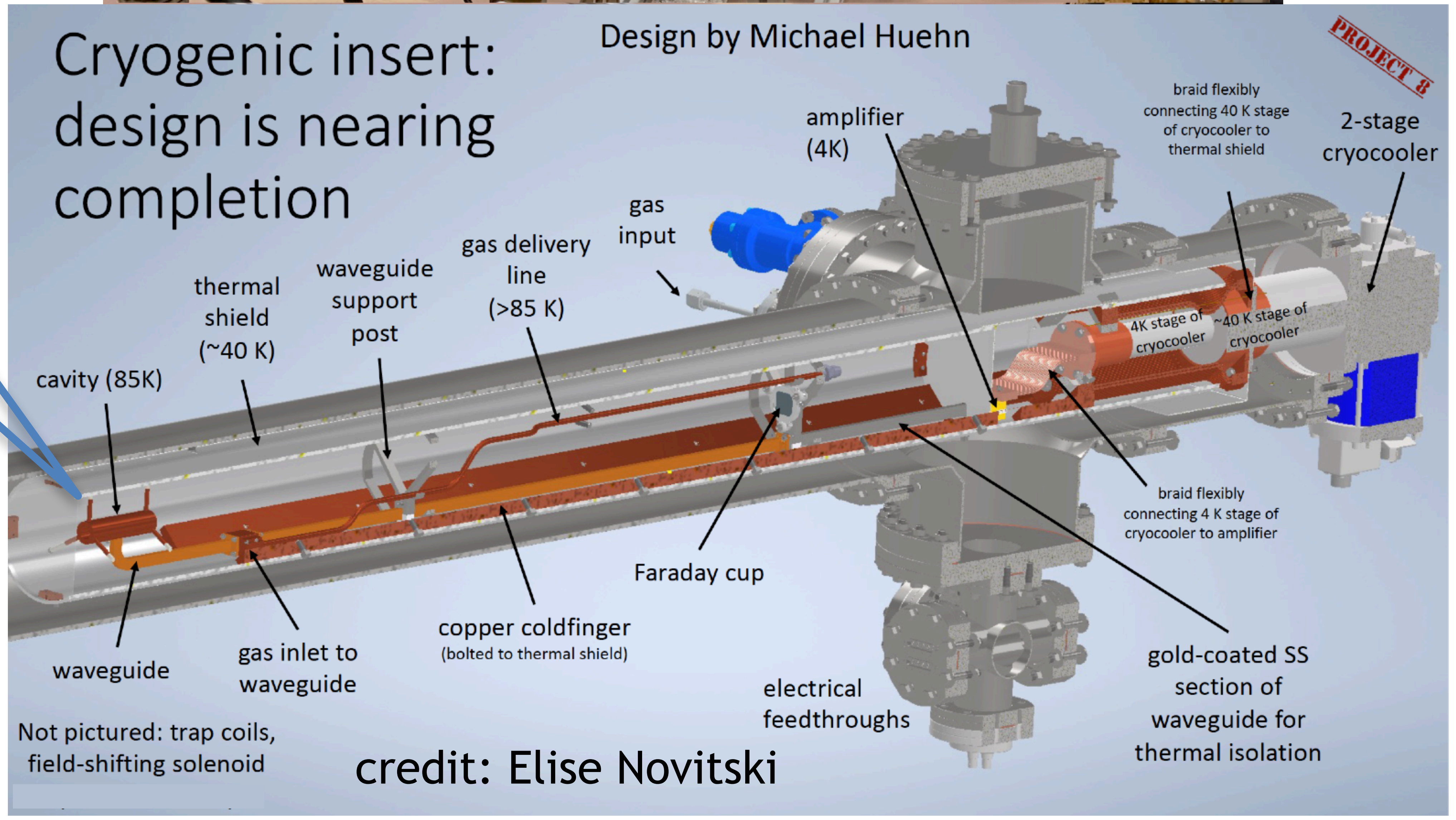

credit: Elise Novitski

Phase III Cavity CRES apparatus (CCA)

Physically open ended cavity with coupling to waveguide

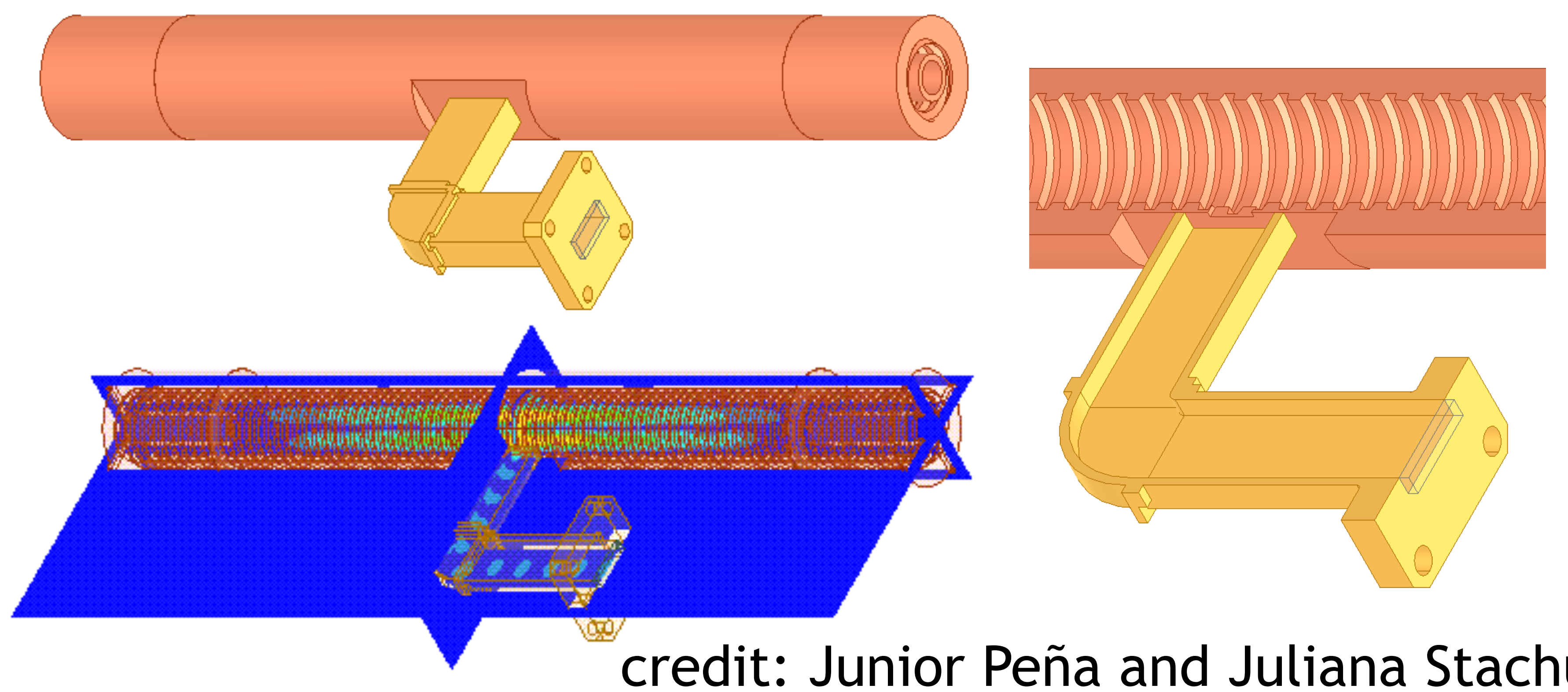

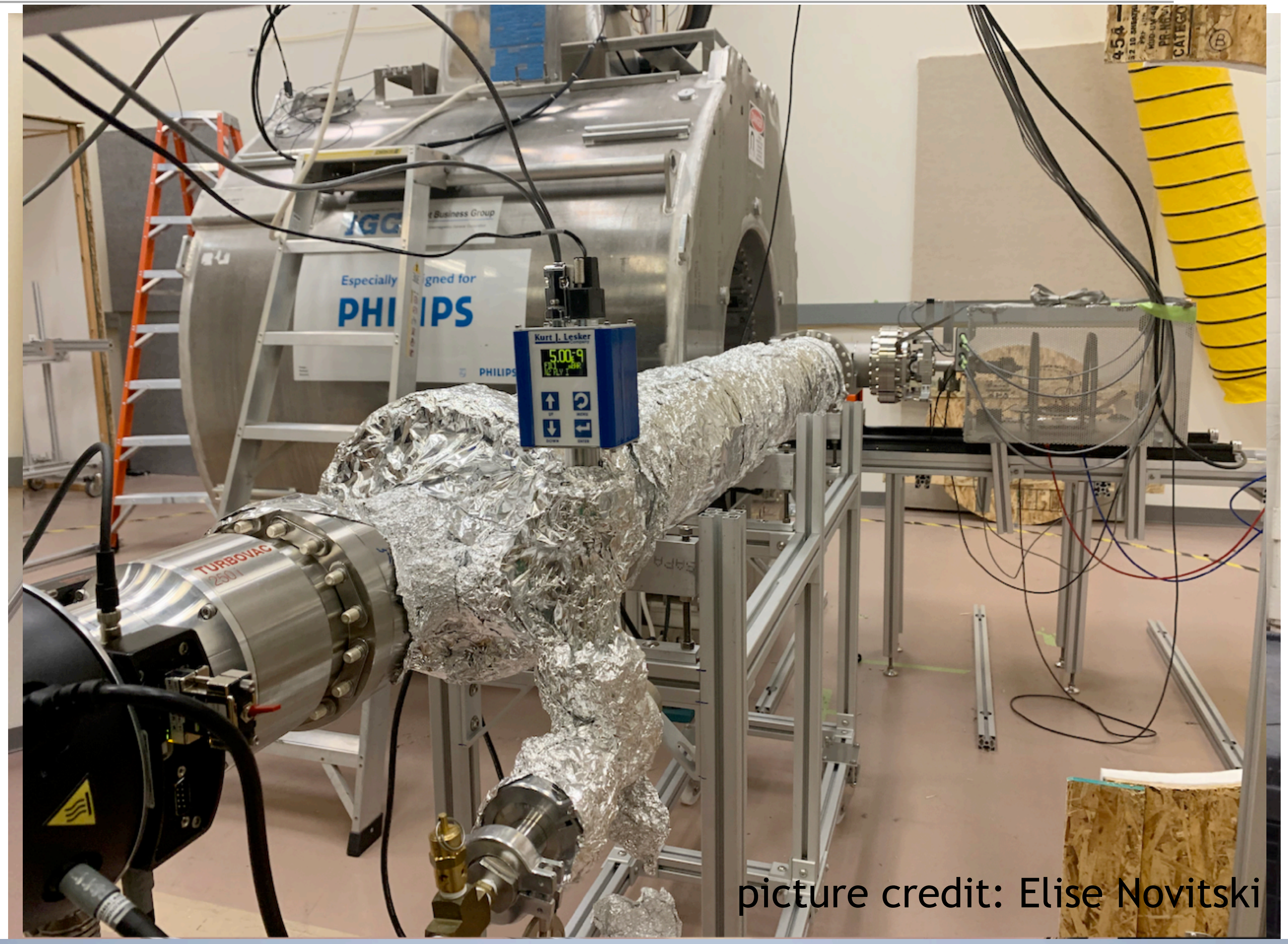

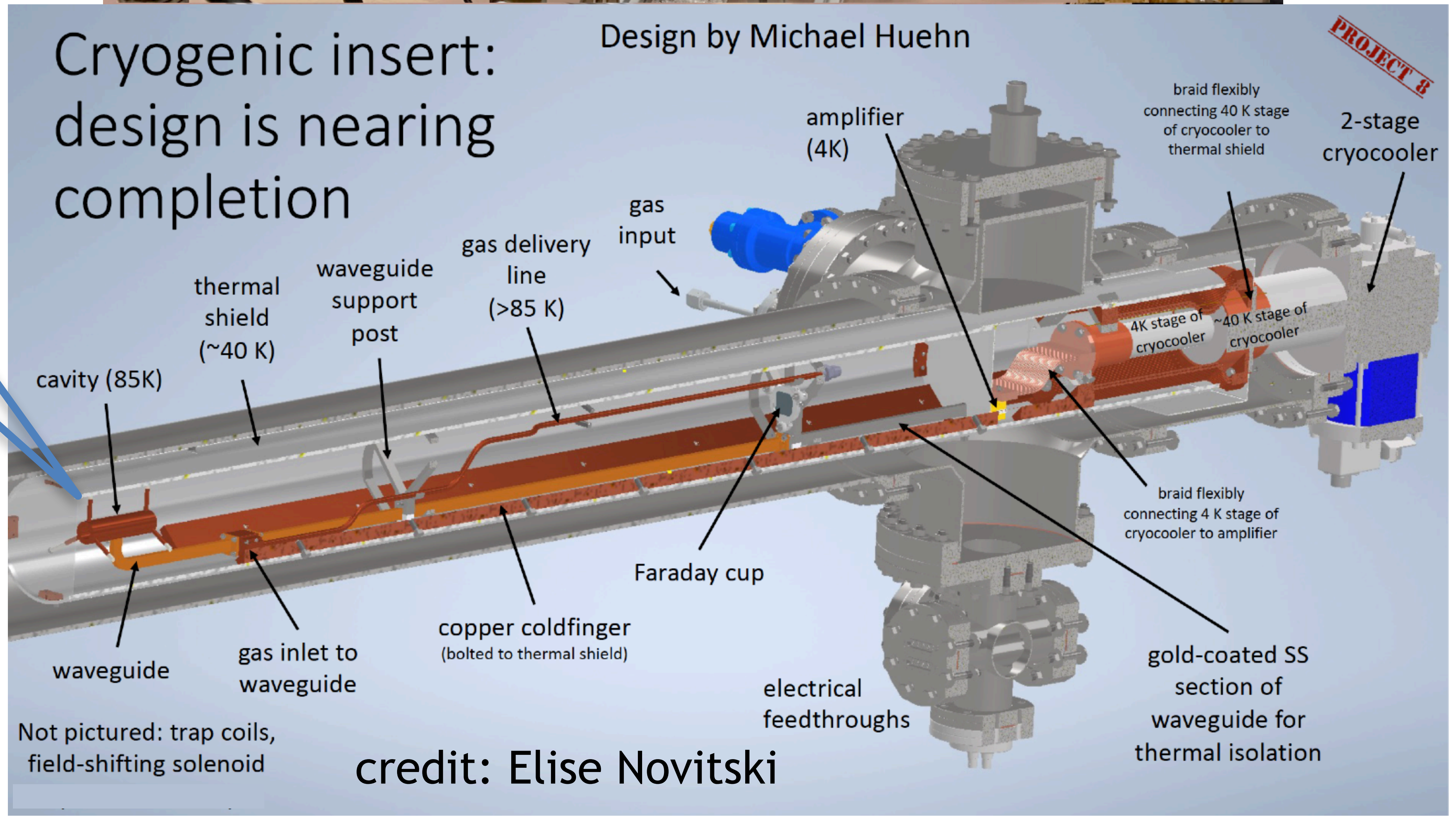

- Need to establish the signal model for e in cavity
- Need to demonstrate sufficient power collection
- Need to demonstrate the analysis capabilities
- Will use a ~1T MRI magnet for re-use of RF instrumentation

This is our next apparatus to come online!

Phase III: Atomic Tritium Demonstrator

Need to confine cold atomic hydrogen/tritium!

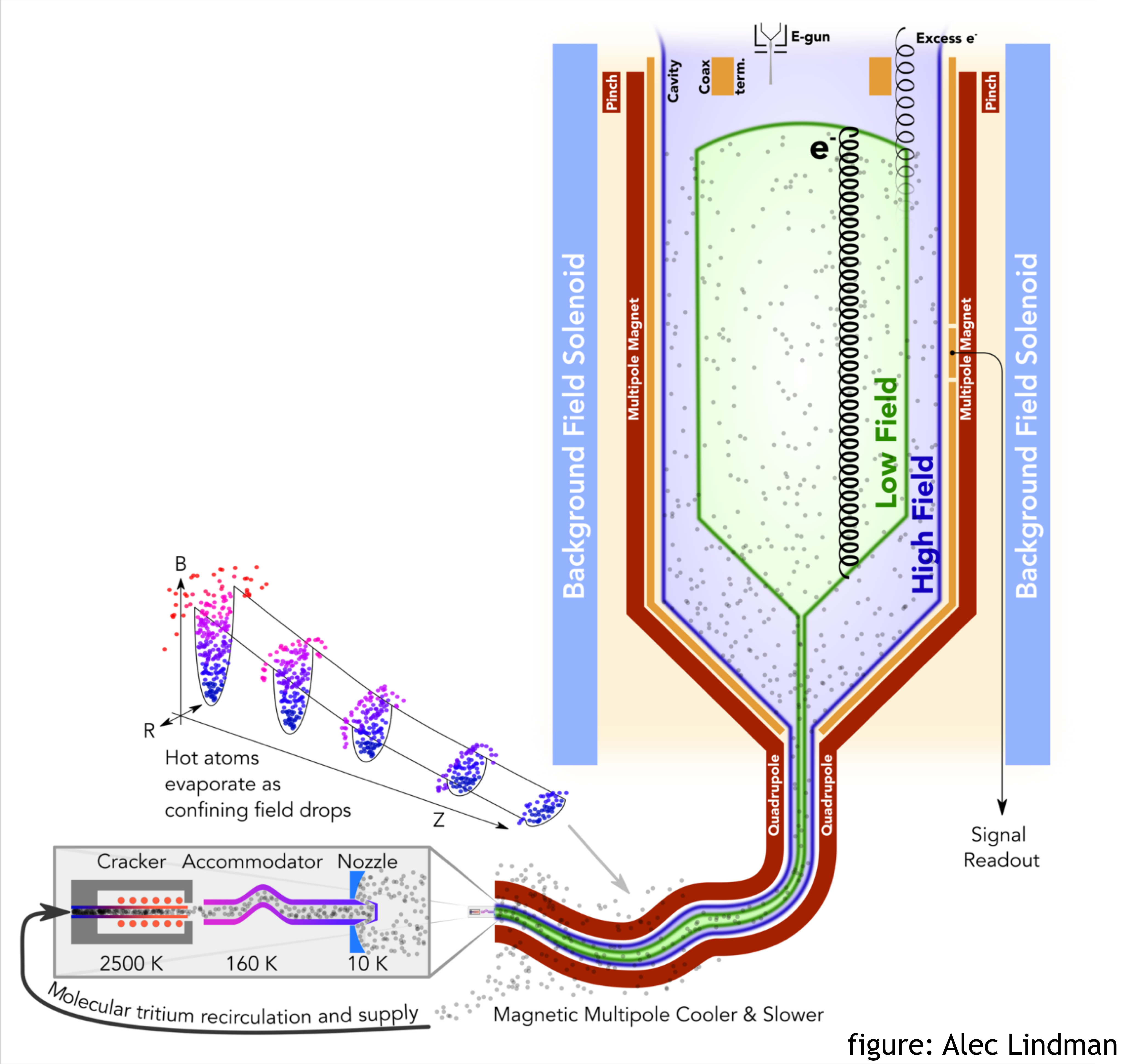

figure: Alec Lindman

Phase III: Atomic Tritium Demonstrator

Need to confine cold atomic hydrogen/tritium!

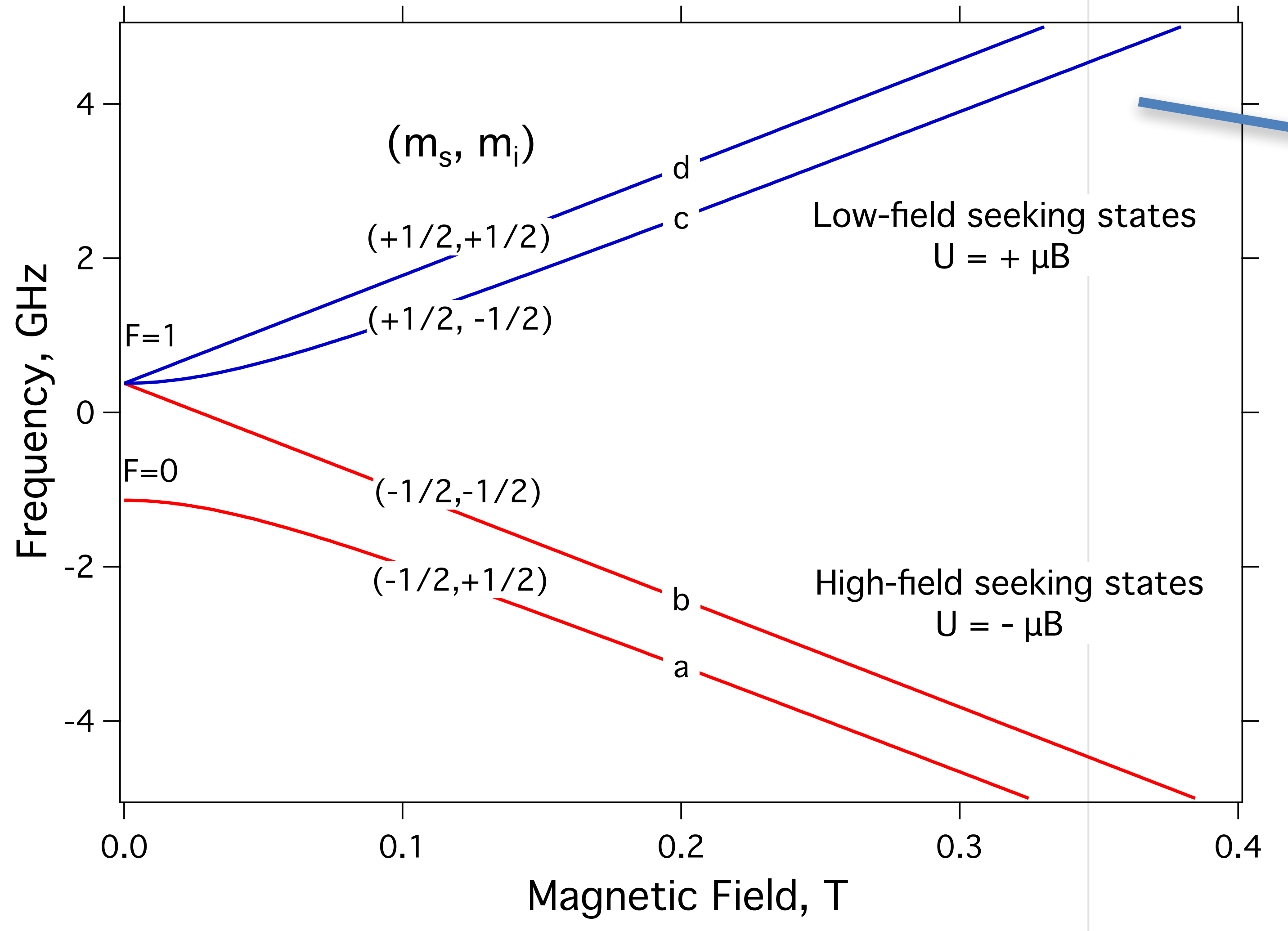

Formaggio, de Gouvêa, Robertson, Physics Reports, Volume 914, 3 June 2021

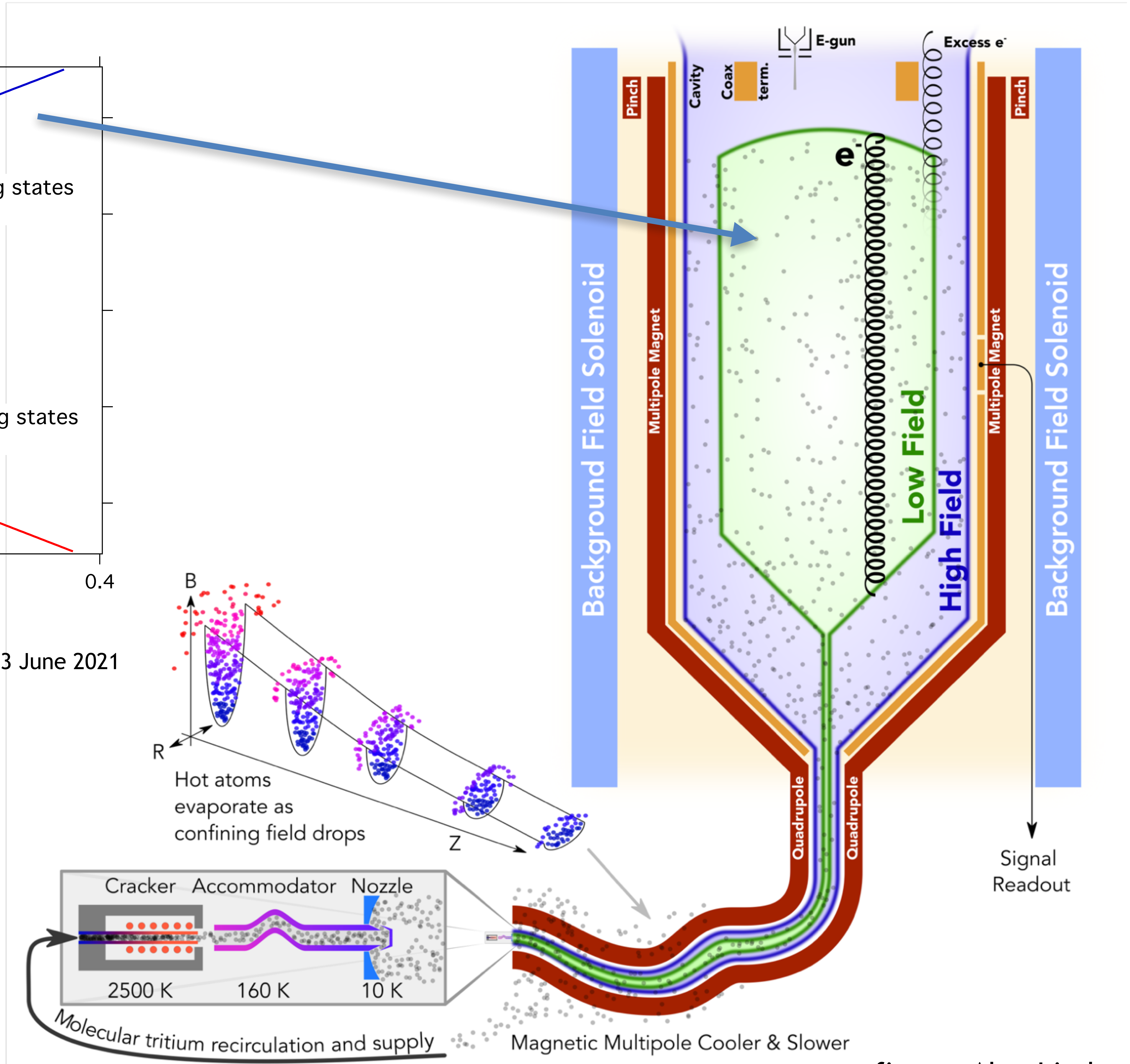

figure: Alec Lindman

Phase III: Atomic Tritium Demonstrator

Need to confine cold atomic hydrogen/tritium!

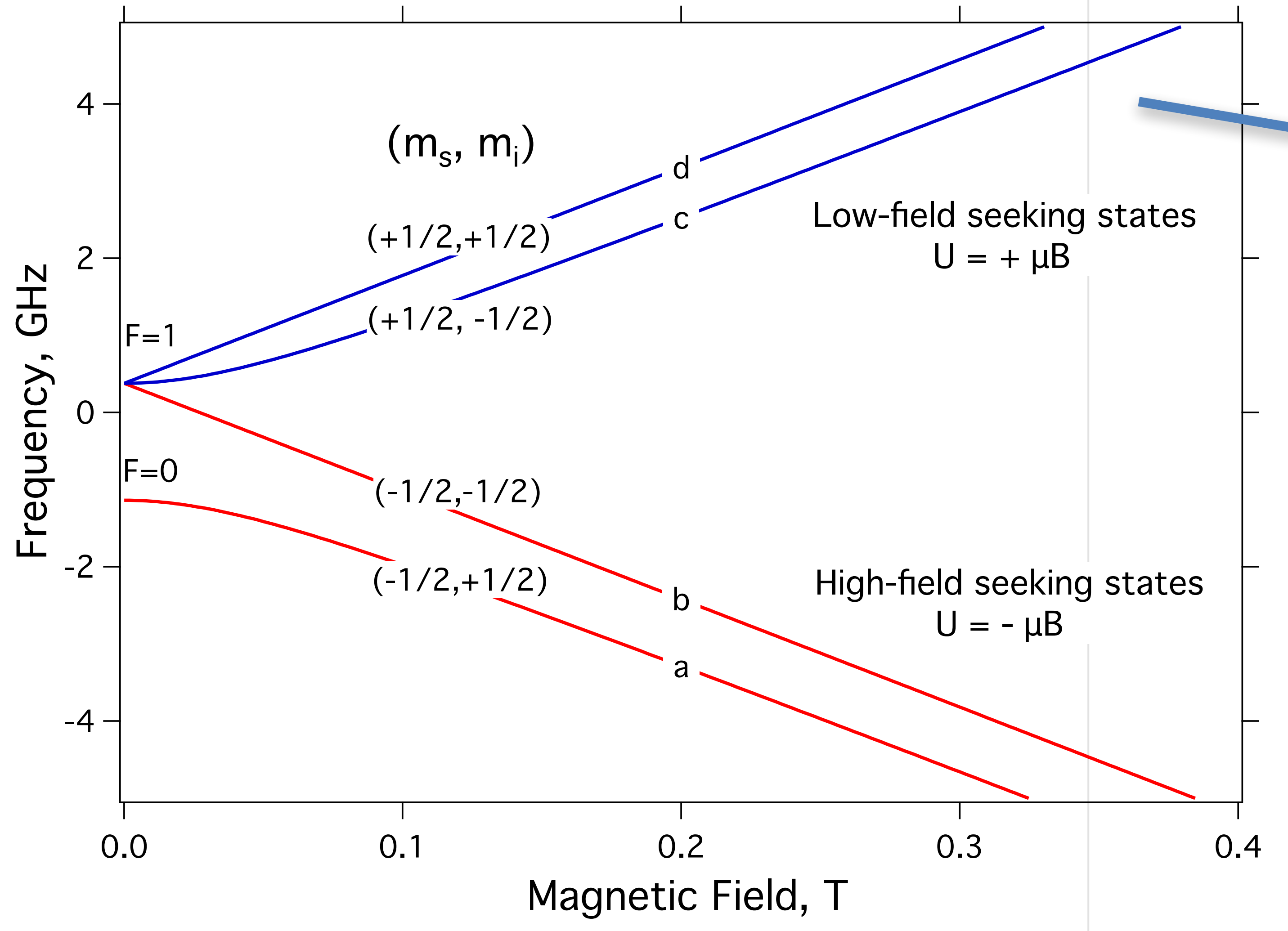

Formaggio, de Gouvêa, Robertson, Physics Reports, Volume 914, 3 June 2021

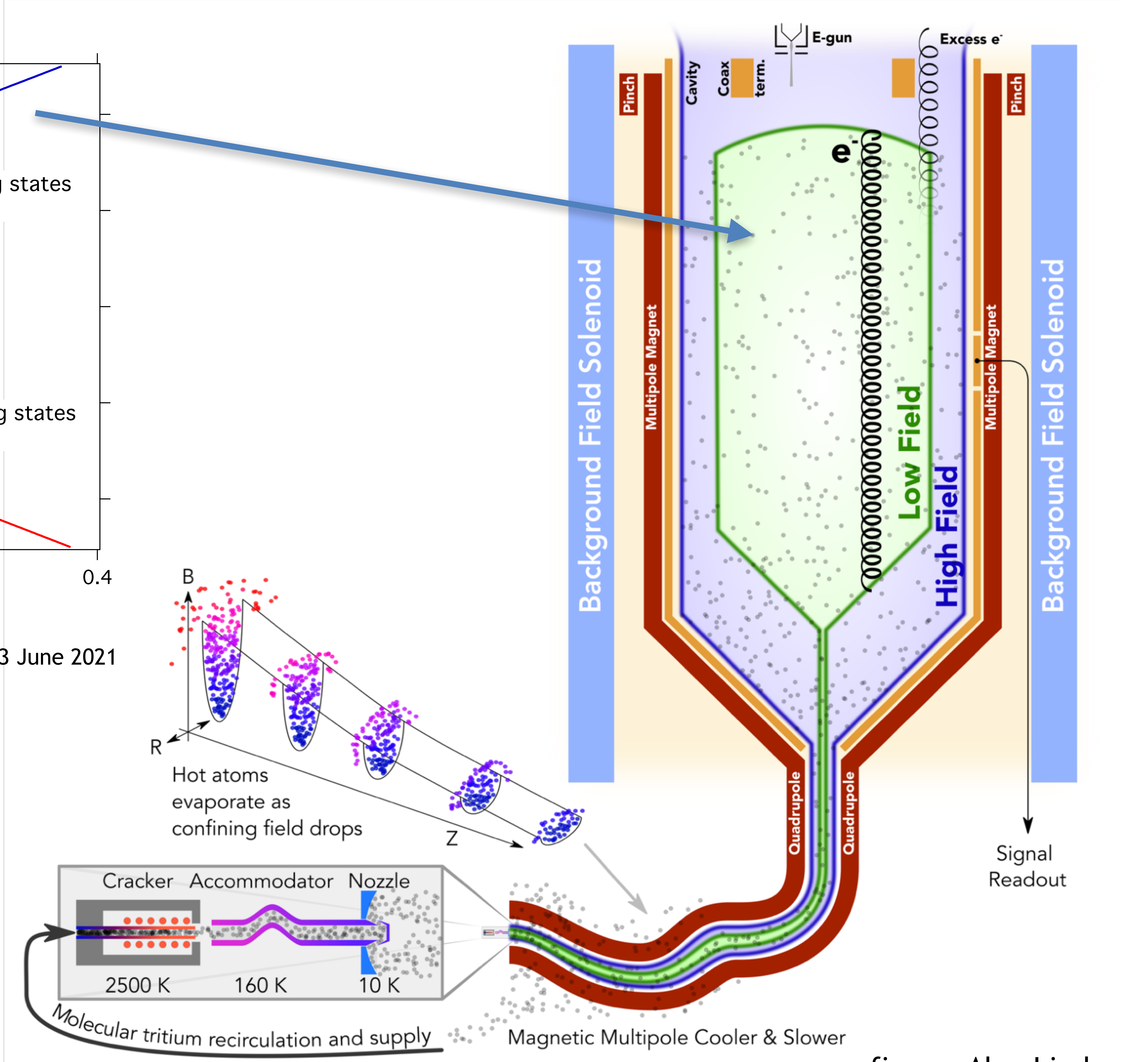

figure: Alec Lindman

Central CRES field should be rather low to reduce dipolar spin flip losses!

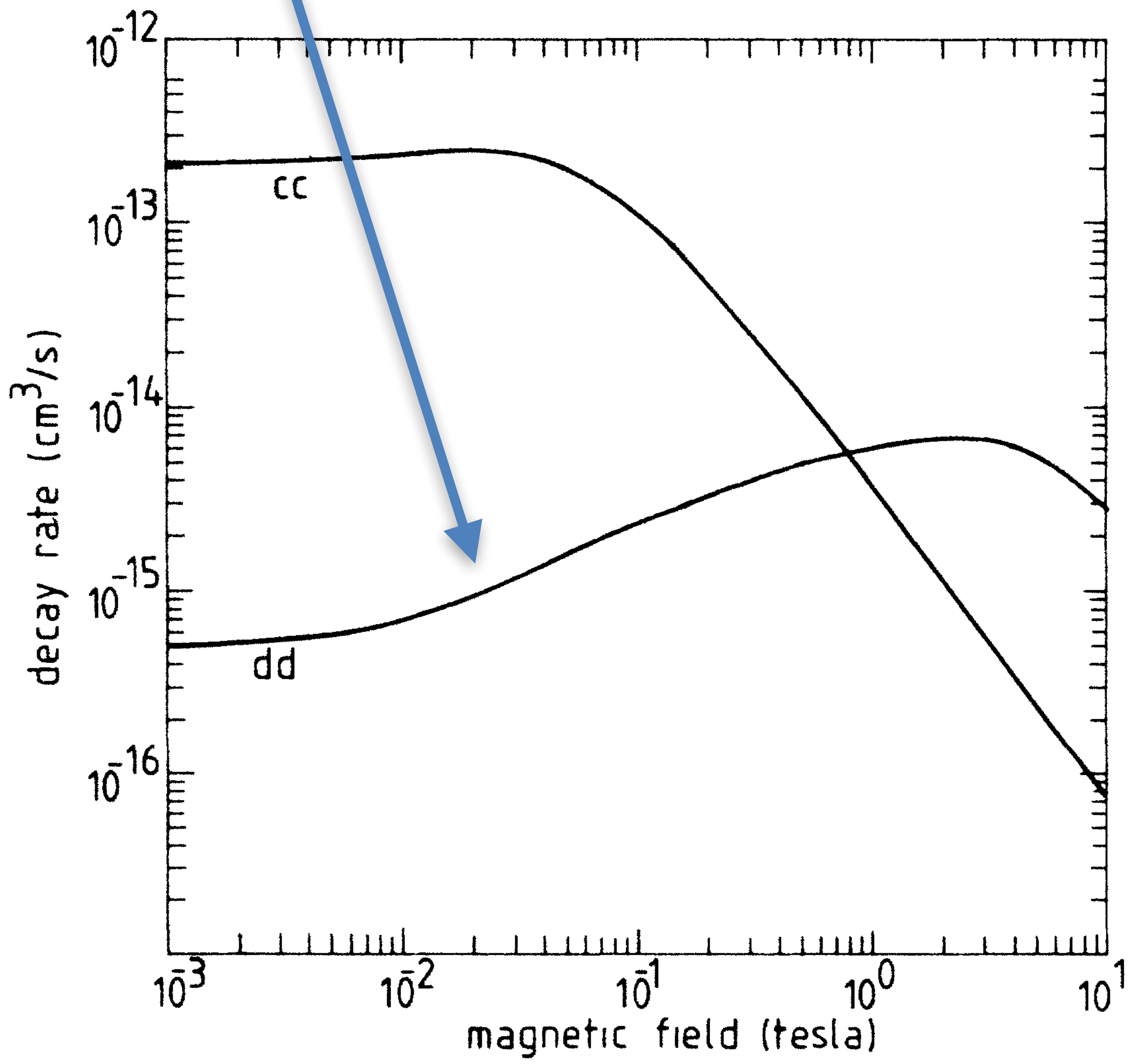

Ad Lagendijk, Isaac F. Silvera, and Boudewijn J. Verhaar Phys. Rev. B 33, 626(R), 1986

The quest for cold atomic tritium starts with molecular hydrogen!

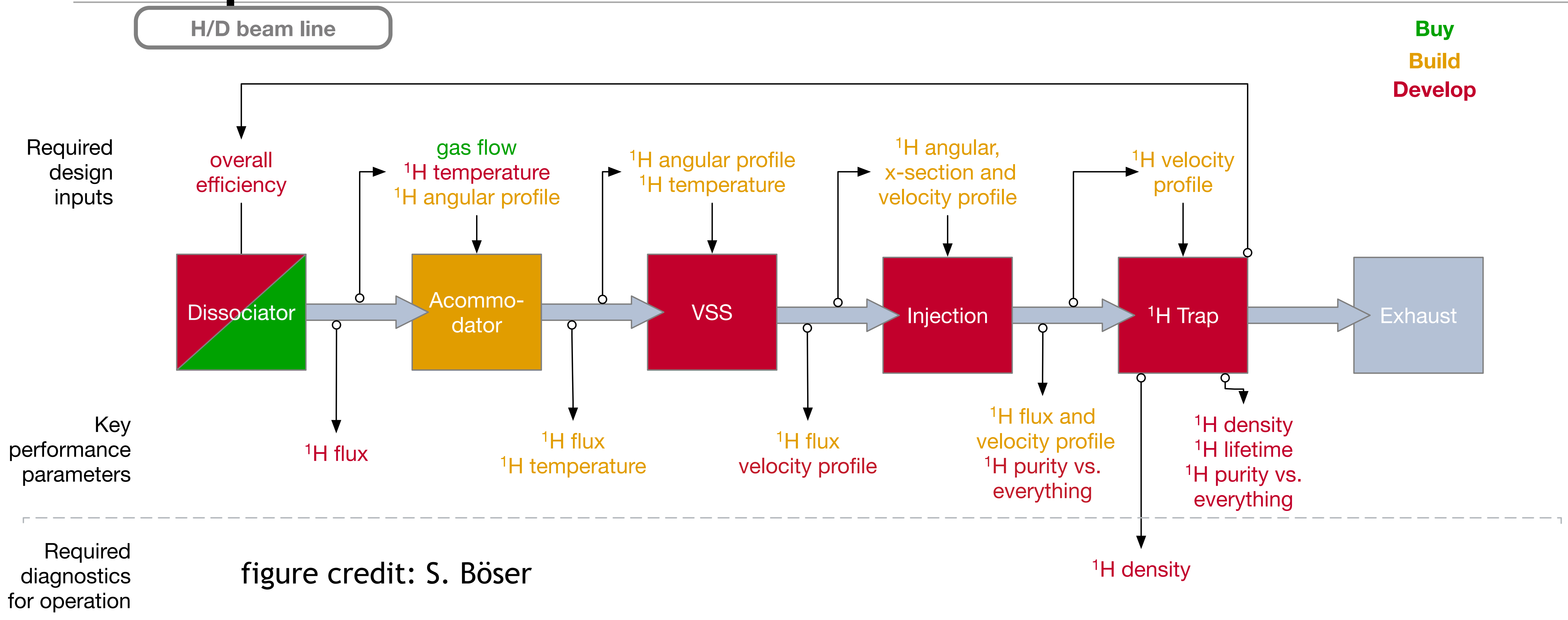

figure credit: RGH Robertson

The quest for cold atomic tritium starts with molecular hydrogen!

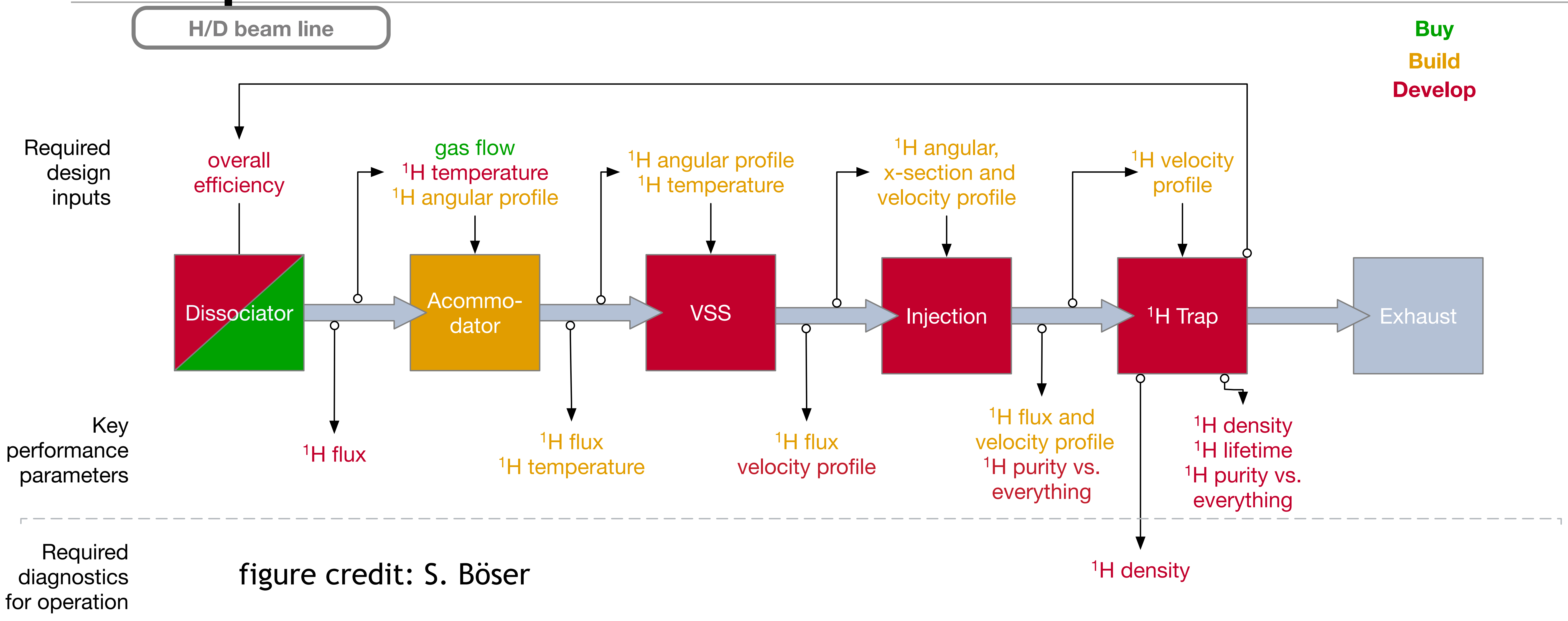

figure credit: S. Böser

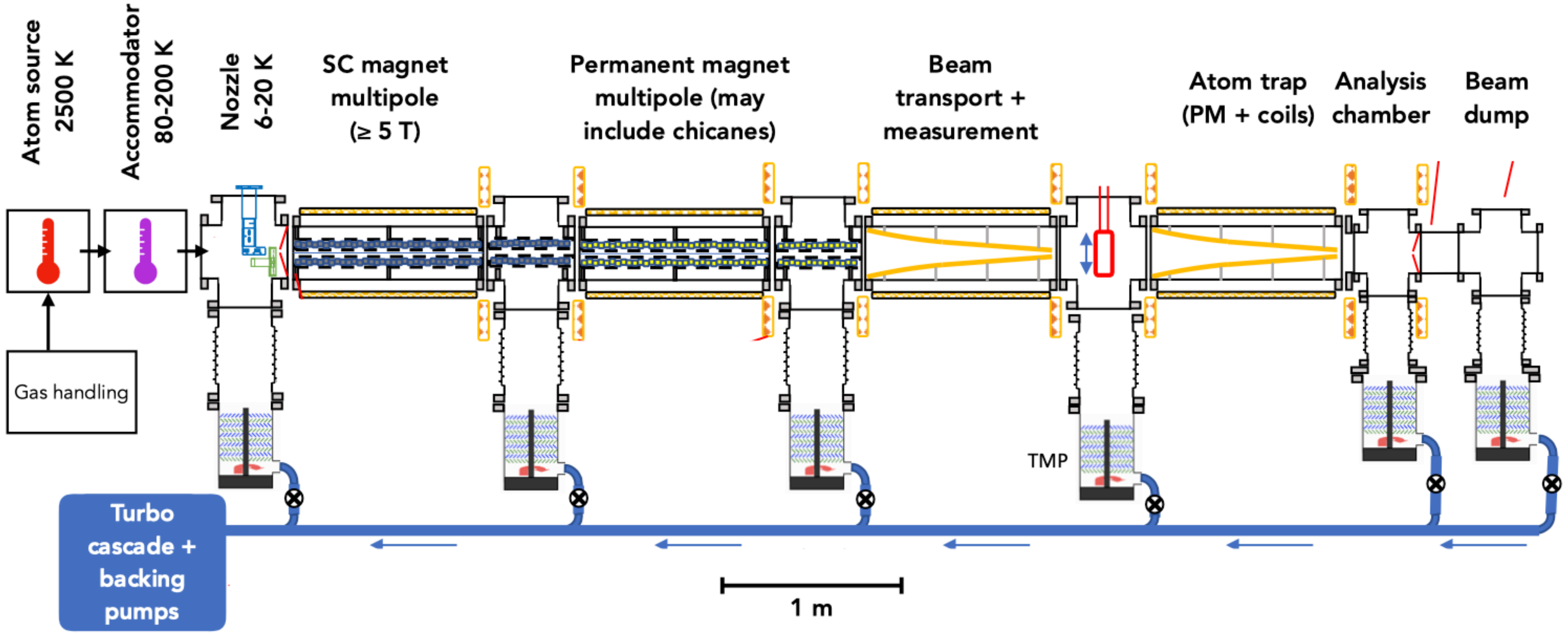

figure credit: RGH Robertson

The quest for cold atomic tritium starts with molecular hydrogen!

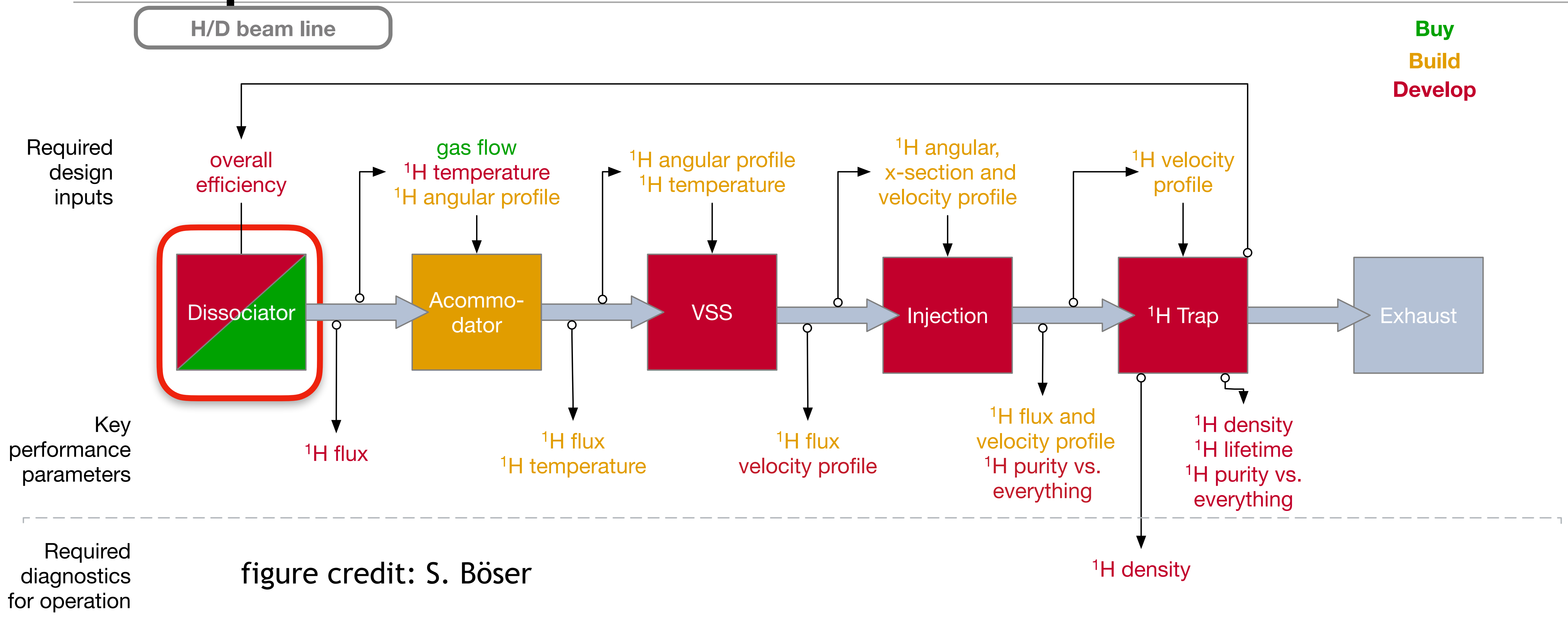

figure credit: S. Böser

Atomic hydrogen flux requirements:

- > 10^{12} cold atoms per second
  ⇒ high decay statistics

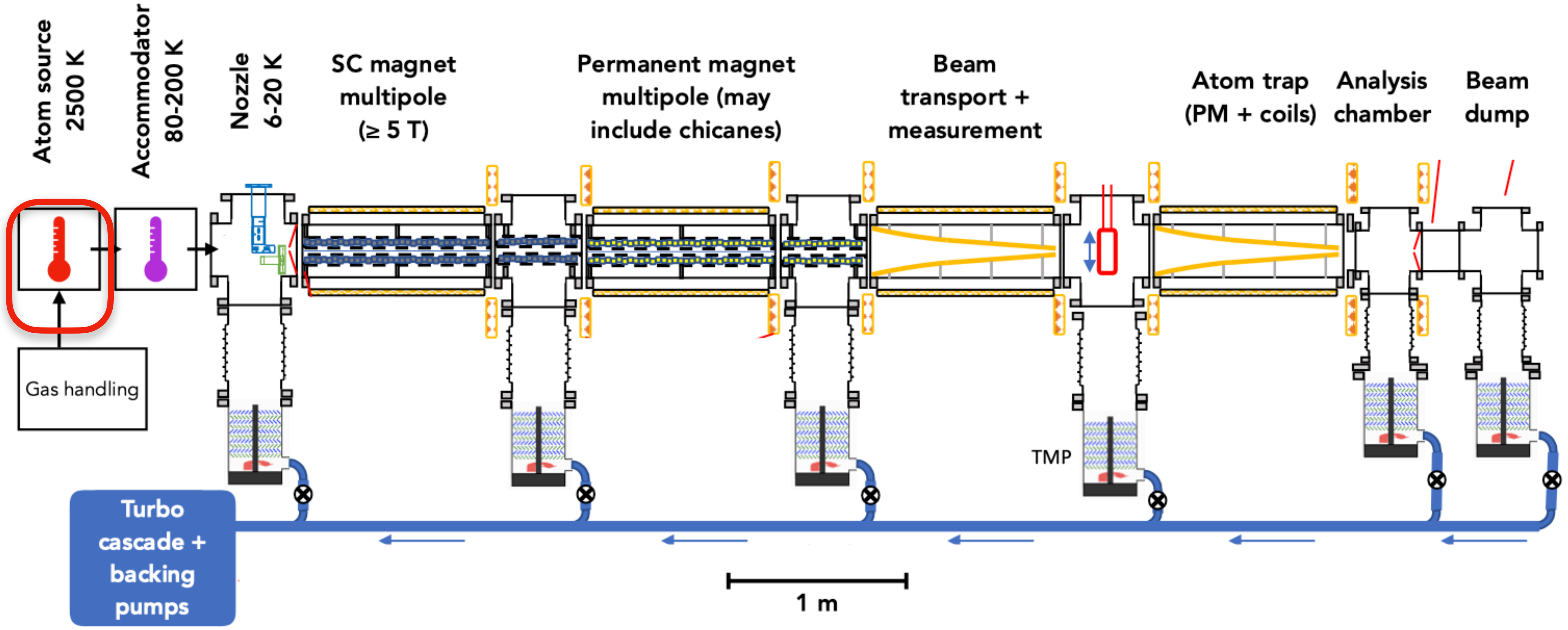

figure credit: RGH Robertson

JG|U

The quest for cold atomic tritium starts with molecular hydrogen!

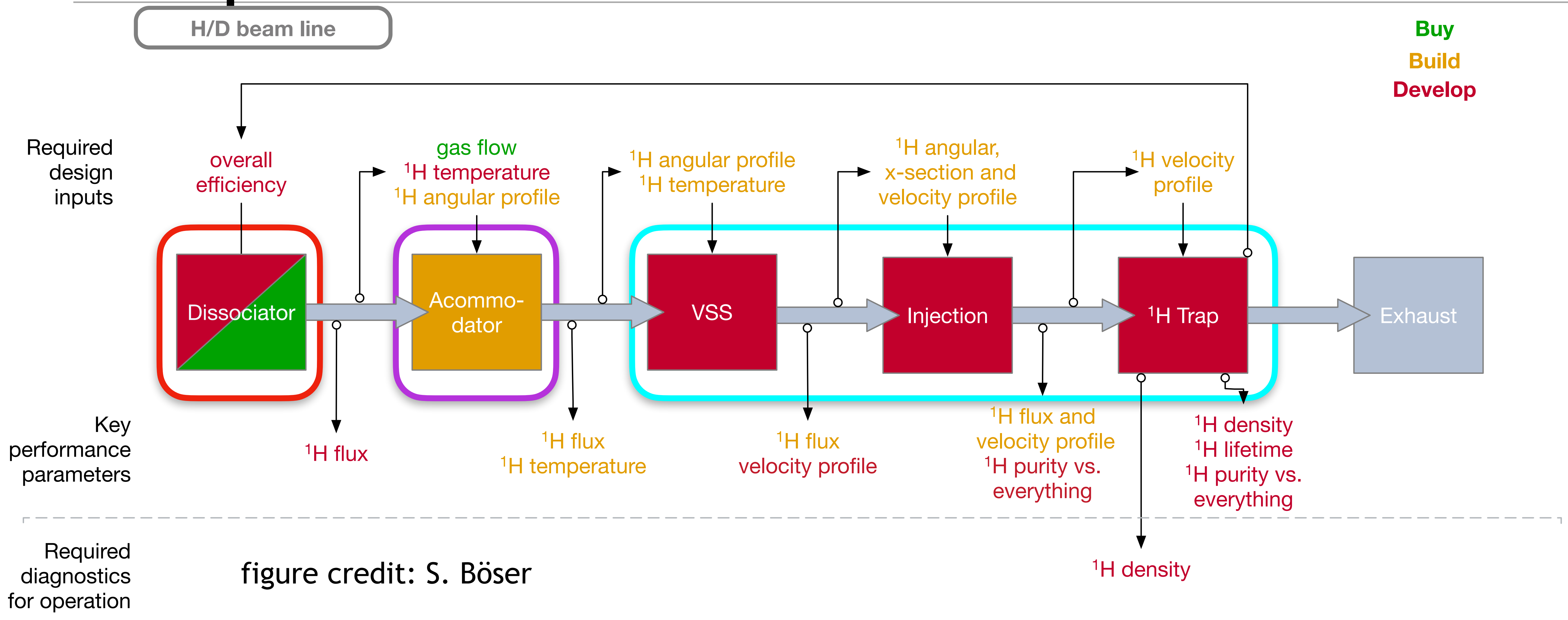

figure credit: S. Böser

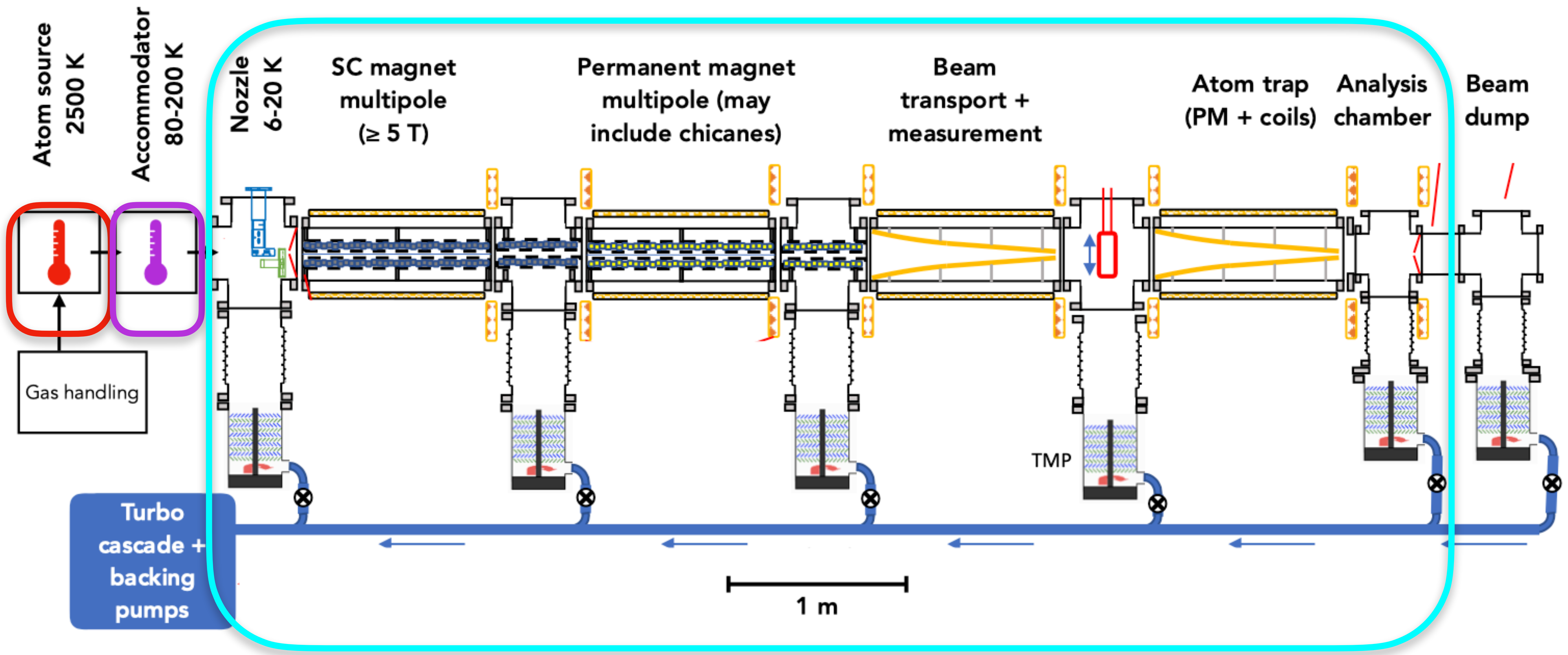

figure credit: RGH Robertson

Atomic hydrogen flux requirements:

- > 10^{12} cold atoms per second
  ⇒ high decay statistics
- Temperatures in the mK range
  ⇒ make atoms magnetically trappable
- Atomic purity: > $10^{4\text{-}5}$ H per H_2
  ⇒ suppress contribution from T_2 decay in endpoint region of T decay

The quest for cold atomic tritium starts with molecular hydrogen!

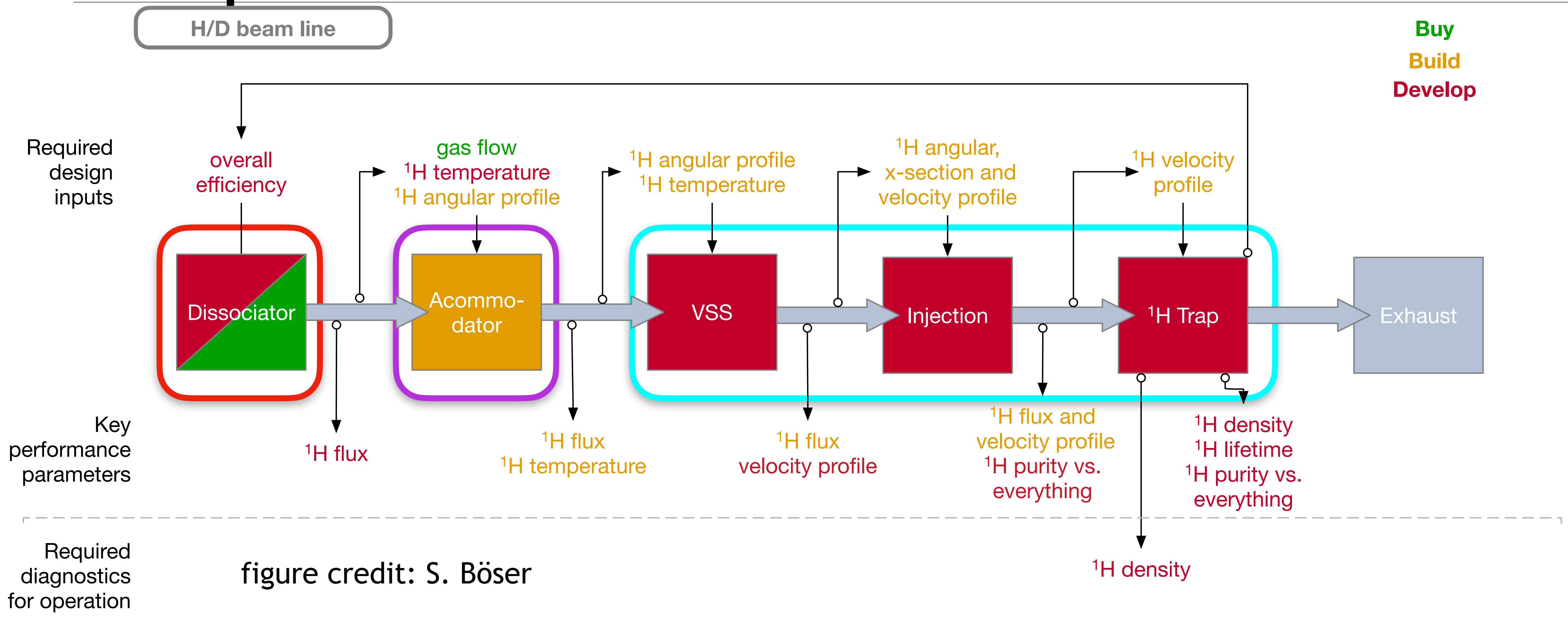

figure credit: S. Böser

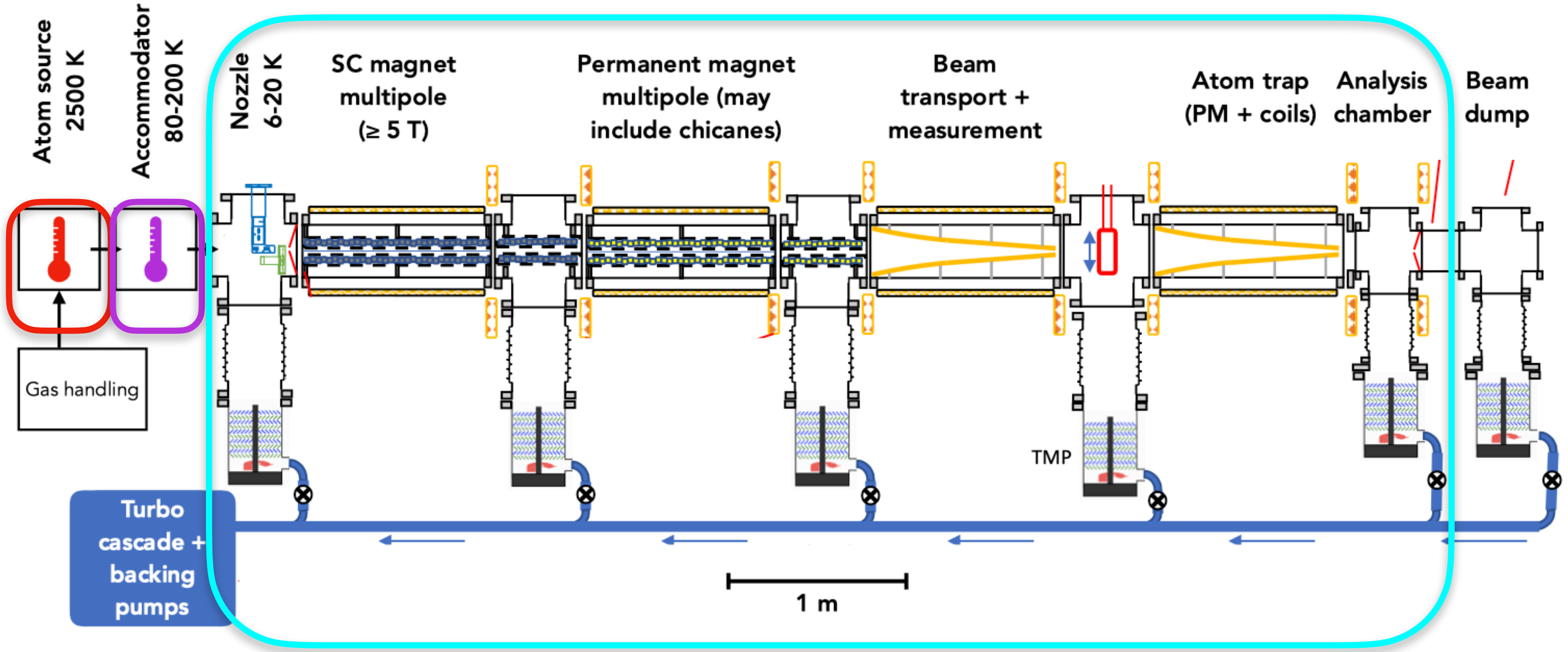

figure credit: RGH Robertson

Atomic hydrogen flux requirements:

- > 10^{12} cold atoms per second
  ⇒ high decay statistics
- Temperatures in the mK range
  ⇒ make atoms magnetically trappable
- Atomic purity: > $10^{4\text{-}5}$ H per H_2
  ⇒ suppress contribution from T_2 decay in endpoint region of T decay
- High efficiency of cold atom production
  ⇒ manageable size of gas handling and purification loop infrastructure

The quest for cold atomic tritium starts with molecular hydrogen!

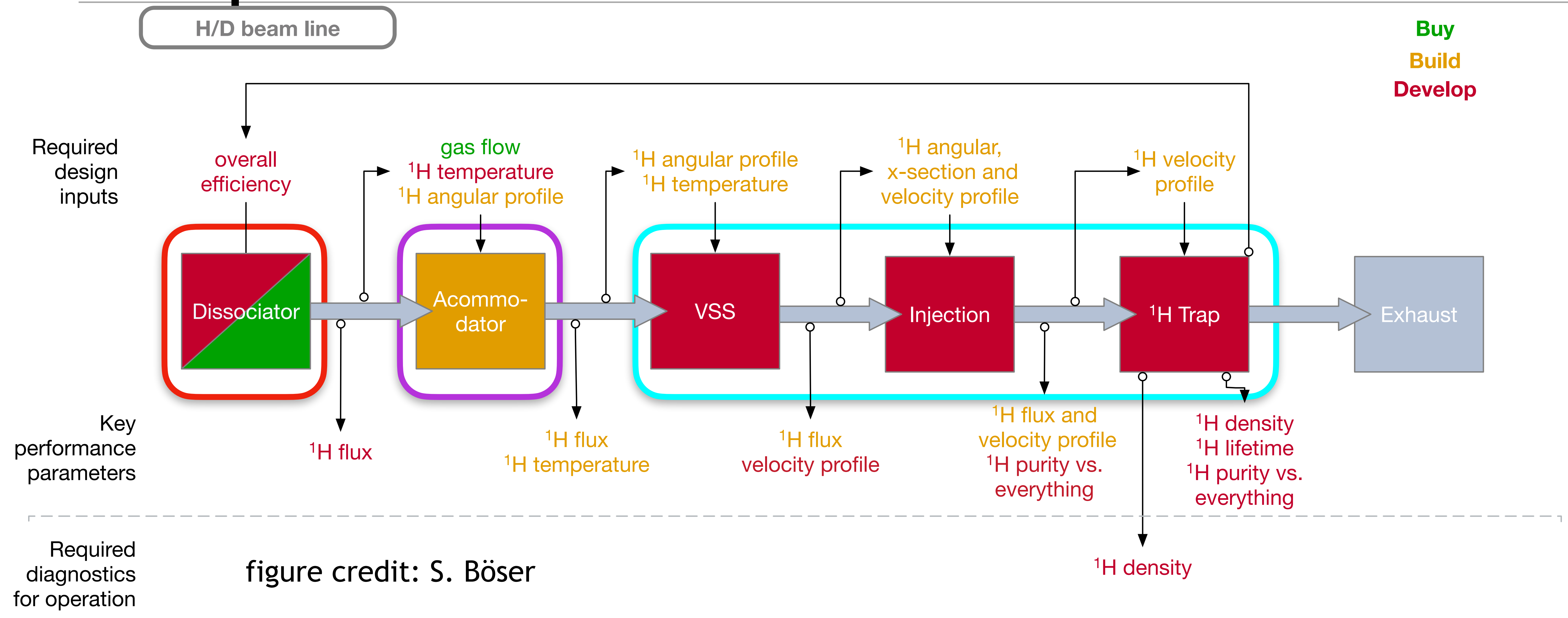

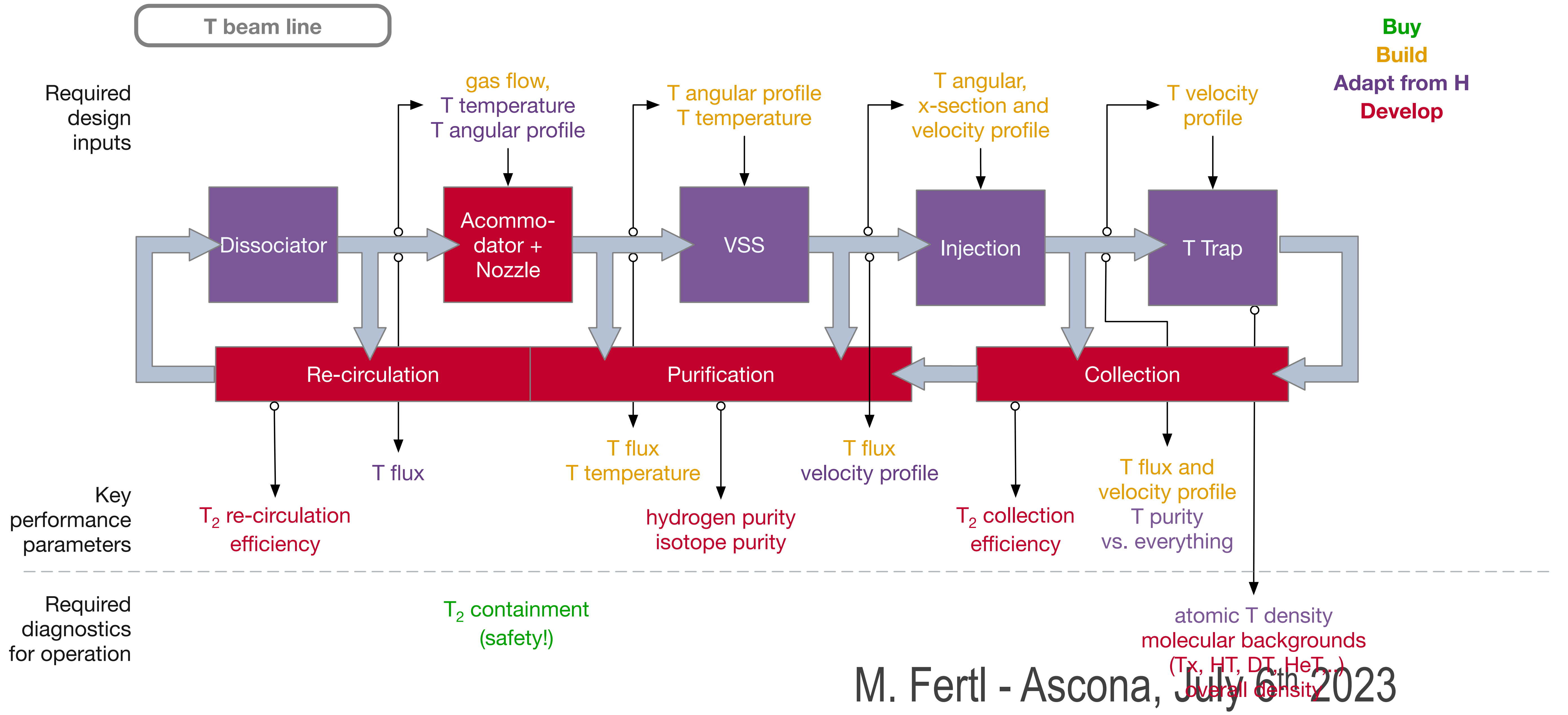

Atomic hydrogen flux requirements:

- > 10^{12} cold atoms per second
  ⇒ high decay statistics
- Temperatures in the mK range
  ⇒ make atoms magnetically trappable
- Atomic purity: > 10^{4-5} H per H_2
  ⇒ suppress contribution from T_2 decay in endpoint region of T decay
- High efficiency of cold atom production
  ⇒ manageable size of gas handling and purification loop infrastructure

Technology development with $H_{(2)}$ and $D_{(2)}$
Later transfer to $T_{(2)}$ infrastructure.

The quest for cold atomic tritium starts with molecular hydrogen!

Thermal cracker:
$H_2 \rightarrow 2\,H$, hot, now!

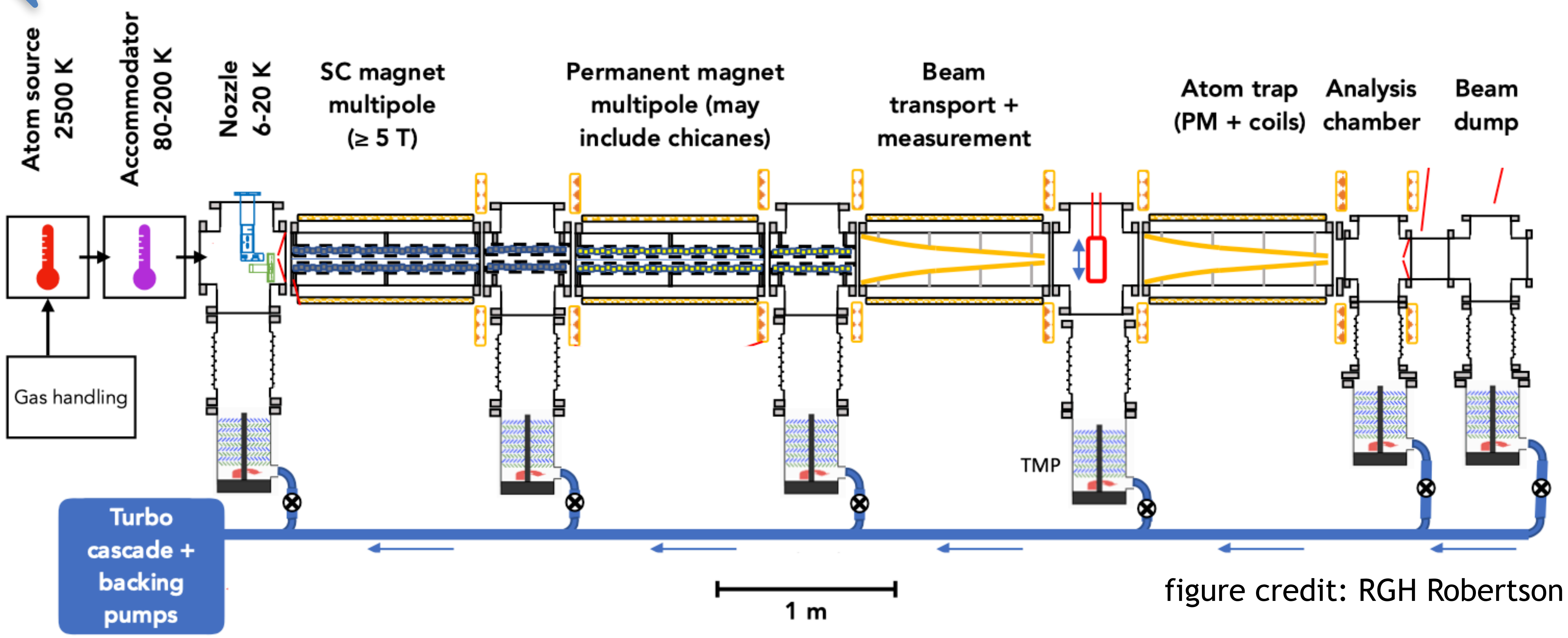

figure credit: RGH Robertson

The quest for cold atomic tritium starts with molecular hydrogen!

Thermal cracker:
$H_2 \rightarrow 2\ H$, hot, now!

Surface accommodation:
Cold surfaces …-2025

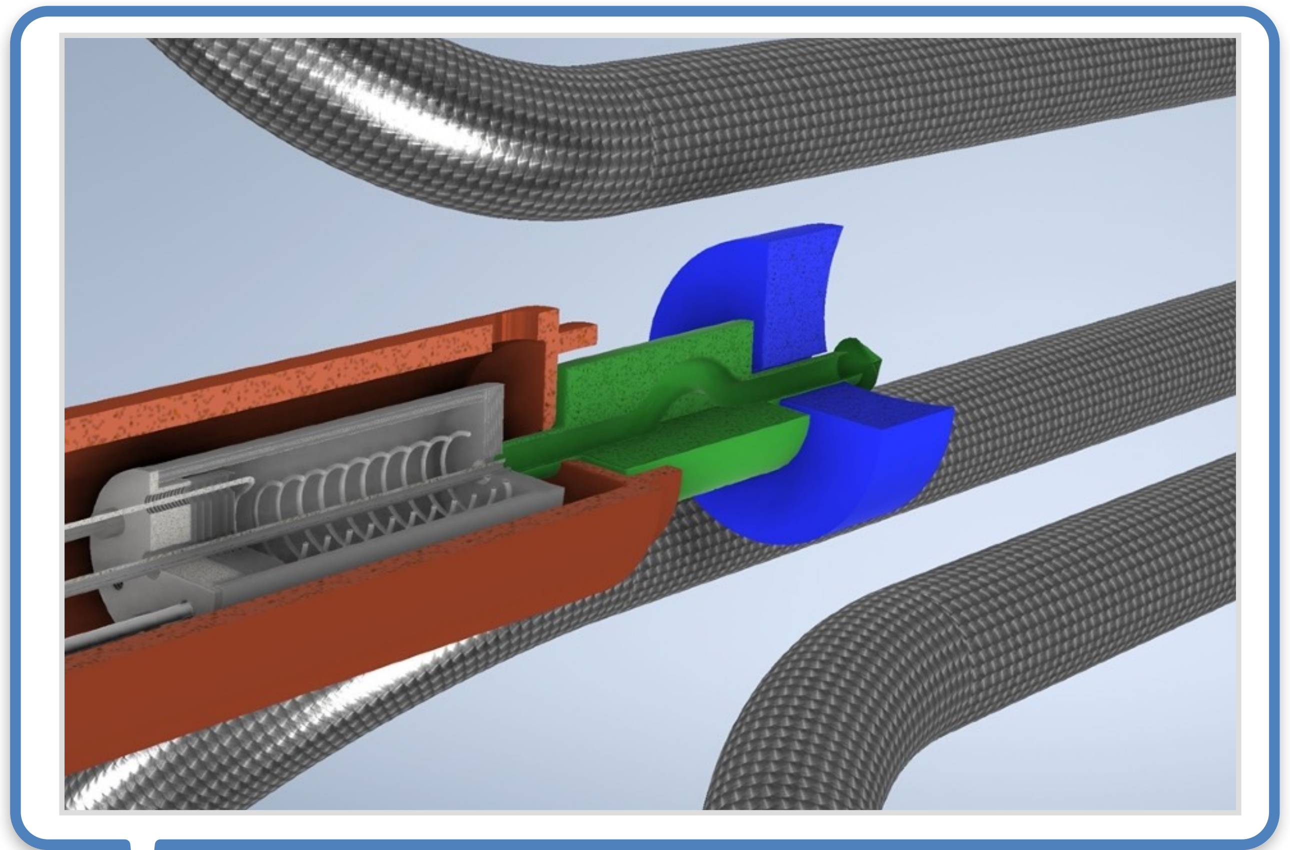

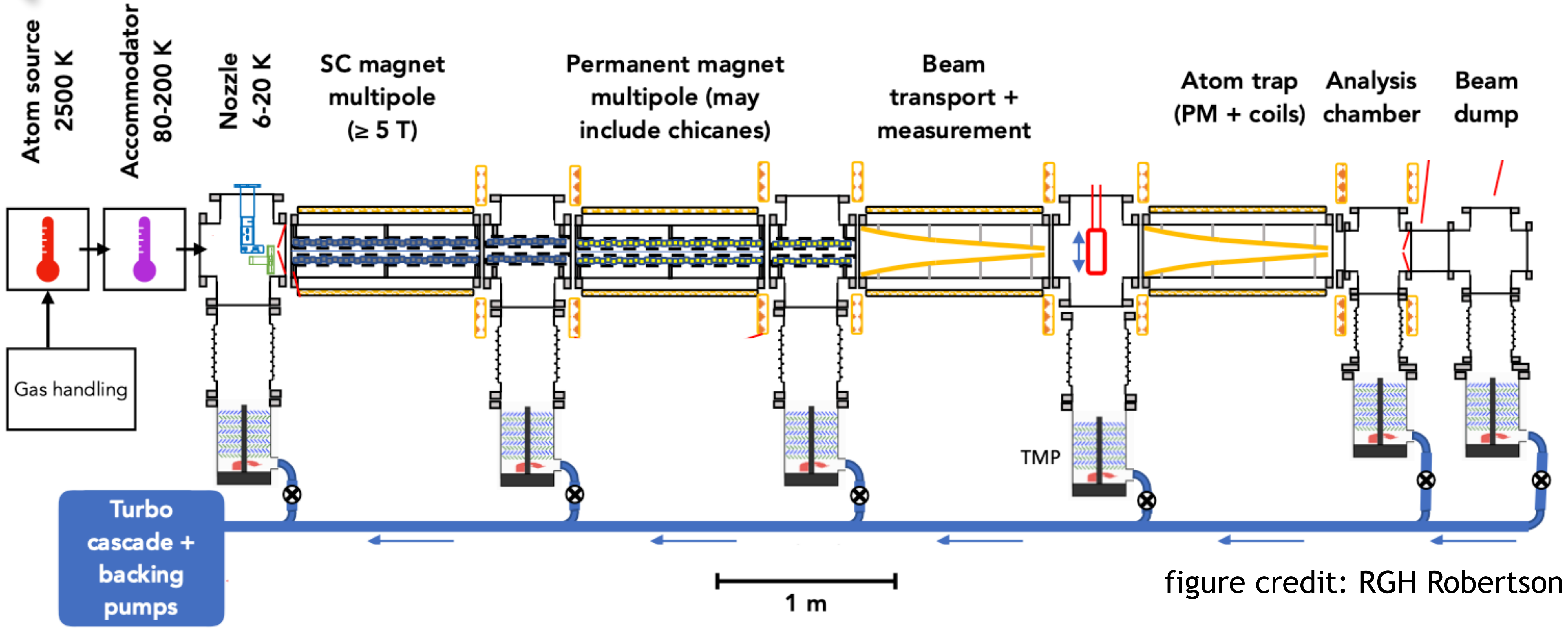

figure credit: RGH Robertson

JG|U

The quest for cold atomic tritium starts with molecular hydrogen!

Thermal cracker:
$H_2 \rightarrow 2\,H$, hot, now!

Surface accommodation:
Cold surfaces …-2025

Magnetic evaporative cooling beamline

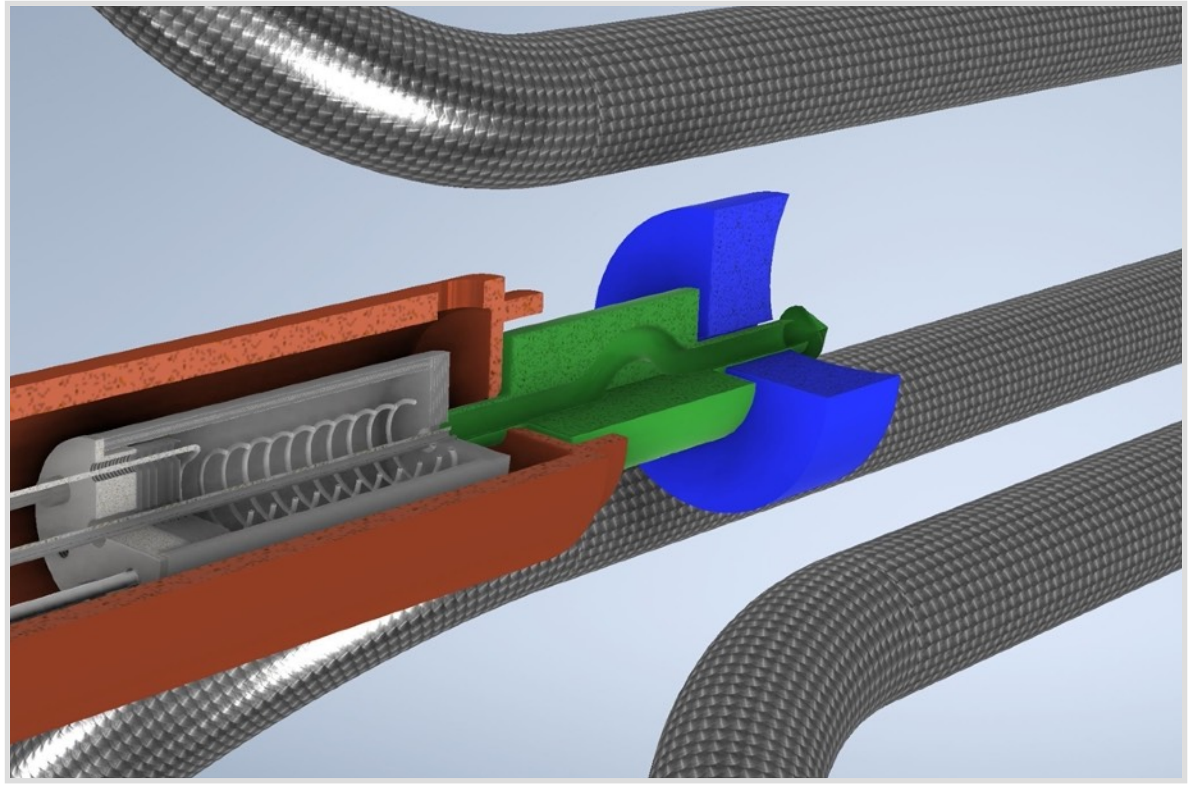

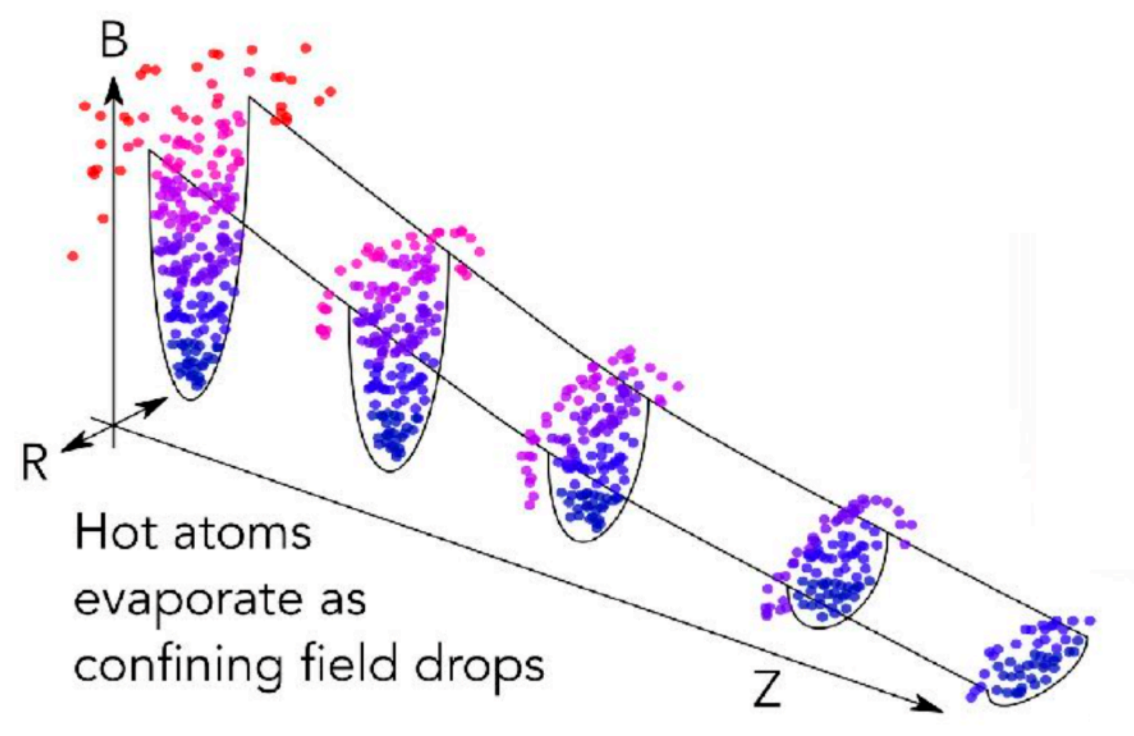

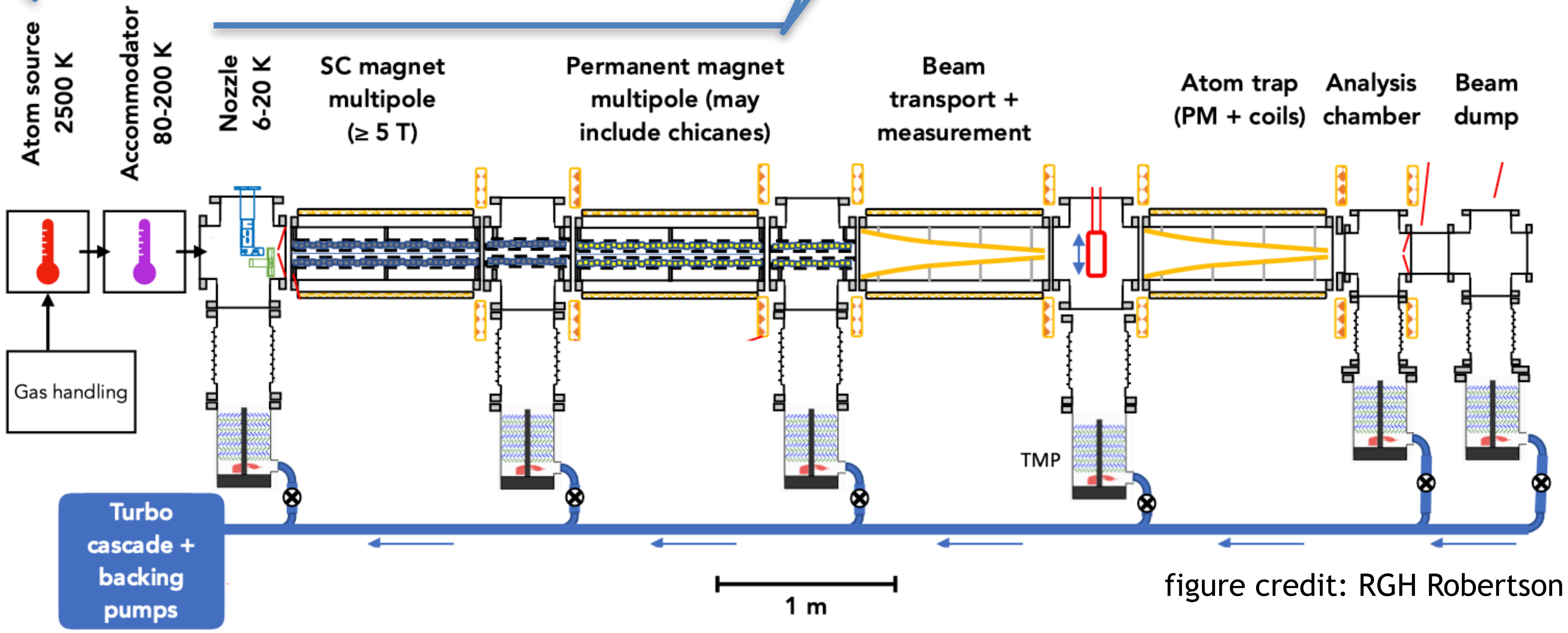

figure credit: RGH Robertson

The quest for cold atomic tritium starts with molecular hydrogen!

Thermal cracker:
$H_2 \rightarrow 2$ H, hot, now!

Surface accommodation:
Cold surfaces …-2025

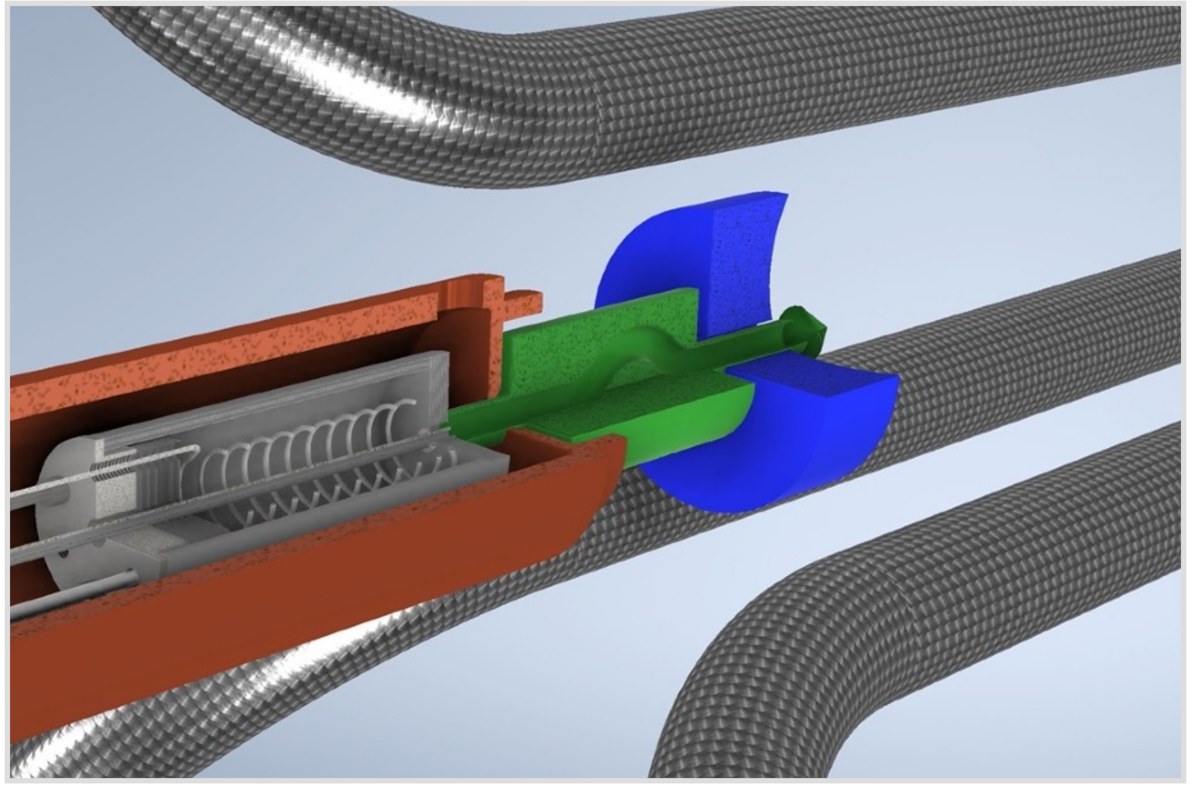

Magnetic evaporative cooling beamline

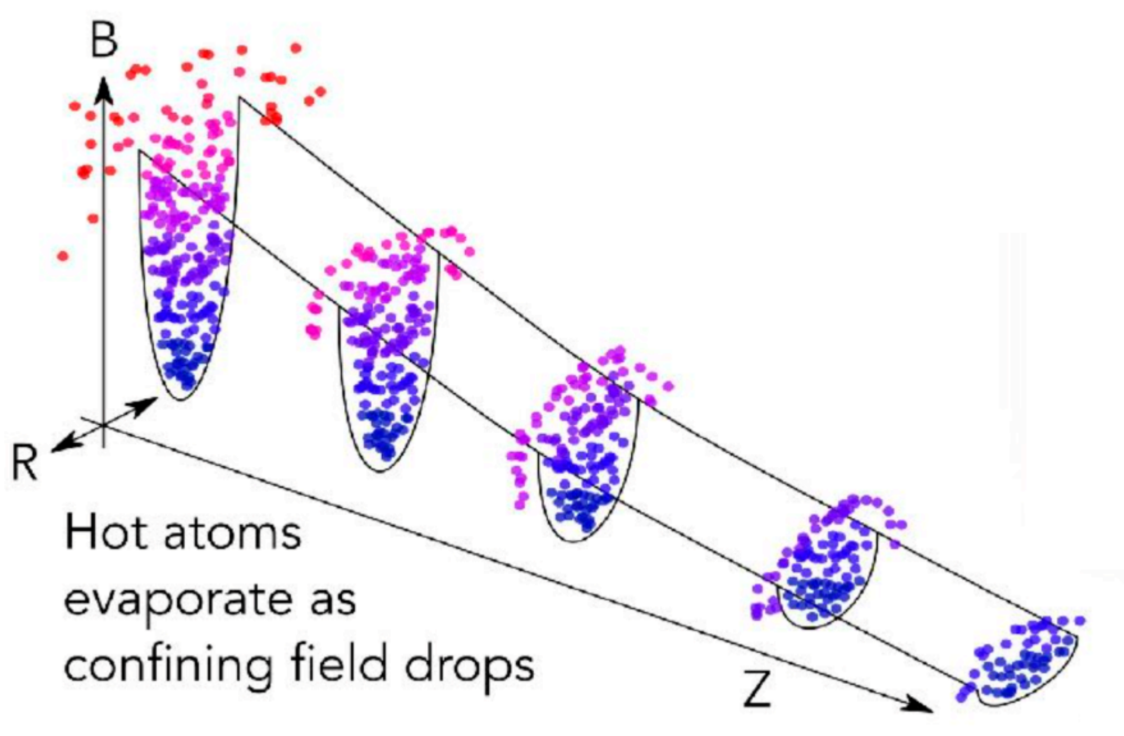

Atomic beam diagnostics:
Wire detector, now!

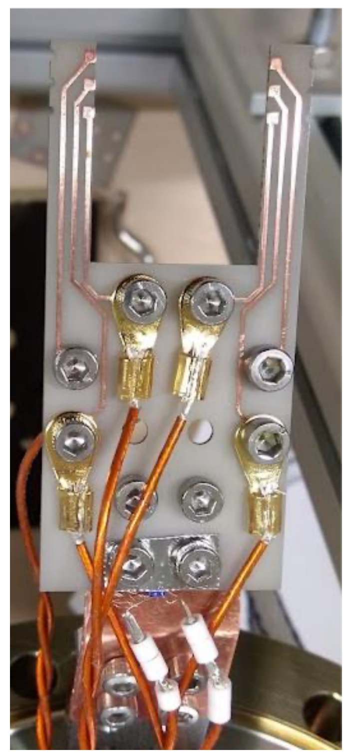

Recombination of H
Heat release
Temperature increase

50 µm wire

Very recent success!

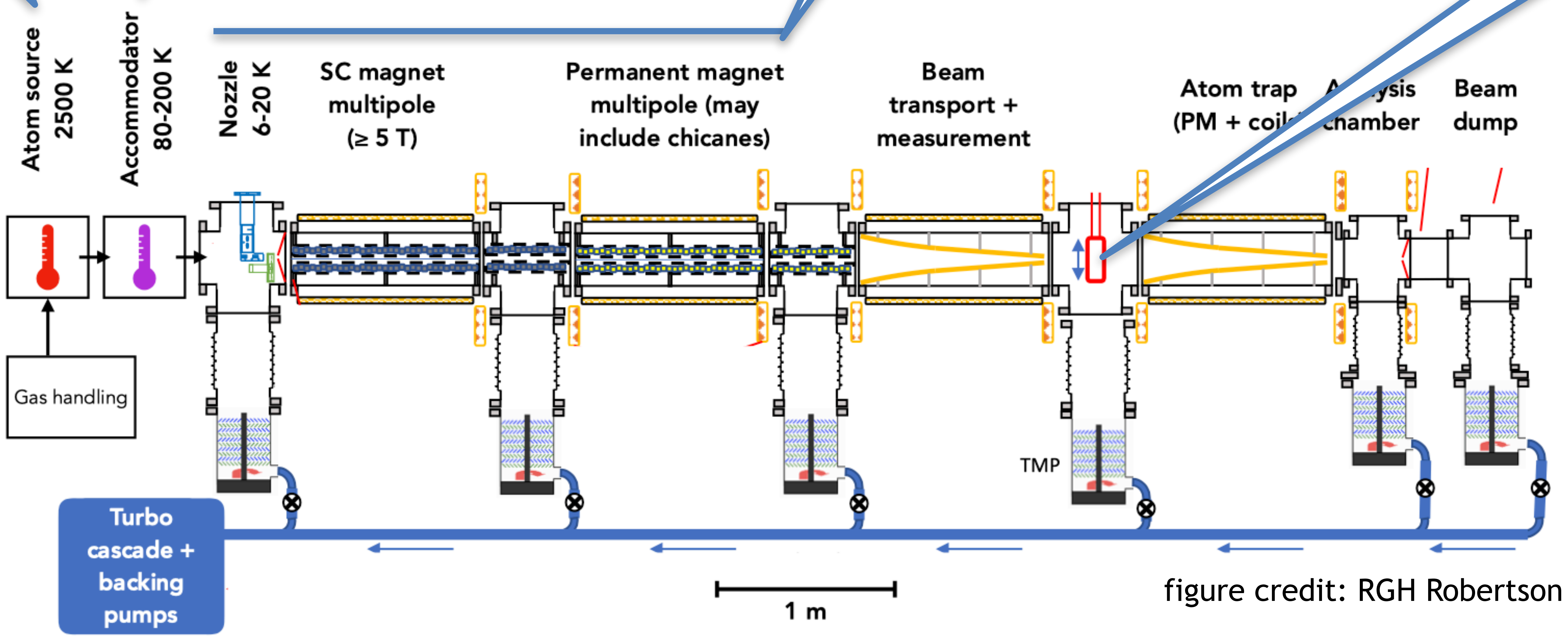

figure credit: RGH Robertson

The commercial thermal cracker!

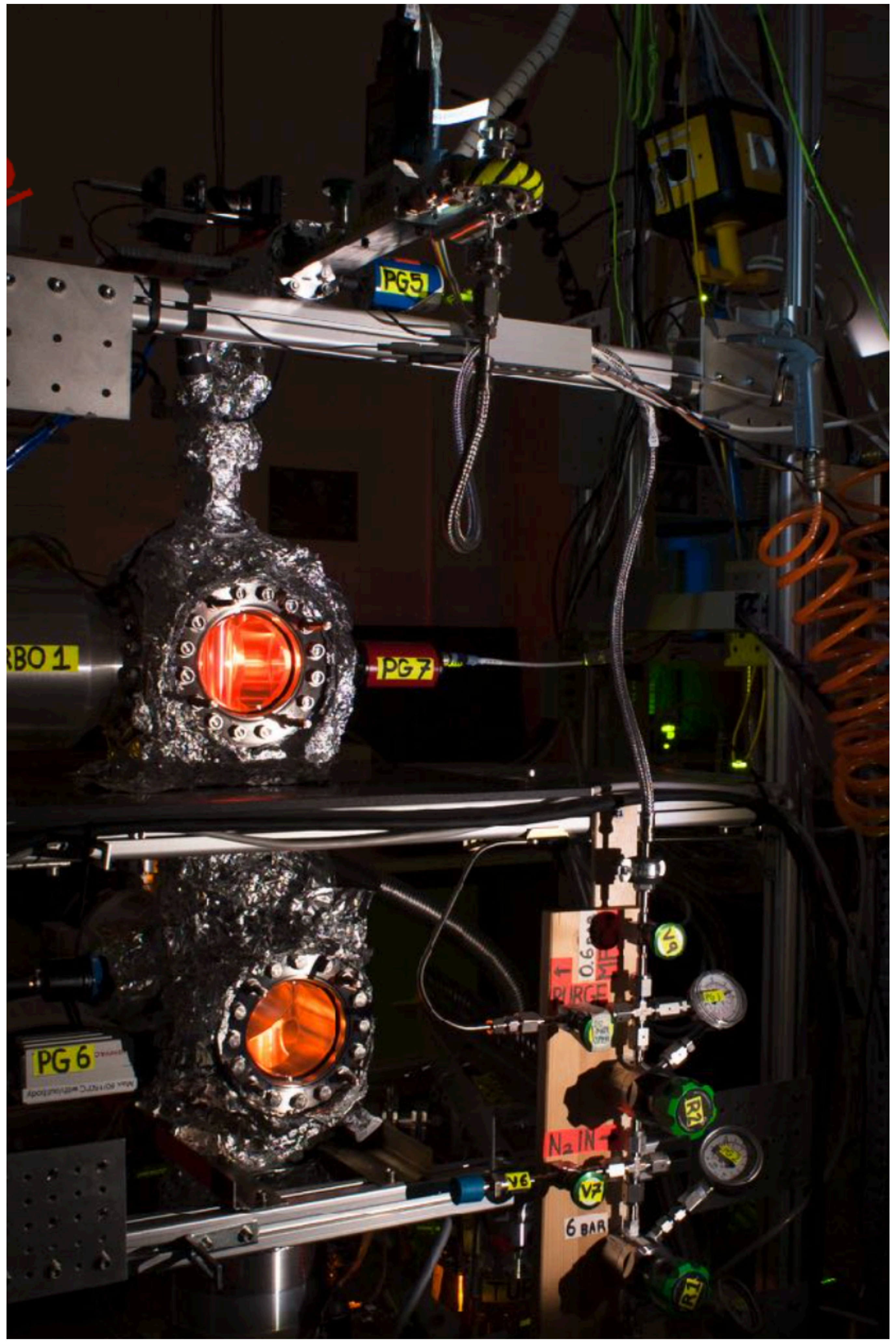

The commercial thermal cracker!

Thermal cracker:
$H_2 \rightarrow 2\ H$

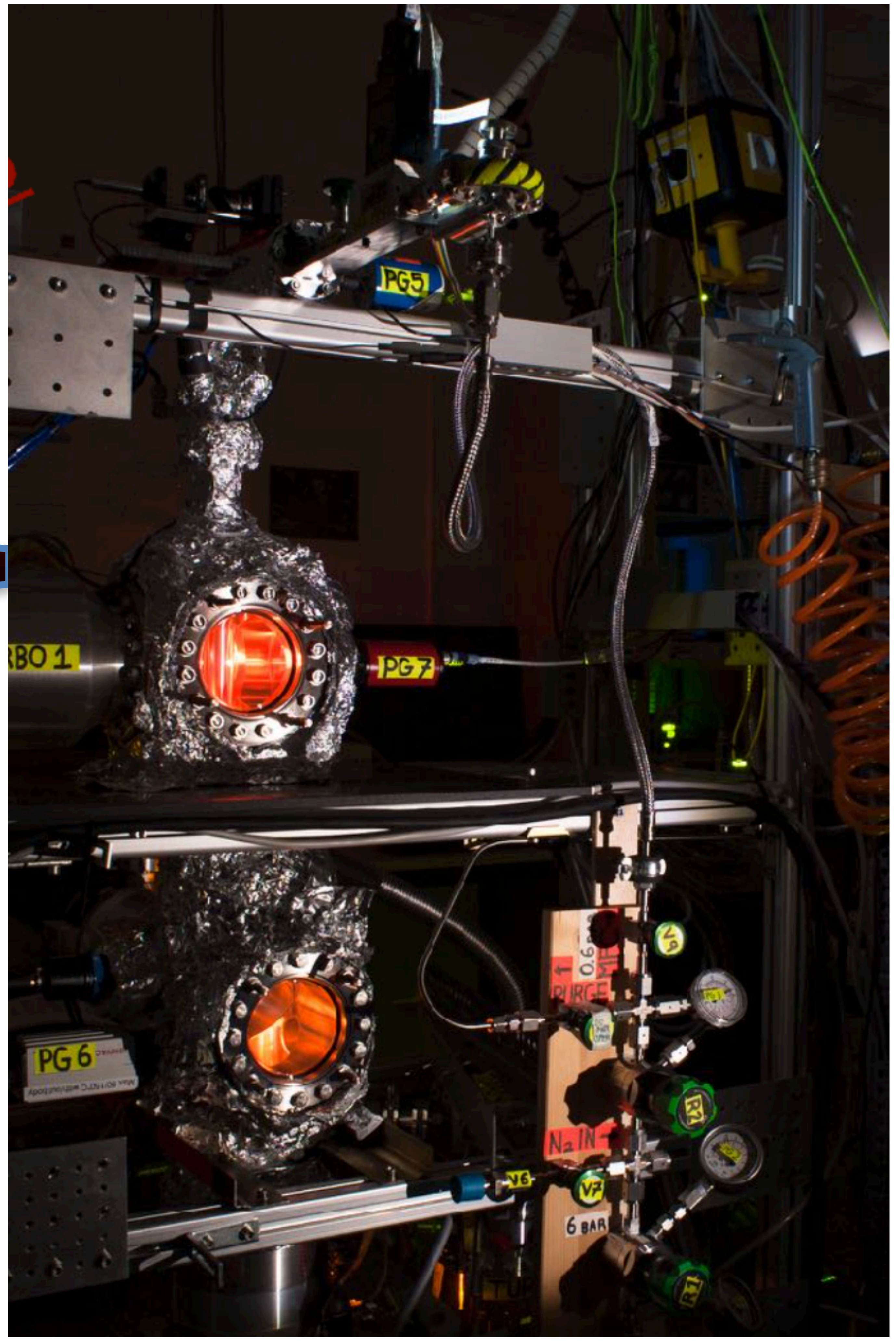

The commercial thermal cracker!

Thermal cracker:
$H_2 \rightarrow 2\ H$

High-resolution mass spectrometer
for AMU 1-10 on z-translator (Hiden)

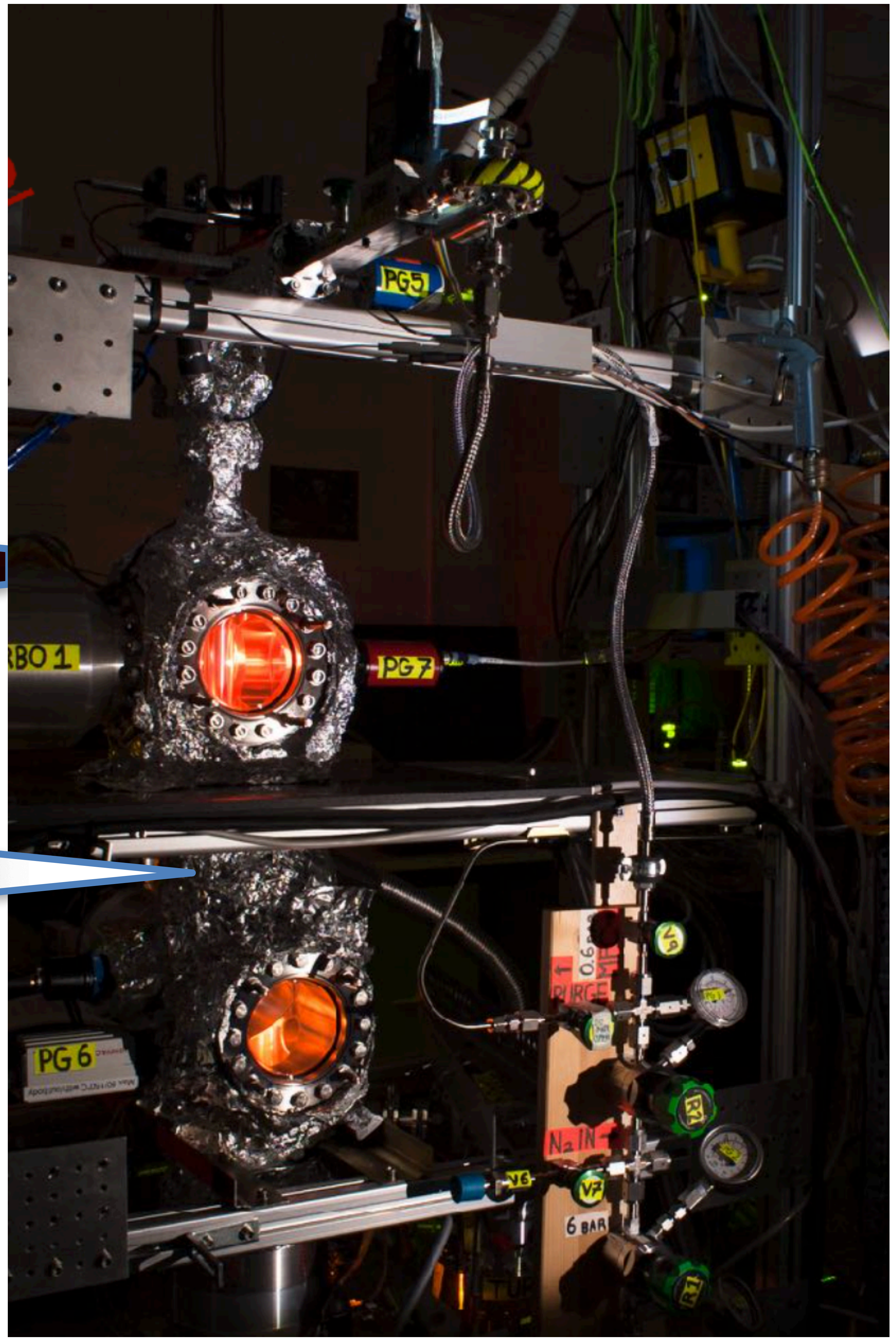

The commercial thermal cracker!

Thermal cracker:
$H_2 \rightarrow 2\,H$

High-resolution mass spectrometer
for AMU 1-10 on z-translator (Hiden)

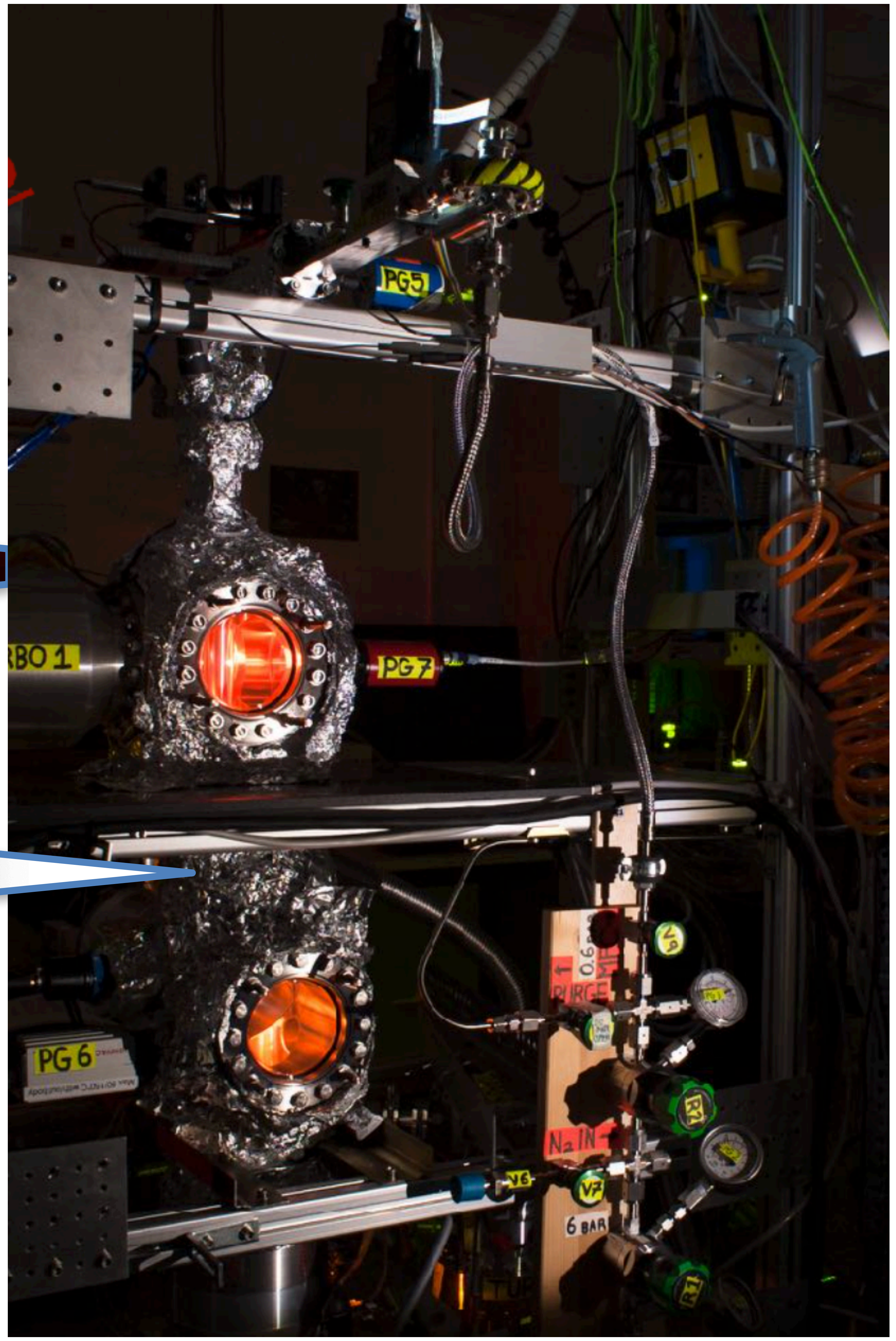

Mass 1 signal of mass spectrometer

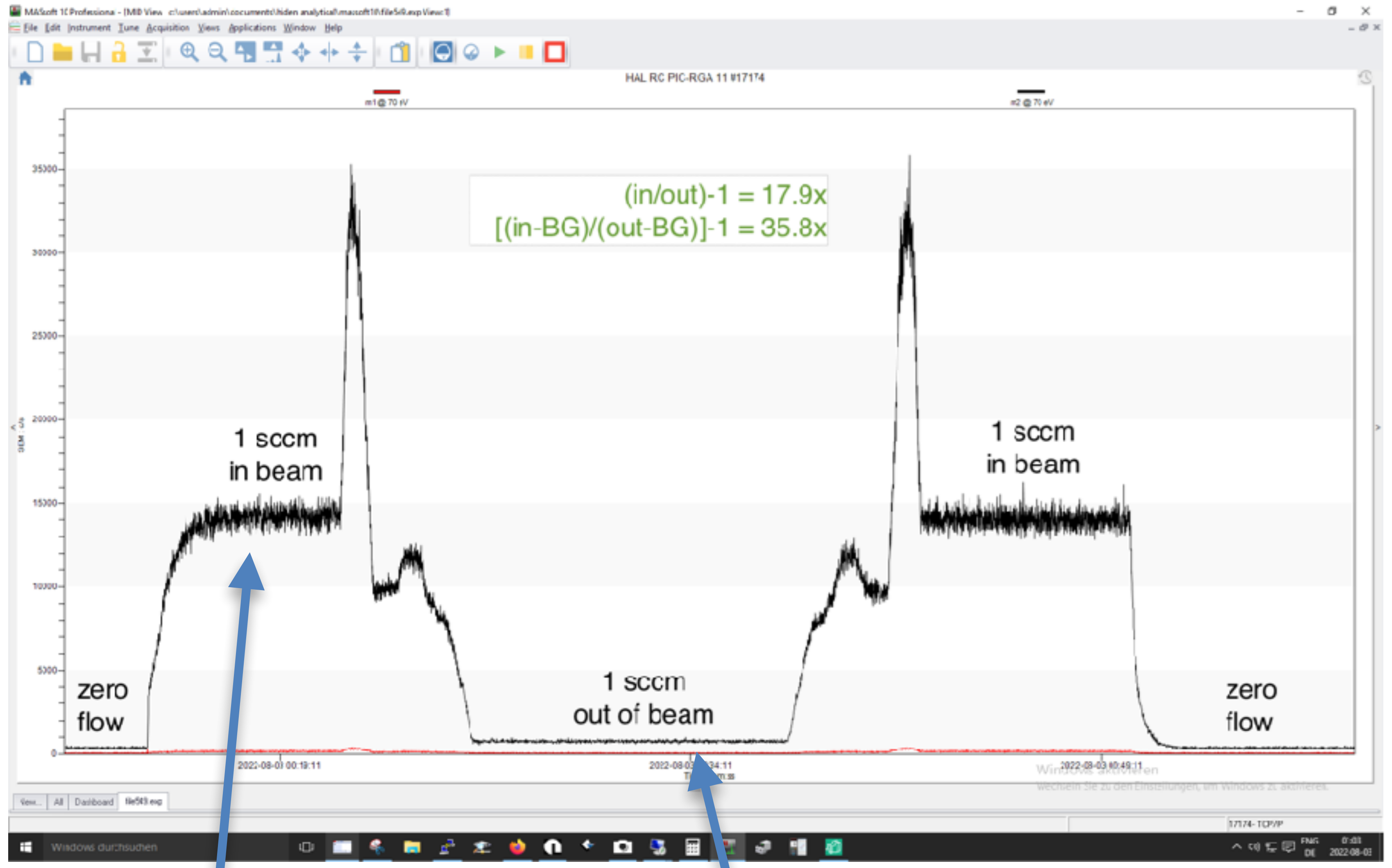

MS in beam
gas flow on

MS out of beam
gas flow on

The commercial thermal cracker!

Thermal cracker:
$H_2 \rightarrow 2\,H$

High-resolution mass spectrometer
for AMU 1-10 on z-translator (Hiden)

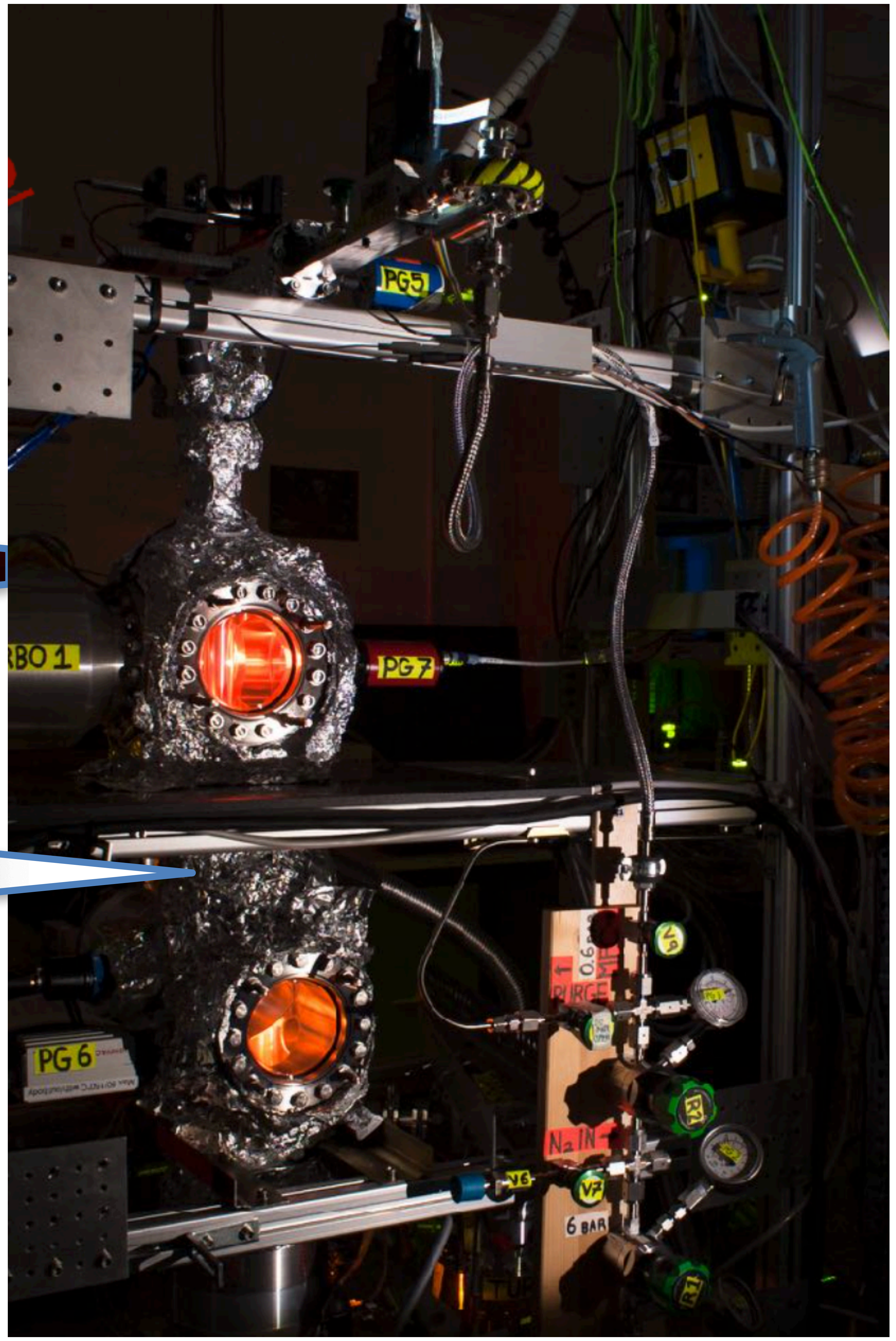

Mass 1 signal of mass spectrometer

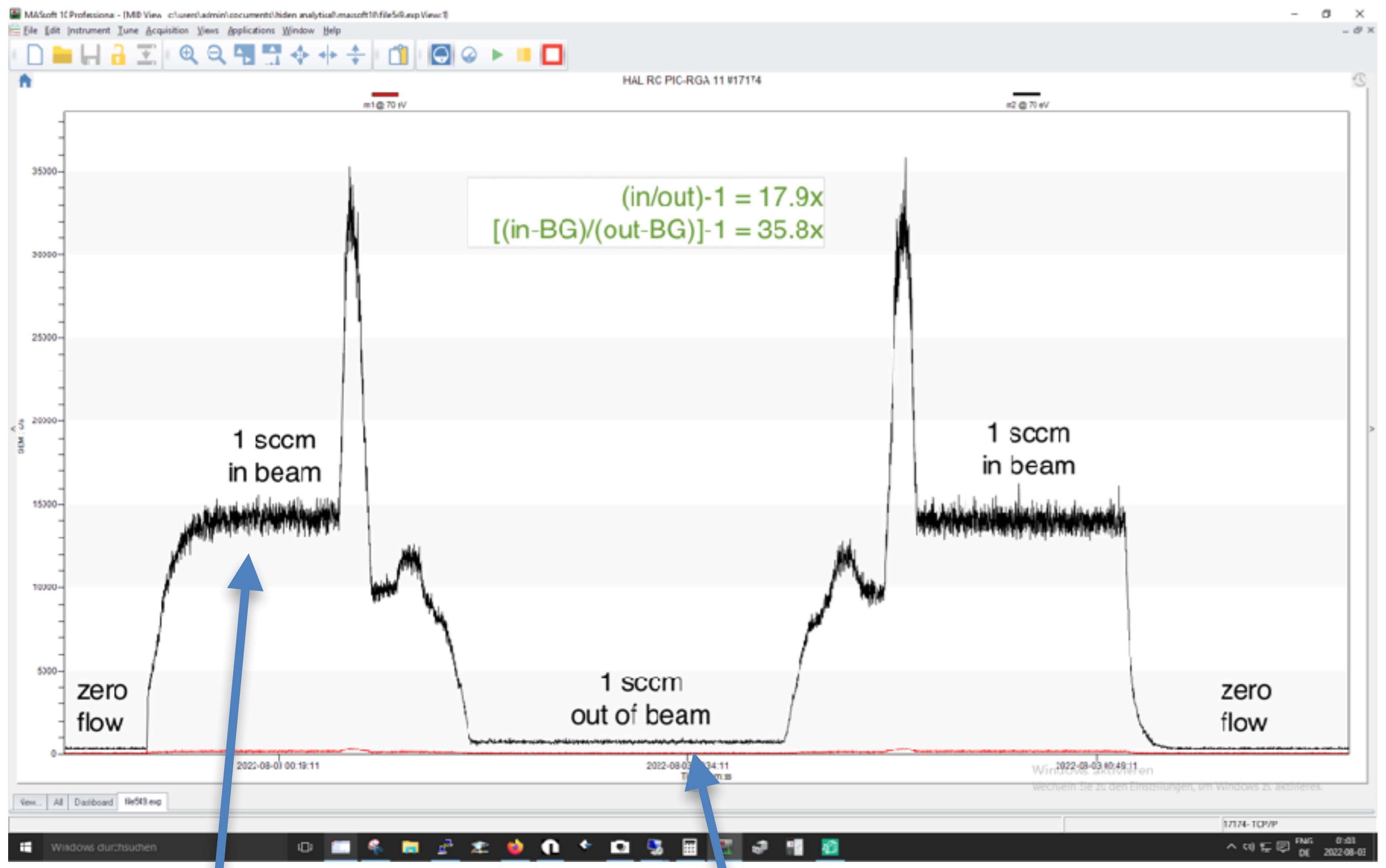

MS in beam
gas flow on

MS out of beam
gas flow on

<u>Biggest challenge:</u>
Derive absolute cracking efficiency
Understand and control H_2 bkgd!
Work in progress!

A wire-based beam monitor

Idea: measure resistance of 50 μm thick wire when hit by H beam

→ recombination to H_2 releases heat

→ calibrate flux vs. temp. increase

A wire-based beam monitor

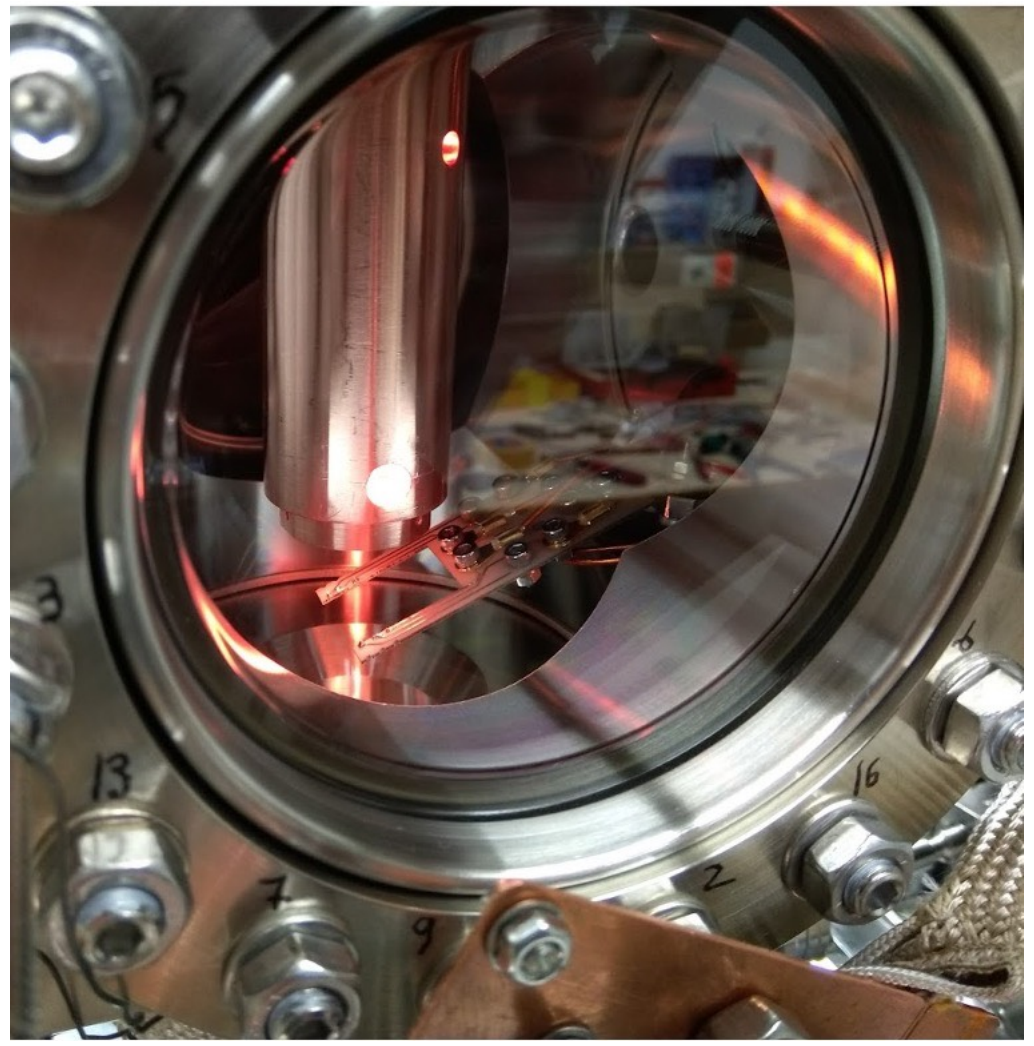

<u>Idea:</u> measure resistance of 50 μm thick wire when hit by H beam
→ recombination to H_2 releases heat
→ calibrate flux vs. temp. increase

figure credits: Ch. Matthé, A. Lindman

A wire-based beam monitor

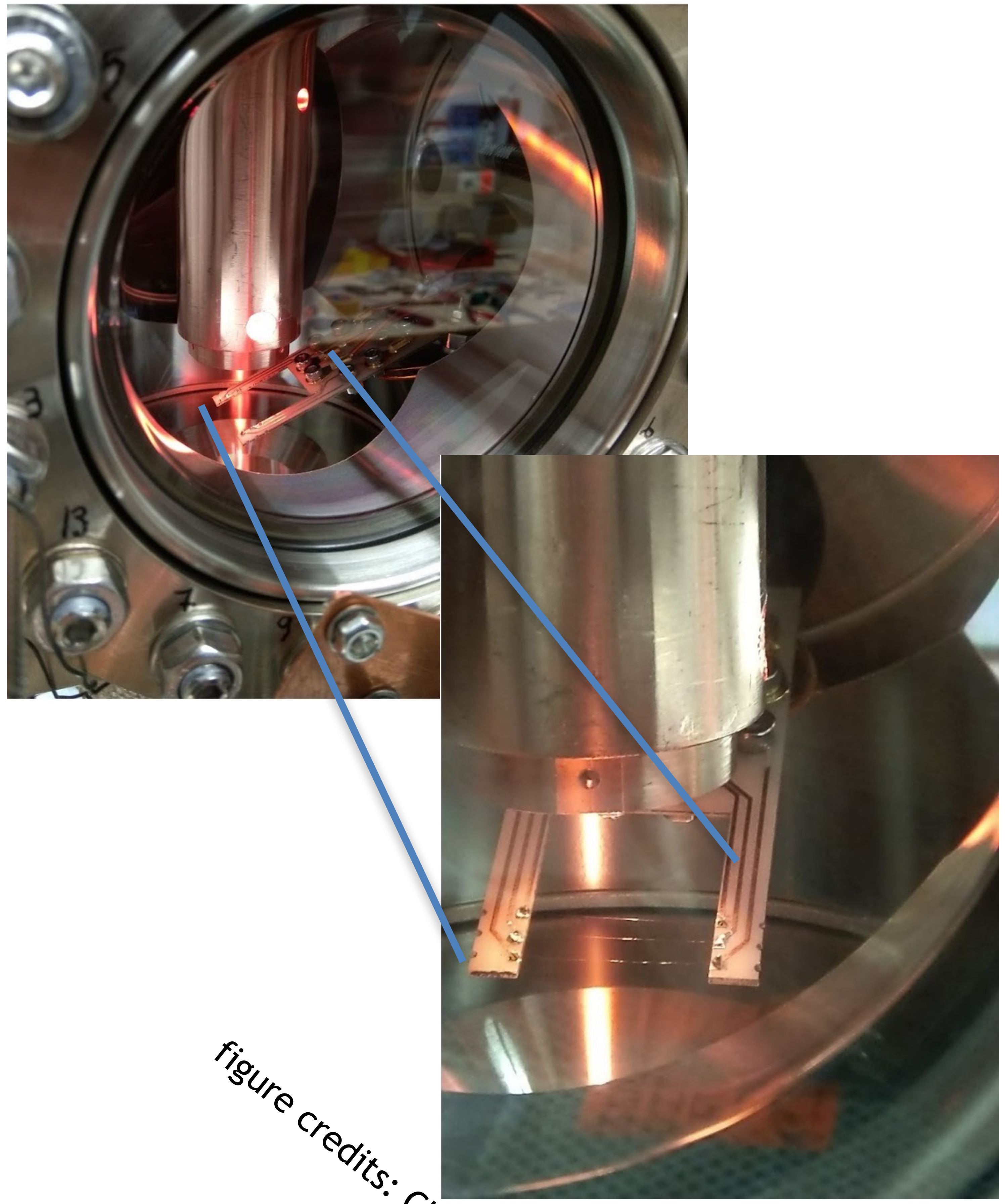

figure credits: Ch. Matthé, A. Lindman

Idea: measure resistance of 50 μm thick wire when hit by H beam

→ recombination to H_2 releases heat

→ calibrate flux vs. temp. increase

A wire-based beam monitor

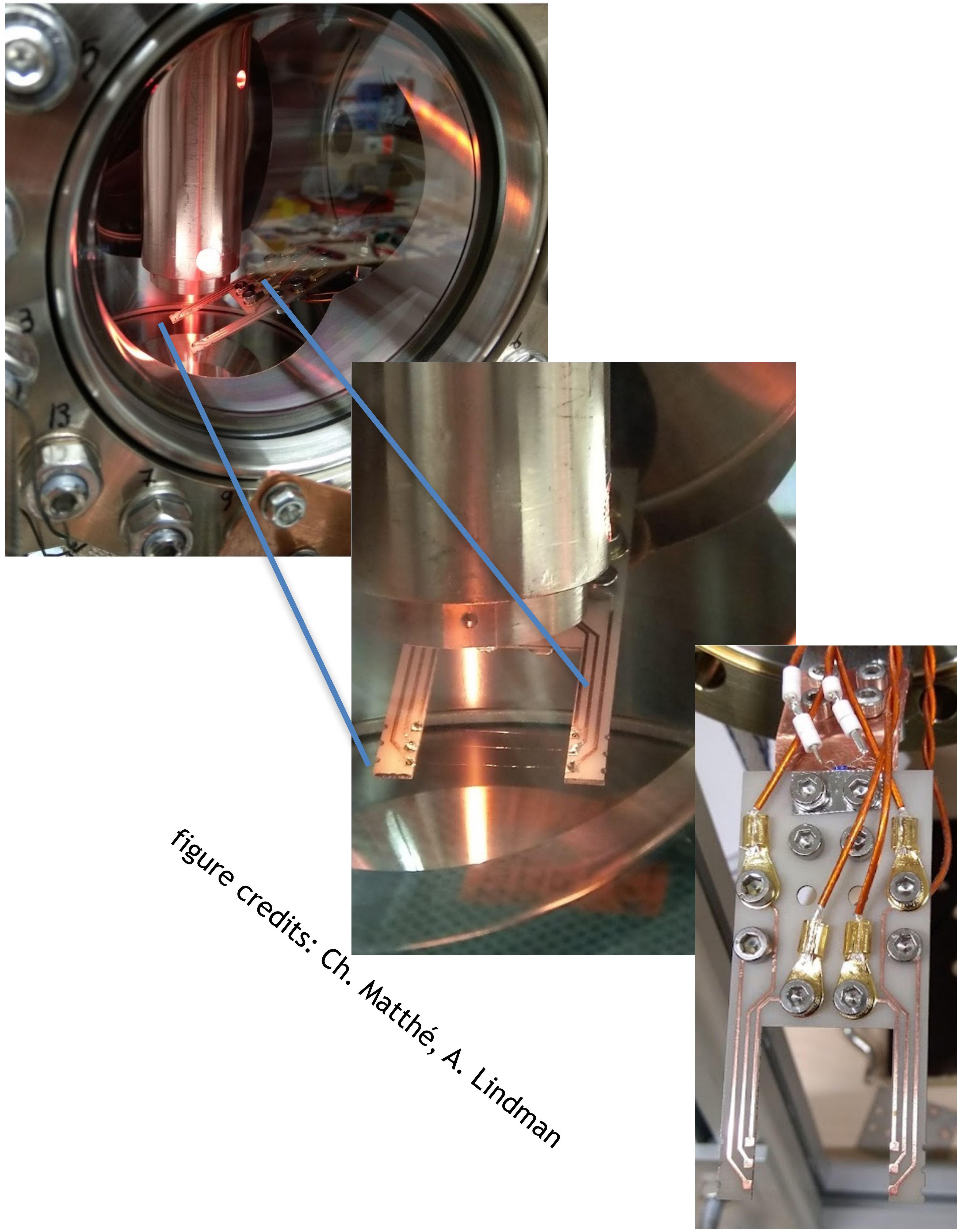

figure credits: Ch. Matthé, A. Lindman

Idea: measure resistance of 50 μm thick wire when hit by H beam

→ recombination to H_2 releases heat

→ calibrate flux vs. temp. increase

A wire-based beam monitor

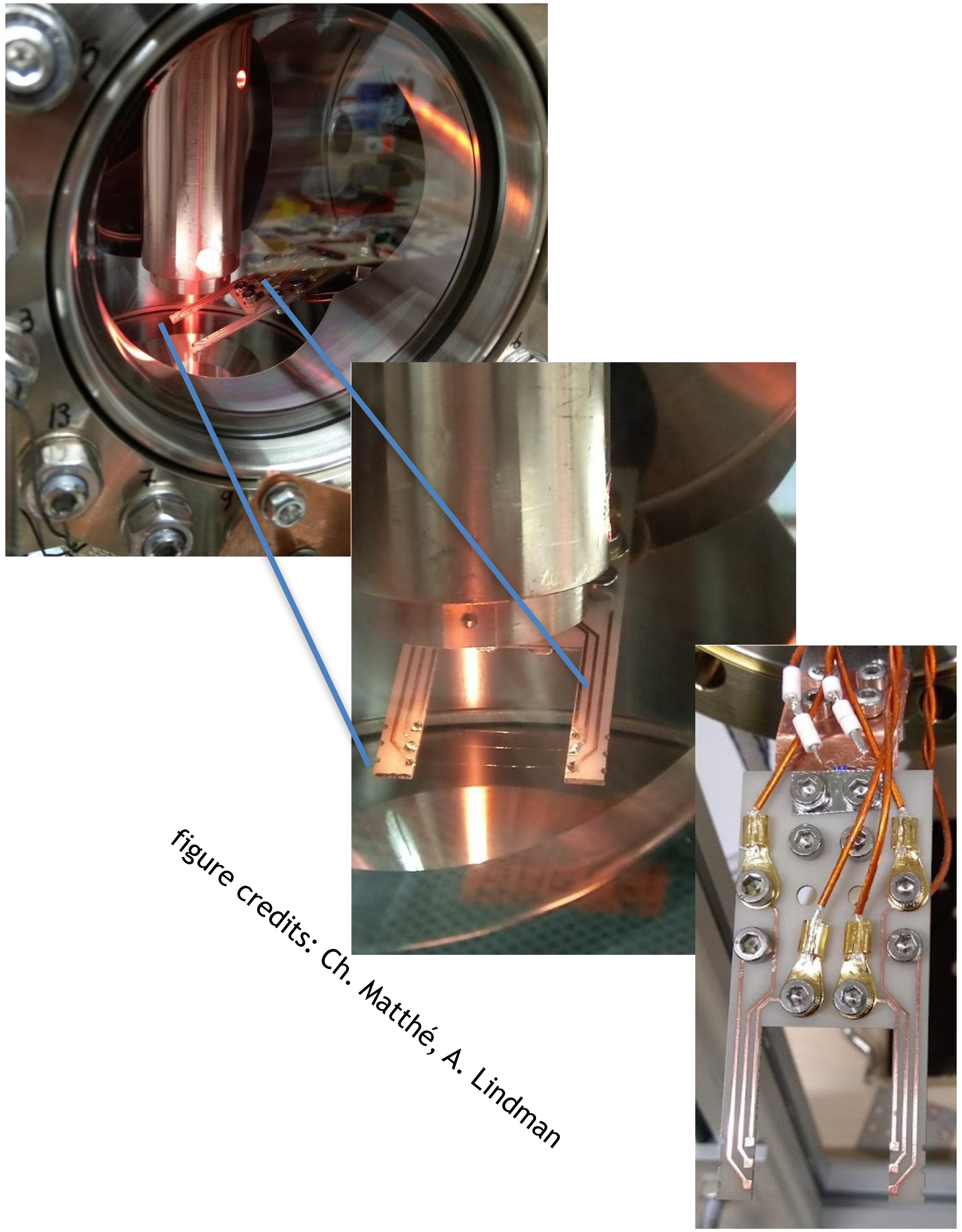

figure credits: Ch. Matthé, A. Lindman

Idea: measure resistance of 50 μm thick wire when hit by H beam

→ recombination to H_2 releases heat

→ calibrate flux vs. temp. increase

Challenge: Very complex interplay between heat sources and sinks

$$\text{Heat Sources} = \text{Heat Sinks}$$

$$F_{beam} + F_{el} = F_{rad} + F_{cond}$$

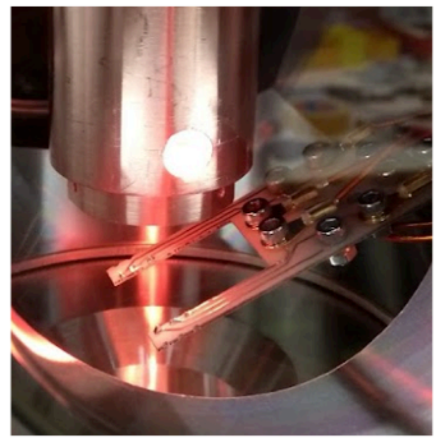

$$+F_{cracker} + F_{beam\ gas} \qquad + F_{residual\ gas}$$

- Blackbody emission from cracker at $\approx 2400\,\mathrm{K}$
  $F_{cracker} \propto T^4_{cracker}$
- Heat exchange with beam gas
  $F_{beam\ gas} \propto a(T_{bg}, T_{wire}) \cdot (T_{bg} - T_{wire})$
  Every Particle yields $a(T) \cdot 1\mathrm{eV}/1.16e4\,\mathrm{K}$
  at 2300K this is $\approx E_{rec}/10$

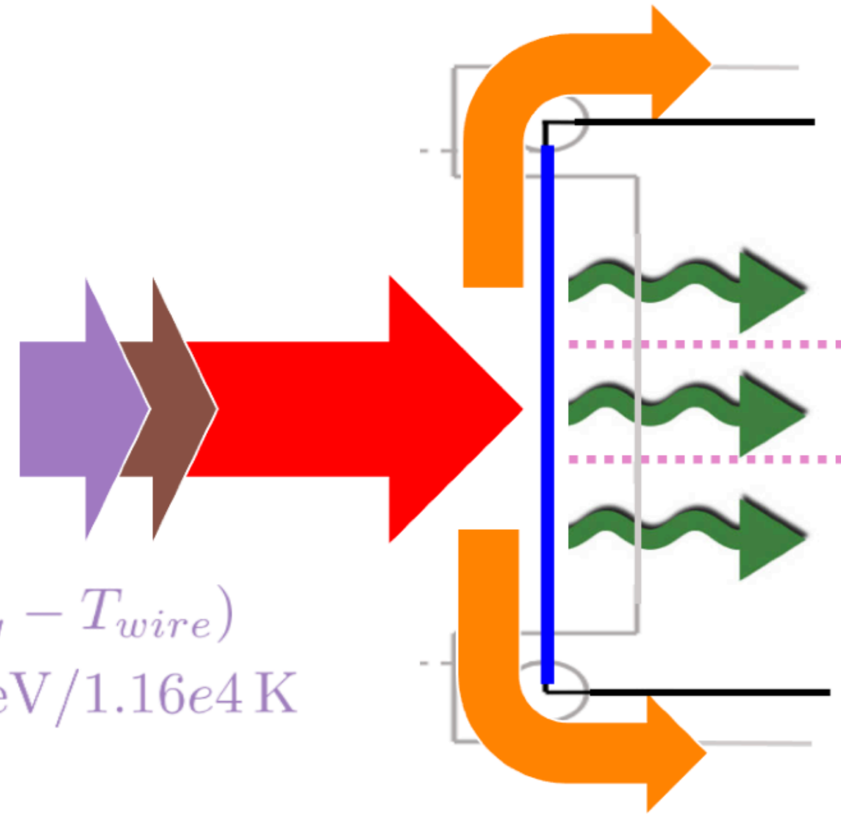

- Heat exchange with residual gas in vacuum
  $F_{res\ gas} \propto a(T_{rg}, T_{wire}) \cdot (T_{rg} - T_{wire})$
- The accommodation factor
  $0 \lesssim a(T_{rg}, T_{wire}) \lesssim 1$
  is a measure of what portion of energy gets deposited in the substrate the gas molecule binds to. It is surface and gas dependent.

A wire-based beam monitor

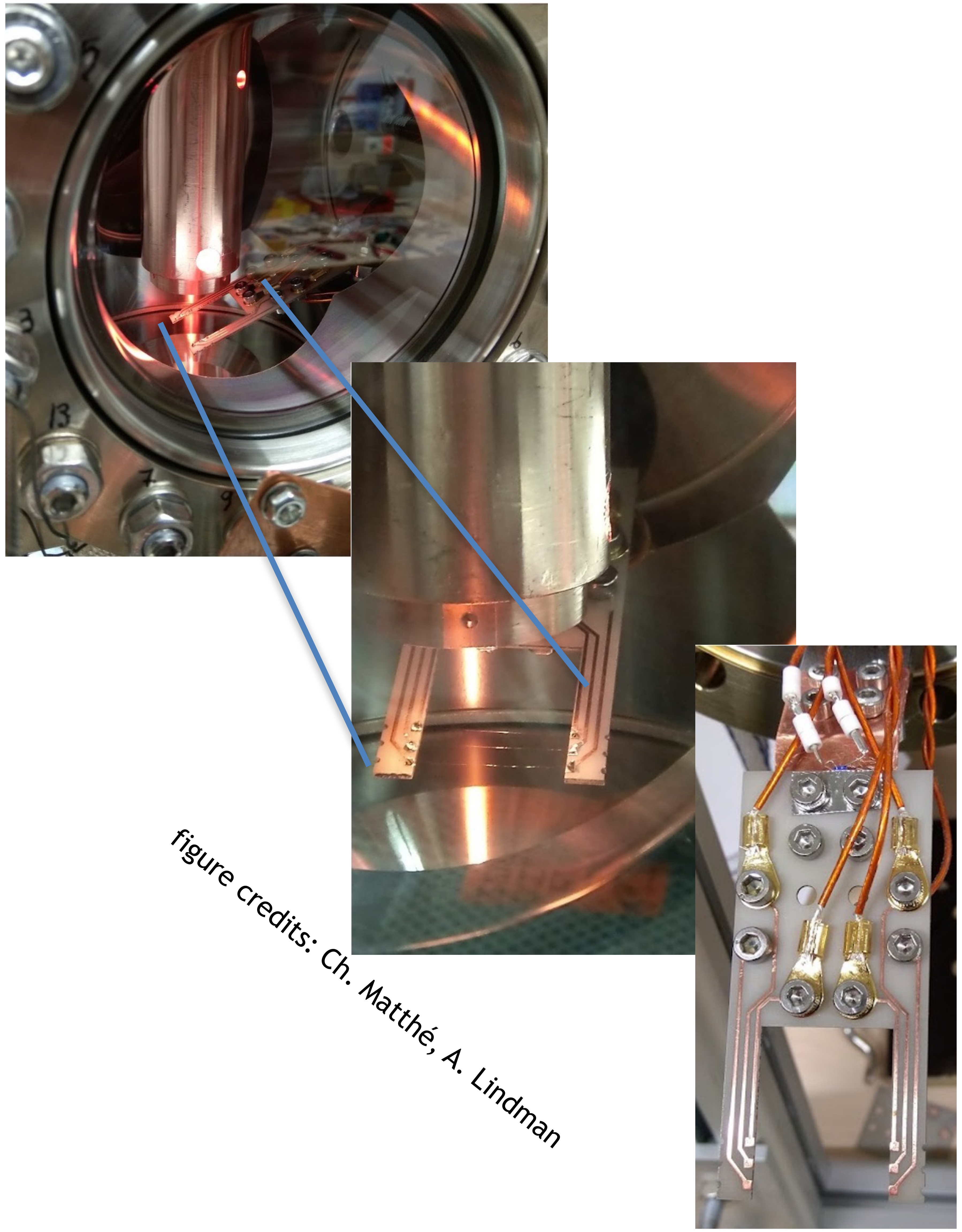

figure credits: Ch. Matthé, A. Lindman

<u>Idea:</u> measure resistance of 50 μm thick wire when hit by H beam

→ recombination to H_2 releases heat

→ calibrate flux vs. temp. increase

<u>Challenge:</u> Very complex interplay between heat sources and sinks

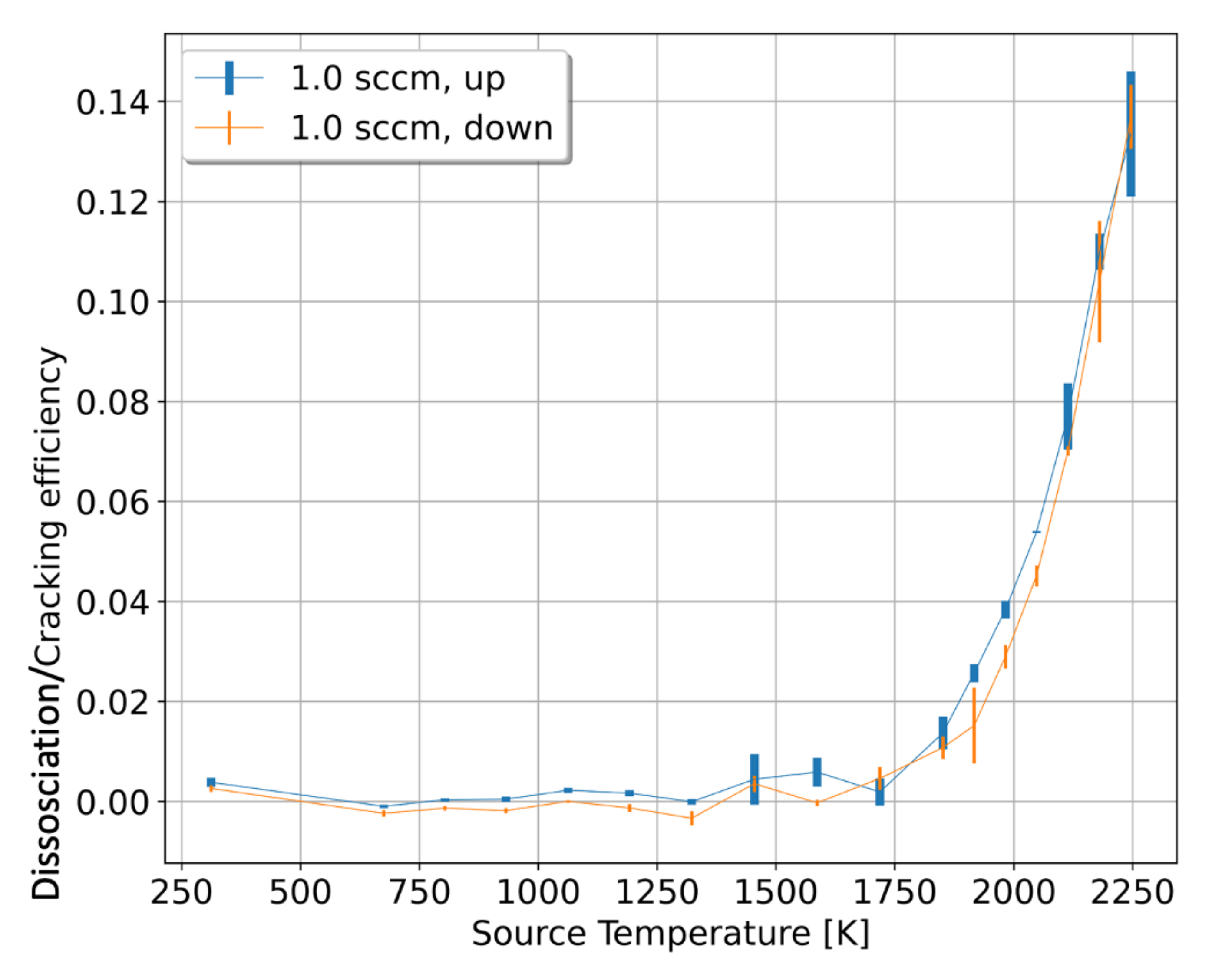

credit: Ch. Matthé

Recently achieved first reproducible signal related to cracker temperature cycle!

Preliminary estimate of cracking efficiency for the first time!

A wire-based beam monitor

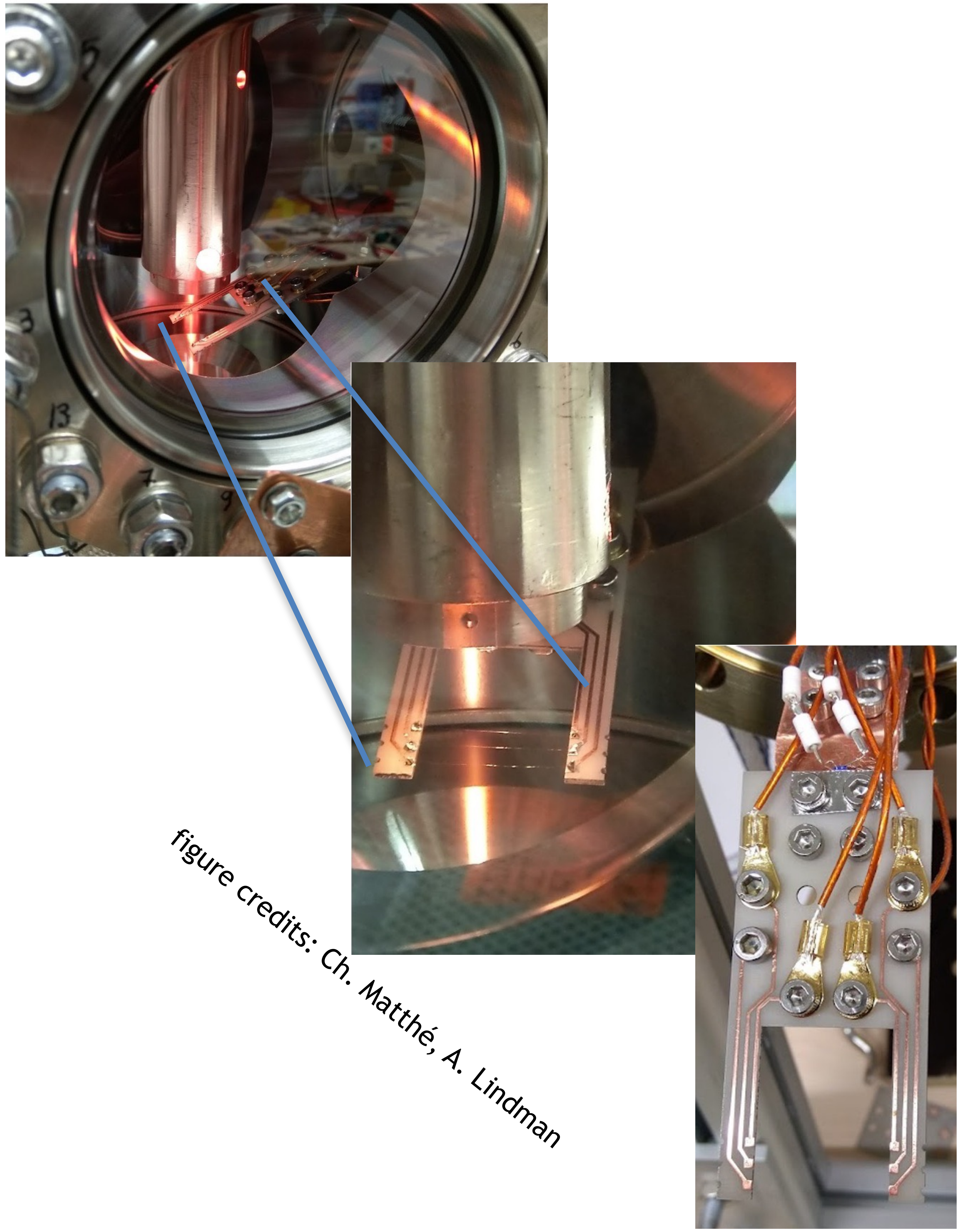

figure credits: Ch. Matthé, A. Lindman

Idea: measure resistance of 50 μm thick wire when hit by H beam

→ recombination to H_2 releases heat

→ calibrate flux vs. temp. increase

Challenge: Very complex interplay between heat sources and sinks

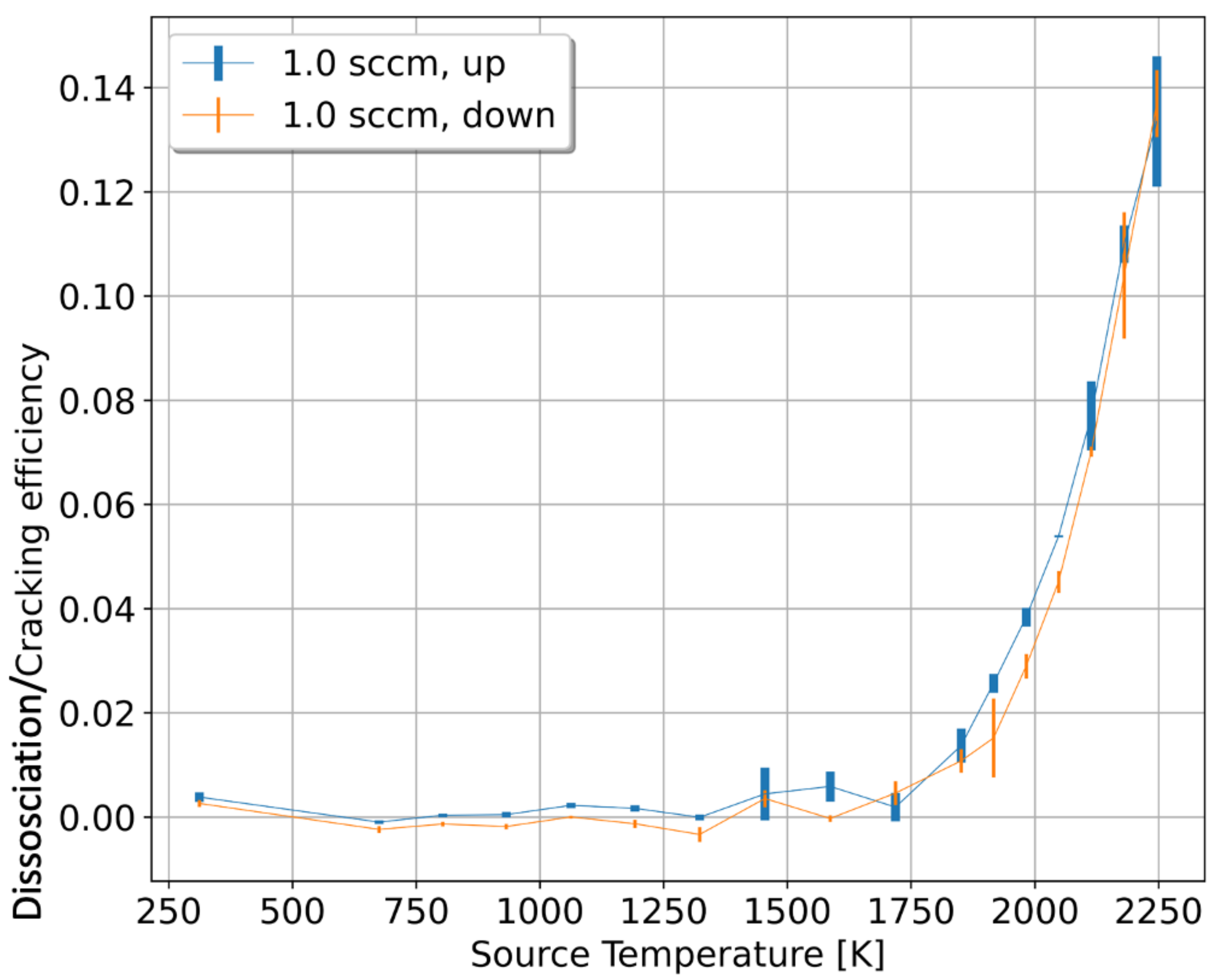

credit: Ch. Matthé

Recently achieved first reproducible signal related to cracker temperature cycle!

Preliminary estimate of cracking efficiency for the first time!

Appeal: Small foot print detectors along beam line as diagnostic tools
Only electrical measurements involved.

Development of magnetic evaporative cooling beam line

Problem: Accommodation on surfaces not possible to mK temperatures → Recombination of atomic hydrogen
Possible Mitigation: evaporative cooling of gas in decreasing trapping potential

Development of magnetic evaporative cooling beam line

Problem: Accommodation on surfaces not possible to mK temperatures → Recombination of atomic hydrogen
Possible Mitigation: evaporative cooling of gas in decreasing trapping potential

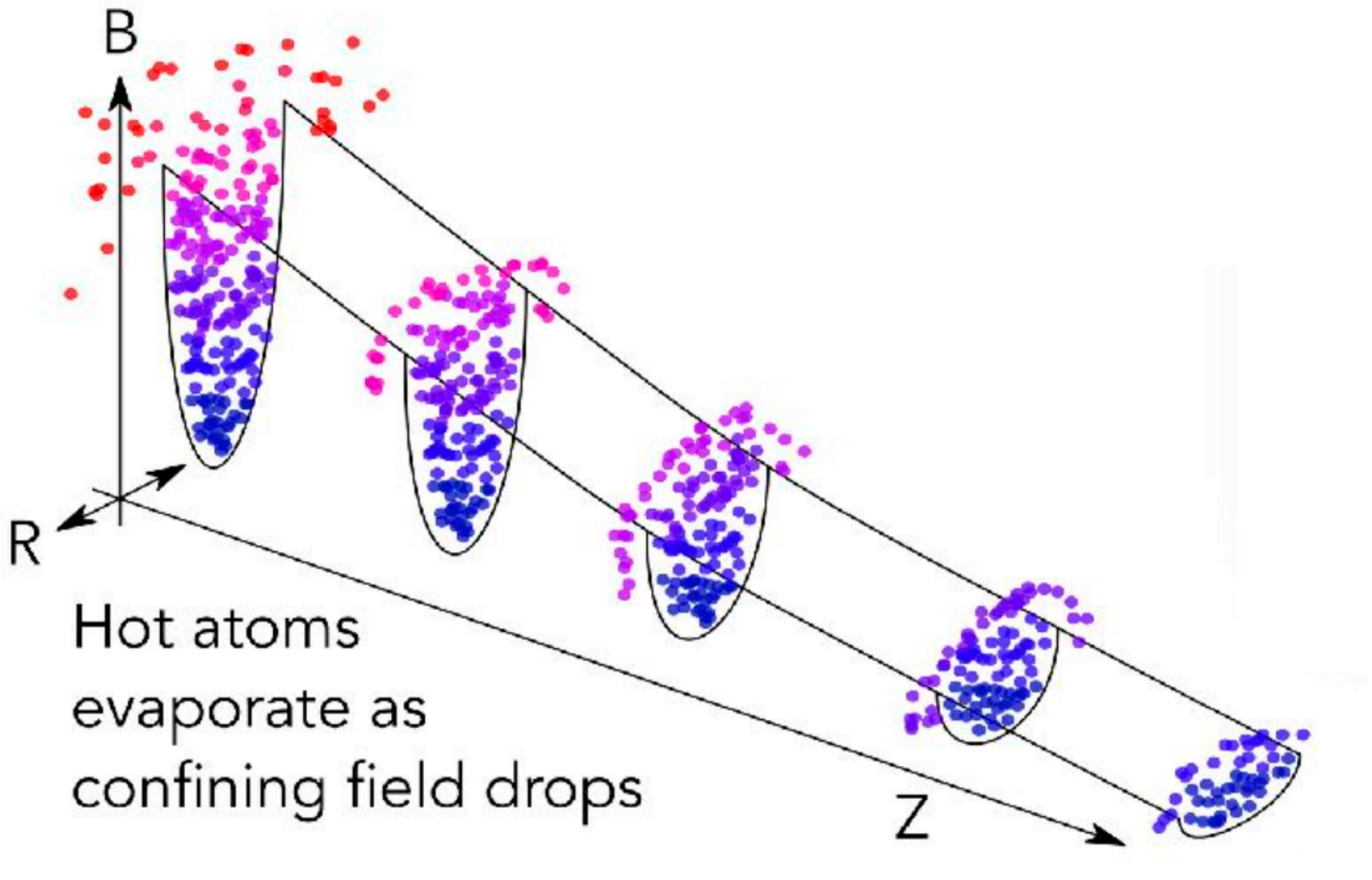

Goal 1: cooling

Radial confinement of atomic H gas: electron magnetic moment and radial gradient field (multipole)

Thermalization: large H density to maintain thermal equilibrium

Evaporation: Radial confinement fields decrease along the beam line
→ only coldest (slowest) atoms remain for injection

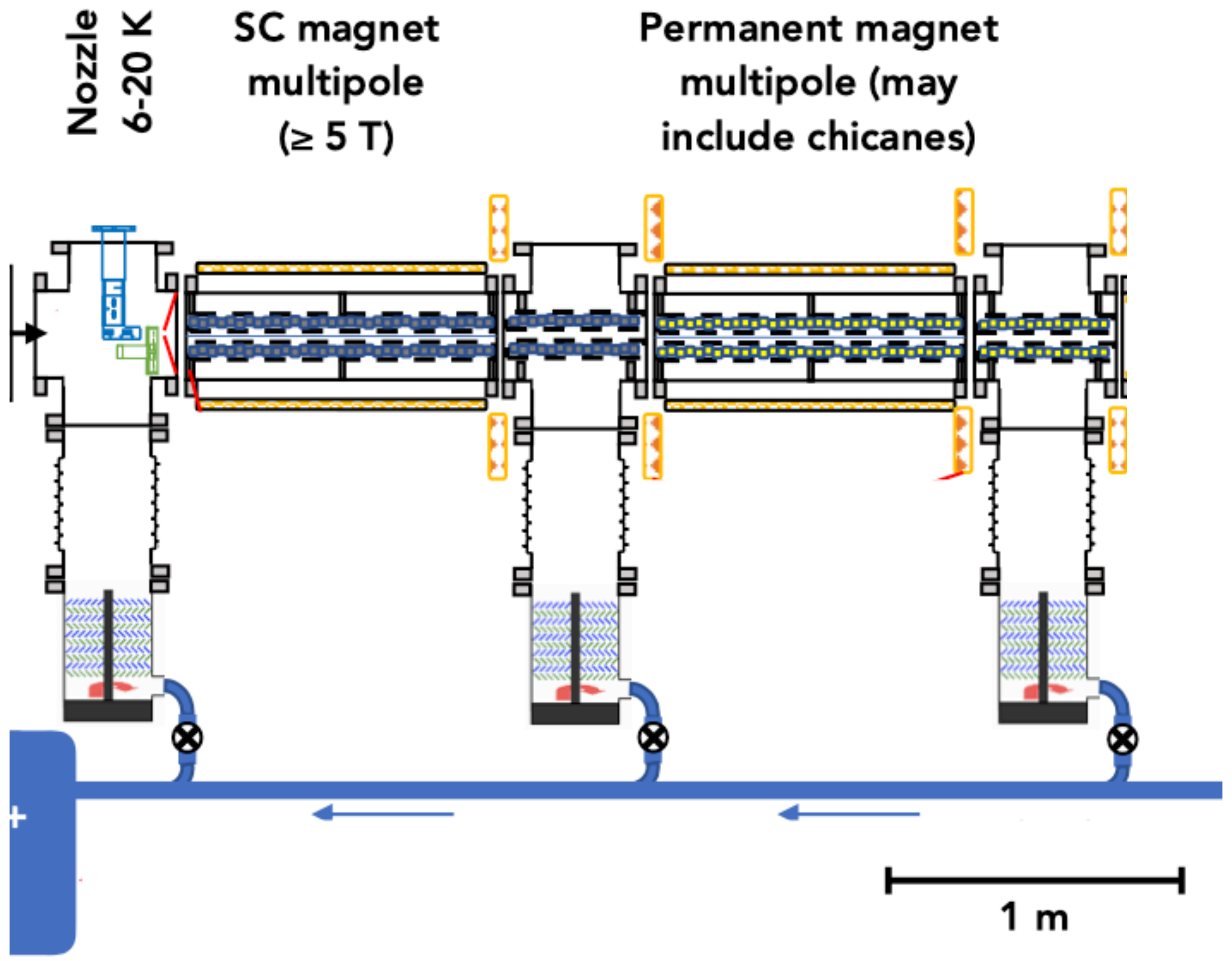

Development of magnetic evaporative cooling beam line

Problem: Accommodation on surfaces not possible to mK temperatures → Recombination of atomic hydrogen
Possible Mitigation: evaporative cooling of gas in decreasing trapping potential

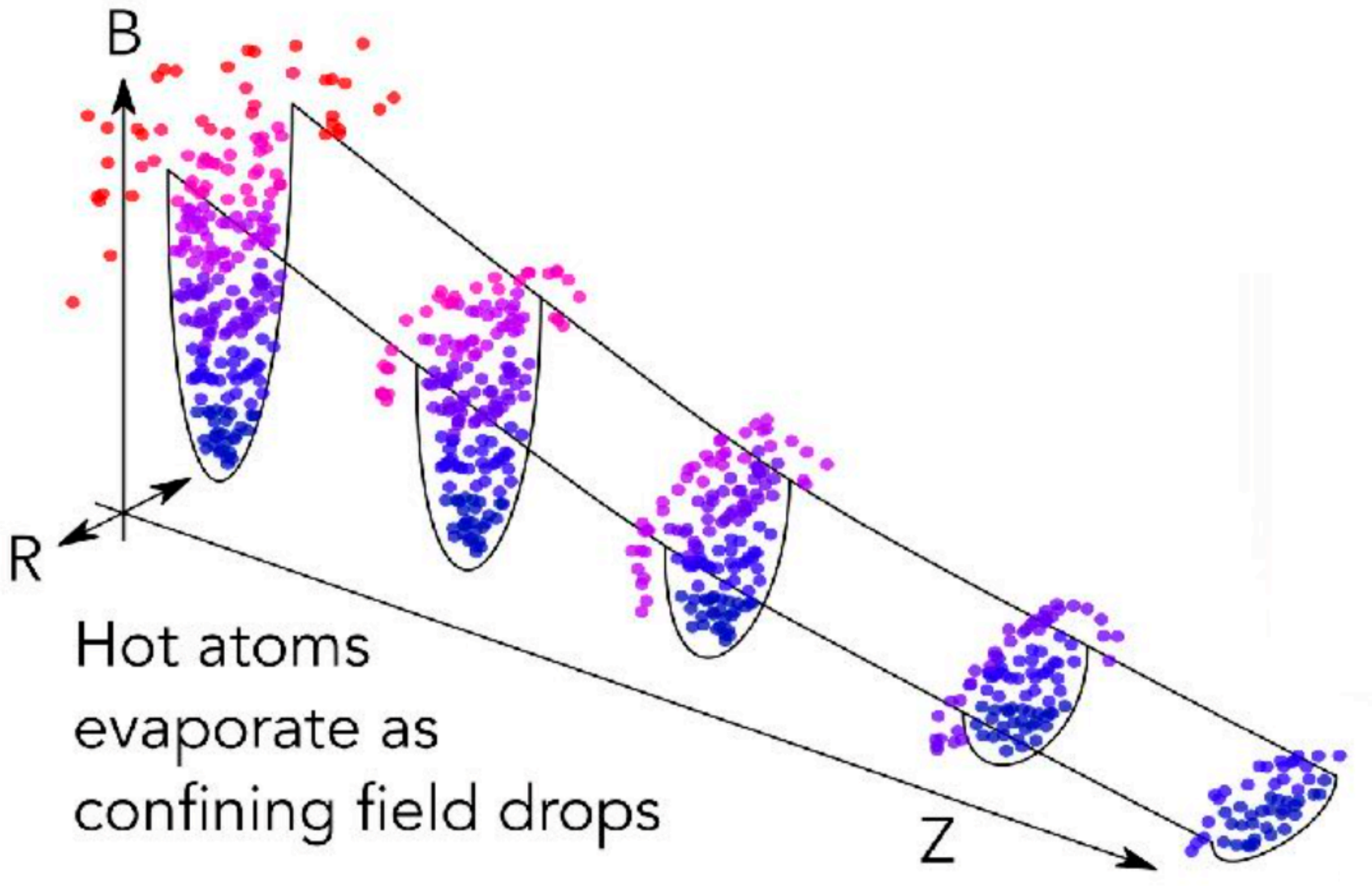

Goal 1: cooling
Radial confinement of atomic H gas: electron magnetic moment and radial gradient field (multipole)

Thermalization: large H density to maintain thermal equilibrium

Evaporation: Radial confinement fields decrease along the beam line
→ only coldest (slowest) atoms remain for injection

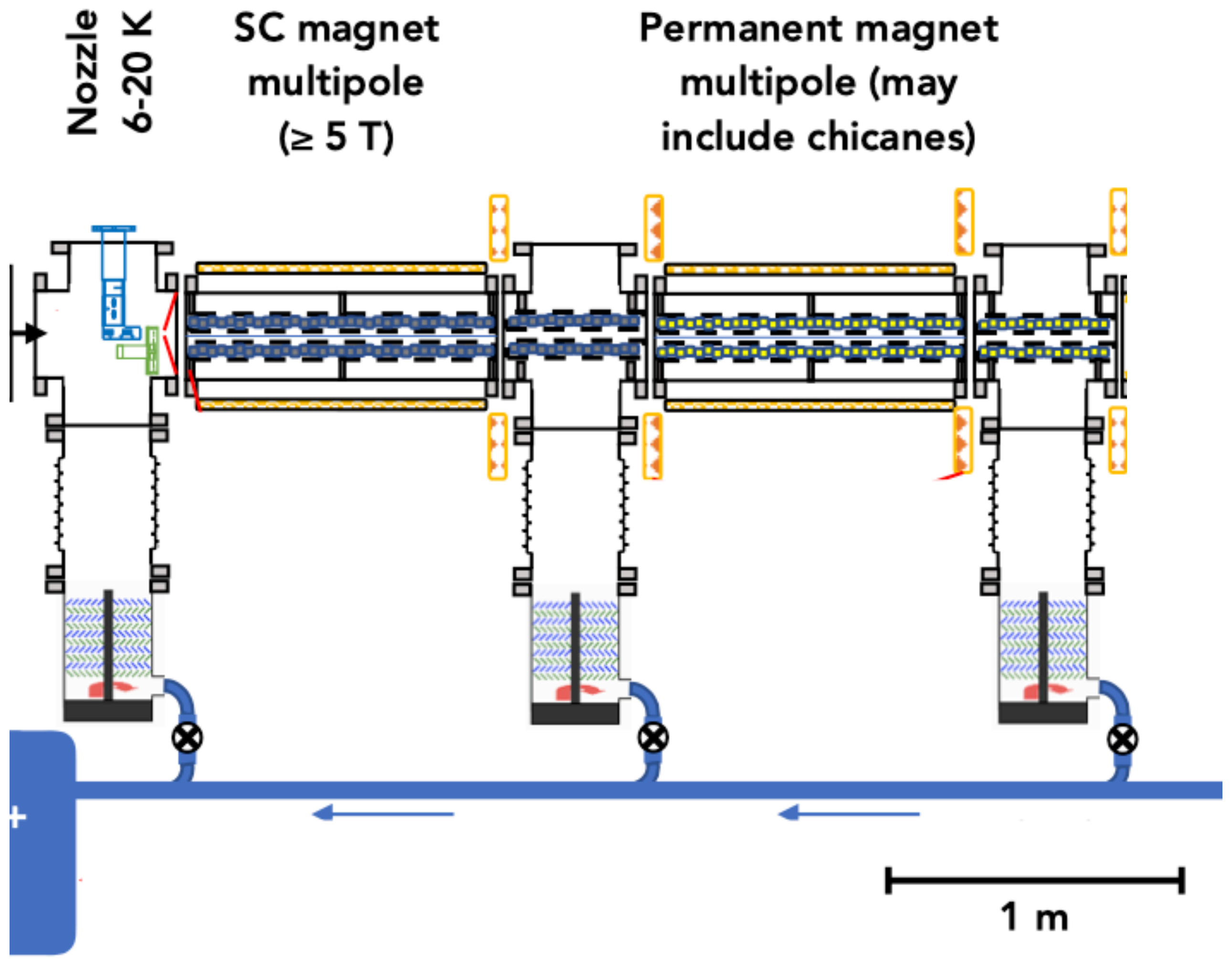

Goal 2: Pure atomic H beam
→ H_2 and helium has no significant magnetic moment
→ H_2 and helium contaminants are not confined and leave radially

Largest challenges:
→ Fully integrated design with SC and permanent magnets
→ cryogenics, UHV, magnetic fields, total gas load

Development of magnetic evaporative cooling beam line

Problem: Accommodation on surfaces not possible to mK temperatures → Recombination of atomic hydrogen
Possible Mitigation: evaporative cooling of gas in decreasing trapping potential

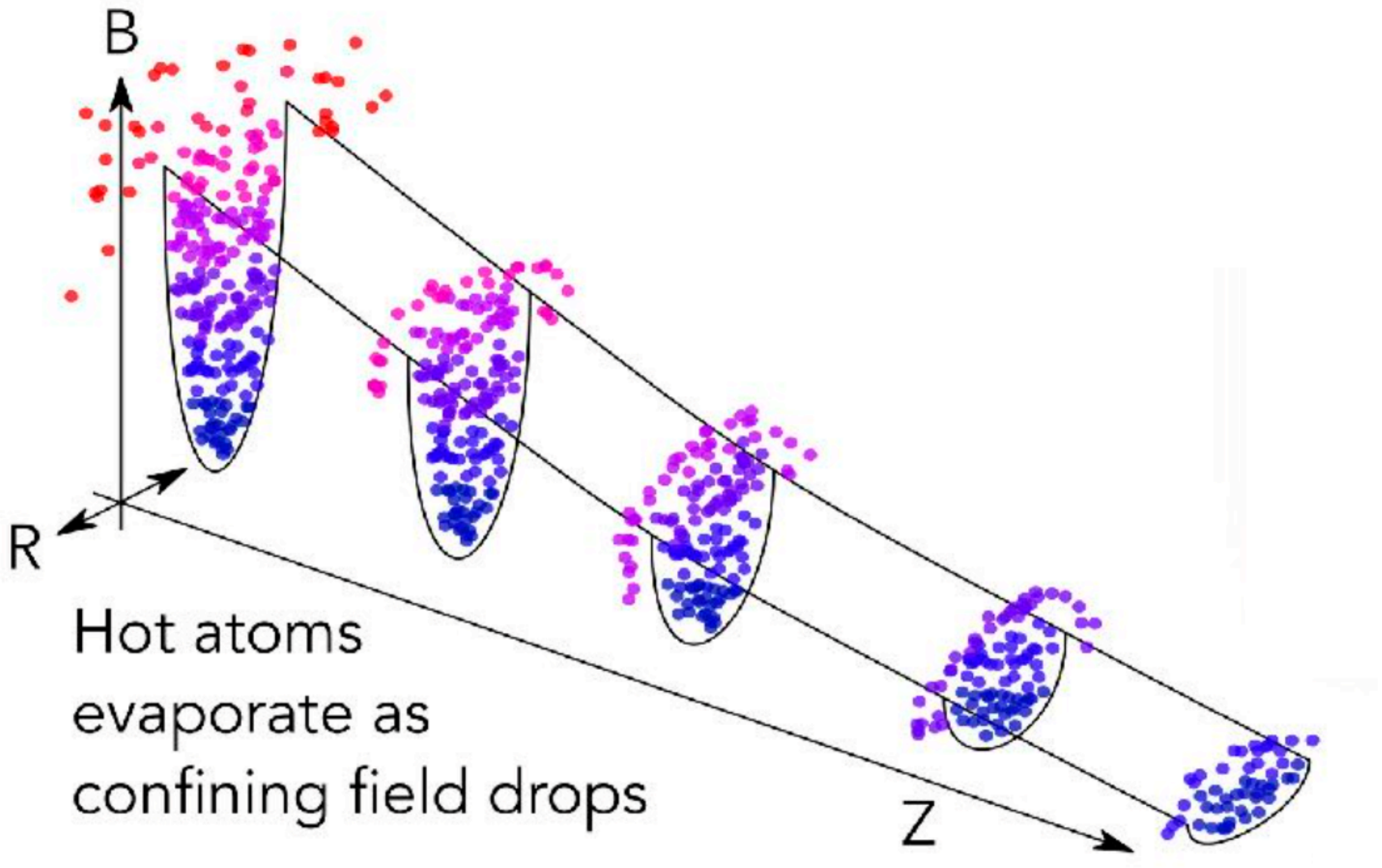

Goal 1: cooling
Radial confinement of atomic H gas: electron magnetic moment
and radial gradient field (multipole)

Thermalization: large H density to maintain thermal equilibrium

Evaporation: Radial confinement fields decrease along the beam line
→ only coldest (slowest) atoms remain for injection

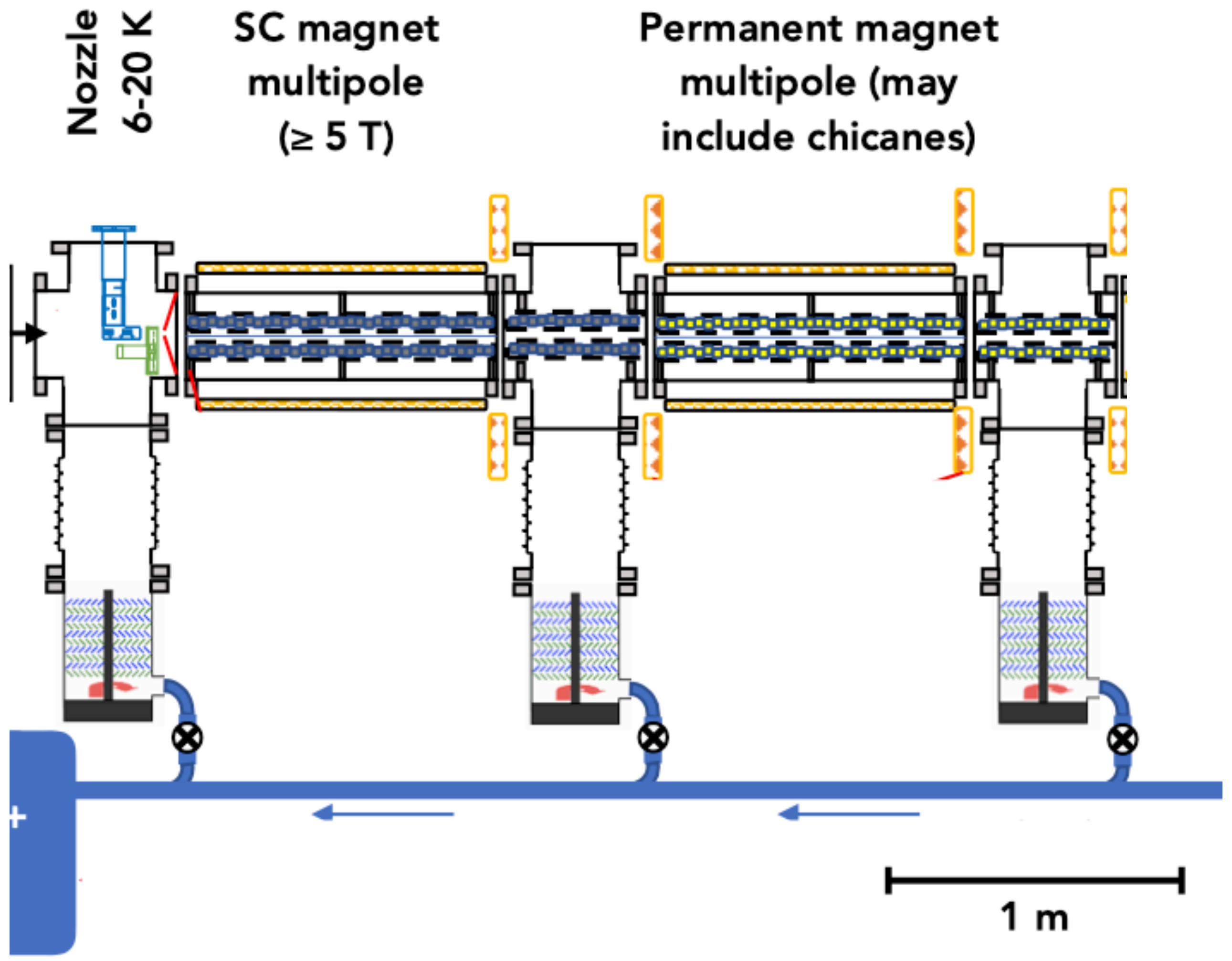

Goal 2: Pure atomic H beam
→ H_2 and helium has no significant magnetic moment
→ H_2 and helium contaminants are not confined and leave radially

Largest challenges:
→ Fully integrated design with SC and permanent magnets
→ cryogenics, UHV, magnetic fields, total gas load

Additional development in the collaboration: Li cooling beam line at Univ. of Texas

Project 8 summary

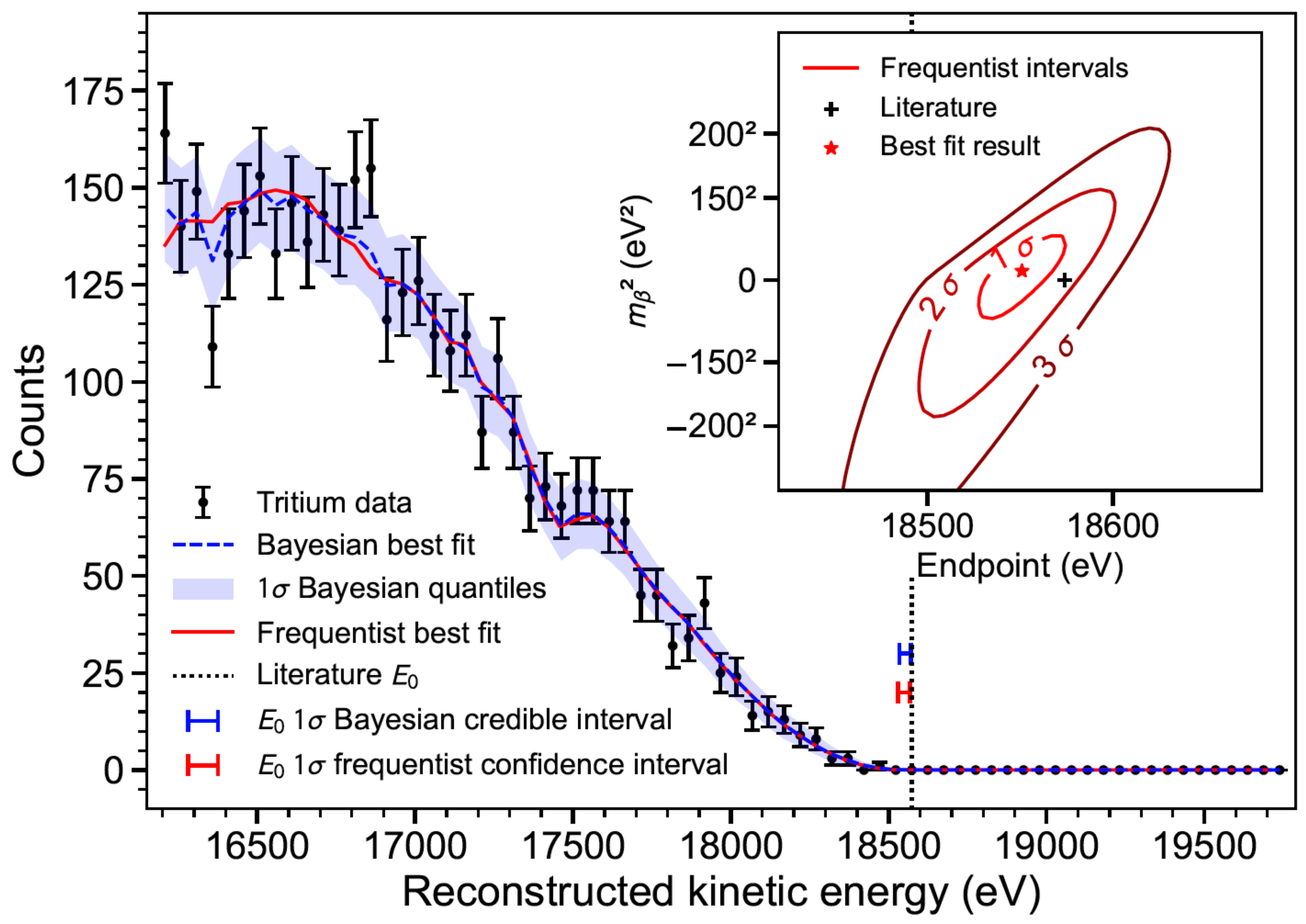

Phase II: First CRES-based neutrino mass limit

T2 endpoint: $E_0^{\text{Freq.}} = \left(18548^{+19}_{-19}\right)$ eV (1σ)

$E_0^{\text{Bay.}} = \left(18553^{+18}_{-19}\right)$ eV (1σ)

Neutrino mass: $m_\beta^{\text{Freq.}} \leq 152\,\text{eV/c}^2$ (90 % C.L.)

$m_\beta^{\text{Bay.}} \leq 155\,\text{eV/c}^2$ (90 % C.I.)

Background rate: $\leq 3 \times 10^{-10}\,\text{eV}^{-1}\text{s}^{-1}$ (90 % C.I.)

Project 8 summary

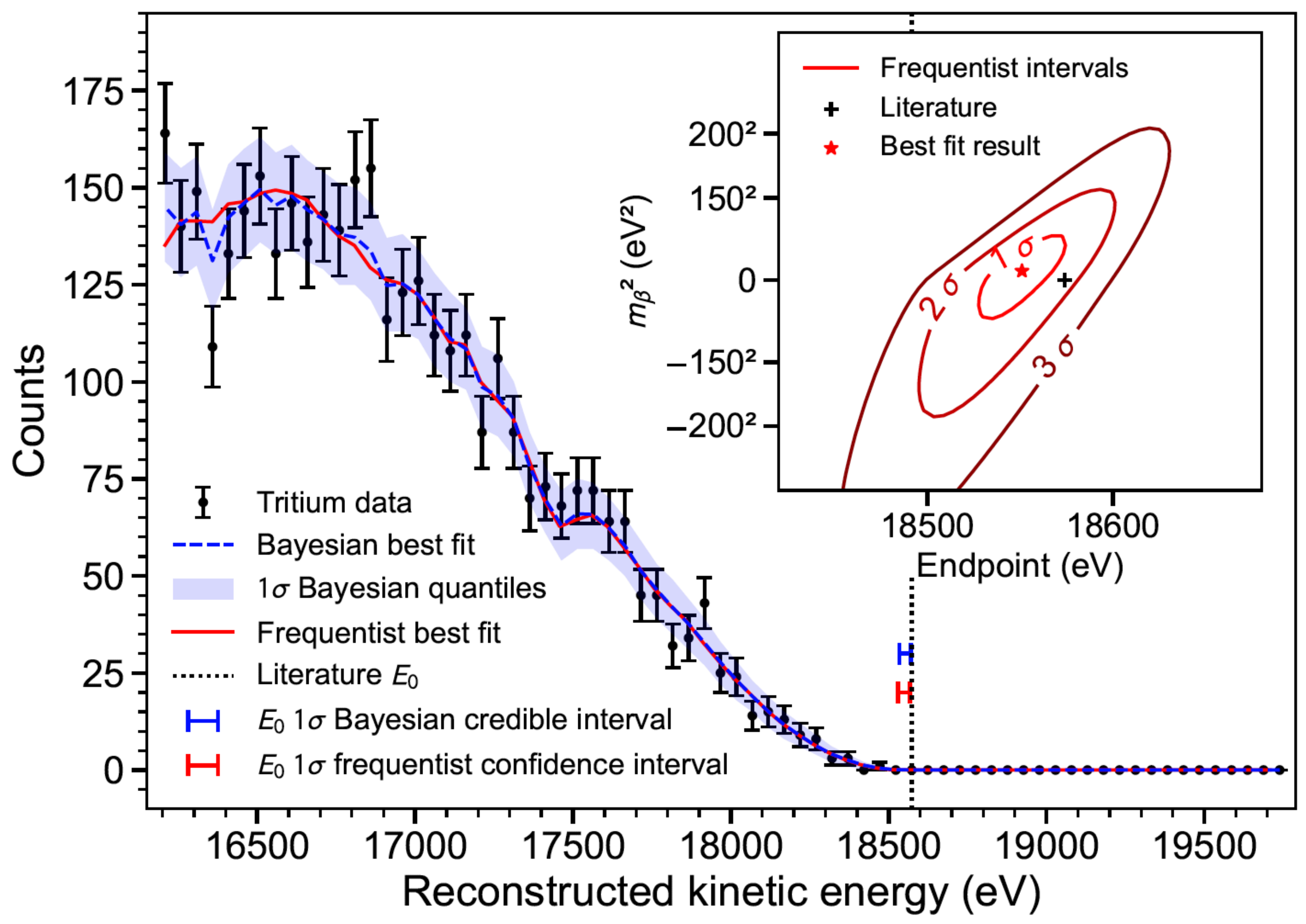

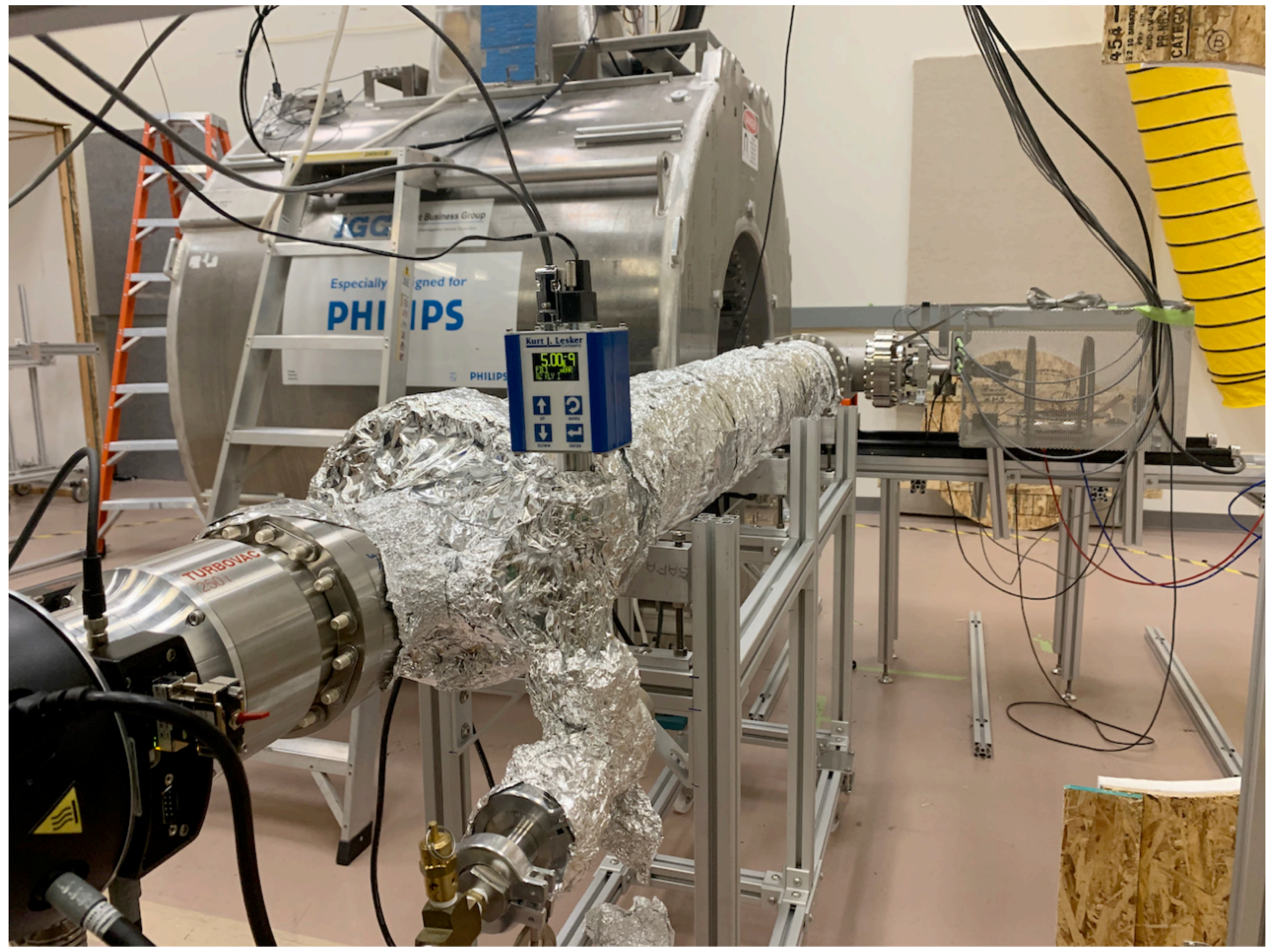

Phase II: First CRES-based neutrino mass limit

T2 endpoint: $E_0^{\text{Freq.}} = \left(18548^{+19}_{-19}\right)$ eV (1σ)

$E_0^{\text{Bay.}} = \left(18553^{+18}_{-19}\right)$ eV (1σ)

Neutrino mass: $m_\beta^{\text{Freq.}} \leq 152\,\text{eV/c}^2$ (90 % C.L.)

$m_\beta^{\text{Bay.}} \leq 155\,\text{eV/c}^2$ (90 % C.I.)

Background rate: $\leq 3 \times 10^{-10}\,\text{eV}^{-1}\text{s}^{-1}$ (90 % C.I.)

Phase III: Intense R&D program to establish the scaling relations to design an experiment with 40 meV mass sensitivity:

- Signal detection in a small RF cavity instead of a waveguide
- Scaling of the gas volume from mm^3 to m^3 and in low field
- Production of trapped cold atomic hydrogen/tritium

^{6}He-CRES: Fierz interference searches with broad-band CRES

Fierz term contribution to differential decay rate

$$w(\langle \mathbf{J} \rangle | E_e, \Omega_e, \Omega_\nu) dE_e d\Omega_e d\Omega_\nu = \frac{F(\pm Z, E_e)}{(2\pi)^5} p_e E_e (E_0 - E_e)^2 dE_e d\Omega_e d\Omega_\nu \times$$

$$\xi \left\{ 1 + a \frac{\mathbf{p}_e \cdot \mathbf{p}_\nu}{E_e E_\nu} + b \frac{m_e}{E_e} + \frac{\langle \mathbf{J} \rangle}{J} \cdot \left[A \frac{\mathbf{p}_e}{E_e} + B \frac{\mathbf{p}_\nu}{E_\nu} + D \frac{\mathbf{p}_e \times \mathbf{p}_\nu}{E_e E_\nu} \right] \right\} ,$$

^{6}He-CRES: Fierz interference searches with broad-band CRES

Fierz term contribution to differential decay rate

$$w(\langle \mathbf{J} \rangle | E_e, \Omega_e, \Omega_\nu) dE_e d\Omega_e d\Omega_\nu = \frac{F(\pm Z, E_e)}{(2\pi)^5} p_e E_e (E_0 - E_e)^2 dE_e d\Omega_e d\Omega_\nu \times$$

$$\xi \left\{ 1 + a \frac{\mathbf{p}_e \cdot \mathbf{p}_\nu}{E_e E_\nu} + b \frac{m_e}{E_e} + \frac{\langle \mathbf{J} \rangle}{J} \cdot \left[A \frac{\mathbf{p}_e}{E_e} + B \frac{\mathbf{p}_\nu}{E_\nu} + D \frac{\mathbf{p}_e \times \mathbf{p}_\nu}{E_e E_\nu} \right] \right\},$$

First order sensitivity to new physics: $b \propto \mathrm{Re}\left(\left| M_\mathrm{F} \right|^2 \frac{C_\mathrm{S} + C'_\mathrm{S}}{C_\mathrm{V}} + \left| M_\mathrm{GT} \right|^2 \frac{C_\mathrm{T} + C'_\mathrm{T}}{C_\mathrm{A}} \right)$

^{6}He-CRES: Fierz interference searches with broad-band CRES

Fierz term contribution to differential decay rate

$$w(\langle \mathbf{J} \rangle | E_e, \Omega_e, \Omega_\nu) dE_e d\Omega_e d\Omega_\nu = \frac{F(\pm Z, E_e)}{(2\pi)^5} p_e E_e (E_0 - E_e)^2 dE_e d\Omega_e d\Omega_\nu \times$$

$$\xi \left\{ 1 + a \frac{\mathbf{p}_e \cdot \mathbf{p}_\nu}{E_e E_\nu} + b \frac{m_e}{E_e} + \frac{\langle \mathbf{J} \rangle}{J} \cdot \left[A \frac{\mathbf{p}_e}{E_e} + B \frac{\mathbf{p}_\nu}{E_\nu} + D \frac{\mathbf{p}_e \times \mathbf{p}_\nu}{E_e E_\nu} \right] \right\} ,$$

First order sensitivity to new physics: $b \propto \mathrm{Re} \left(\left| M_F \right|^2 \frac{C_S + C_S'}{C_V} + \left| M_{GT} \right|^2 \frac{C_T + C_T'}{C_A} \right)$

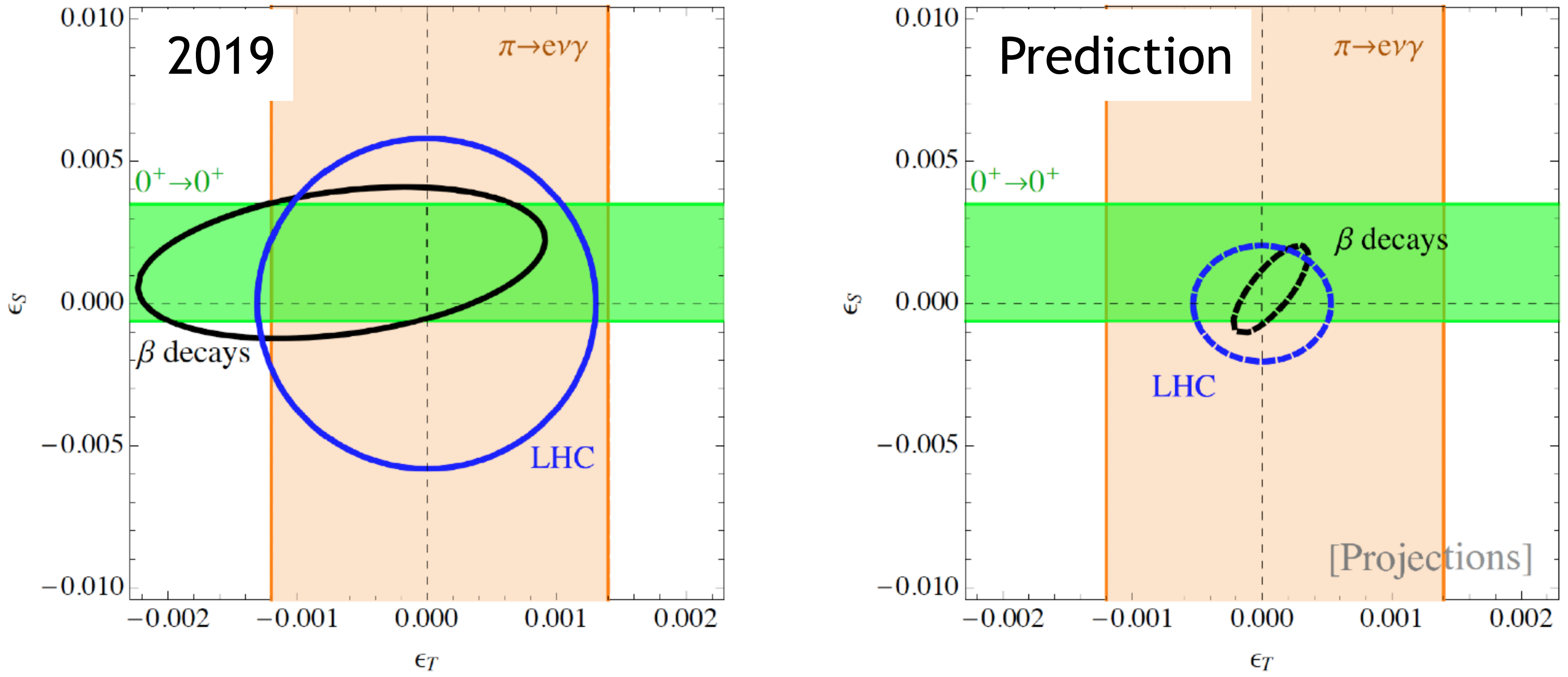

Gonzalez-Alonso, et al., Progress in Particle and Nuclear Physics, Volume 104, January 2019, Pages 165-223

^{6}He-CRES: Fierz interference searches with broad-band CRES

Fierz term contribution to differential decay rate

$$w(\langle \mathbf{J}\rangle|E_e,\Omega_e,\Omega_\nu)dE_e d\Omega_e d\Omega_\nu = \frac{F(\pm Z,E_e)}{(2\pi)^5} p_e E_e (E_0-E_e)^2 dE_e d\Omega_e d\Omega_\nu \times$$

$$\xi\left\{1 + a\frac{\mathbf{p}_e\cdot\mathbf{p}_\nu}{E_eE_\nu} + b\frac{m_e}{E_e} + \frac{\langle \mathbf{J}\rangle}{J}\cdot\left[A\frac{\mathbf{p}_e}{E_e} + B\frac{\mathbf{p}_\nu}{E_\nu} + D\frac{\mathbf{p}_e\times\mathbf{p}_\nu}{E_eE_\nu}\right]\right\},$$

First order sensitivity to new physics: $b \propto \mathrm{Re}\left(|M_F|^2\frac{C_S+C_S'}{C_V} + |M_{GT}|^2\frac{C_T+C_T'}{C_A}\right)$

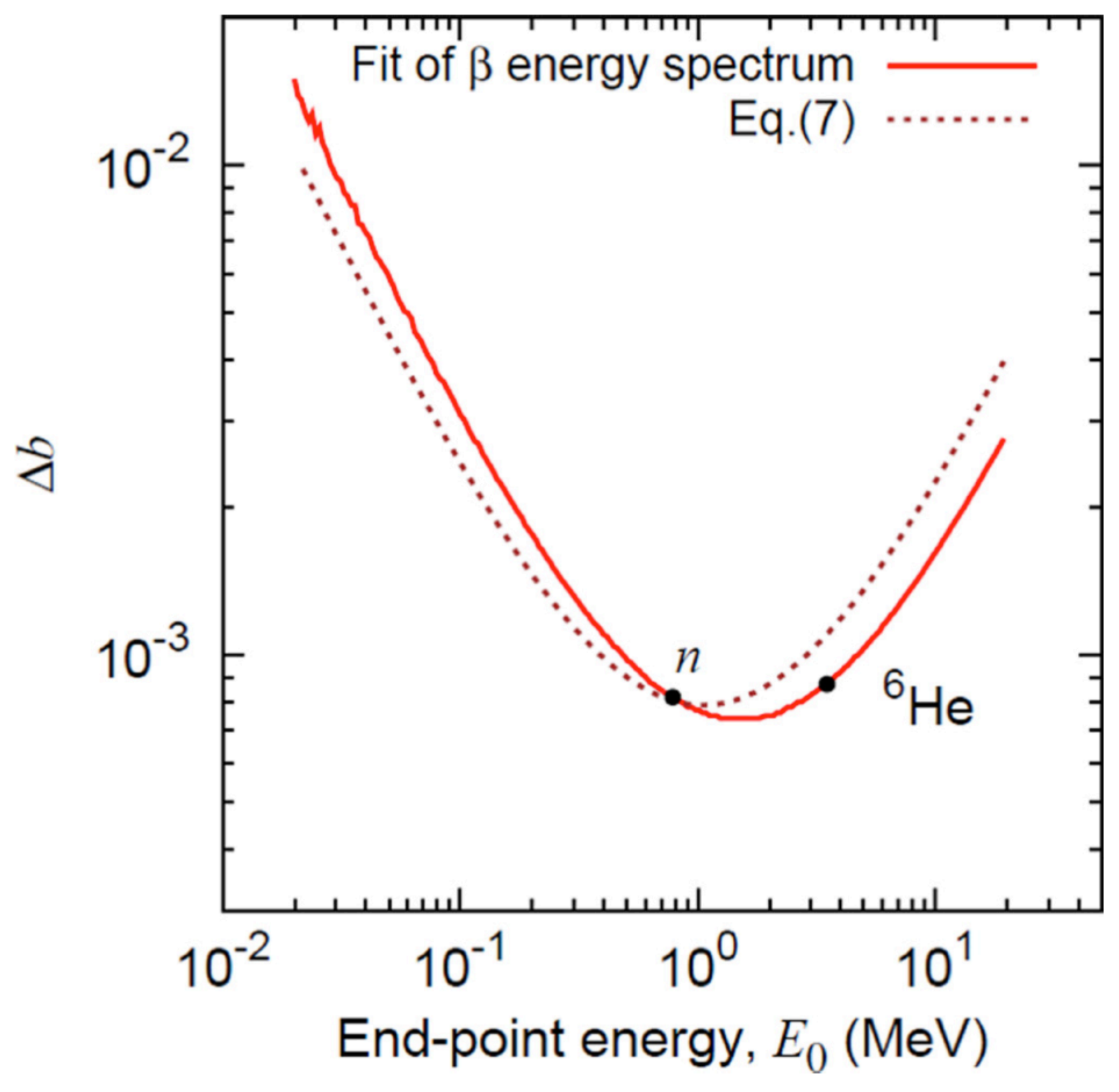

M. Gonzalez-Alonso and O Naviliat-Cuncic, PRC 94, 035503 (2016)

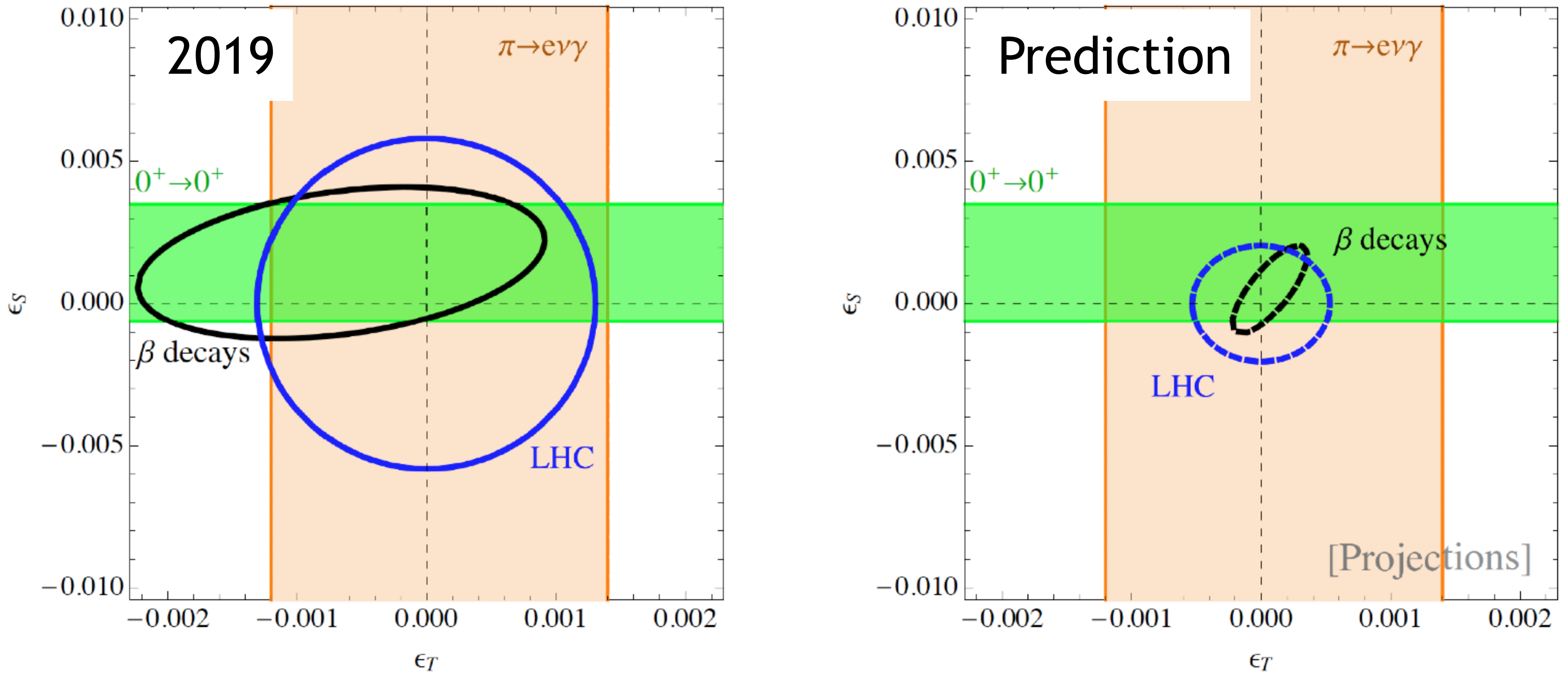

Gonzalez-Alonso, et al., Progress in Particle and Nuclear Physics, Volume 104, January 2019, Pages 165-223

<u>^{6}He:</u>

1. 100 % Gamow-Teller transition ⇒ C_T sensitivity
2. No γ emission with β^- decay
3. Short half-life time: 807 ms
4. Theoretically well understood

<u>Neutrons:</u>

Most fundamental semi-leptonic weak decay

First cyclotron radiation signals from MeV-scale e± from $^{6}He/^{19}Ne$ decays

arXiv:2209.02870

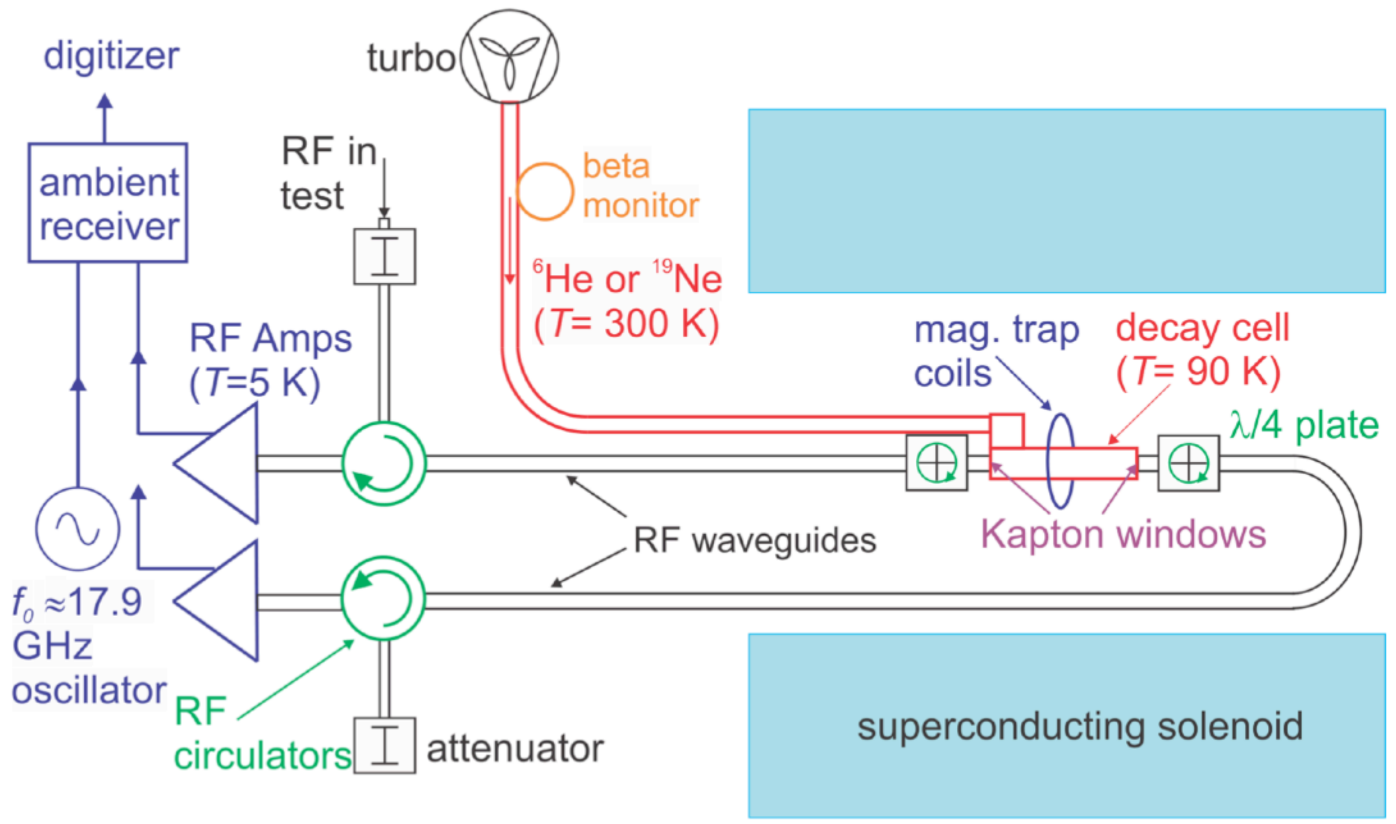

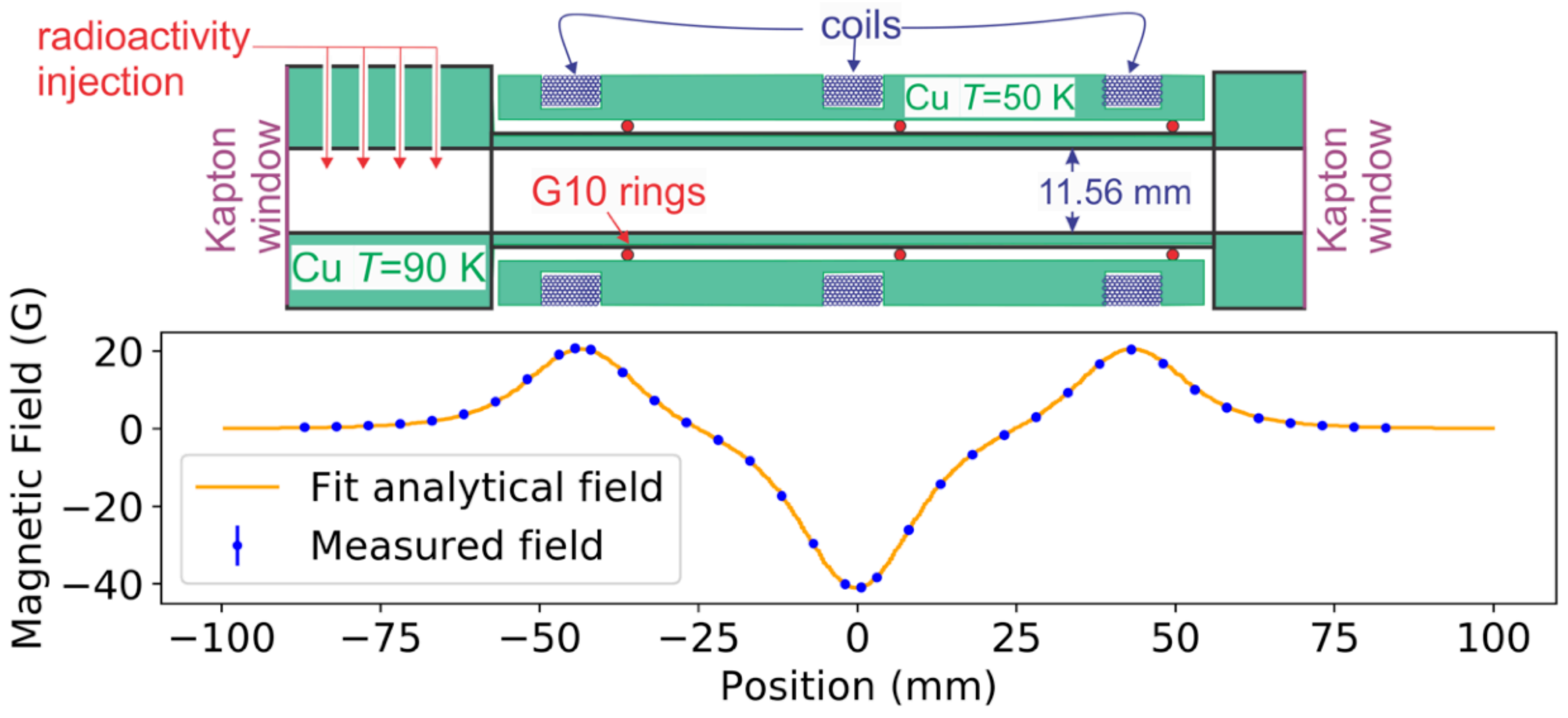

First cyclotron radiation signals from MeV-scale e± from ^{6}He/^{19}Ne decays

arXiv:2209.02870

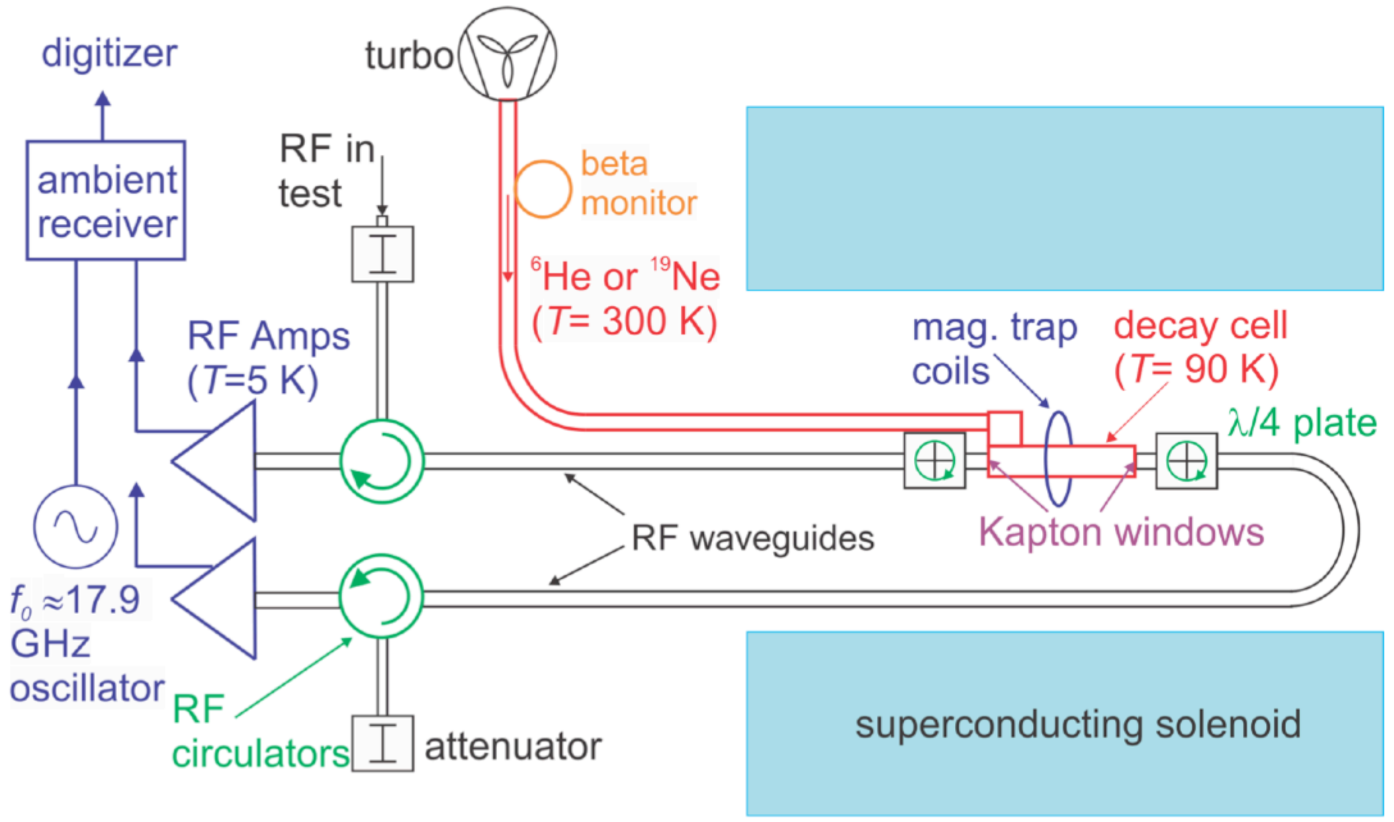

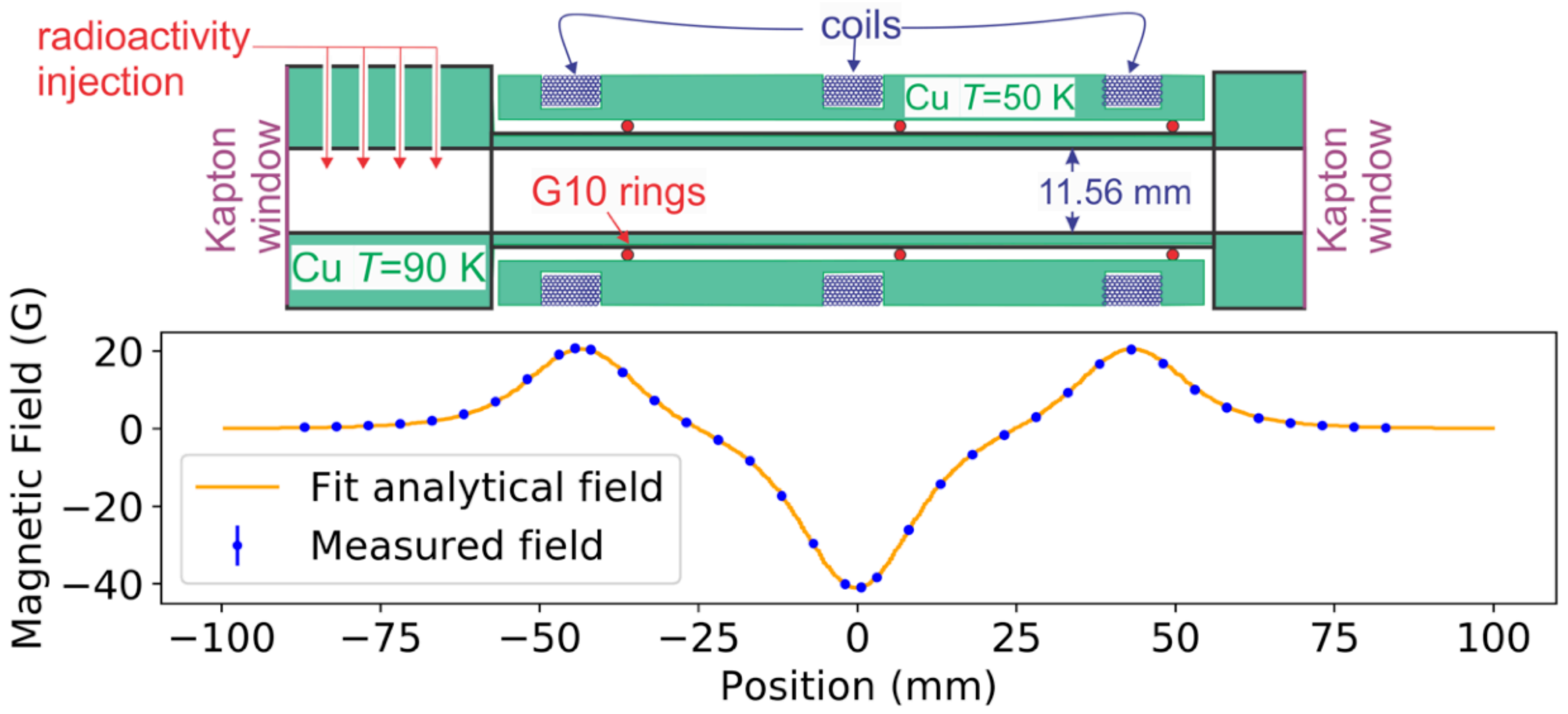

Very high-density of ^{6}He tracks at 2T

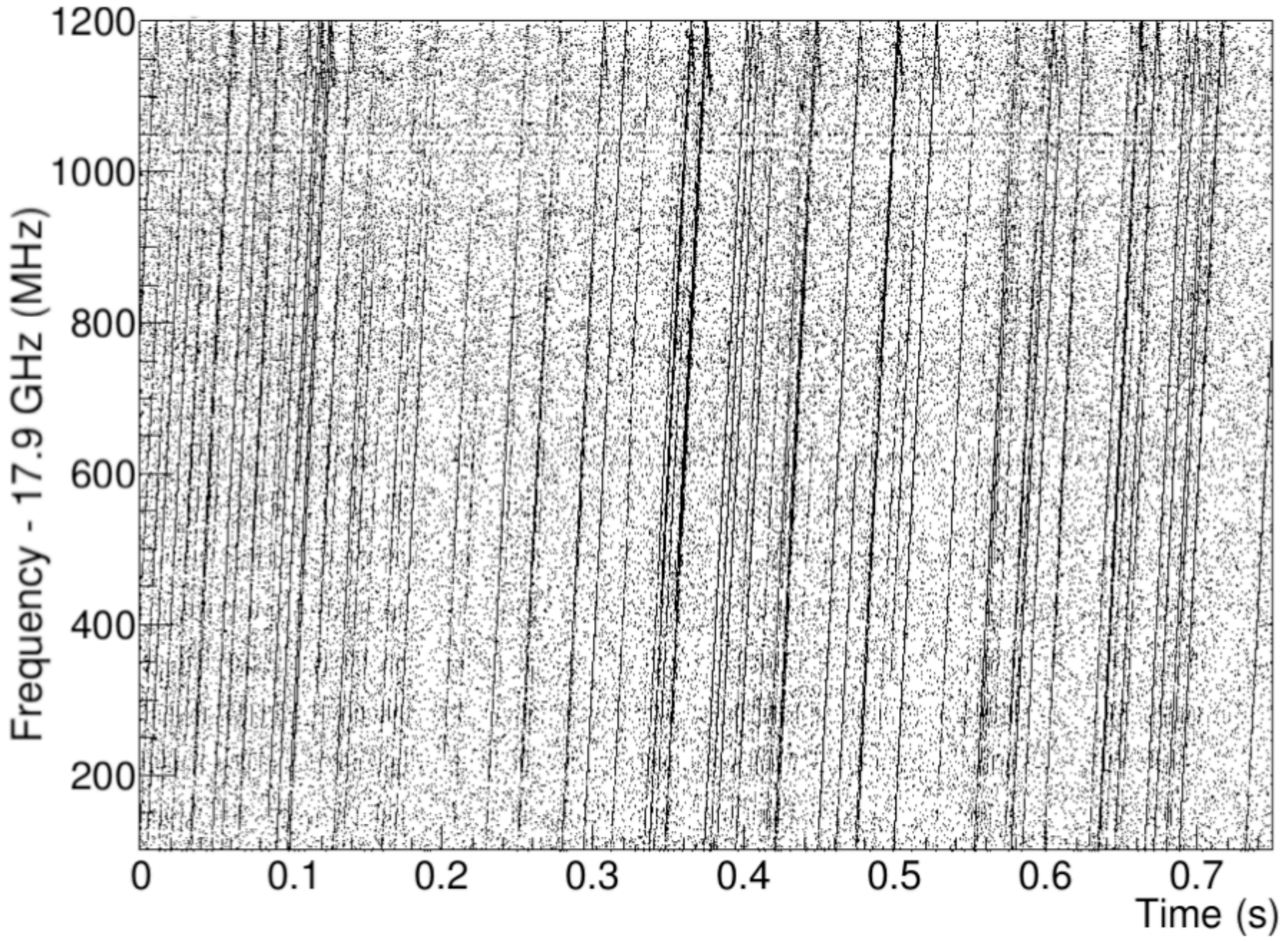

First cyclotron radiation signals from MeV-scale e± from ^{6}He/^{19}Ne decays

arXiv:2209.02870

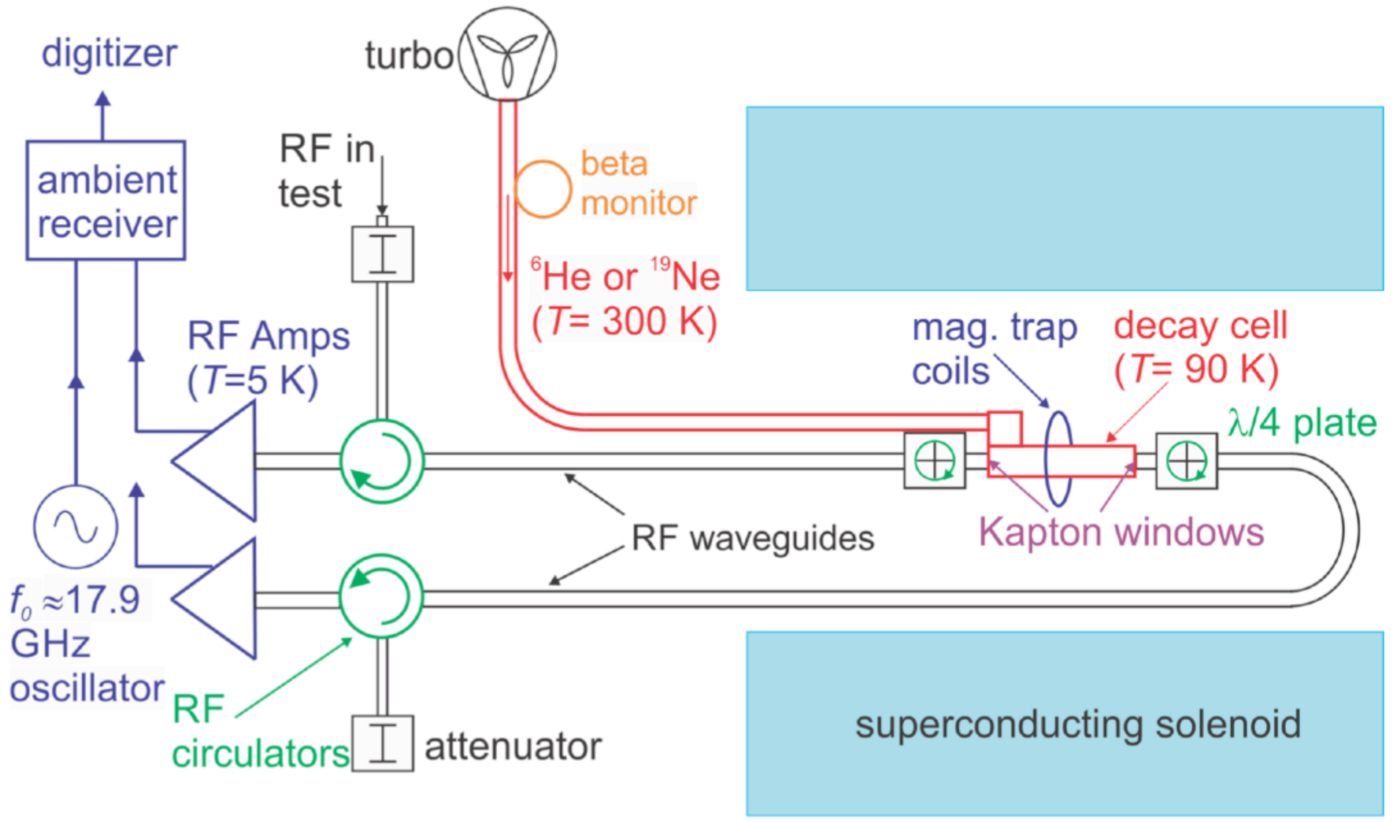

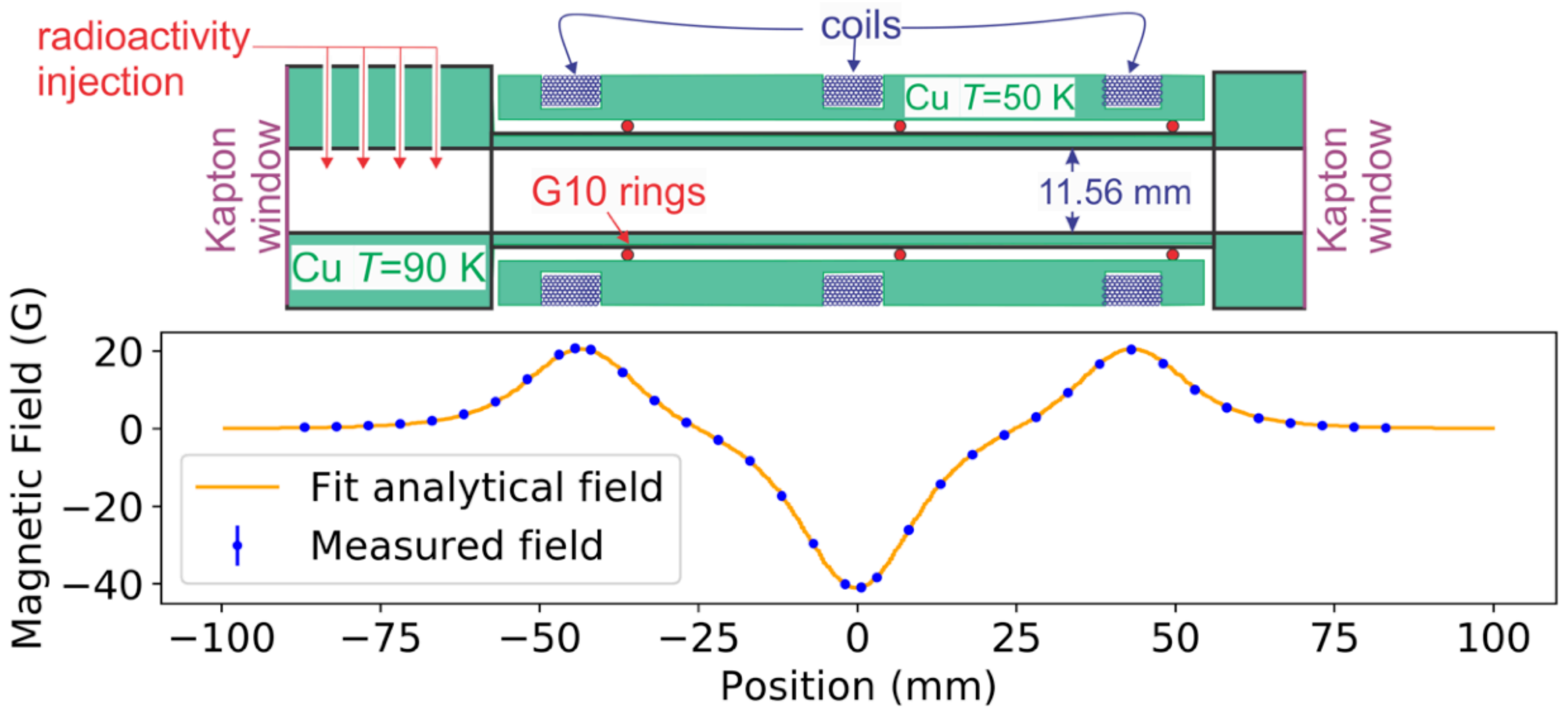

Very high-density of ^{6}He tracks at 2T

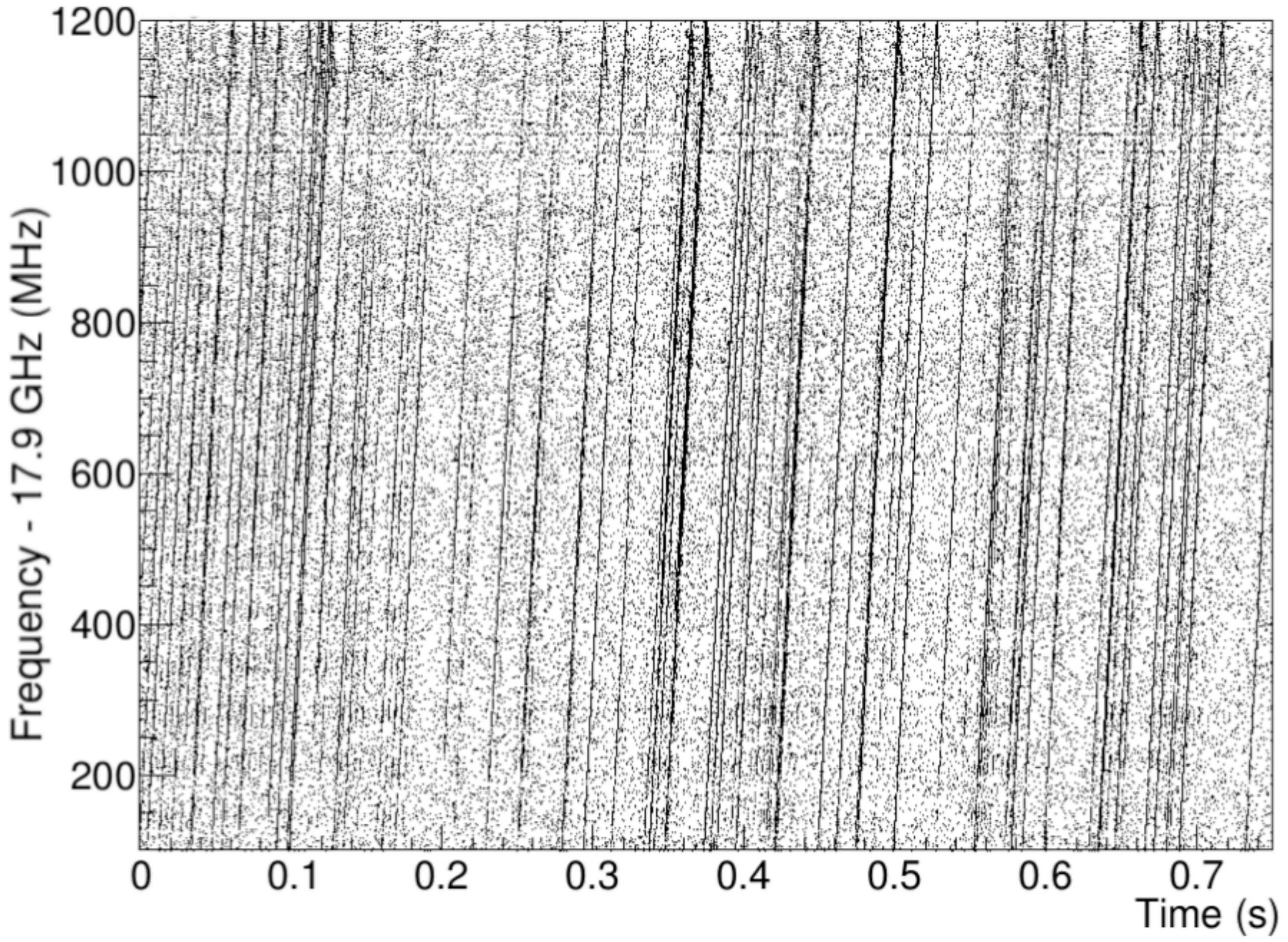

Two ^{19}Ne tracks in detail

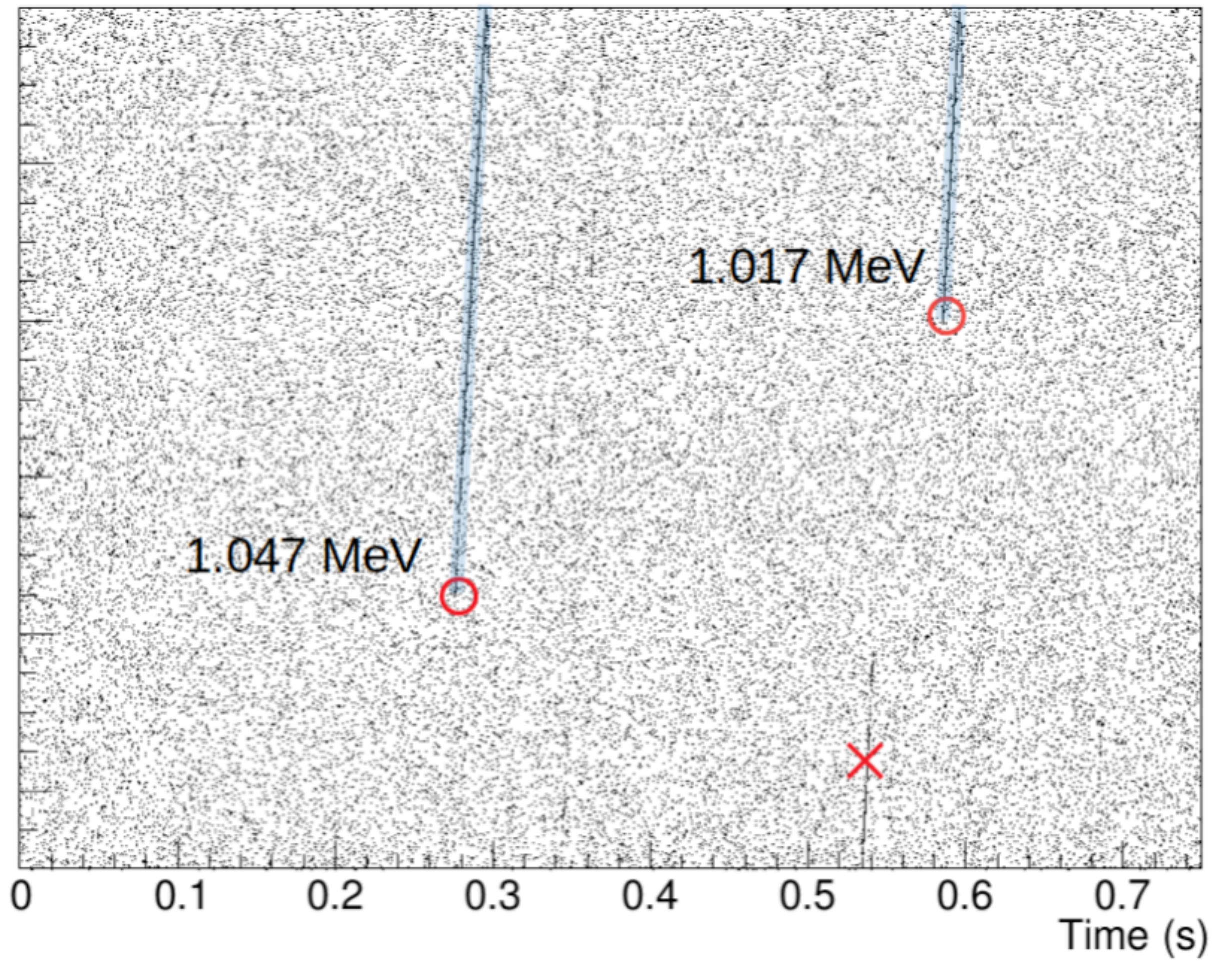

First cyclotron radiation signals from MeV-scale e± from ^{6}He/^{19}Ne decays

arXiv:2209.02870

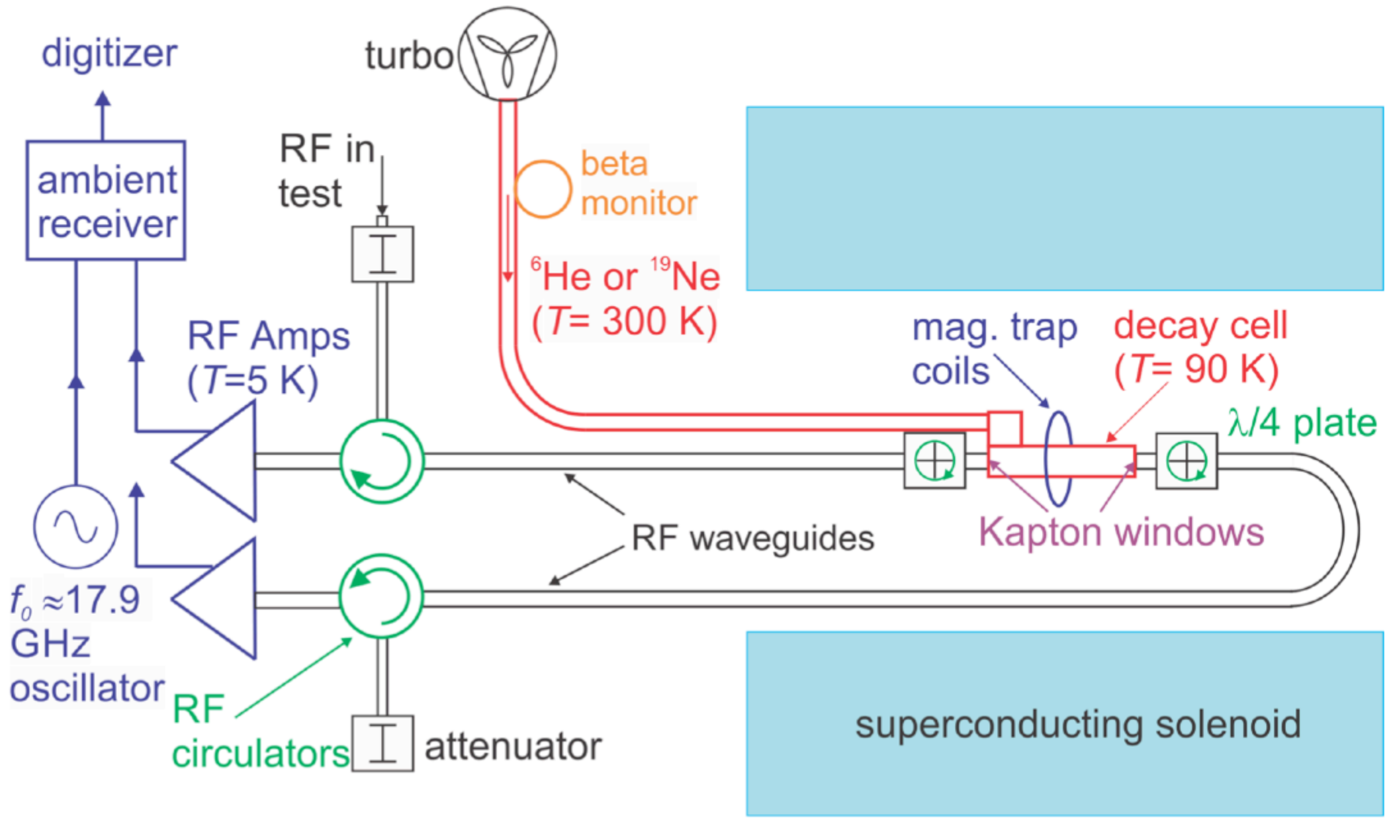

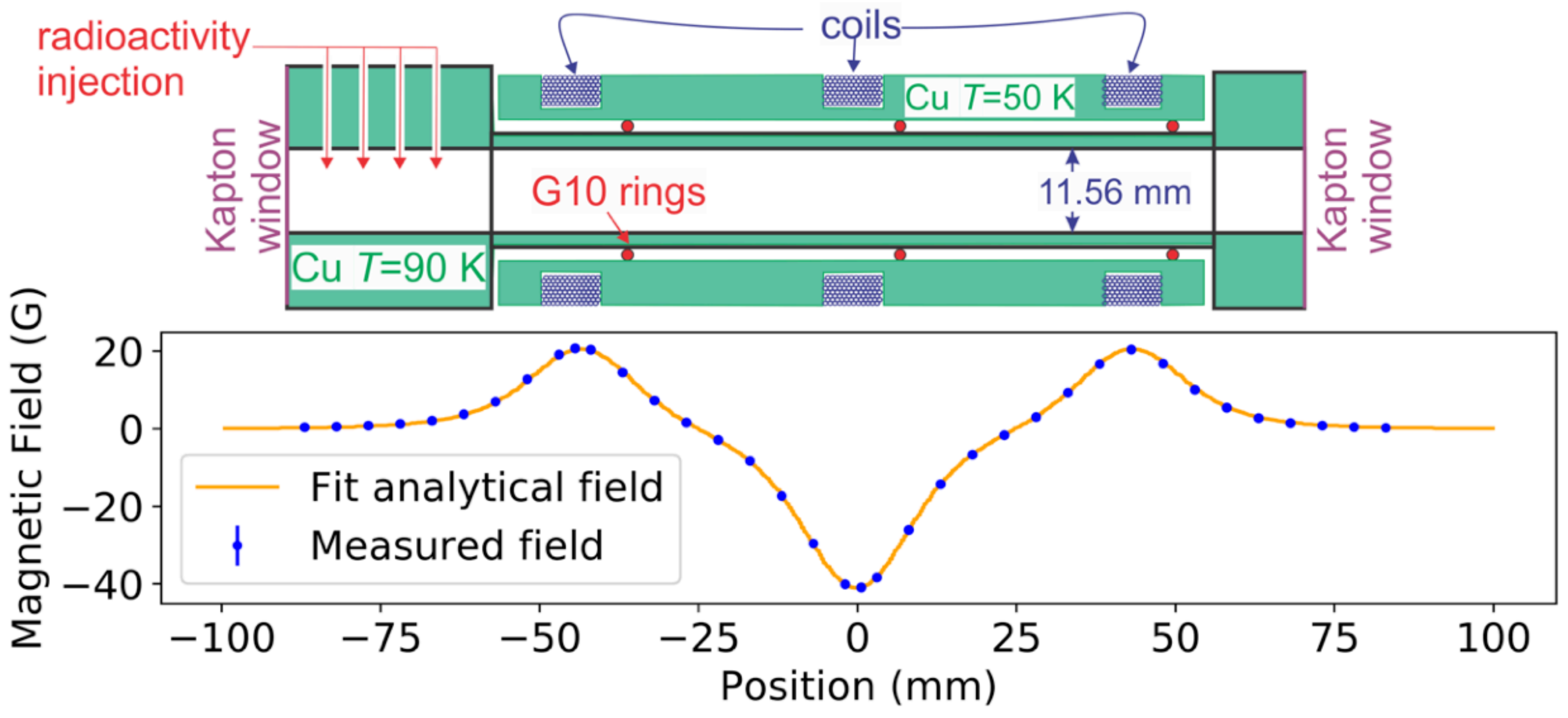

Very high-density of ^{6}He tracks at 2T

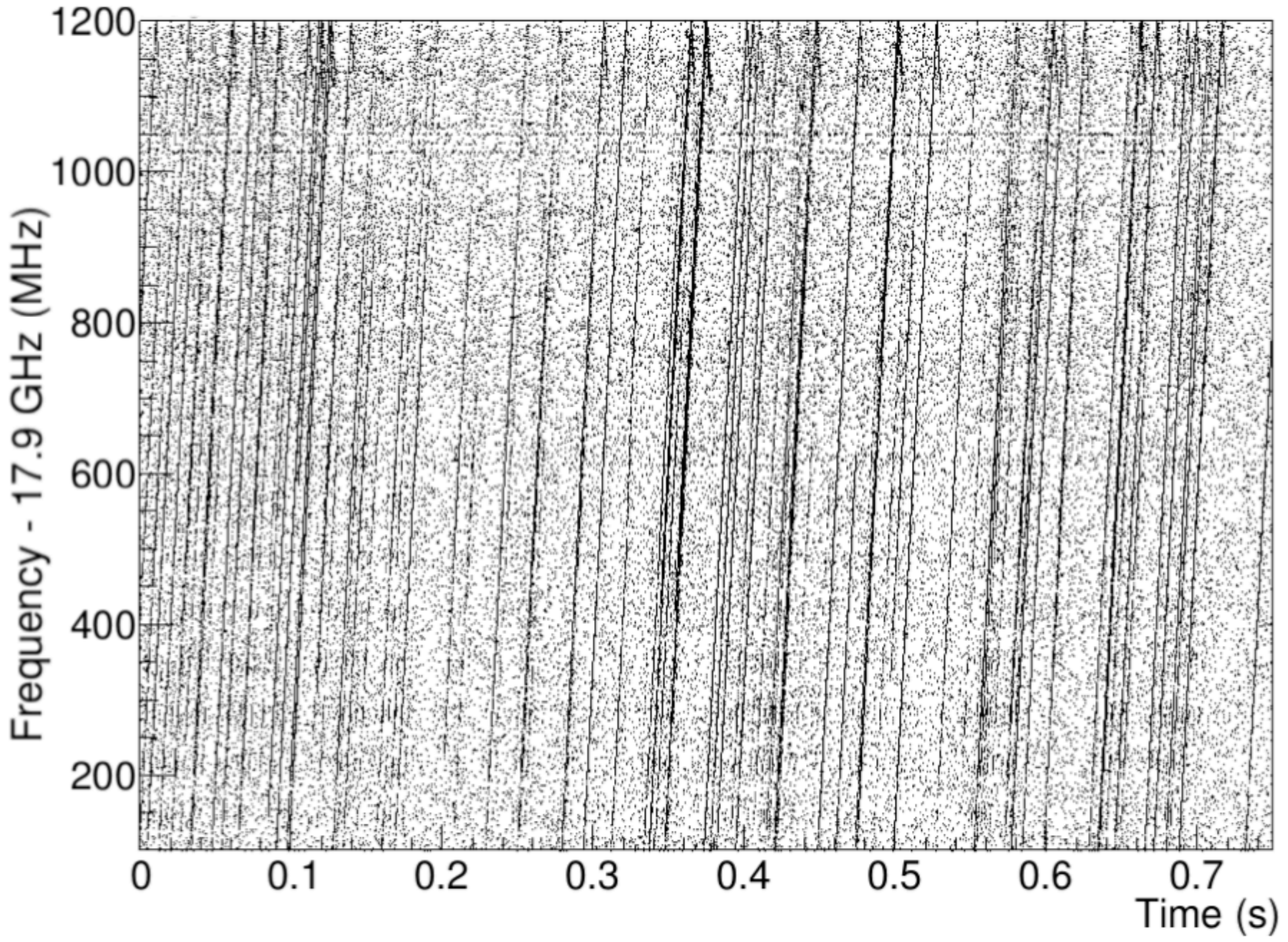

Two ^{19}Ne tracks in detail

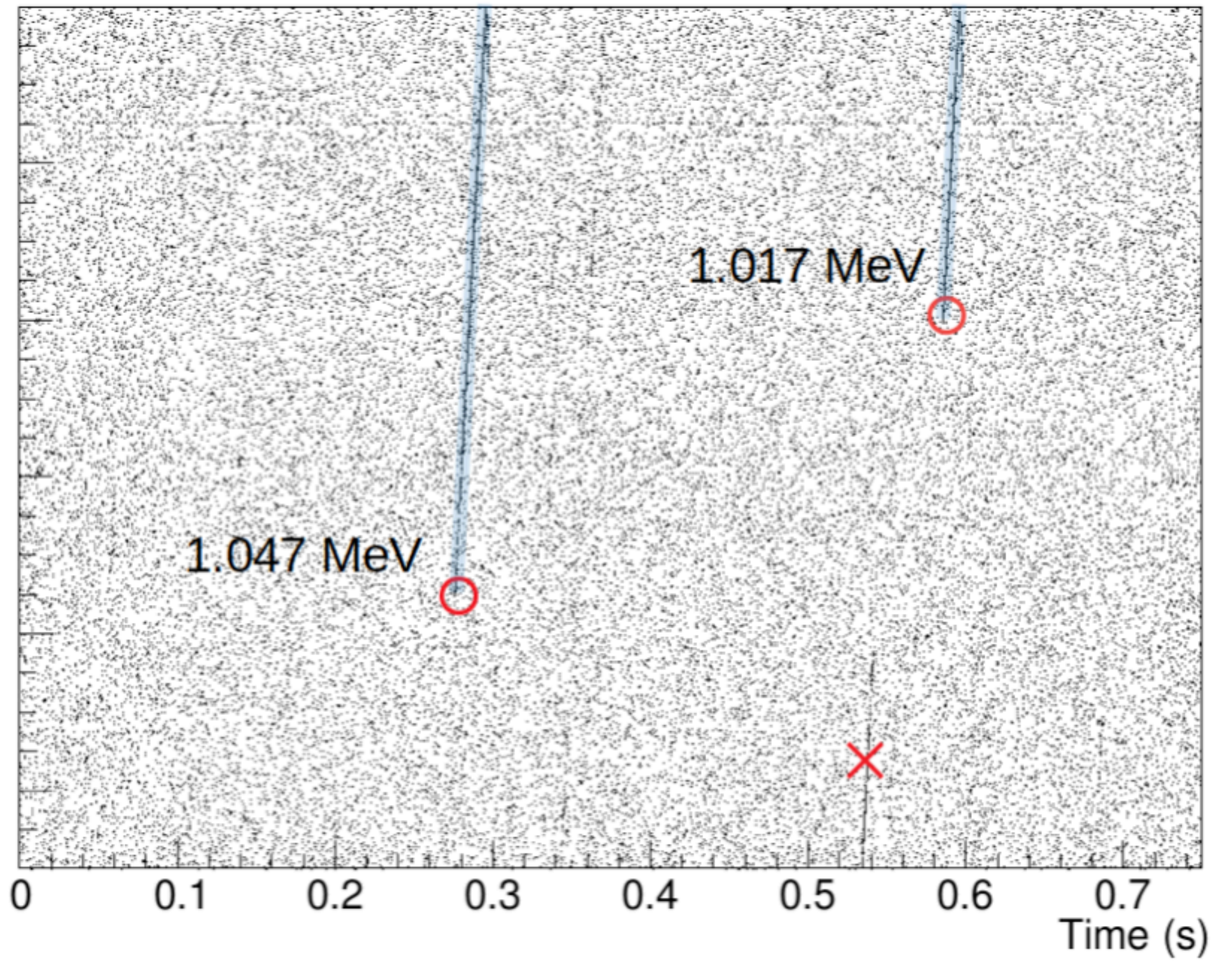

^{19}Ne track affected by waveguide resonance

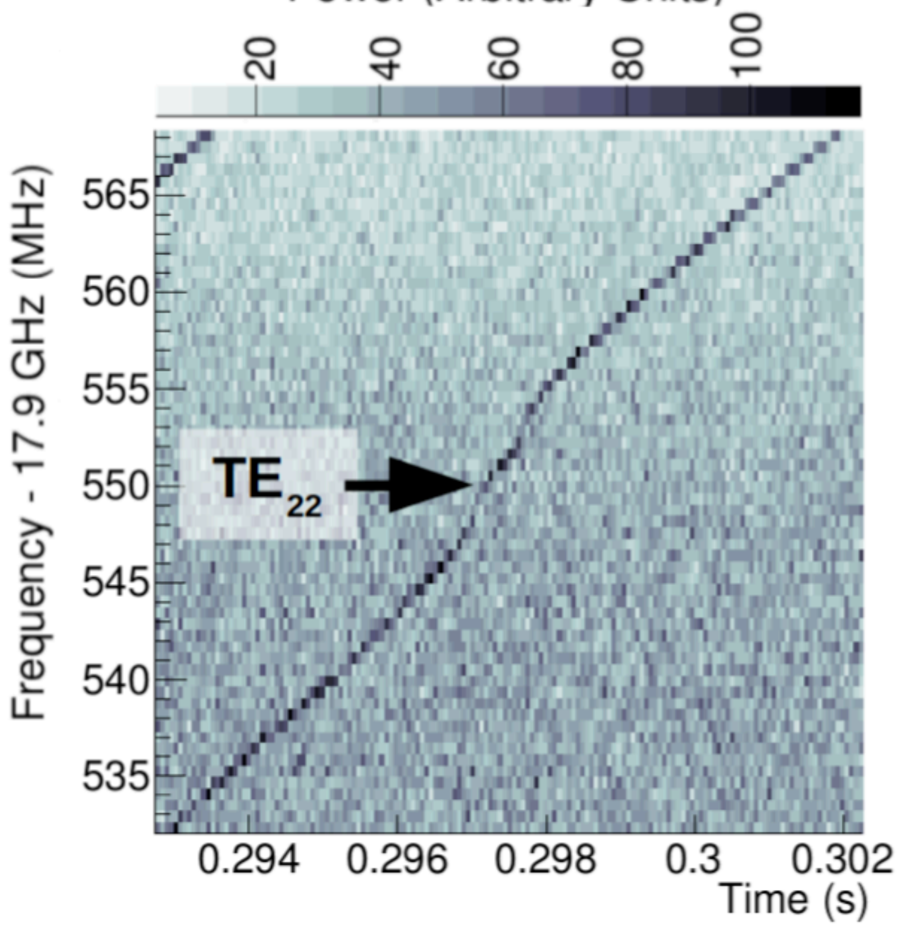

First cyclotron radiation signals from MeV-scale e± from ^{6}He/^{19}Ne decays

Energy band sampled
for fixed RF bandwidth

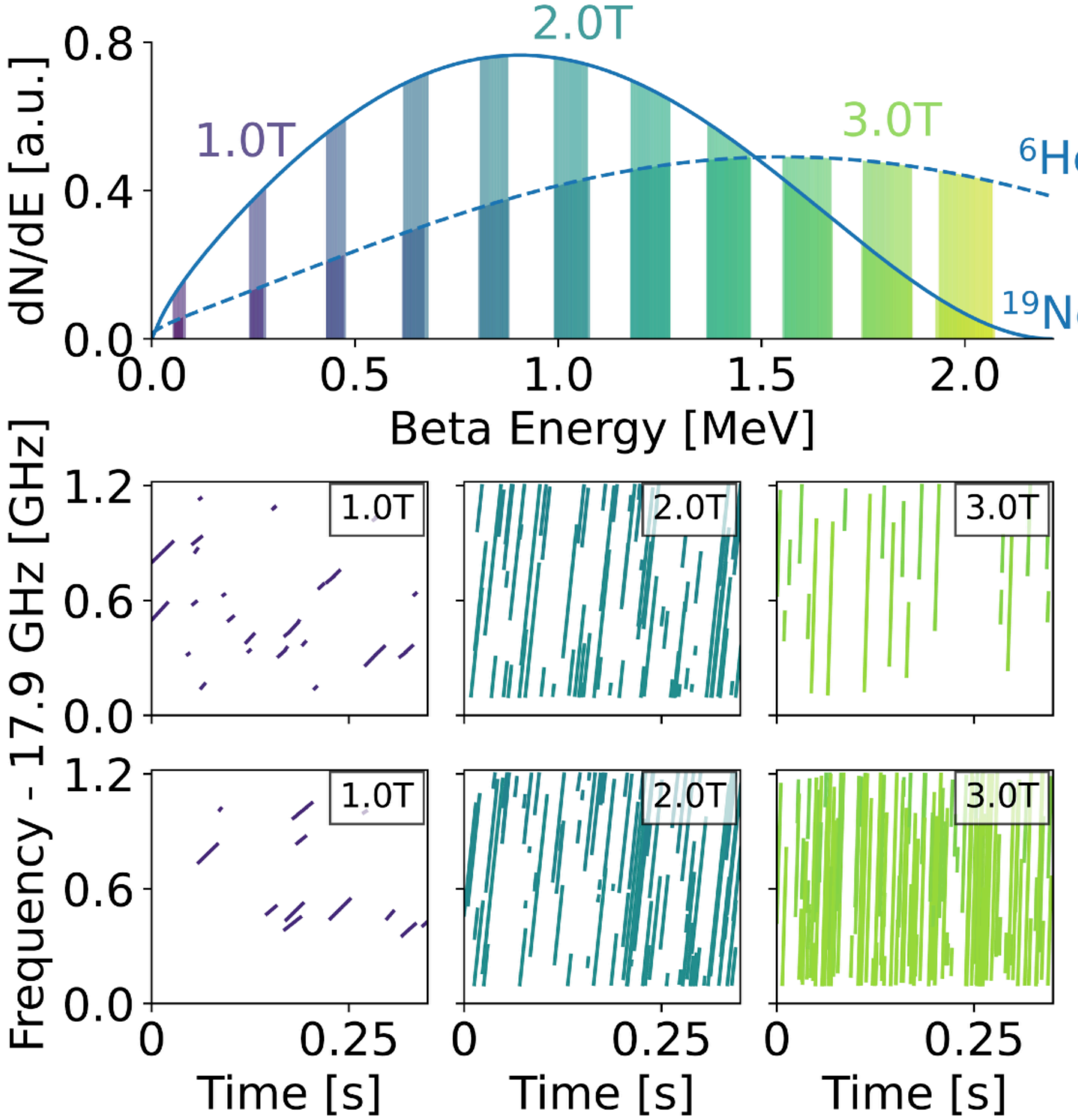

Ratio measurement of
^{19}Ne and ^{6}He spectra

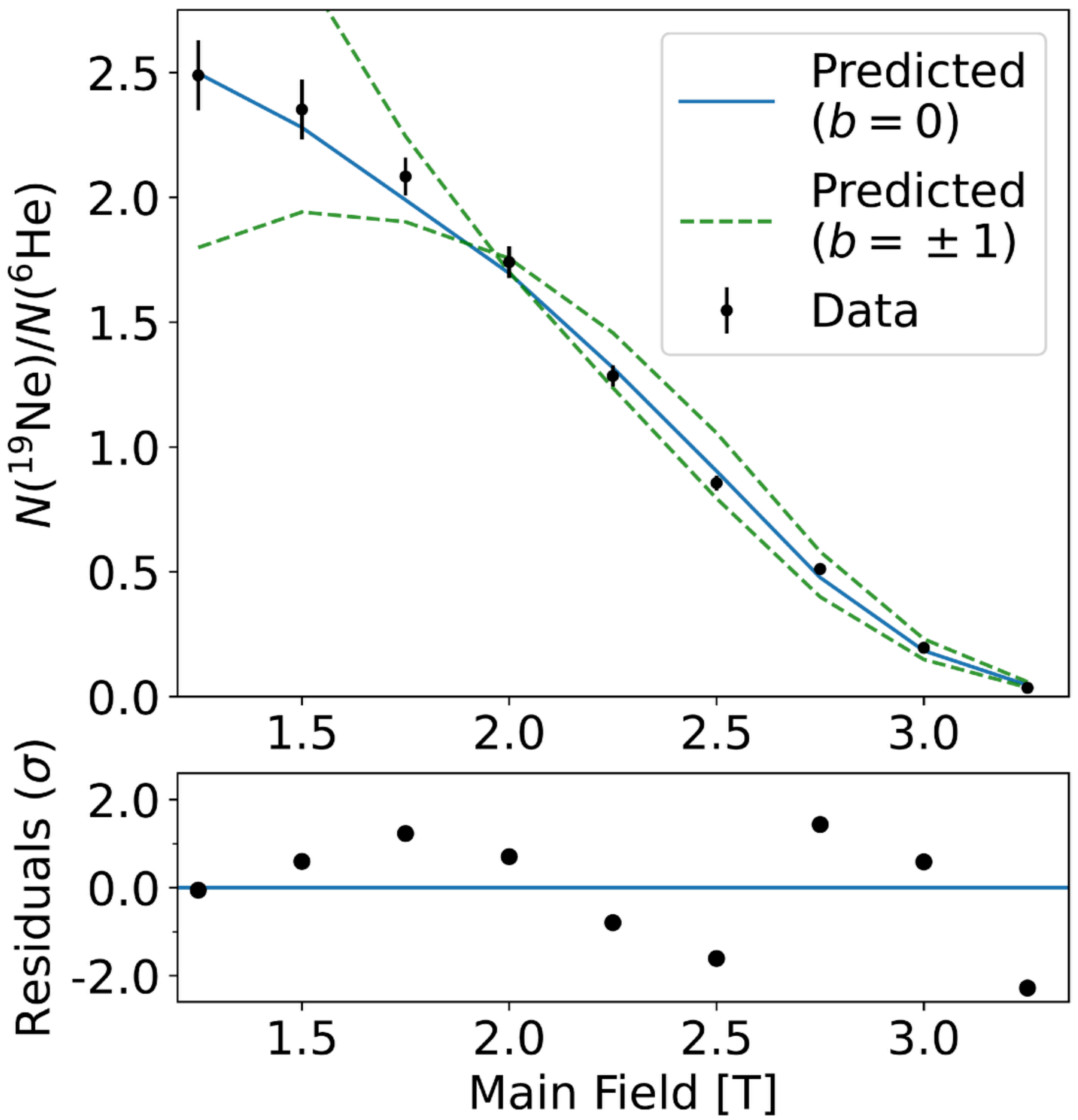

Strong multimodal
coupling in waveguide cell

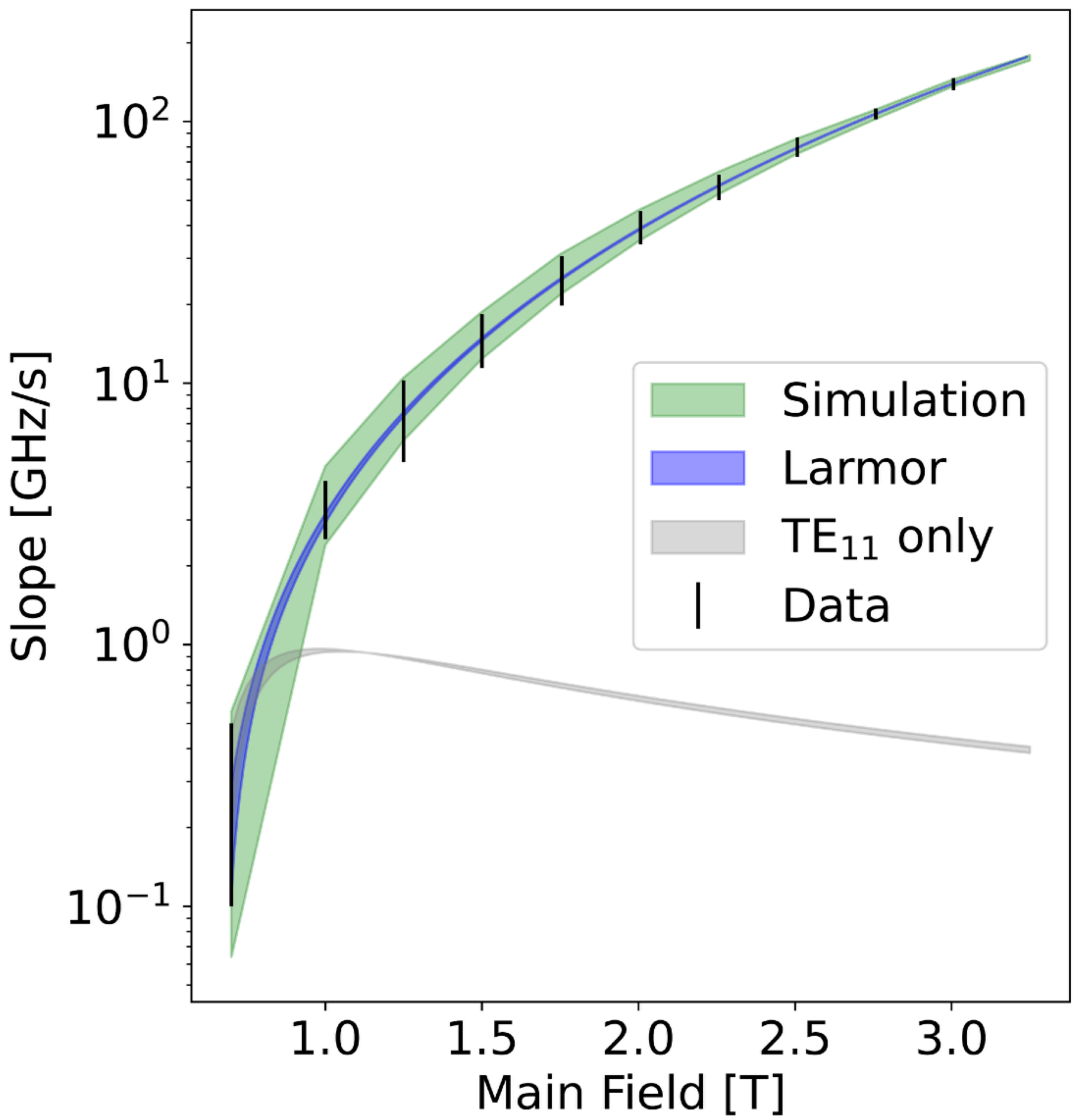

arXiv:2209.02870v2

First cyclotron radiation signals from MeV-scale e± from ^{6}He/^{19}Ne decays

Energy band sampled for fixed RF bandwidth

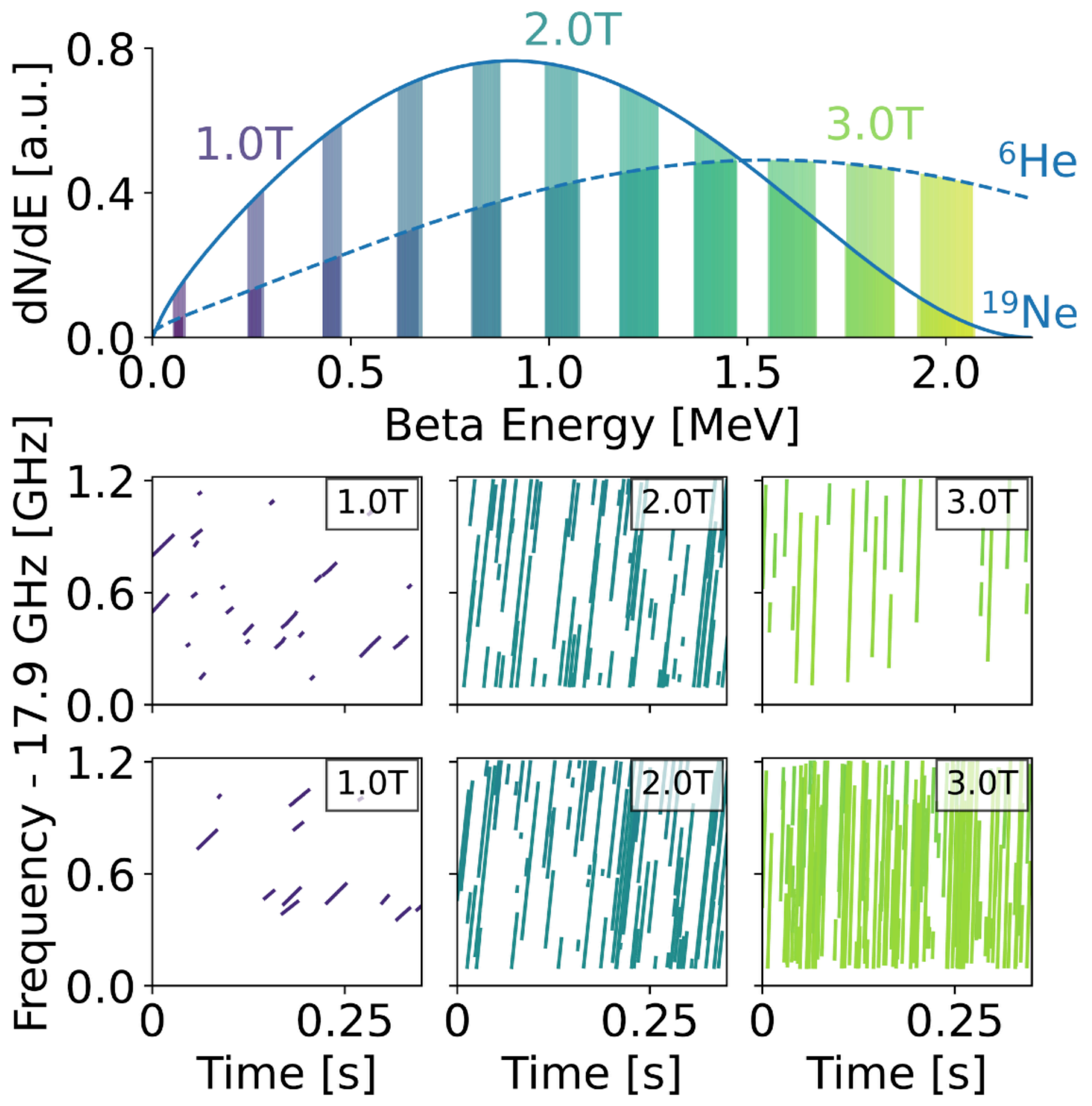

Ratio measurement of ^{19}Ne and ^{6}He spectra

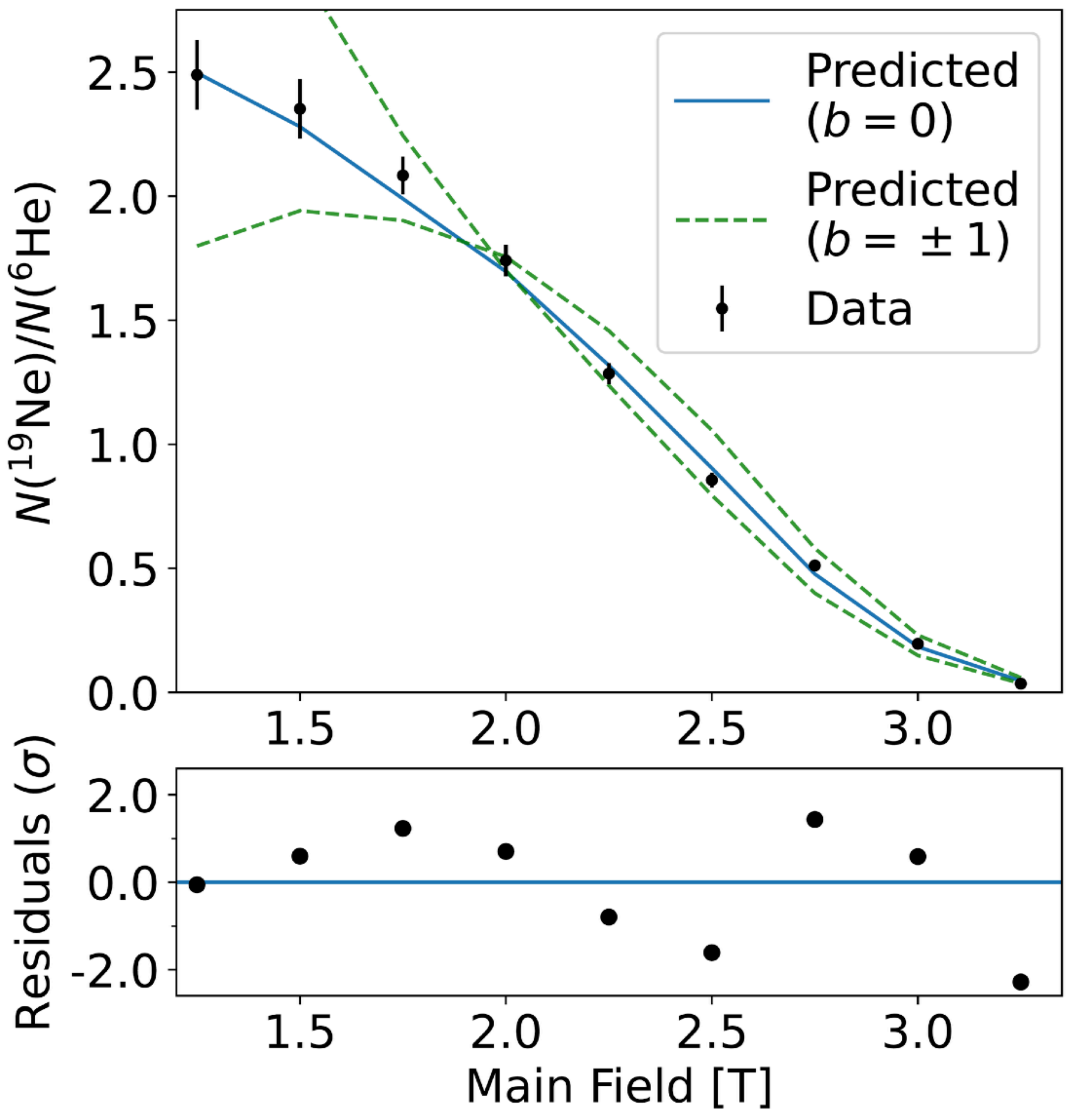

Strong multimodal coupling in waveguide cell

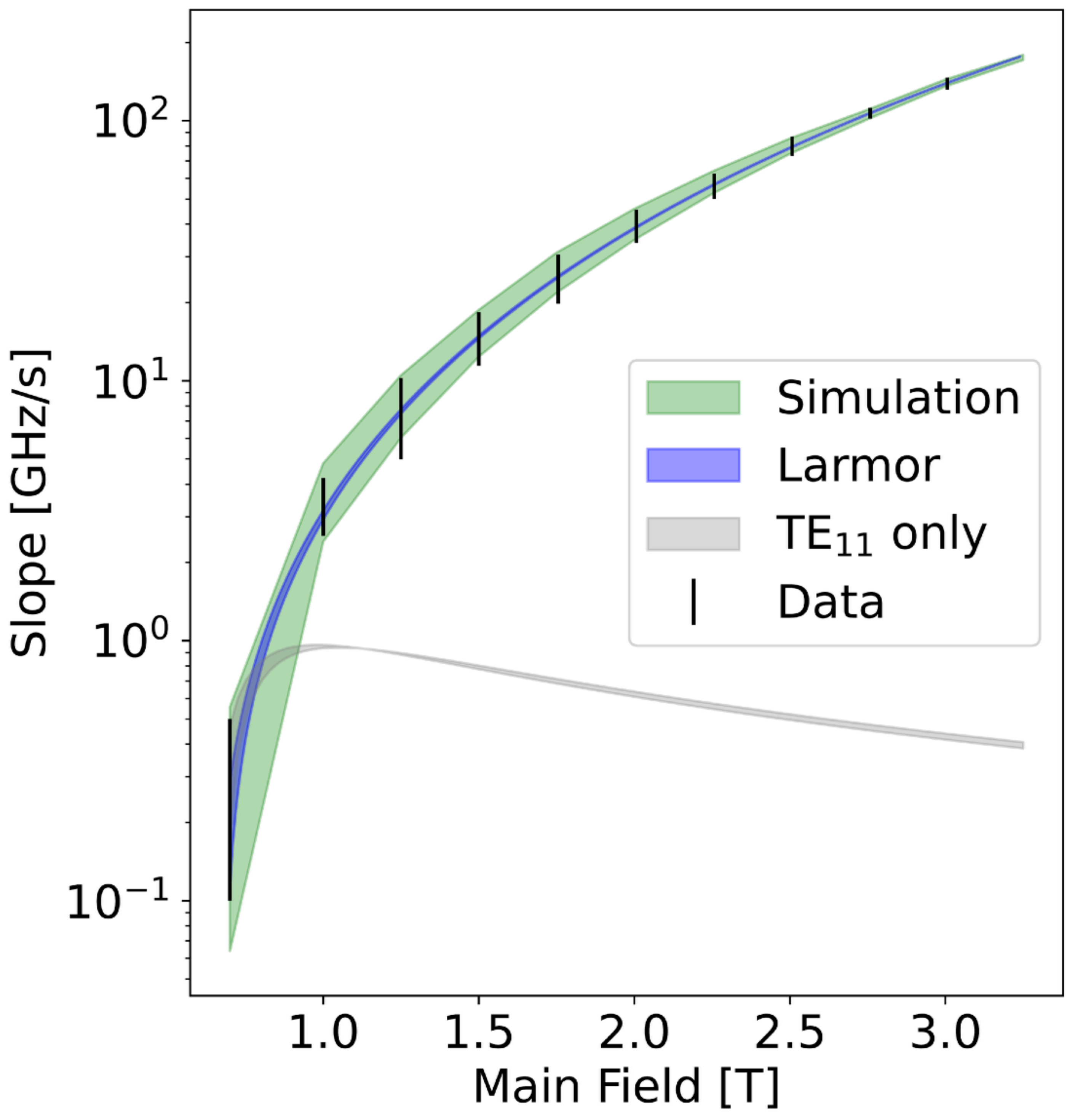

arXiv:2209.02870v2 Established viability of CRES across the full beta-decay energy range!

Summary

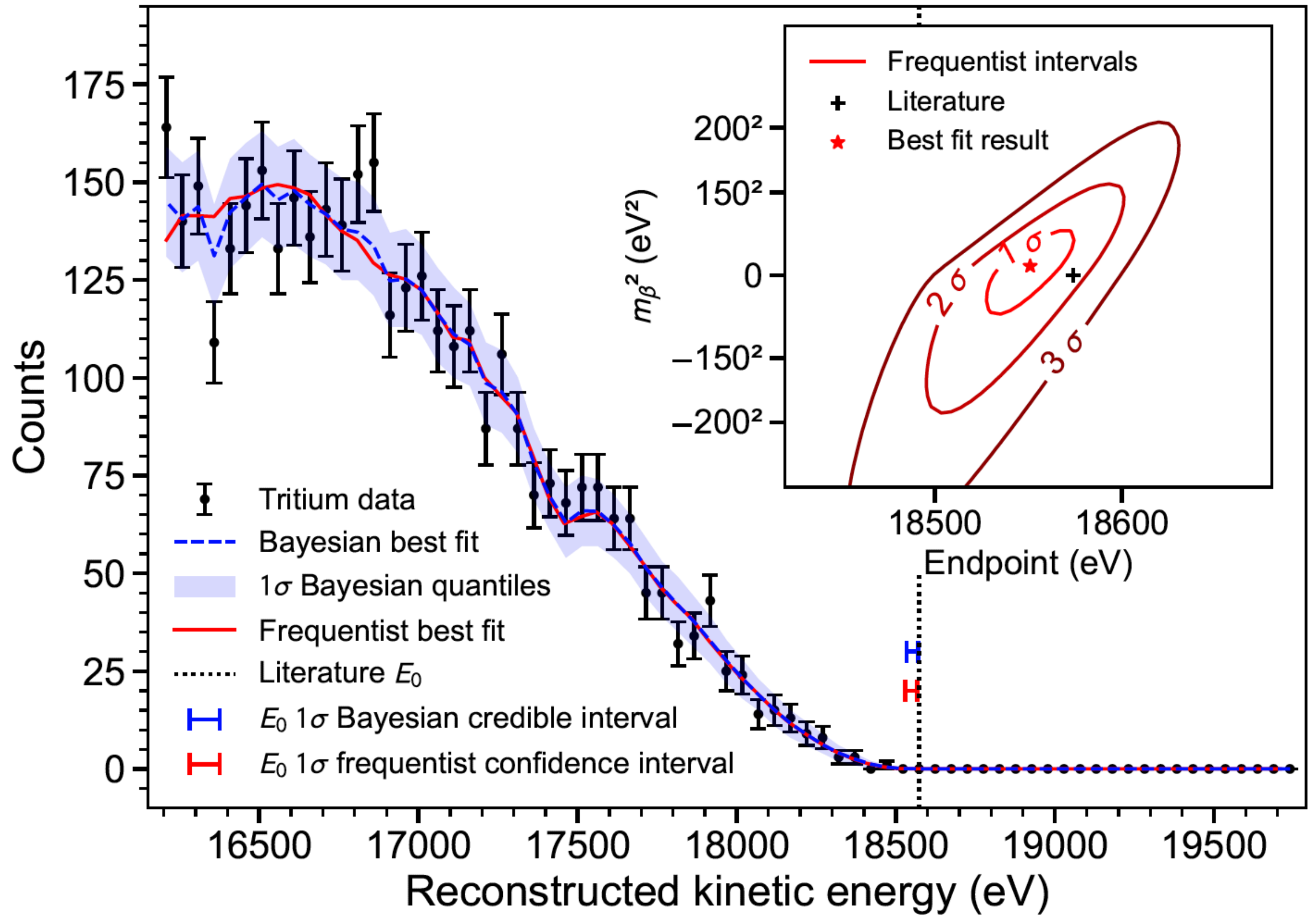

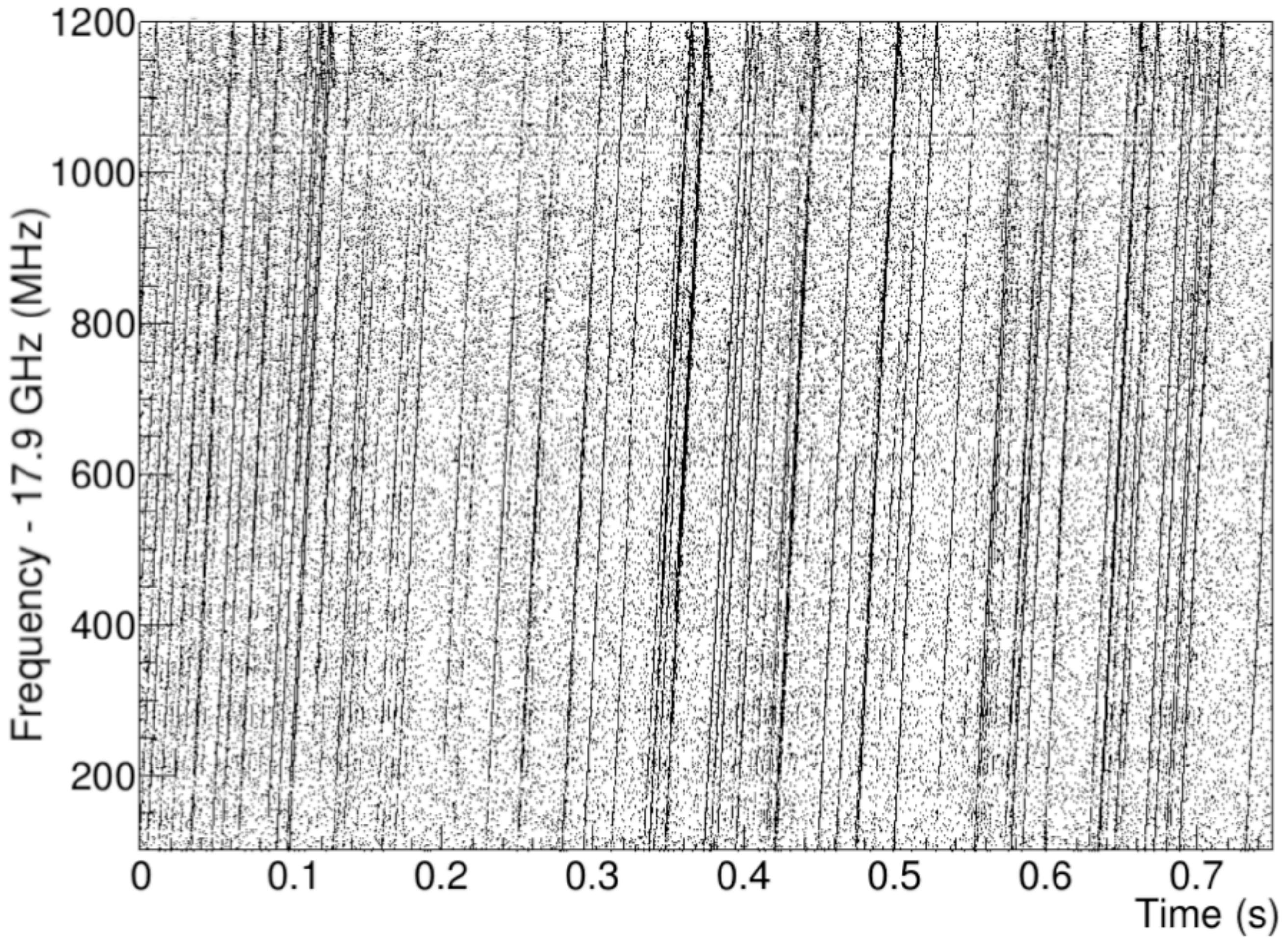

- CRES established as promising technique for next generation neutrino mass experiment

- Project 8 Phase II demonstrated background-free operation, control of systematics, first CRES m_β limit

- Work ongoing toward key technology demonstrations on the path to the 40 meV experiment

- First cyclotron radiation emission signals from MeV-scale $e^\pm$ pave the way for wide-application frequency based precision spectroscopy.

Acknowledgments: Project 8 and ^{6}He collaborations

B. Monreal, R. Mohiuddin, Y.-H. Sun Case Western Reserve University

C.-Y. Liu University of Illinois, Urbana-Champaign

W. Pettus Indiana University

S. Böser, M. Fertl, A. Lindman, Ch. Matthé, B. Mucogllava, R. Reimann, F. Thomas, L. A. Thorne

Johannes Gutenberg University Mainz

T. Thümmler Karlsruhe Institute of Technology

A. Poon, Lawrence Berkeley National Laboratory

K. Kazkaz Lawrence Livermore National Laboratory

J. A. Formaggio, M. Li, J.I. Peña, J. Stachurska, W. Van De Pontseele Massachusetts Institute of Technology

J. K. Gaison, N. S. Oblath, D. Rosa de Jesus, J. R. Tedeschi, B. A. VanDevender

Pacific Northwest National Laboratory

P.T. Surukuchi University of Pittsburgh

B. Jones University of Texas, Arlington

M. C. Carmona-Benitez, L. de Viveiros, R. Mueller, A. Ziegler Pennsylvania State University

C. Claessens, P. J. Doe, S. Enomoto, A. Marsteller, E. Novitski, R. G. H. Robertson, G. Rybka

University of Washington

K. M. Heeger, J. A. Nikkel, L. Saldaña, P. L. Slocum, P.T. Surukuchi, A. B. Telles, T. E. Weiss

Yale University

PROJECT 8

N. Buzinsky, W. Byron, W. DeGraw, B. Dodson, A. Garcia, G. Garvey, B. Graner, H. Harrington, K.S. Khaw, K, Knutsen, E. Novitski, R.G.H. Robertson, G. Rybka, E. Smith, M. Sternberg, D.W. Storm, H.E. Swanson, X. Zhu

University of Washington

M. Fertl

Johannes Gutenberg University Mainz

M. Guigue, X. Huyan, N. S. Oblath, J.R. Tedeschi, B.A. VanDevender

Pacific Northwest National Laboratory

L. Hayen, D.D. Stancil, A. Young

North Carolina State University

L. Hayen, A. Young

The Triangle Universities Nuclear Laboratory, Durham

D. McClain, D. Melconian

Texas A&M University

P. Müller, G. Savard,

Argonne National Laboratory

F. Wietfeldt

Tulane University

^{6}He-CRES

This work is supported by the PRISMA+ Cluster of Excellence at the Johannes Gutenberg University of Mainz, the US DOE Office of Nuclear Physics, the US NSF, and internal investments at all institutions.

We are looking for new group members to join our efforts in Mainz

JG|U
JOHANNES GUTENBERG UNIVERSITÄT MAINZ

PROJECT 8

Cluster of Excellence
PRISMA+
Precision Physics, Fundamental Interactions and Structure of Matter

To strengthen its neutrino physics research program, the University of Mainz offers

1 PhD position (EG13/2)

at the Cluster of Excellence PRISMA+ to work on “Project 8”, a next generation neutrino mass experiment (http://www.project8.org).

Neutrino oscillations provide a clear indication that neutrinos are not massless as assumed in the Standard Model of particle physics. Yet the masses of the neutrinos are several orders of magnitude lower than those of other fermions, and only upper limits have been set so far. Today, the most sensitive method to observe neutrino masses in the laboratory is the observation of the tritium β-decay spectrum endpoint region.

Towards this goal, the Project 8 collaboration has developed the novel method of Cyclotron Radiation Emission Spectroscopy (CRES), in which the electron energy is determined by its radio frequency emission when trapped in a magnetic field. Recently, we have succeeded in measuring the tritium spectrum with a small volume inside a waveguide, read out by a single antenna. In order to scale up to the final experiment, several techniques will need to be developed and tested.